THE UNIVERSITY
of EDINBURGH

Inhibition of pH regulation as a therapeutic strategy in breast cancer

James Meehan

Doctor of Philosophy

The University of Edinburgh

2016

Declaration

I declare that this thesis has been composed by me, and that the work was performed by me, except where otherwise stated. The work presented in this thesis has not been submitted for any other degree or professional qualification.

James Meehan

Acknowledgements

Firstly, I would like to thank my supervisors Dr Simon Langdon and Dr Carol Ward. I consider myself extremely lucky to have been given the opportunity to work with the both of them for the past number of years, and I thank them both for their constant support. I could not have asked for better supervisors, and I am very grateful to them both. Thanks also to Professor Ian Kunkler for support and advice offered over the course of my PhD, in addition to the help received in obtaining further funding.

I would like to thank the College of Medicine and Veterinary Medicine for providing the opportunity for me to undertake my PhD at the University of Edinburgh. Similarly, I would like to give my appreciation to the Breast Cancer Institute (BCI) and the Aitken Breast Cancer Fund, who helped fund my stay in Edinburgh, in addition to contributing to my lab expenses and conference attendances. I would also like to thank the METOXIA consortium for helping to fund the project.

I would also like to thank the following people for their contributions to my project:
Tissue collection- Professor Michael Dixon and Lorna Renshaw
Explant studies- Dr Carol Ward
Xenograft studies- Dr Simon Langdon and Edward Jarman
Contributions to data analysis- Dr Arran Turnbull
Sample collection for gene expression analysis- Dr Arran Turnbull, Edward Jarman, Carlos Martinez Perez, Xrisy Xintaropoulou
Tissue sectioning- Helen Caldwell
IGMM Imaging Facility- Dr Ahmed Fetit and Matthew Pearson

Thank you to everyone within the Division of Pathology Laboratories for making me feel so welcome.

I would also like to thank Daniel for being such a great friend for the past 5 years.

Thank you to my family, especially my father Vincent, who has supported me my whole life.

Finally, I would like to thank Sarah for her unending kindness and support, especially over the past few months.

Abstract

The abnormal regulation of H^+ ions, leading to a reversed pH gradient in cancer cells when compared to normal cells, is considered to be one of the most distinctive features of cancer. However, this characteristic has yet to be fully exploited as a therapeutic target in cancer. This project assessed whether targeting pH regulating proteins, which permit cancer cells to survive in the hostile hypoxic and acidic tumour microenvironment, could produce an effective therapeutic response in breast cancer. The pH regulating proteins carbonic anhydrase IX (CAIX), Na^+/H^+ exchanger 1 (NHE1) and vacuolar (H^+)-ATPase (V-ATPase) were the focus of this thesis. Initial experiments were conducted in 2D tissue culture before progressing into 3D, using models that more faithfully re-create the *in vivo* tumour microenvironment.

Expression analysis conducted with MCF-7, MDA-MB-231 and HBL-100 human breast cancer cell lines cultured in 2D, and in 3D as multicellular tumour spheroids, showed that protein and mRNA levels of CAIX were very responsive to lower O_2 concentrations. Both MDA-MB-231 and HBL-100 cells displayed large increases in CAIX expression levels in hypoxia, with the HBL-100 cell line exhibiting the largest change in CAIX mRNA (42-fold increase) and protein (78-fold increase) levels in 0.5% O_2 conditions. Hypoxia inducible factor 1-α (HIF-1α) controls the expression of CAIX, but the induction of CAIX in hypoxic MCF-7 cells was lower in comparison to the other cell lines, despite the presence of similar levels of HIF-1α. The differences in CAIX expression observed between the cell lines was consistent with a varying activity of factor inhibiting HIF-1 (FIH-1), an oxygen sensor that controls signalling through HIF-1α, as siRNA targeting FIH-1 led to increased levels of CAIX in hypoxic MCF-7 cells. While NHE1 protein levels did increase in hypoxic conditions in MCF-7 cells in 3D, overall, the expression levels of both NHE1 and V-ATPase were not as responsive to changes in O_2 concentrations when compared to CAIX across differing O_2 conditions in each of the cell lines.

Inhibitors targeting CAIX, NHE1 and V-ATPase were all shown to reduce cancer cell number in 2D culture conditions. Differing O_2 conditions changed the sensitivity

of these cell lines to CAIX inhibition. Cells cultured in 20% O_2 conditions were responsive to CAIX inhibition, while acute hypoxic cells cultured in 0.5% O_2 displayed an increased resistance to drug treatment. Chronically hypoxic cells, which had spent over 10 weeks in 0.5% O_2 before treatment, exhibited a re-sensitisation to CAIX inhibition.

3D invasion assays demonstrated that CAIX inhibition significantly reduced the invasion of cells from MDA-MB-231 spheroids into collagen type 1 in both 20% O_2 and 0.5% O_2 conditions, while drugs targeting either NHE1 or V-ATPase had no such inhibitory effects. Preliminary clonogenic assays, used to assess radiation sensitivity and performed with MDA-MB-231 spheroids, indicated that inhibitors targeting CAIX and NHE1 led to a significant decrease in colony formation when combined with irradiation, compared to either drug treatment or irradiation alone.

Further invasion assays, carried out with primary tissue derived from human patients, showed that drugs targeting CAIX retained their inhibitory effects when tested on heterogeneous cancer material of varying tumour subtypes. CAIX inhibition also exhibited anti-cancer effects *in vivo* on mouse MDA-MB-231 xenografts, significantly reducing the proliferation and growth of tumours within mice.

Together, this work demonstrates that inhibitors targeting the pH regulation mechanisms of cancer cells have potential in the treatment of breast cancer, highlighted by their capacity to affect cancer cell number, cancer cell invasion, and their ability to combine with irradiation. Of the 3 pH regulatory molecules studied, CAIX appears to be the target with the most therapeutic potential.

Lay Summary

Hydrogen ions (H^+ ions) are one of the most important and reactive ions present in a cell. Alterations in the concentrations of H^+ ions, measured as changes in pH, can affect many processes that occur within a cell. Because of the importance of pH to cellular function, cells have developed the ability to control the amount of H^+ ions within them through the expression of pH regulating proteins.

The regulation of H^+ ions in cancer cells is different to the regulation of H^+ ions in normal cells in the body. In fact, the abnormal regulation of pH within cancer cells is thought of as one of the most distinctive features of cancer. However, this characteristic has yet to be fully exploited in the treatment of cancer. The aim of this project therefore was to assess the effects of drugs targeting pH regulatory proteins that have been linked with cancer, evaluating whether inhibiting these proteins could produce an effective therapeutic response in breast cancer. The pH regulating proteins carbonic anhydrase IX (CAIX), Na^+/H^+ exchanger 1 (NHE1) and vacuolar (H^+)-ATPase (V-ATPase) were the focus of this thesis.

The uncontrolled proliferation of cancer cells within the tumour leads to some cells being pushed further and further away from blood vessels, inhibiting the delivery of O_2 and the removal of wastes, leading to hypoxia (a lack of O_2) and the formation of an acidic environment. Hypoxia has been shown to induce the expression of pH regulating proteins that enable the survival of cancer cells within this hostile environment. Initial experiments assessed the expression of CAIX, NHE1 and V-ATPase in hypoxic conditions. Breast cancer cell lines were used in these experiments. The results showed that CAIX expression levels were very responsive to changes in O_2 concentrations, with large increases in the amount of this target observed in hypoxic conditions. However, the extent of CAIX expression differed between the cell lines studied. The expression of CAIX is controlled by an oxygen sensor within the cell called hypoxia inducible factor 1-α (HIF-1α), and despite the presence of similar levels of this protein in each of the cell lines, the levels of CAIX were still reduced in one of the cell lines. Further work showed that the differences in

CAIX expression seen between the cell lines were consistent with the varying activity of another oxygen sensor present in the cell called factor inhibiting HIF-1 (FIH-1), as reductions in the levels of FIH-1 led to increases in the amount of CAIX. While NHE1 protein levels did increase in hypoxic conditions in one of the cell lines, overall, the hypoxic expression levels of both NHE1 and V-ATPase were much more consistent when compared to CAIX.

The anti-cancer effects of drugs targeting the 3 pH regulation proteins were also assessed. Inhibitors targeting CAIX, NHE1 and V-ATPase were shown to reduce cancer cell number. However, the sensitivity of the cells to CAIX inhibition varied with the oxygenation of the cells. Aerobic (well-oxygenated) cells were responsive to CAIX inhibition, while cells present in hypoxic conditions for up to 5 days showed an increased resistance to drug treatment. However, the presence of cells for 20 weeks in hypoxic conditions led to a re-sensitisation to CAIX inhibition.

The invasion and migration of cancer cells from the breast to other parts of the body is the main cause of breast cancer mortality. pH regulating proteins have been linked to this process. Invasion assays, conducted to assess the effects of drugs targeting pH regulation molecules on the invasion of cancer cell lines, showed that inhibiting CAIX reduced the amount of invasion in both aerobic and hypoxic conditions. However, no such inhibitory effects were seen with drugs targeting either NHE1 or V-ATPase. Further invasion assays carried out with tissue derived from human breast cancer patients showed that CAIX inhibitors retained their effects in this more complex cancer model. The abnormal pH of cancer cells has also been linked with a resistance to radiotherapy. Preliminary experiments indicated that drugs targeting both CAIX and NHE1 were able to improve the effects of irradiation. Finally, *in vivo* experiments showed that CAIX inhibitors reduced the proliferation and growth of tumours in mice.

Together, this work demonstrates that inhibitors targeting the pH regulation mechanisms of cancer cells have potential in the treatment of breast cancer. Of the 3

pH regulatory molecules studied, CAIX appears to be the target with the most therapeutic potential.

Abbreviations

1,3-BPG	1,3-bis-phosphoglycerate
2-PG	2-phosphoglycerate
3-PG	3-phosphoglycerate
6PG	6-phosphogluconate
6PGδL	6-phosphogluconolactone
6PGDH	6-phosphogluconate dehydrogenase
6PGL	6-phosphogluconolactonase
AH	Acute hypoxic
ALDOA	Aldolase A
ANOVA	Analysis of variance
APS	Ammonium persulphate
ASCT2	Alanine, serine, cysteine-preferring transporter 2
ATP	Adenosine-5'-triphosphate
BCA	Bicinchoninic acid
CA	Carbonic anhydrase
CBP	Creb binding protein
CDK4	Cyclin dependent kinase 4
CDKN2A	Cyclin-dependent kinase inhibitor 2A
CH	Chronic hypoxic
CITED2	CBP/p300 Interacting Transactivator With Glu/Asp Rich Carboxy-Terminal Domain 2
$CoCl_2$	Cobalt chloride
C-TAD	C-terminal transactivation domain
DHAP	Dihydroxyacetone
DMA	Dimethylamiloride
DMEM	Dulbecco's modified Eagle's Media
DMSO	Dimethyl sulfoxide
DNA	Deoxyribonucleic acid
E4P	Erythrose 4-phosphate
ECM	Extracellular matrix
ECT	Electron transport chain
ENO1	Enolase 1
ER	Oestrogen receptor
F1,6BP	Fructose-1,6-bisphosphate
F6P	Fructose-6-phosphate
$FADH_2$	Flavin adenine dinucleotide, reduced
FCS	Fetal calf serum
FIH-1	Factor inhibiting HIF-1
FIJI	Fiji is just ImageJ
FISH	Fluorescent in situ hybridisation
G3P	Glyceraldehyde 3-phosphate
G6P	Glucose-6-phosphate
G6PDH	Glucose 6-phosphate dehydrogenase
GAPDH	Glyceraldehde 3-phosphate
GLS1	Glutaminase 1
GLS2	Glutaminase 2
GLUT	Glucose transporter
GSH	Glutathione
h	Hour
HER1	Receptor tyrosine-protein kinase erbB-1
HER2	Receptor tyrosine-protein kinase erbB-2
HER3	Receptor tyrosine-protein kinase erbB-3
HIF	Hypoxia inducible factor
HK	Hexokinase
HRE	Hypoxic response element

IGMM	Institute of Genetics and Molecular Medicine
IGRT	Image guided radiotherapy
IHC	Immunohistochemistry
IHT	Interstitial hypertension
IMRT	Intensity-modulated radiotherapy
IORT	Intra-operative radiotherapy
LDHA	Lactate dehydrogenase A
LFQ	Label-free quantitation
MCT	Monocarboxylate transporter
MEGM	Mammary epithelial cell growth media
min	Minute
MMP	Matrix metalloproteinase
MRI	Magnetic resonance imaging
mRNA	Messenger RNA
mTOR	Mammalian target of rapamycin
NADH	Nicotinamide adenine dinucleotide
NADPH	Nicotinamide adenine dinucleotide phosphate
NEAA	Non-essential amino acid
NHE	Na^+-H^+ exchanger
NMR	Nuclear magnetic resonance
N-TAD	N-terminal transactivation domain
OD	Optical density
ODDD	O_2-dependent degradation domain
OH^-	Hydroxide
OXPHOS	Oxidative phosphorylation
PARP	Poly (ADP-ribose) polymerase
PBS	Phosphate buffered saline
PDH	Pyruvate dehydrogenase
PEP	Phosphoenolpyruvate
PFK-1	Phosphofructokinase 1
PGI	Phosphoglucose isomerase
PGK1	Phosphoglycerate kinase
PGM	Phosphoglycerate mutase
PHD	Prolyl hydroxylase domain
PI3K	Phosphoinositide 3-kinase
PKM	Pyruvate kinase M
PKM2	Pyruvate kinase M2
PPI	Proton pump inhibitor
PPP	Pentose phosphate pathway
PR	Progesterone receptor
PTEN	Phosphatase and tensin homolog
R5P	Ribose 5-phosphate
re-ox	Re-oxygenated
RNA	ribonucleic acid
ROS	Reactive oxygen species
RPE	Ribulose 5-phosphate epimerase
RPI	Ribose 5-phosphate isomerase
rpm	Revolutions per minute
Ru5P	Ribulose 5-phosphate
S7P	Sedoheptulose 7-phosphate
SDS	Sodium dodecyl sulphate
SEM	Standard error of the mean
SERD	Selective oestrogen receptor down regulator
SERM	Selective oestrogen receptor modulator
SRB	Sulforhodamine B
TAL	Transaldolase
TCA	Trichloroacetic acid
TIMP-2	Tissue inhibitor of metalloproteinase-2

TKT	Transketolase
TNM	Tumour, node, metastasis
TPI	Triose-phosphate isomerase
V-ATPase	Vacuolar H^+-ATPase
VHL	Von Hippel-Lindeau
Xu5P	Xylulose 5-phosphate

List of Figures

List of Tables

Contents

1 Chapter 1: Introduction

1.1 Breast cancer incidence and survival

Breast cancer is the most common cancer to occur in women. GLOBOCAN statistics show that approximately 1,670,000 women were diagnosed with breast cancer worldwide in 2012, with 522,000 breast-cancer related deaths occurring in that same year [1]. In the UK, over 53,000 cases of breast cancer were reported in 2013, with breast cancer being responsible for over 11,000 deaths in 2014 alone [2]. It is thought that the incidence of breast cancer in women around the world will rise to approximately 3,200,000 cases per year by 2050 [3]. These figures reveal the scale of breast cancer incidence and the effect it has on societies around the world, along with the need for more effective methods of detection and treatment [4].

1.2 Hallmarks of cancer

In 2000, Hanahan and Weinberg published a paper proposing that cancer cells have unique capabilities that enable them to survive, proliferate and metastasise [5]. Altogether, six different abilities were proposed: (i) sustaining proliferative signalling, (ii) evading growth suppressors, (iii) activating invasion and metastasis, (iv) enabling replicative immortality, (v) inducing angiogenesis and (vi) resisting cell death. Research conducted in the decade following this paper led to the authors modifying the original 6 core hallmarks, adding two emerging hallmarks along with two enabling characteristics [6]. The two emerging hallmarks added to the original 6 were (i) deregulating cellular energetics and (ii) avoiding immune destruction. The enabling characteristics, which the authors say make it possible for cancer cells to acquire the differing hallmarks, were (i) genomic instability and mutation and (ii) tumour-promoting inflammation (figure 1). Hanahan and Weinberg propose that these hallmarks, in combination with the enabling characteristics, are a foundation for understanding the biology of cancer.

Figure 1. The hallmarks of cancer.

The acquired abilities of cancer cells that allow them to survive, proliferate and metastasise are shown. Genome instability and mutation, in addition to tumour-promoting inflammation, are characteristics that enable cancer cells to acquire these abilities or hallmarks. Figure adapted from [6].

1.3 Anatomy and physiology of the breast

The breast is composed of both adipose and glandular tissue supported by a fibrous connective tissue called Cooper's ligaments. The glandular tissue is organised into lobes, with each lobe consisting of numerous lobules. The lobules themselves are made up of alveoli, the glandular physiological units of the breast. While not active in non-pregnant females, these structures change during lactation and acquire secretory features, discharging milk into the lumen of ducts, which store and transport milk to the nipples during lactation. The ducts are lined by cells that can contract, opening the ducts and assisting in the flow of milk (figure 2)[7]. The breast is well supplied by both blood vessels and the lymphatic system, enabling the delivery of O_2 and nutrients, along with the removal of wastes (reviewed in [8]).

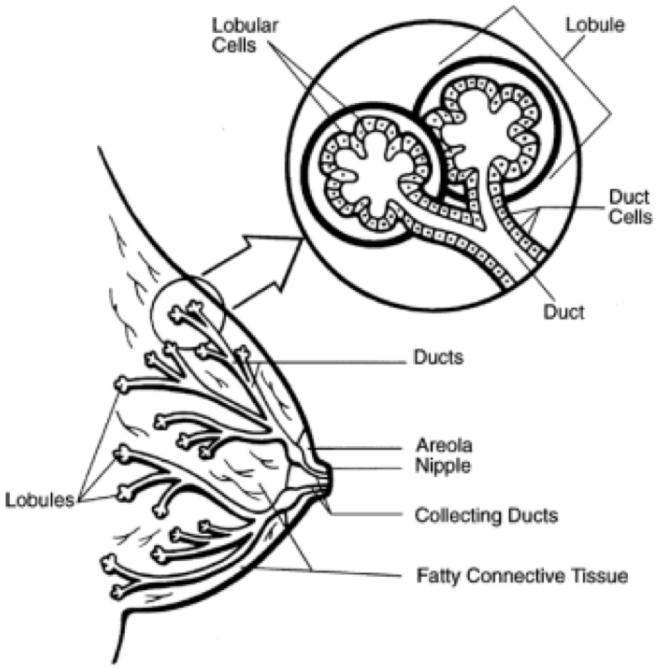

Figure 2: Anatomy of a normal mammary gland.

The connective tissue supports the glandular tissue of the breast, which is made up of lobes, with each lobe organised into lobules. The lobules themselves are made up of lobular cells, also known as alveoli. The milk secreted from the alveoli is transported to the nipple via the ducts. Figure adapted from [9].

1.4 Histological subtypes, staging and molecular classification

Cancer can be classified according to the tissue or cell type it is derived from. Carcinomas (arise from the epithelial cells of the body), sarcomas (develop from the connective tissue or muscles), leukaemias (cancer arising from blood cells), lymphomas and myelomas (begin in the immune system), and cancers of the central nervous system are the main types of cancer that occur. Breast cancer develops from cells present in the tissue of the breast, with the majority of breast tumours characterised as carcinomas [10].

1.4.1 Histological subtypes

Breast cancers can be classified based on the invasion of tumour cells into the surrounding tissue. Tumours that have not invaded are labelled as in situ breast cancers, while tumours that have invaded are categorised as invasive or infiltrating. In situ breast tumours are further divided into either ductal or lobular depending on

both the cytological features and growth patterns of the cells of the cancer [11]. Invasive carcinomas can also be sub-classified into different histological subtypes. The main invasive cancer subtypes include invasive ductal, invasive lobular, mixed (has features of both invasive ductal and invasive lobular), medullary, tubular, mucinous and papillary carcinomas [11]. The invasive ductal subtype is the most common of all of the invasive cancers that occur [12].

1.4.2 Staging, grading, NPI and prognosis

The stage of a cancer assesses the tumour size and whether it has spread. Breast cancers are staged according to the TNM (tumour, node, metastasis) system. Briefly, this system of staging is based on the size of the cancer, whether it has spread to lymph nodes, and whether the tumour has metastasised to other parts of the body [13]. In addition to breast cancer staging, the degree of differentiation of the cells of the tumour is also analysed in a process called grading. The grading system developed by Bloom and Richardson [14], and modified by Elston and Ellis [15], gives scores dependent on the proportion of glandular/tubule formation, the degree of nuclear polymorphism and the proportion of mitotic nuclei. Breast cancers with a low grade usually have a good clinical outcome, while breast cancers with a high grade score are more aggressive and have a greater likelihood of recurring after treatment (reviewed in [16]). The Nottingham Prognostic Index (NPI) is another method which has been developed to help predict patient outcome, and is based on a combination of the tumour size in cm (S), lymph-node stage (N) and grade (G) assembled into a prognostic index formula (NPI = [0.2 x S] + N + G) [17]. As the NPI numerical value rises, the prognosis worsens, with patients stratified into NPI groups ranging from ‘good’ to ‘very poor’ based on the overall value obtained [18]. Breast cancer staging, grading and the NPI are extremely helpful tools for both patients and doctors, enabling patients to understand their conditions better, while also helping doctors to plan treatments.

1.4.3 Molecular subtypes of breast cancer

The analysis of gene expression patterns of breast cancer has led to the identification of distinct molecular subtypes of cancer. These subtypes have been classified as: (i) normal breast like (genetic signature similar to adipose tissue), (ii) luminal A (ER^+ [oestrogen-receptor positive], PR^+ [progesterone-receptor positive], $HER2^-$ [human epidermal growth factor negative]), luminal B (ER^{low}, $HER2^{low}$, $PR^{+/-}$), (iii) $HER2^+$ (ER^-, PR^-, $HER2^+$), (iv) basal-like (ER^-, $HER2^-$, PR^-; with expression of cytokeratin 5 and 14), (v) triple negative (ER^-, PR^-, $HER2^-$) and apocrine (ER^-, PR^-, $HER2^{+/-}$) [19-21]. While both breast cancer staging and grading do have some prognostic value, they do not take into account these molecular markers that can predict response to the identified targeted therapies (see section 1.5.3).

The use of some of these molecular markers to further classify carcinomas has been accepted in breast cancer diagnosis. Analysis of PR, ER and HER2 levels through immunohistochemistry (IHC) is used to guide treatment, determining which patients are most likely to respond to therapies targeting these molecules [22, 23]. ER and PR expression staining is currently measured using the Allred score, which ranges from 0 to 8 depending on the proportion and intensity of staining [24]. A scoring system ranging from 0 to 3+ is used to measure HER2 over-expression, with 0 and 1+ values considered negative for over-expression, while a value of 2+ is considered weakly positive and 3+ is strongly positive [25]. The HER2 IHC staining results can be verified by identifying the number of HER2 gene copies through fluorescent in situ hybridization (FISH) [25].

While the traditional tissue-based testing mentioned above uses a single marker approach, other panel-based molecular tests have recently been developed to classify clinical cases of breast cancer into the different subtypes. The PAM-50 Breast Cancer Institute Classifier assay is one such assay that uses the mRNA levels of 50 genes to categorise breast cancer tissue into the different molecular subtypes, with the MammaPrint assay also including an option for molecular subtype testing [20].

1.5 Treatment of breast cancer

Treatment for breast cancer can be classified into either systemic or local therapy. Chemotherapy, hormone therapy and targeted therapies are examples of systemic therapies, which are given either by mouth or intravenously, and reach cancer cells throughout the body. Surgery and radiotherapy are examples of local therapy. Overall, there are 3 different types of breast cancer that clinicians treat: (i) non-invasive breast cancer; (ii) breast cancer that has invaded locally into the surrounding tissue or regional lymph nodes ; (iii) breast cancer that has metastasised to other parts of the body. The type of treatment, and the combinations of treatments, that the patient receives depends on which of the above cancers the patient is diagnosed with, in addition to the subtype, stage and molecular classification of the tumour (see section 1.4).

1.5.1 Chemotherapy

Chemotherapy is a form of treatment that involves the administration of cytotoxic drugs that damage targets such as DNA and tubulin in replicating cells, thereby leading to cell death. Paul Ehrlich, a German scientist whose interests included the use of drugs to treat cancer, coined the term chemotherapy in the early 1900s, defining it as the use of chemicals to treat infectious diseases (reviewed in [26]). The start of the modern era of chemotherapy can be traced to the 1940s, with the discovery that nitrogen mustard induced tumour regression in a patient with non-Hodgkin's lymphoma (reviewed in [26, 27]).

Many different chemotherapy drugs are available for the treatment of breast cancer, with different combinations used for breast cancer treatment. These are outlined in table 1. While these drugs target highly proliferative cancer cells in the tumour, there are also non-malignant cells in the body with high proliferation rates that are similarly affected. This can lead to many adverse side effects, including nausea and vomiting, weight loss, hair loss, fatigue, and a compromised immune system [28].

As a result of these wide-ranging side effects, treatments are usually given in cycles, with drugs given for periods ranging between 1 and 5 days, followed by a break of up to 4 weeks. Drug treatment, followed by a break, makes up one cycle. Up to 8 treatment cycles may be given to patients suffering from breast cancer, depending on the drugs used and the stage of the cancer [29]. In addition to variations in the number of cycles received, the timing of chemotherapy treatment can also differ between patients. Treatment given before surgery, with the purpose of shrinking the tumour before the surgical procedure, thus reducing the extent of surgery required, is known as neoadjuvant chemotherapy. This approach is used for the treatment of primary non-operable breast cancer, locally advanced operable breast cancer, and inflammatory breast cancer [30]. Treatment provided after surgery, in an attempt to prevent metastasis or cancer recurrence, is termed adjuvant chemotherapy, and has been shown to improve overall patient survival by approximately 10% [31].

Main drugs used in chemotherapy
Cyclophosphamide
Epirubicin
Fluorouracil
Methotrexate
Mitomycin
Mitozantrone
Doxorubicin
Docetaxel
Gemcitabine

Common combinations
CMF→ cyclophosphamide, methotrexate, fluorouracil
FEC→ fluorouracil, epirubicin, cyclophosphamide
FEC-T→ fluorouracil, epirubicin, cyclophosphamide, taxotere
E-CMF→ epirubicin followed by CMF
AC→ doxorubicin, cyclophosphamide
EC→ epirubicin cyclophosphamide
MMM→ methotrexate, mitozantrone, mitomycin
MM→ methotrexate, mitozantrone

Table 1: Chemotherapy drugs and combinations.

1.5.2 Hormone therapy

Oestrogen and progesterone are hormones that control the growth and activity of normal cells, but which can also affect cancer cells if they express the appropriate receptors. These hormones are synthesised by the ovaries in pre-menopausal women [32, 33], with oestrogen also produced in the body fat in post-menopausal women [32]. Around 80% of breast cancers diagnosed are either oestrogen receptor (ER) or progesterone receptor (PR) positive [34], with the presence of ER or PR frequently driving tumour growth and progression [35, 36]. Hormone therapy removes or blocks the actions of hormones on these receptors.

Different types of hormone treatment are used to treat breast cancer depending on whether or not the patient has gone through menopause. Selective oestrogen receptor modulators (SERMs), such as tamoxifen, are an example of one form of hormone therapy used mostly in pre-menopausal women [37]. SERMs work by blocking the ER on breast cancer cells, thereby removing the growth-promoting effects of oestrogen on the tumour. Fulvestrant (Faslodex) is an example of a selective oestrogen receptor down regulator (SERD) that not only inhibits ER, but also accelerates ER degradation [38].

Suppressing the production of oestrogen from the ovary, and thereby lowering the amount of oestrogen available to the tumour, is another form of hormone therapy used to treat pre-menopausal patients. Blocking the production of luteinising hormone, which usually acts to stimulate the production of oestrogen from the ovaries, is one form of treatment used. Goserelin (Zoladex) is an example of a luteinising hormone blocker employed in the clinic [39]. Surgery to remove the ovaries themselves is another method used to reduce the production of oestrogen in the body [39].

Oestrogen can also be synthesised from androgens in the tissues of the body in post-menopausal women, a reaction catalysed by aromatase [40]. Letrozole (Femara), anastrozole (Arimidex) and exemestane (Aromasin) are examples of aromatase inhibitors used in these patients that work either through competing with substrates

binding to aromatase, or by mimicking the substrates of aromatase and inactivating the enzyme, thereby reducing the amount of oestrogen produced [40].

As in chemotherapy, hormone therapy can be given in a neoadjuvant or an adjuvant setting. Hormone therapy can also be employed as a primary treatment in those patients with ER positive breast cancer who are unsuitable for general anaesthetic and cannot undergo surgery [41]. Hormone therapy used in this context is known as primary endocrine therapy.

1.5.3 Targeted therapy

Targeted therapies have been developed to disrupt molecules and pathways that are over-expressed or deregulated in cancers. However, even though the agents used in targeted therapy are directed specifically at cancer cells, adverse side effects can still occur with these treatments (reviewed in [42]).

HER2 is an example of a molecule, over-expressed in around 20% of breast cancers [43], which can be targeted in breast cancer patients. Activation of the HER2 receptor leads to the stimulation of a number of signalling pathways associated with cell growth and proliferation [44]. Trastuzumab (Herceptin), an antibody targeting HER2, is a targeted therapy currently used in the clinic. It functions by binding to HER2 and blocking the cellular signalling pathways initiated by the receptor, thereby inhibiting the growth and survival of HER2-dependant tumours [45]. Trastuzumab can be given in neoadjuvant, adjuvant and metastatic settings, and has been shown to improve the overall survival rates of breast cancer patients with over-expressed levels of this receptor [46].

Pertuzumab is another monoclonal antibody used as a targeted therapy that operates by binding the HER2 receptor at a different site from trastuzumab, inhibiting ligand-dependent signalling between HER2 and HER3. These 2 monoclonal antibodies have complementary mechanisms of action as a result of their different binding sites (reviewed in [47]), and clinical trials have shown the benefits and tolerability of combined treatment [48, 49].

Lapatinib, a dual tyrosine kinase inhibitor of HER2 and epidermal growth factor receptor (EGFR or HER1), is another example of targeted therapy in clinical use [50]. Both Trastuzumab and lapatinib have been combined with chemotherapy [51, 52] and hormone therapy [51, 53], leading to improved patient outcomes compared to single agent treatment. Further studies have also shown the benefits of combining trastuzumab and lapatinib together in breast cancer treatment [54, 55].

Other forms of targeted therapy involving trastuzumab include trastuzumab emtansine (Kadcyla), which consists of a monoclonal antibody combined to a chemotherapy drug. With this treatment, trastuzumab directs the conjugate to the HER2 over-expressing breast cancer cells, inhibiting HER2 signalling, while the emtansine causes cancer cell death through impeding microtubule assembly [56]. Another instance of a targeted therapy in clinical use is everolimus. This drug inhibits the mammalian target of rapamycin (mTOR) pathway, which is an intracellular signalling pathway involved in the regulation of the cell cycle, thereby inhibiting cancer cell growth [57].

1.5.4 Surgery

Breast cancer treatment generally involves the surgical removal of tumour tissue. There are various types of surgery [58], with the surgical procedure carried out dependent on both the size of the tumour and whether or not it has metastasised. Lumpectomies are carried out on small tumours, and involve the removal of only the breast lump and a small area of the surrounding normal tissue, which is then checked for the presence of any cancer cells. Quadrantectomies involve the removal of about a quarter of the breast tissue, with further surgery required if cancer cells are discovered at the edges of the removed tissue. These procedures are often termed breast-conserving surgery [58].

Women who have larger tumours, who have a tumour present in the middle of the breast, or who have cancerous tissue present in more than one area of the breast, require more extensive surgery. These procedures are termed mastectomies, and

involve the removal of the central part of the breast close to the nipple. There are a variety of mastectomy procedures carried out [58]. A simple mastectomy involves the removal of the entire breast, leaving the lymph nodes and tissue below the breast. A modified radical mastectomy is the same as a simple mastectomy, with the underarm lymph nodes removed as well. A radical mastectomy is the most extensive operation, in which the entire breast, lymph nodes and chest wall muscles under the breast are removed.

For many years radical mastectomies were the main surgery implemented for breast cancer of any size. However, randomised studies showed that removal of the whole breast was not always necessary, as patients who underwent breast-conserving surgery followed by radiotherapy had a similar survival rate to patients who had mastectomies [59-61]. Breast reconstruction surgery is usually carried out following the surgical removal of cancer tissue. This procedure can be performed at the same time as the breast cancer surgery (immediate reconstruction), or at a later date (delayed reconstruction) [58].

1.5.5 Radiotherapy

Radiotherapy, first used in the treatment of cancer in the 1890s (reviewed in [62]), still plays a major role in the management of breast cancer today, despite the multitude of advances made in both systemic therapy and surgery since that time. Radiotherapy involves the use of ionizing radiation to kill cancer cells. Brachytherapy is one form of radiotherapy, comprising the placing of radioactive material beside breast tumours inside the body [63]; however, external radiotherapy is another form of radiotherapy that is much more commonly performed.

Radiotherapy is traditionally performed post-surgery, after breast conserving surgery and sometimes after mastectomies, and functions to eradicate any residual tumour cells left behind post-surgery [64]. The considerable benefit of adjuvant radiotherapy to patients suffering from breast cancer is well recognised, with studies showing a significant reduction in breast cancer recurrence and mortality in patients that have received radiotherapy [65-68]. In addition to treatment after surgery, radiotherapy

also has a role in the management of advanced breast cancer subsequent to systemic therapy, when inflammatory changes preclude surgical intervention [64]. The effect of neo-adjuvant radiotherapy, in combination with chemotherapy, has recently been assessed in phase 1 clinical trials [69].

Adjuvant radiotherapy is broken up into fractions, which involves giving patients repeated smaller doses of radiation within a course of treatment. Radiation treatment can last from 3 to 5 weeks, with fractions given once a day every weekday [70]. The aim of these treatments is to distribute an effective dose of radiation to the tumour tissue whilst minimising damage to the surrounding healthy tissue. The favourable effects of adjuvant radiotherapy on long-term survival can be counterbalanced by an increase in the percentage of non-breast cancer related deaths, including vascular mortality [68]. A linear relationship has been found between the dose of radiation the heart receives and the rate of major coronary events [71]. There have been numerous studies investigating mechanisms to reduce the dose the heart receives during breast cancer radiotherapy. Strategies such as prone patient positioning and patient breathing techniques have been shown to be effective in reducing the irradiation dose received by the heart [72]. Recent developments in the field of radiotherapy involve the application of intensity-modulated radiotherapy (IMRT) and image guided radiotherapy (IGRT), which have led to the improved accuracy in radiation treatment [72, 73]. Intra-operative radiotherapy (IORT) is another method of radiotherapy that has been developed [74] that is currently undergoing clinical trials (HTA - 10/104/07). Instead of giving a course of irradiation treatment post-surgery, this technique sees patients receiving a single dose during surgery, with the aim of avoiding the irradiation of normal tissues surrounding the tumour.

1.6 Physiology of breast cancers

Blood capillaries are present in close proximity to metabolically active tissues within the body, enabling the effective exchange of nutrients and metabolites between the blood and cells of the tissue [75]. The breast is well vascularised [8], ensuring that normal cells within the breast are provided with sufficient O_2 and nutrients, enabling them to perform their functions. Tumour cells also require O_2 and nutrients to

survive, along with the ability to remove metabolic wastes. As tumours grow and develop, some cells within the tumour can be pushed further and further away from the blood vessels, preventing their access to metabolites and O_2 [76, 77]. The ability of tumour cells to induce the formation of new blood vessels from existing blood vessels, through the process known as angiogenesis, is one of the hallmarks of cancer fundamental to tumour biology [6].

While angiogenesis only occurs in particular physiological conditions in healthy adults, it is much more persistent within tumours [78]. However, studies show that these newly made blood vessels within tumours have many structural abnormalities compared to the normal vasculature (figure 3) [79, 80]. These defects lead to blood flow that can vary considerably between differing breast tumours [79]. The characteristics of newly formed blood vessels lead to areas within tumours where the O_2 concentrations are low. Cells within these areas are described as being hypoxic.

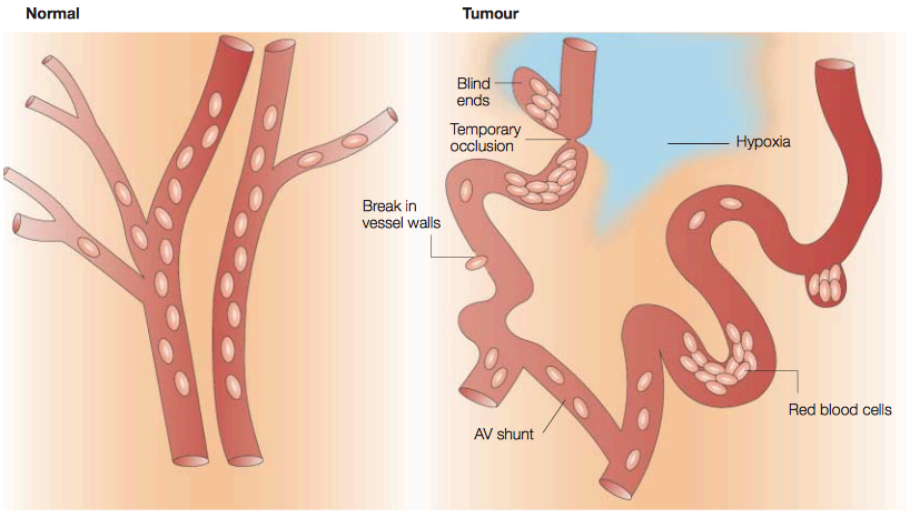

Figure 3: Differences in the vasculature of normal and cancerous tissue.

The blood vessels of normal tissue are well-organised and lead to the oxygenation of all areas of the tissue. Tumour vasculature, however, have incomplete vessel walls along with sluggish and irregular blood flow, leading to areas of tissue that are not adequately supplied with oxygen. Image adapted from [81].

1.7 Hypoxia

Hypoxia is defined as a state of reduced O_2 availability. The O_2 concentration in air is 21%, however, most tissues in mammals function in O_2 concentrations ranging from 2-9% O_2. Tissues with O_2 concentrations $\leq$ 2% O_2 are usually defined as hypoxic, with tissues in $\leq$ 0.02% O_2 conditions defined as severely hypoxic [82].

1.7.1 Mechanisms leading to hypoxia

There are two main mechanisms that lead to the formation of hypoxia in tumours. Gray and Thomlinson discerned the first in 1955 (figure 4). They identified a connection between the necrotic areas that formed in tumour tissues and distance from blood vessels, with this distance being consistent with the diffusion properties of O_2 [77]. This type of hypoxia is known as diffusion limited hypoxia, or steady state hypoxia. In 1968 a study was published which provided an example of diffusion limited hypoxia that is more typical in solid tumours, with tumour tissue observed surrounding blood vessels, and necrosis evident in areas of the tumour further away from the blood vessels [76]. Diffusion limited hypoxia occurs as a result of cells closest to the blood vessel consuming much of the available O_2. The O_2 concentration decreases as distance from the blood vessel increases, leading to the development of hypoxic cells [83]. The distance from the blood vessel at which this form of hypoxia develops is variable, as the diffusion distance of O_2 depends on how much of the O_2 is used by the cells closest to the blood vessel, in addition to how much O_2 is being carried in the blood [84]. This type of hypoxia is also known as chronic hypoxia, as cells can be exposed to low levels of O_2 through this mechanism for a considerable time [84].

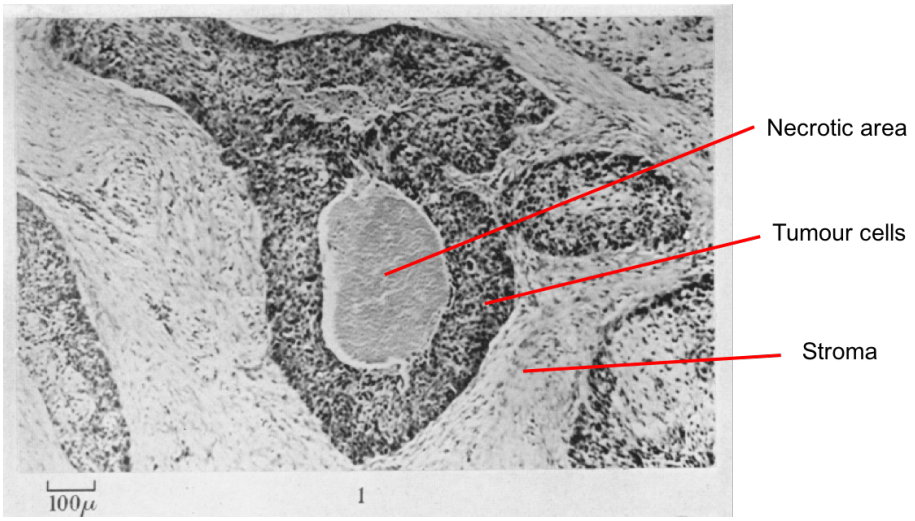

Figure 4: Visualisation of hypoxia in tumours.

Figure adapted from a paper by Gray and Thomlinson [77], which was the first to visualise the presence of hypoxia in tumours. Their paper describes the presence of tumour regions enclosed by vascular stroma, with necrotic areas present in the centre of many of the pieces of tumour tissue. The size of the region of viable tumour cells between the stromal tissue and necrotic tumour tissue was in a similar range to their calculated diffusion distance of O_2. They therefore suggested that O_2 was being consumed by the tumour cells as it diffused in from the stroma, leading to the formation of necrotic areas in the centre of the tumour, with hypoxic cancer cells adjacent to these necrotic areas.

For many years it was thought that diffusion-limited hypoxia was the only form of hypoxia to exist in tumours. However, late in the 1970s it was suggested that hypoxia could develop in tumours through a differing mechanism termed perfusion-limited hypoxia, or cycling hypoxia, which can lead to the re-oxygenation of previously hypoxic cancer cells [85]. The development of hypoxia through this process was confirmed in the 1980s [86]. This form of hypoxia arises from disturbances in the blood flow through the tumour vasculature, thereby preventing the delivery of O_2 from red blood cells. Blockage of the vasculature by circulating tumour cells, or the collapse of abnormal blood vessels, are possible causes for the cessation of blood flow (reviewed in [87]). This type of hypoxia is also known as acute hypoxia, as it can be transient in nature.

This classification of hypoxia into two groups, which many refer to as acute (perfusion limited) and chronic (diffusion limited) hypoxia, is perhaps an oversimplification. These two groups can be further broken down into subgroups.

Acute hypoxia can been subdivided into ischemic hypoxia (no blood flow at all due to complete blockage, leading to no O_2 delivery) and hypoxemic hypoxia (still a small amount of blood flow with abnormally low levels of O_2). Chronic hypoxia can be further divided into diffusion-limited hypoxia, hypoxemic hypoxia (reduced O_2 content in the blood for long periods of time), and IHT (interstitial hypertension)-induced hypoxia (lack of flow due to compromised perfusion) [84].

More recently, a third form of tumour hypoxia, termed macroscopic regional hypoxia, has also been identified [88, 89]. In tumours, blood vessels and their branches can continue for many millimetres through the tumour tissue. At the arterial end of the blood vessel there is the highest concentration of O_2. However, towards the venous end the concentration of O_2 decreases as the cells present nearer the arterial end consume O_2. This produces a gradient in O_2 concentration within the blood vessel, and can lead to cancer cells at the distal parts of the vessel being hypoxic, despite being in close proximity to the vasculature.

1.7.2 Hypoxic levels within normal and breast cancer tissue

Because of a lack of suitable methods for the measurement of O_2 tensions within human tissues, it was challenging for clinicians and scientists to assess tumour hypoxia within patients for many years after its initial observation in the 1950s [90]. While there are a number of methods in development for analysing the oxygenation levels of tissues in the body (reviewed in [91, 92]), a non-invasive technique that accurately measures O_2 levels within tissues still does not exist. The Eppendorf pO_2 histograph is one technique that has been used to analyse the oxygenation of tissues in the human body [93-96]. This method consists of using an O_2 electrode that is placed into the tissue and provides histograms of O_2 partial pressures. Studies carried out assessing the O_2 concentrations in both normal and cancerous breast tissue showed that the O_2 concentration of breast tumours was distinctly lower than that of normal tissue [93]. The median O_2 concentration measured in normal breast tissue was found to be around 8.5% O_2, while the median O_2 concentration in locally advanced breast cancer tissue was 3.9% O_2. Severe hypoxia was prevalent in many of the breast tumours analysed, with nearly 60% of cancers having areas of tissue

with O_2 tensions of under 0.33% O_2. This contrasted greatly with normal breast tissues, in which O_2 concentrations below 1.6% O_2 were not found [93]. Another study assessing the oxygenation status of breast cancers using the same method also showed the extensive presence of hypoxia in breast tumour tissue [95].

1.7.3 Hypoxia and treatment resistance

The abnormal structure of the tumour blood supply, leading to hypoxia, has many consequences for cancer and its treatment. In fact, hypoxia was one of the first modifiers of treatment outcome recognised for cancer, and remains one of the most important influences of responsiveness today [97]. The efficacy of systemic therapy is adversely affected, as the irregular vasculature hinders the delivery of blood-borne drugs to many of the cancer cells in the tumour. This leads to a heterogeneous distribution of drugs within cancers, compromising chemotherapy, hormone therapy and targeted therapy (reviewed in [98]). The hypoxia created by the inefficient delivery of O_2 also has an effect on systemic therapy, as the hypoxic conditions lead to a decrease in the proliferation rate of cancer cells [99-101]. Since many of the cytotoxic agents used in cancer treatment function by targeting rapidly dividing cells, the effects of these cytotoxic agents can also be reduced [100].

From 1909 onwards, many different studies indicated that O_2 levels could influence the radio-sensitivity of cells (reviewed in [82]). Research conducted in the early 1950s by Gray et al confirmed this effect, when they demonstrated that cells which were anoxic at the time of irradiation were more resistant to treatment than cells which were well oxygenated [102]. At a given dose of irradiation, hypoxic cancer cells tolerate a dose 2-3 times higher than aerobic cells, recognised as the O_2 enhancement effect. Radiotherapy can lead to the generation of free radicles within the cell that may react with DNA. The presence of even low concentrations of O_2 can ‘fix’ (make permanent) any radiation-induced DNA damage before this damage can be repaired by radical scavengers in the cell. This is known as the oxygen fixation hypothesis (reviewed in [82] and [103]). This process leads to a molecular change in the DNA that is not repairable, and can lead to reproductive cell death if the cell tries to divide [104].

1.8 Cancer cell metabolism and HIF

The reprogramming of energy metabolism to support the growth and proliferation of cancer cells (reviewed in [105, 106]) is recognised as an attribute that is extremely important in the development and progression of cancer. This characteristic is now considered an emerging hallmark of cancer [6].

1.8.1 Glycolysis, the citric acid cycle, and oxidative phosphorylation

The breakdown of glucose is the dominant form of energy production in most animal cells. There are 2 main parts in the production of energy from glucose. Part 1 (reviewed in [107, 108]) occurs in the cytosol of the cells, and involves the breakdown of glucose to pyruvate, which is accompanied by the production of small amounts of NADH (nicotinamide adenine dinucleotide, reduced) and ATP (adenosine triphosphate) (figure 5A). This process is known as glycolysis, and does not require O_2. Part 2 (reviewed in [107, 109, 110]) comprises the citric acid cycle and oxidative phosphorylation (figure 5B). The citric acid cycle involves converting pyruvate into acetyl-CoA, followed by the consumption of acetyl-CoA molecules, leading to the production of NADH, $FADH_2$ (flavin adenine dinucleotide, reduced) and ATP. In a process termed oxidative phosphorylation (OXPHOS), the NADH and $FADH_2$ produced in the cell pass their electrons down the electron transport chain, leading to the generation of large amounts of ATP. Part 2 occurs in the mitochondria and requires O_2. While most aerobic cells in the body derive their energy from glycolysis followed by OXPHOS, low O_2 conditions lead to a reduction in mitochondrial respiration within cells [111]. One of the ways through which hypoxic cancer cells adapt their metabolism to low O_2 conditions is through the hypoxia inducible factors (HIFs).

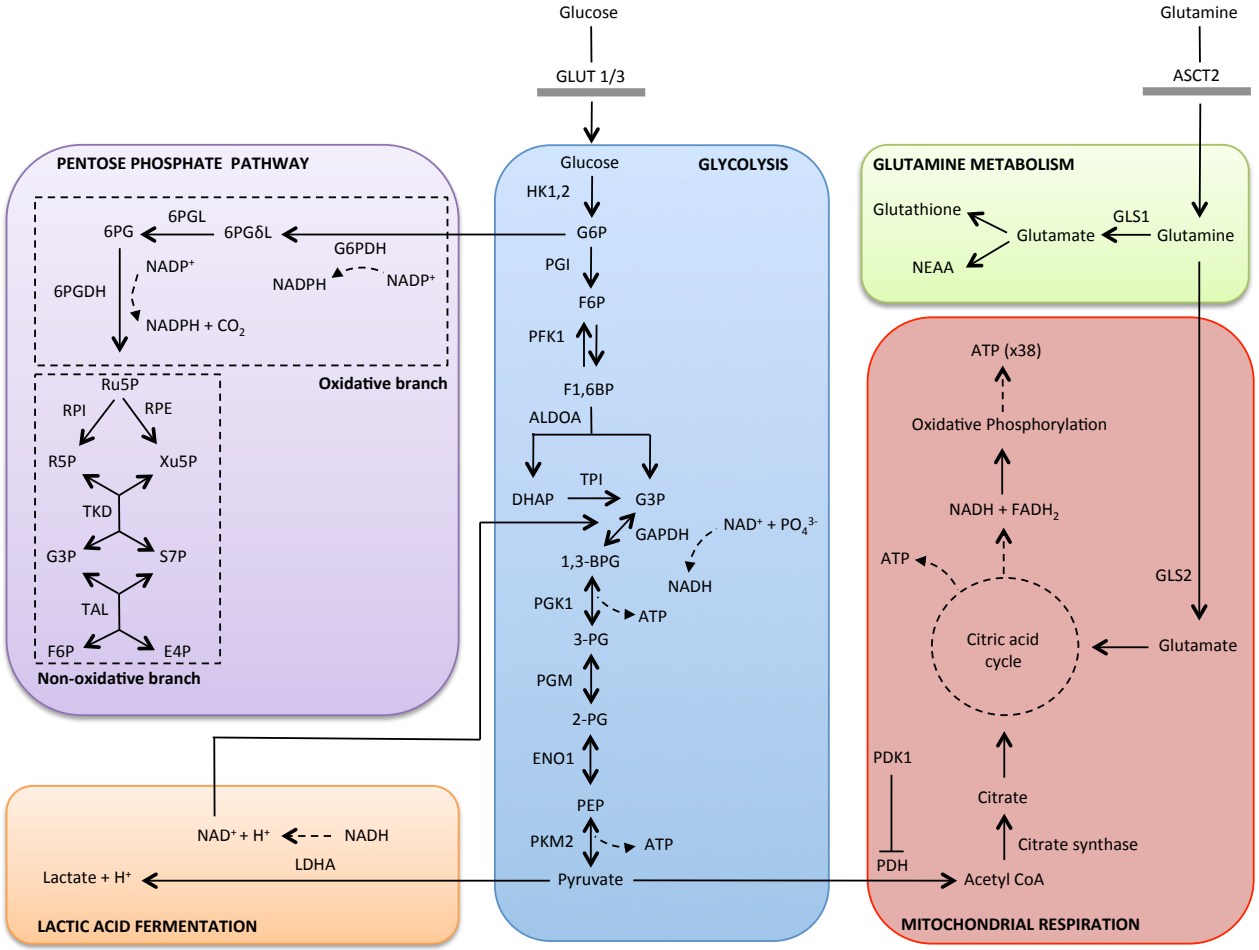

Figure 5: Simplified diagram of cellular metabolism.

See next page for description

(A) Glycolysis. *Glycolysis is a sequence of reactions that can be thought of as comprising three main stages. (i) The conversion of glucose into fructose 1,6-bisphosphate, which traps glucose in the cell. (ii) Cleavage of the fructose 1,6-bisphosphate into two three-carbon fragments that are inter-convertible. (iii) The transfer of energy to NADH and ATP when the three-carbon fragments are oxidized to pyruvate. Glycolysis does not require O_2 to function. Despite the production of some ATP during glycolysis, pyruvate still contains most of the energy that was present in glucose.* **(B) Mitochondrial respiration**. *Vast amounts of energy can be produced through the citric acid cycle and oxidative phosphorylation in the presence of O_2. Firstly, pyruvate is shuttled into the mitochondrion of the cells and is converted into an acetyl group, which is attached to coenzyme A, leading to the formation of acetyl CoA. Acetyl CoA combines with another molecule to form citrate. Citrate enters a sequence of reactions called the citric acid cycle, which produces ATP and CO_2 along with large amounts of the electron carriers NADH and $FADH_2$. The electrons from NADH and $FADH_2$ are subsequently passed along the electron transport chain present in the mitochondria, leading to the production of large amounts of ATP and the consumption of O_2 through oxidative phosphorylation.* **(C) Lactic acid fermentation.** *Hypoxic cancer cells, along with many normoxic cancer cells, rely on glycolysis for the production of energy. However, an energy-producing pathway that ceases at pyruvate is unable to continue for long as NAD^+ is consumed in this pathway, and there is only a limited amount of NAD^+ present in a cell. Lactic acid fermentation, a process in which pyruvate is converted into lactic acid, leads to the regeneration of NAD^+, thus enabling the continuation of glycolysis.* **(D) Pentose phosphate pathway (PPP).** *The PPP is mainly an anabolic pathway that consists of 2 parts; the oxidative branch and the non-oxidative branch. The oxidative branch, using glucose-6-phosphate (G6P) as the substrate, consists of 3 reactions and leads to the generation of NADPH. The non-oxidative branch of the PPP primarily functions to generate ribose-5-phosphate (R5P). Other reactions of the non-oxidative branch convert 5-carbon sugars into 6 (fructose 6-phosphate) and 3 (glyceraldehyde-3-phosphate) carbon sugars, which can be used by the glycolytic pathway.* **(E) Glutamine metabolism.** *ASCT2 mediates the uptake of glutamine into the cell. The imported glutamine is then converted into glutamate either in the cytosol by GLS1, or by GLS2 in the mitochondria. The glutamate present in the cytosol is a source of non-essential amino acids (NEAAs), and is also a precursor of glutathione. The glutamate present in the mitochondria can enter the citric acid cycle.*

GLUT glucose transporter; HK hexokinase; G6P glucose-6-phosphate; PGI phosphoglucose isomerase; F6P fructose- 6-phosphate; PFK-1 phosphofructokinase 1; F1,6BP fructose-1,6-bisphosphate; ALDOA aldolase A; DHAP dihydroxyacetone phosphate; G3P glyceraldehyde 3-phosphate; TPI triose-phosphate isomerase; GAPDH glyceraldehyde 3-phosphate dehydrogenase; 1,3-BPG 1,3-bis-phosphoglycerate; PGK1 phosphoglycerate kinase 1; 3-PG 3-phosphoglycerate; PGM phosphoglycerate mutase; 2-PG 2-phosphoglycerate; ENO1 enolase 1; PEP phosphoenolpyruvate; PKM2 pyruvate kinase M2; ATP adenosine-5'-triphosphate; PDH pyruvate dehydrogenase; PDK1 pyruvate dehydrogenase kinase; LDHA lactate dehydrogenase A; NADH nicotinamide adenine dinucleotide; PO43- phosphate; G6PDH glucose 6-phosphate dehydrogenase; 6PGδL; 6-phosphogluconolactone; 6PGL 6-phosphogluconolactonase; 6PG 6-phosphogluconate; NADPH nicotinamide adenine dinucleotide phosphate; CO_2 carbon dioxide; 6PGDH 6-phosphogluconate dehydrogenase; Ru5P ribulose 5-phosphate; RPI ribose 5-phosphate isomerase; RPE ribulose 5-phosphate epimerase; R5P ribose 5-phosphate ; Xu5P xylulose 5-phosphate; TKT transketolase; S7P sedoheptulose 7-phosphate; TAL transaldolase ; E4P erythrose 4-phosphate; ASCT2 alanine, serine, cysteine-preferring transporter 2; GLS1 glutaminase 1; GLS2 glutaminase 2; NEAA non-essential amino acid

1.8.2 HIF

Activation of the hypoxia inducible factor (HIF) pathway is one of the main mechanisms that enable hypoxic cancer cells to survive in their low O_2 environment. HIFs are O_2-responsive transcription factors, and are master regulators of genes involved in the control of many different processes, including metabolism, proliferation, angiogenesis and migration (reviewed in [112]).

HIFs consist of both an α and a β subunit. There are 3 different isoforms of the alpha subunit (HIF-1α, HIF-2α and HIF-3α) and only 1 beta subunit (HIF-1β) (reviewed in [82]). In contrast to HIF-1β, the HIFα proteins are sensitive to changes in the levels of O_2 (figure 6). HIFα protein stability is controlled through a region called the O_2-dependent degradation domain (ODDD) [113]. Under high O_2 concentrations, HIF-specific prolyl hydroxylase domain (PHDs) proteins, which require O_2 for activity, hydroxylate the proline residues present within the ODDD [114-116]. Hydroxylation within the ODDD of the α subunit leads to its recognition by the von Hippel-Lindeau (VHL) tumour suppressor protein, which catalyses the transfer of ubiquitin onto the HIFα protein [113, 117, 118]. HIFα hydroxylation, and the subsequent poly-ubiquitination, leads to the proteasomal degradation of the protein [113, 119]. PHD proteins are inhibited in lower O_2 conditions [114], leading to the accumulation of the HIFα subunits and translocation to the nucleus. When present in the nucleus, the HIFα subunit dimerizes with HIF-1β [120], and the HIFα-HIFβ heterodimer binds to hypoxic response elements (HREs) present in target genes [121].

HIF-1α and HIF-2α, the 2 principle mediators of the cellular response to hypoxia, have distinct roles within cells. This is reflected in their stabilisation at different O_2 tensions, their differing temporal response, and their selectivity with regard to transcriptional targets (reviewed in [122]). In contrast to the HIF-1α and HIF-2α subunits, HIF-3α is thought to have a dominant negative function, reducing the gene expression induced by the other subunits [123].

In addition to the ODDD, which regulates HIFα stability, HIFα subunits contain two transactivation domains termed N-TAD (N-terminal transactivation domain) and C-

TAD (C-terminal transactivation domain) [124, 125], which are areas where co-regulatory proteins can bind and control gene expression [126-128]. While the PHD proteins control the levels of HIFα in differing O_2 conditions, the extent of expression through stabilised HIF is controlled by another protein, factor inhibiting HIF-1 (FIH-1). FIH-1 is an additional O_2 sensor present in cells that has been described as a negative regulator of HIF transcriptional response [129, 130]. While the PHD proteins are inactivated in low O_2 conditions, FIH-1 has been shown to retain its activity in hypoxia [131, 132], catalysing the hydroxylation of an asparaginyl residue in the C-TAD of HIFα. This hydroxylation impairs the interaction between C-TAD and the transcriptional co-activator p300/CREB binding protein (CBP) [130, 133], thus impairing the expression of C-TAD sensitive genes (figure 6).

Since HIF-1α was originally recognized due to its response to hypoxic conditions, it has become apparent that HIF signalling can be influenced by O_2-independent factors. Increased HIF signalling can be induced in normoxic conditions by various genetic alterations that lead to the activation of oncogenes (ERBB2 and SRC) and the inactivation of tumour suppressor genes (VHL, PTEN and CDKN2A)[134, 135]. Most of these genetic alterations can lead to HIF signalling in aerobic conditions through either increasing the synthesis or decreasing the ubiquitination of HIF-1α. Other O_2-independent factors have also been linked to HIF-1α signalling in normoxic conditions, including signalling through growth factors [136, 137] and lactate or pyruvate accumulation [138, 139].

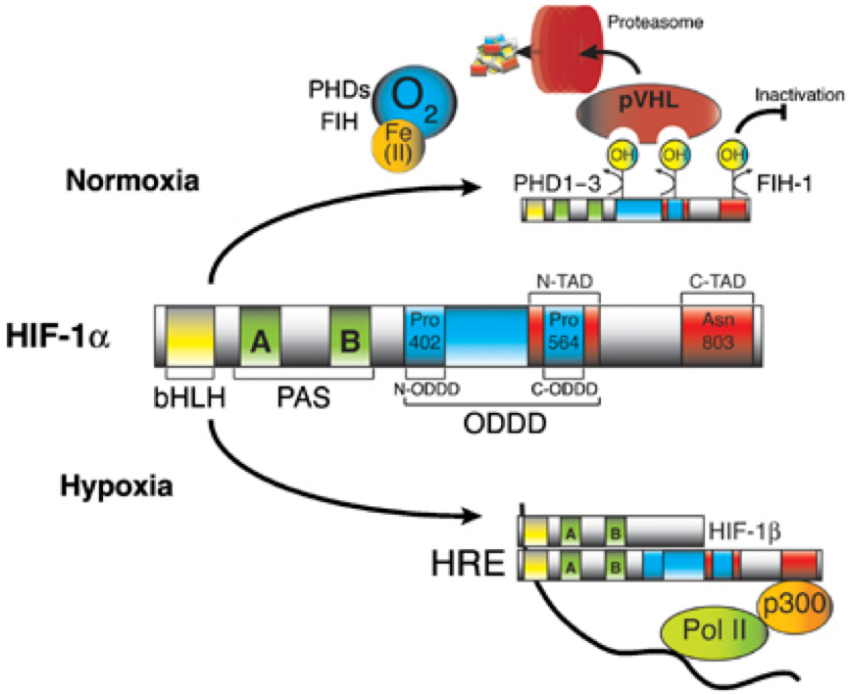

Figure 6: Regulation of HIF signalling.

PHDs (prolyl hydroxylase domain) are Fe^{2+}-dependent proteins that control the levels of HIF-1α in the cell. In oxygenated conditions, these proteins hydroxylate the proline residues within the ODDD (oxygen-dependent degradation domain) of HIF-1α. This leads to the binding of the VHL (von Hippel-Lindau) protein to HIF-1α, resulting in the ubiquitination and subsequent proteasomal degradation of HIF-1α. When O_2 levels drop, the PHDs are inactivated, leading to the accumulation of HIF-1α in the cell. The stabilised HIF-1α translocates to the nucleus and dimerises with HIF-1β, which is facilitated by the bHLH (basic helix loop helix) and the PAS (Per/ARNT/Sim) domains present in both proteins. The heterodimer then binds to hypoxic response elements (HREs) within the regulatory regions of target genes, leading to the expression of genes involved in hypoxic response through RNA polymerase II. Factor inhibiting HIF-1 (FIH-1) is another oxygen sensor present in the cells that controls the extent of signalling through stabilised HIF-1α. FIH-1 hydroxylates the asparaginyl residue within the C-terminal transactivation domain (C-TAD) of HIF-1α, preventing the binding of the transcriptional co-activator p300/CREB binding protein (CBP) to HIF-1α, leading to only partial HIF signalling through stabilised HIF-1α. More severe hypoxic conditions inhibit FIH-1, enabling the binding of co-activators to HIF-1α, leading to full HIF signalling. Image adapted from [140].

1.8.3 HIF and glycolysis

Oxygen is vital for cell survival as it is necessary for the production of large amounts of energy through OXPHOS (reviewed in [107, 109]). However, as already mentioned (see section 1.8.1), hypoxic cancer cells are unable to rely on this process for energy production due to their low O_2 levels. The HIF pathway helps cancer cells survive in reduced O_2 concentrations by causing two alterations in the metabolism of hypoxic cancer cells: through the stimulation of glycolysis and the inhibition of

OXPHOS.

Although HIF-1α and HIF-2α control the expression of overlapping sets of genes, the effects of HIF-1α on metabolism have been more thoroughly investigated. HIF-1α increases the expression of many of the enzymes involved in the glycolytic pathway, including hexokinase 2 (HK2), aldolase A (ALDA), phosphoglycerate kinase 1 (PGK1), enolase 1 (ENO1), and pyruvate kinase M (PKM) [141-143]. To ensure that there is sufficient glucose to support the amplified rate of glycolysis, HIF-1α also induces the expression of the plasma membrane glucose transporters GLUT1 and GLUT3 [144-146].

In addition to instigating increased rates of glycolysis, HIF-1α also affects mitochondrial respiration through blocking the citric acid cycle and oxidative phosphorylation (reviewed in [147]). Under sufficient O_2 conditions, the pyruvate derived from glucose is usually converted into acetyl-CoA by pyruvate dehydrogenase (PDH), which then enters the citric acid cycle [110]. HIF-1α inhibits mitochondrial respiration through inducing the expression of pyruvate dehydrogenase kinase 1 (PDK1) [148-151], which inactivates PDH (reviewed in [152, 153]), thus depriving the citric acid cycle of citrate. HIF-1α also reduces mitochondrial respiration through the down-regulation, inhibition and degradation of proteins involved in oxidative phosphorylation, such as mitochondrial complex 1 [154] and cytochrome C oxidase subunit 4 (COX4) [155]. In addition to blocking the citric acid cycle and OXPHOS, HIF-1α also leads to reduced mitochondrial biogenesis [156] and an induction of mitochondrial degradation [157]. Overall, these changes help hypoxic cancer cells adapt their metabolism to the low O_2 environment through the induction of a highly glycolytic phenotype.

1.8.4 The Warburg Effect

While hypoxic cancer cells adapt to their low O_2 environment by inducing glycolysis, there are also cancer cells in the body present in normoxic conditions that also exhibit a highly glycolytic phenotype. This observation was first made in the 1920s by Otto Warburg [158], and was later termed the Warburg Effect [159].

Warburg originally suggested that an 'irreversible injuring of respiration' was the cause of the aerobic glycolysis [160], with normoxic cancer cells increasing their rate of glycolysis to deal with the lack of ATP generation through dysfunctional mitochondrial [160]. However, research performed in the decades following Warburg's paper indicated that defects in the mitochondria were a rare occurrence, and therefore could not explain the aerobic glycolysis seen in cancer cells [161]. More recent work showing that cancer cells maintain the ability to produce ATP via OXPHOS indicate that the mitochondria within cancer cells are not dysfunctional [162, 163].

The causes of the Warburg effect are still unknown today, nearly a century after it was first observed. One suggestion put forward involves hypoxia, with some proposing that the low O_2 conditions present in tumours leads to cancer cells adapting their metabolism through increasing their rate of glycolysis. This adaptation enables these cancer cells to survive in the hypoxic environment, and leads to a dependence on glycolysis in these cells that persists even in aerobic conditions [164]. Conversely, studies have shown that the induction of aerobic glycolysis is an early event in cancer development, emerging from oncogenic mutations in the early stages of cancer [165]. Therefore, even though hypoxia has an important role in the metabolic reprogramming of cancer cells in low O_2 environments, it has been suggested that hypoxia is a delayed event and is not the reason behind the Warburg effect [166]. However, while hypoxia may not play a role in the genesis of the Warburg effect, the HIF pathway may still have a part to play, as the loss of tumour suppressors (such as PTEN, VHL and p53) or the activation of oncogenes (including SRC, Ras and PI3K), along with other O_2 independent factors, can lead to HIF-1α stabilisation in normoxic conditions (see section 1.8.2), thus inducing aerobic glycolysis.

It is thought that the Warburg Effect benefits cancer cells and encourages cancer cell proliferation [166]. However, exactly how the Warburg Effect is advantageous for cancer cells is still debated, because although the rate of ATP production is increased in these cells, aerobic glycolysis is an inefficient way of producing ATP compared to

mitochondrial respiration (reviewed in [167]). Some believe that cells with a higher rate but lower yield of ATP production may have an advantage when competing for shared energy resource such as glucose [168], of which there is only a limited amount in the tumour microenvironment [169-171]. There are those that disagree with the reasoning that the increased rate of ATP production through aerobic glycolysis aids in proliferation. Studies conducted in the late 1960s showed that energy consumption not associated with proliferation in mammalian cells is very high [172], leading to the belief that cells actually require more ATP for normal cellular maintenance than they do for proliferation [167]. This means that ATP levels in proliferating cancer cells may never be a limiting factor [167].

Anabolic or biosynthetic pathways are a vital part of cancer cell metabolism, as they enable the production of the macromolecules required for cell division and cancer growth (reviewed in [105]). Another hypothesis put forward to explain the existence of the Warburg Effect is that it increases the availability of precursors for these anabolic pathways, with the production of ATP not representing a major component of this phenotype [105]. Studies presenting evidence that functional mitochondrial are required for tumourigenesis [173-175], in addition to other work showing that limiting ATP production through the inhibition of glycolysis does not prevent oncogenesis [176], leads some to believe that aerobic cancer cells rely on mitochondrial respiration for the production of energy [105].

Several papers explain the Warburg Effect as a ‘switch’ from OXPHOS to glycolysis [164, 166]. However, more recent work has provided evidence against the idea of a ‘switch’ occurring, with studies showing that cancer cells exhibit the ability to enhance both lactate production and the citric acid cycle in parallel [177-179]. One possible way through which this might be achieved in cancer cells is through enhanced enzyme expression and substrate delivery [105].

1.8.5 Lactic acid fermentation

Within the glycolytic pathway, conversion of glyceraldehyde 3-phosphate (G3P) to 1,3-bis-phosphoglycerate (1,3-BPG), catalysed by glyceraldehyde 3-phosphate

dehydrogenase (GAPDH), leads to the reduction of NAD^+ to NADH. As there is only a limited amount of NAD^+ in a cell, this molecule must be regenerated for glycolysis to continue (reviewed in [107, 108]).

In cells undergoing low levels of glycolysis, mitochondrial shuttles (the most commonly known is the malate-aspartate shuttle) restore NAD^+ levels in the cytosol, with the concomitant generation of NADH in the mitochondria. The NADH generated in the mitochondria passes its electrons down the electron transport chain, and the NAD^+ produced in the cytosol enables the continuation of glycolysis (reviewed in [167]). During glycolysis in normal cells, these shuttles are able to regenerate sufficient NAD^+ for glycolysis to persist. However, the rate of NAD^+ consumption is vastly increased in both hypoxic and aerobic cancer cells as a result of their highly glycolytic phenotype, which results in the mitochondrial shuttles being unable to regenerate NAD^+ at a fast enough rate (reviewed in [167]). Cancer cells therefore require other methods to maintain NAD^+ levels.

The major mechanism through which highly glycolytic cells restore their NAD^+ levels is through lactic acid fermentation (reviewed in [107, 108]) (figure 5C). In this process, NADH transfers its electrons to pyruvate, leading to the production of lactic acid and the regeneration of NAD^+, thus enabling glycolysis to continue in these cells. Normoxic and hypoxic cancer cells, through both oncogenic transformation and HIF-1α stabilisation, are adapted to increase the rate of lactic acid fermentation. Hypoxia and HIF-1α stabilisation induce the expression of pyruvate dehydrogenase kinase 1 (PDK1) (see section 1.8.3) and lactate dehydrogenase (LDHA) [151, 180]. PDK1 inactivates pyruvate dehydrogenase (PDH) (see section 1.8.3), inhibiting the conversion of pyruvate to acetyl CoA, thereby impeding mitochondrial respiration and increasing the amount of pyruvate present in the cells. The amplified levels of LDHA, which catalyses lactic acid fermentation, leads to an increase in the conversion rate of this pyruvate to lactate [151]. In this way, cancer cells are adapted to produce NAD^+ at a fast enough rate to help ensure their high rate of glycolysis can continue.

1.8.6 The pentose phosphate pathway

Instead of using glycolysis, followed by either oxidative phosphorylation or lactic acid fermentation, glucose can take an alternative pathway termed the pentose phosphate pathway (PPP) (reviewed in [181, 182]) (figure 5D). The PPP is principally an anabolic pathway that supports the synthesis of macromolecules through the production of NADPH (nicotinamide adenine dinucleotide phosphate, the majority of which is used in reductive biosynthesis reactions in the cell [183, 184]), and ribose [185] (required for nucleotide biosynthesis). The contributions of the PPP are very important in the production of the raw materials required for cell proliferation [185]. The PPP is a crucial pathway in cancer cells as a result of their high proliferative rate.

Apart from contributing to the production of raw materials required for cell proliferation, the PPP also has a part to play in controlling the levels of reactive oxygen species (ROS) produced in cells due to metabolism. Electrons transported through the electron transport chain (ECT) during OXPHOS can react with O_2, leading to the formation of ROS [186]. It has been estimated that between 0.2-2% of the O_2 consumed by the mitochondria is released as ROS (reviewed in [187]). A build up of ROS within the cells can cause damage to cellular components and induce cell death [188]. Antioxidants reduce the effects of these ROS, with glutathione being one of the most important anti-oxidants present in the cell [189]. However, GSH cannot be produced in the mitochondria, and must instead be imported from the cytosol [189]. The production of GSH requires the presence of NADPH; the PPP, through the production of NADPH, has a role to play in the generation of GSH in cells (reviewed in [181, 182]). This aspect of the PPP is especially important in cancer cells as a result of their increased rates of metabolism and ROS generation [190].

Studies have indicated that rapidly dividing cancer cells can modulate the PPP, leading to increased levels of nucleic acids and NADPH, thereby enabling increased proliferation and leading to greater control over oxidative stress levels [182]. For example, hyperactivation of a number of pro-oncogenic signalling pathways, such as

the PI3K/Akt, Ras and Src pathways, are thought to promote the post-translational modification and activation of glucose 6-phosphate dehydrogenase (G6PDH) [182], an enzyme which catalyses the first committed step of the PPP. The expression levels of transaldolase (TAL), another enzyme involved in the PPP, have also been shown to be up-regulated in cancer cells [191].

1.8.7 Glutamine metabolism

There are energy sources other than glucose available to cells. Glutamine is an example of one such source (figure 5E). The essential requirement of glutamine for cells in culture was first observed in 1948 by Albert Fischer [192], and later by Harry Eagle in 1956 [193]. Later experiments provided evidence that glutamine was being used to produce energy in cells [194]. These observations led to the concept that glutamine metabolism was a major component of the metabolic phenotype of cancer cells [195].

Glutamine is a non-essential amino acid that can be synthesised within cells. However, during periods of stress or rapid growth, the demand for this amino acid can outstrip the supply, causing glutamine to become conditionally essential [196]. Some cells are unable to survive in environments lacking glutamine, exhibiting a phenotype known as ‘glutamine addiction’ [197]. Metabolism of glutamine in the citric acid cycle produces reducing equivalents for oxidative phosphorylation, thereby functioning as a source of energy [198], while also replenishing the citric acid cycle intermediates that have been extracted for biosynthesis [199]. Even though OXPHOS is inhibited in low O_2 conditions [111], mitochondrial respiration can still occur in hypoxia [200]. Studies have shown that glutamine can also be used as a fuel for OXPHOS in hypoxic cancer cells [201], while other work has highlighted the vital role glutamine metabolism has for cancer cell survival in conditions of either hypoxia or glucose deficiency [202]. The dependence of breast tumours on glutamine seems to differ with the tumour subtype, as basal-type breast cancers have been shown to have an increased dependence on glutamine compared to luminal breast cancers [203, 204].

Proliferating cells are required to synthesise a number of different nitrogen-containing molecules, including nonessential amino acids and nucleotides. In addition to its other roles in metabolism, glutamine (containing 2 atoms of reduced nitrogen) acts as a major structural building block for the synthesis of many different nitrogen-containing compounds (reviewed in [106]).

1.8.8 Metabolic co-operation

Tumours are heterogeneous environments, containing regions under the influence of different O_2 conditions, along with various cell types, producing many opportunities for metabolic co-operation [205]. Monocarboxylate transporters (MCTs) function in the bidirectional transport of lactate across the plasma membranes of cells, with MCT1 and MCT4 representing the isoforms most extensively expressed in cancer cells (reviewed in [206]). For many years, the lactate produced by hypoxic cancer cells was considered as a waste product. However, recent work has shown that aerobic cancer cells can use this lactate for the production of energy [207, 208]. This work led to the conception of the metabolic symbiont model, wherein the lactate produced by hypoxic cancer cells is exported by MCT4, and taken up through MCT1 into the normoxic cancer cells, where it fuels metabolism. This spares glucose for the highly glycolytic hypoxic cancer cells within the tumour, helping them survive within their hostile microenvironment [207]. Further evidence that lactate can be used as a fuel for mitochondrial respiration has recently been published [178].

Metabolic co-operation between cancer and stromal cells has also been proposed. In one model, termed the Reverse Warburg Effect, cancer cells induce aerobic glycolysis in the neighbouring stromal fibroblasts, with the tumour cells taking up the metabolites released from the stromal cells and using them for energy production [209]. Breast cancer cells are thought to induce the Reverse Warburg Effect in stromal cells through initiating the down-regulation of caveolin-1 (Cav-1) [210], a transformation suppressor protein present in fibroblasts [211]. Other evidence of metabolic co-operation between cancer cells and stromal cells has been found in studies on ovarian cancer, with ovarian cancer cells using fatty acids produced in adipocytes to fuel mitochondrial respiration [212].

1.9 Metabolism and pH

Hydrogen (H^+) ions, or protons, are one of the most important and reactive ions present in a cell. Changes in the concentration of H^+ ions leads to changes in pH of the cell (reviewed in [213]). Proteins act as pH buffers in the cell, with H^+ ions usually present at low concentrations in biological solutions as they are generally bound to proteins. The binding or release of protons to and from proteins can change the ionization state of a protein, thereby changing protein function [214]. Therefore changes in the concentration of H^+ ions within the cell, or changes in intracellular pH (pHi), can affect many different cellular processes (reviewed in [215]). This highlights the importance of regulating pH in cells, controlling H^+ ion concentration to suit protein function.

Numerous processes contribute to the production of acids in cells, and the production of energy from glucose is one such process (reviewed in [213]). Under well-oxygenated conditions in normal cells, the respiration of glucose to CO_2 leads to the production of ATP, a process that consumes an H^+ ion ($ADP^{3-} + HPO_4^{2-} \rightarrow ATP^{4-} + OH^-$). This disturbance in the acid-base equilibrium is later cancelled out by the breakdown of ATP. The main source of acidity from cells undergoing mitochondrial respiration is therefore the CO_2 that is produced, which can react with water ($H_2O + CO_2 \leftrightarrow HCO_3^- + H^+$), leading to the formation of H^+ ions. In hypoxia, ATP production through glycolysis is linked to lactic acid fermentation (glucose + $2xADP^{3-} + 2xHPO_4^{2-} \rightarrow 2xATP^{4-} + 2xlactate^-$). This process does not lead to the generation or consumption of H^+ ions. However, the subsequent breakdown of ATP does lead to the release of protons, thus explaining how anaerobic metabolism produces acid [213, 216].

Normal cells in the body possess mechanisms to counter the effects of the acid produced by metabolism. The CO_2 produced from respiration can passively diffuse across the plasma membrane, with some studies indicating the presence of specialised gas channels in cells that increase membrane permeability to CO_2 [217]. However, others believe that the contribution of these channels to the movement of CO_2 out of the cell is not significant [218]. The H^+-lactate produced from anaerobic

metabolism has a much lower lipid:water partition coefficient than CO_2, and is unable to pass freely through the plasma membrane (reviewed in [213]). Cells must therefore possess other extrusion methods to remove these products of metabolism to help keep the pHi at an optimum level.

Cells express many pH-regulating proteins whose primary function is to control pHi. MCTs, already introduced in section 1.8.8, are one such group of proteins. These transporters translocate the H^+-lactate across the plasma membranes of cells, thus reducing the acid load produced from metabolism [219]. The rate of diffusion of metabolic products, such as CO_2 and H^+-lactate, is dependent on the concentration gradients of these products across the plasma membrane. In normal tissue with a structured and well-developed vasculature, the efficient blood perfusion leads to favourable diffusion gradients and efficient solute flux (reviewed in [213]). Both normoxic and hypoxic cancer cells are more reliant on glycolysis for energy production than normal cells in the body (see sections 1.8.3 and 1.8.4). This increased dependence on glycolysis in cancer cells leads to the production of increased amounts of acids within these cells in comparison to normal cells. The chaotic tumour vasculature results in inadequate perfusion within cancer tissues and the build-up of CO_2 and H^+-lactate in the extracellular environment, impairing the outward diffusion of these metabolic products (reviewed in [213]). The increased acid production through glycolysis, combined with impaired diffusion, would lead to an acidic pHi and probable cell death if additional compensatory mechanisms did not exist. As such, an adaptive feature of cancer cells is the over-expression or elevated activity of a number of pH regulating proteins.

Some of the main proteins involved in the regulation of cancer cell pH include the anion exchangers (AE1, AE2, and AE3) (reviewed in [220]), the Na^+/HCO_3^- co-transporters (NBCs) (reviewed in [220]) and the monocarboxylate transporters (MCT1, MCT2, MCT3 and MCT4) (reviewed in [206]). The carbonic anhydrases, the Na^+/H^+ exchangers, and the vacuolar (H^+)-ATPases are 3 other groups of proteins that have also been linked with the control of pH within tumours (figure 7). These 3 proteins are the focus of this thesis.

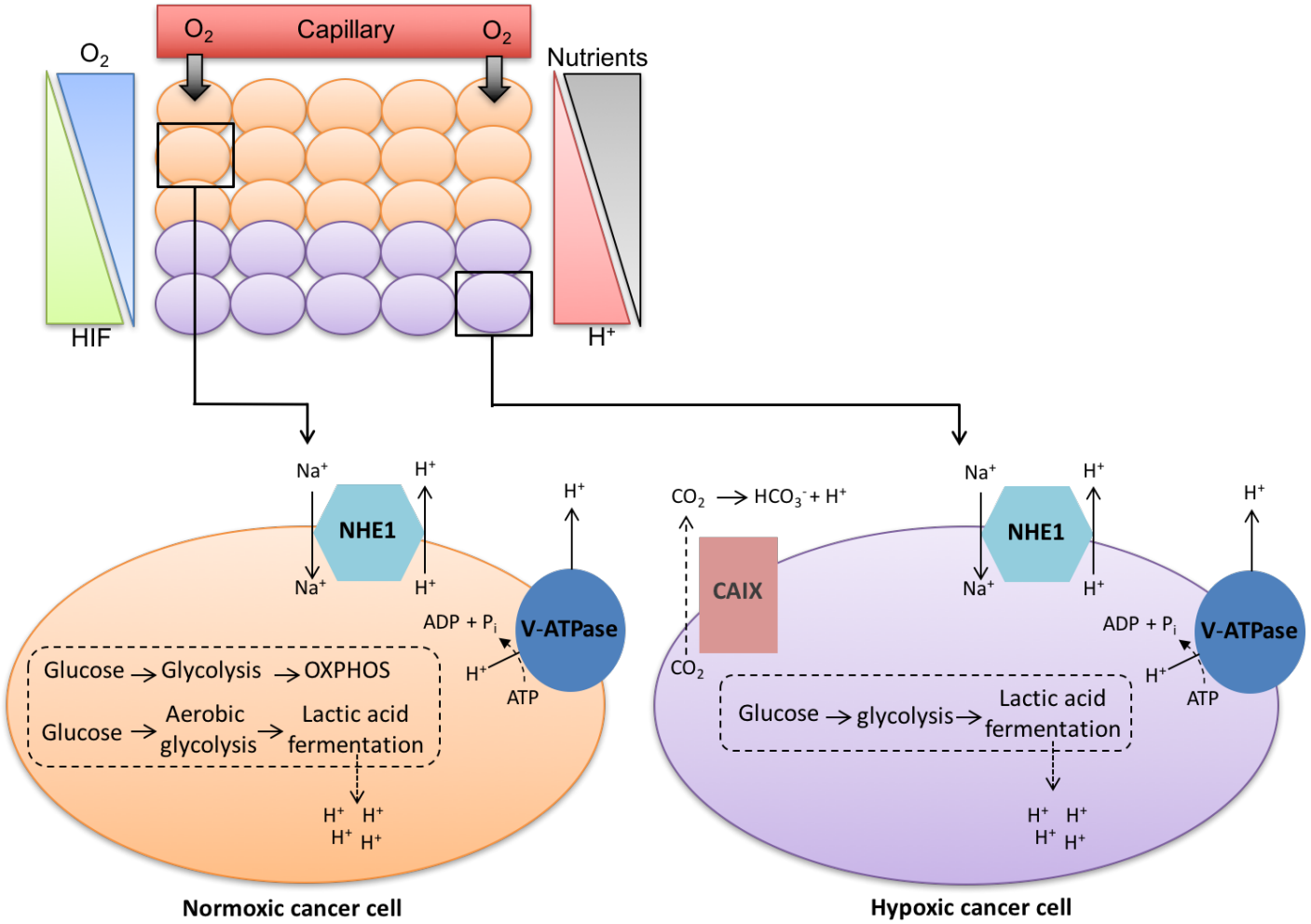

Figure 7: Cancer cell metabolism, HIF and pH.

See next page for description

Figure 7: Cancer cell metabolism, HIF and pH. *As cancer cells are pushed further away from blood vessels, the level of O_2 and nutrients available to the cells decreases. Normoxic cells can produce energy either through oxidative phosphorylation (OXPHOS) or through aerobic glycolysis (Warburg Effect). Hypoxic cancer cells, however, are unable to acquire energy through OXPHOS due to low O_2 levels. Activation of the hypoxia inducible factor (HIF) family of transcription factors is one of the principle oxygen-responsive signalling pathways that allows the adaptation of hypoxic cancer cells to this hostile microenvironment. HIF signalling shifts energy production from OXPHOS in the mitochondria towards glycolysis, allowing hypoxic cancer cells to continue to produce energy despite the low O_2 levels. This shift towards glycolysis may also occur in normoxic cancer cells as a result of genetic alterations leading to increased HIF signalling in well-oxygenated conditions. The increased dependency on glycolysis leads to the production of increased amounts of H^+ ions, which can lead to changes in the pHi of cancer cells if not dealt with. To help cope with the excess H^+ ions being produced, cancer cells up-regulate/activate a number of pH regulating proteins; these proteins include CAIX, NHE1 and V-ATPase.*

1.10 Carbonic anhydrases

Carbonic anhydrases (CAs) are metalloenzymes that have a bound zinc atom in the active site of the protein that is essential for enzymatic activity. Sixteen carbonic anhydrase isoforms have been identified in primates, with 15 of these present in humans (reviewed in [221]). These isoforms differ in their catalytic activity, subcellular localization, and their sensitivity to inhibitors. There are secreted (CAVI), cytosolic (CAI, CAII, CAIII, CAVII and CAXIII), mitochondrial (CAVA and CAVB), and membrane-bound (CAIX, CAXII, CAXIV and CAXV) forms of the protein. Three inactive isoforms (CAVIII, CAX and CAXI), which lack catalytic function, have also been identified (reviewed in [221]). The carbonic anhydrase family of proteins are involved in many different physiological functions. These include ion transport, bone resorption, the secretion of gastric and pancreatic juices, and pH regulation [222].

As already discussed (see section 1.9), membrane-permeant CO_2 is a form in which much acid is removed from cells. This CO_2 is generated either from oxidative phosphorylation or from the reaction of metabolic acids with HCO_3^-. The poor perfusion of tumour tissues inhibits the diffusion of CO_2 out of cancer cells (see section 1.9). The spontaneous hydration reaction involving CO_2 ($CO_2 + H_2O \leftrightarrow HCO_3^- + H^+$) reduces the concentration of CO_2 outside of the cells, increasing the diffusion rate of CO_2 across the plasma membrane (reviewed in [223]). However,

this reaction is very slow. Carbonic anhydrases facilitate CO_2 diffusion from cancer cells by catalysing the extracellular hydration of CO_2, leading to the generation of H^+ and HCO_3^-, thereby maintaining a steeper efflux gradient for CO_2 [223, 224]. Some of the membrane-bound carbonic anhydrase proteins are thought to interact with HCO_3^- transporters, forming a transport metabolon. In this complex, the carbonic anhydrase proteins supply the membrane-impermeant HCO_3^-, which is then translocated across the membrane by HCO_3^- transporters [222, 225].

1.10.1 CAIX

Carbonic anhydrase IX (CAIX) (figure 8A) is one member of the carbonic anhydrase family that is associated with cancer, with higher levels of this protein connected to increased tumour aggressiveness and progression, resulting in a poor prognosis in a number of different cancers [226]. CAIX expression is rarely seen in most postnatal tissues, with CAIX only observed in cells of the stomach and intestine [227]. However, ectopic expression of CAIX can also occur in tumours. The stabilization of HIF-1α in the hypoxic areas of tumours leads to high levels of CAIX expression in these regions [228-230].

This link between hypoxia, HIF and CAIX has led to interest in the use of CAIX as a biomarker to distinguish the presence of hypoxia in cancer [231]. However, the use of CAIX as a biomarker for hypoxia has been hampered by the results of several studies conducted on cervical cancer, where tumour oxygen tension levels and HIF staining did not always correlate with CAIX expression [232-234]. These discrepancies may be explained by 3 observations: (i) it can take several hours after initial HIF-1α stabilization for CAIX expression to be seen, which could explain the absence of CAIX in cells that have only recently become hypoxic and have stained positive for HIF-1α [235]. (ii) HIF-1α is an extremely labile protein that degrades rapidly in well-oxygenated conditions. Re-oxygenation of previously hypoxic areas may therefore be leading to an absence of HIF-1α and the retention of CAIX [235]. (iii) While hypoxia is the major inducer of CAIX expression in cancers, stabilisation of HIF-1α through oncogenic mutations, or through other O_2-independent

mechanisms (see section 1.8.2), could also lead to increased CAIX levels in normoxic conditions.

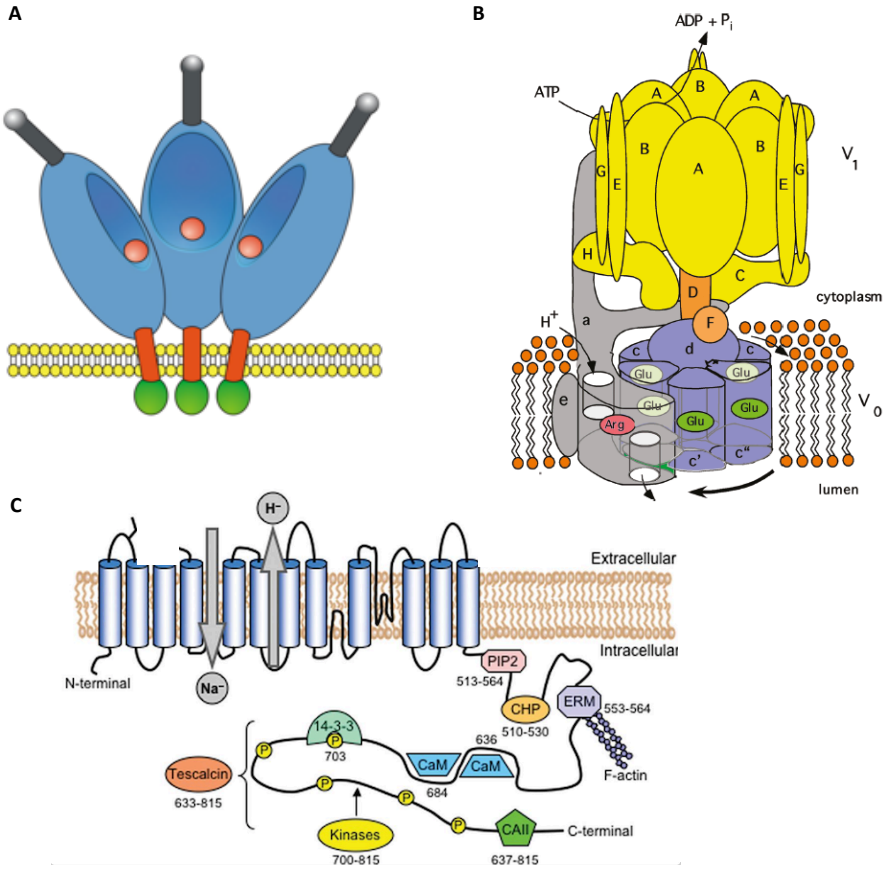

Figure 8: Protein structures.

(A) *CAIX consists of a large extracellular domain, a single-pass transmembrane region, and a short intracellular tail. The extracellular portion contains a well-conserved CA domain that binds zinc and hydrates CO_2 extracellularly, along with a proteoglycan-like region that is thought to mediate CAIX function, in addition to having a role in cell adhesion. The cytoplasmic tail present intracellularly contains 3 putative phosphorylation sites that may have a part to play in the regulation of the protein. CAIX proteins are believed to assemble as either dimers or trimers on the plasma membranes of cells, stabilised by the formation of disulfide bonds (reviewed in [236, 237]. Image adapted from ref [236]).* **(B)** *The V-ATPase complex consists of 2 domains, the peripheral V_1 domain and the integral V_0 domain, each of which is composed of many different subunits. ATP hydrolysis results in the rotation of a central motor consisting of D, F, d and proteolipid (c, c', and c'') subunits. This leads to the uptake of H^+ ions by glutamic acid residues through hemichannels present in the protein, and the transport of these H^+ ions through to the other side of the membrane (reviewed in [238, 239]. Image adapted from [238]).* **(C)** *The NHE1 protein consists of a short N-terminal intracellular region, a membrane-spanning region consisting of 12 transmembrane domains, and a large intracellular C-terminal tail. The membrane domain of NHE1 functions in the transport of ions, extruding one Na^+ ion in exchange for one Na^+ ion, while the cytoplasmic domain of NHE1 functions in the regulation of activity of the protein. NHE1 can also regulate cytoskeleton organisation through its C-terminal domain (reviewed in [240, 241]. Image adapted from [240]*

1.10.2 CAXII

CAXII is another protein that has been linked with cancer [242-244]. However, this link is not as well evidenced as that observed for CAIX, with fewer studies carried out to date on CAXII. Therefore, less is known about the role of this carbonic anhydrase isoform. CAXII is also a transmembrane protein that catalyses the extracellular hydration reaction of CO_2, thus aiding in the cellular control of pH [245]. In contrast to CAIX, which is only rarely expressed in normal tissues within the body, CAXII expression is much more widespread (reviewed in [236, 246]). In a study comparing CAXII and CAIX levels in normal adult tissues, there was largely no overlap in CAXII and CAIX expression, with the CAXII isoform detected at high levels in the colon, kidney, oesophagus, pancreas, rectum and brain [243]. However, the overexpression of CAXII has been found in numerous types of cancer, including breast cancer [243, 244]. Like CAIX, CAXII levels are also increased in hypoxia [242, 243]. However, the molecular mechanism through which CAXII expression is induced in low O_2 conditions is not currently known, as the presence of a functional HRE that could bind HIF has yet to be identified in the CAXII promoter region (reviewed in [236]).

1.11 NHE1

The Na^+-H^+ exchanger 1 (NHE1) is a pH regulating protein that removes an H^+ ion from the cytoplasm in exchange for the influx of a Na^+ ion in a 1:1 ratio (figure 8C) (reviewed in [241]). Ten isoforms of the Na^+-H^+ exchanger have been identified so far (NHE1-NHE10), of which NHE1 is the best characterised. As a result of its presence in nearly all cell types, NHE1 expression is widespread in the human body, with NHE1 detected in the heart, the vasculature, the kidney, different parts of the gastrointestinal tract and the central nervous system, along with many other organs in the body (reviewed in [241]). This protein has been shown to have roles in numerous processes within cells in addition to its central role in pH regulation, including migration, proliferation, vesicle trafficking and cell signalling (reviewed in [241]). Structurally, the NHE1 protein consists of a large cytoplasmic domain at the C-terminal end of the protein, followed by a transmembrane domain consisting of 12

membrane-spanning regions, and a short N-terminal cytoplasmic domain (reviewed in [241]).

In normal cells above a set pHi value the NHE1 protein remains inactive. Allosteric H^+ binding sites present on NHE1 make this protein very sensitive to changes in the pHi [247]. When the pH drops below a certain level in the cell, H^+ ions bind to these allosteric binding sites, activating NHE1 and leading to the extrusion of a proton in exchange for the influx of a Na^+ ion, thereby alkalinizing the pHi. The allosteric H^+ binding sites allow NHE1 to vary its activity in response to small changes in the concentrations of intracellular H^+ ions [247], enabling these proteins to maintain pHi within a limited range. Studies support the idea that NHE1 may actually function as a dimer [248], and that this dimeric interaction may control the pH-dependent regulation of NHE1 [249].

Considerable work has been carried out assessing the post-translational regulation of NHE1. Secreted stimuli including hormones, cytokines, growth factors, and physical stimuli including shear stress, integrin-mediated adhesion and osmotic cell shrinkage, can all regulate the activity of NHE1 (reviewed in [241]). The binding of proteins and lipids, along with phosphorylation of the C-terminal tail of NHE1, are other forms of post-translational modification identified that affect NHE1 activity (reviewed in [241]). Translocation of the NHE1 protein to or from the plasma membrane is another way in which protein activity can be controlled [250].

Aside from NHE1 activity, NHE1 expression levels are regulated by a multitude of different influences. Growth factors [251] and reactive oxygen species [252] have been shown to lead to increased NHE1 expression levels. NHE1 expression levels are higher in some cancers, with amplified levels of NHE1 observed in hepatocellular carcinoma tissue compared to normal liver tissue [253]. The relationship between hypoxia and NHE1 expression in cancer is not as evident as that seen with hypoxia and CAIX. However, certain studies indicate that hypoxia may influence NHE1 expression in some cell types, with reports of NHE1 regulation by HIF-1α, along with increases in NHE1 levels in low O_2 conditions [254-256].

1.12 V-ATPase

The vacuolar (H^+)-ATPases (V-ATPases) are ATP-dependent proton pumps made up of 2 domains connected by multiple stalks. The peripheral domain (V_1) consists of 8 subunits (A-H) and functions to hydrolyse ATP. The second domain (V_0) is made up of 6 proteolipid subunits arranged in a ring, and functions in the translocation of H^+ ions across the membrane (figure 8B) (reviewed in [238, 239]). V-ATPase proteins act by a rotary mechanism, wherein the hydrolysis of ATP at the V_1 domain drives rotation of the central stalk and the attached proteolipid subunits of the V_0 domain. The subunits of the V_0 domain contain acidic residues that are capable of undergoing reversible protonation. These subunits pick up H^+ ions as they are rotated and transport the H^+ ions across the membrane (reviewed in [238, 239]).

V-ATPases have a role to play in the acidification of intracellular compartments, contributing to processes such as receptor-mediated endocytosis and the digestion of internalized macromolecules in lysosomes (reviewed in [238, 239]). Besides their presence on the membranes of intracellular organelles, V-ATPase complexes have also been shown to be present on the plasma membranes of specialized cells, where they act to pump H^+ ions out of the cell. This function of V-ATPases has connected them to normal physiological processes such as such as bone resorption, sperm maturation and renal acidification (reviewed in [238, 239]).

Since V-ATPase proteins function in numerous cellular compartments, mechanisms are required to target the complexes to differing cellular sites. There are varying V-ATPase subunit isoforms produced for each subunit (reviewed in [238]). Studies have shown that V-ATPase complexes may selectively form to contain specific combinations of subunit isoforms in different tissues [257], and some believe that these unique combinations of subunit isoforms may drive the localization of the V-ATPase complex [239]. In addition to the possibility that the whole V-ATPase complex subunit signature may play a part in localization, other studies have shown that the information needed for V-ATPase targeting may be present within subunit a of the V_0 domain. Altogether there are 4 isoforms of the a subunit (a1-a4) (reviewed

in [238]), with V-ATPase complexes with the a3 isoform shown to targeted to the plasma membranes of mouse osteoclast cells [258].

In addition to the presence of V-ATPase on the surfaces of specialized cells in the body, studies have also reported the existence of the V-ATPase complex on the plasma membranes of cancer cells [259, 260], where they are thought to play a role in pH control. In fact, some hypothesize that cancer cells primarily control pH through the V-ATPase complex, rather than through other pH regulating proteins such as NHE1 or bicarbonate transporters [261].

Regulation of V-ATPase activity in cells is mainly accomplished through 3 mechanisms: (i) reversible dissociation of the V_1/V_0 complex, (ii) changes in complex density at the plasma membrane through the reversible fusion of V-ATPase carrying vesicles, and (iii) alterations in the efficiency of coupling of H^+ movement with ATP hydrolysis (reviewed in [238, 239, 262]). While regulation of gene expression is a common method for cells to control the activity of many proteins, the combined gene regulation of a multi-subunit complex such as V-ATPase, which is made up of at least 13 different polypeptides, is cumbersome [262]. Therefore most cells in the body are thought to regulate V-ATPase activity through the above 3 mechanisms. However, examples of the overexpression of certain subunits of the V-ATPase complex have been found in oral squamous carcinoma cells [263, 264]. V-ATPase subunit expression levels are also increased after treatment with cisplatin [265, 266]. While these studies show some evidence of V-ATPase expression differences in cancer cells compared to normal cells, little has been published to date connecting hypoxia/HIF to V-ATPase expression.

1.13 pH and cancer

The activation and/or up-regulation of pH regulating proteins on the plasma membranes of cancer cells leads to the alkalinisation of the pHi and the acidification of the extracellular pH (pHe) of tumour cells, resulting in pHi and pHe values in these cells that differ greatly from those in normal cells. Studies conducted using microelectrodes to measure the pH values of cancerous tissue and normal tissue,

which were later confirmed with NMR and MRI techniques, have shown that the pHe of cancer cells is regularly lower than the pHe of normal tissue, whereas the pHi values of cancer cells is more alkaline compared to normal cells (reviewed in [267, 268]). The abnormal regulation of H^+ ions in cancer cells, leading to the formation of this reversed pH gradient in cancer cells and tissues when compared to normal cells and tissues within the body, is a phenomenon that is increasingly being considered as one of the most differential characteristics of cancer [269]. This reversed pH gradient has a large effect on both cancer cell biology and the treatment of cancer.

1.13.1 pH and invasion/migration

The invasion and metastasis of tumour cells to other parts of the body is the main cause of cancer mortality, with 90% of deaths from solid tumours resulting from metastasis [270]. Many of the different processes underlying cell invasion/migration are dependent on pH. The assembly of actin filaments drives the formation of lamellipodium and invadopodia, membrane structures that protrude into the extracellular matrix (ECM) and enable cell migration. At pHi values of greater than 7.2, the assembly of actin filaments increases as a result of the increased activity of actin-binding proteins, thereby increasing cell motility (reviewed in [215, 271]). In addition to the assembly of actin filaments, cell migration requires the remodelling of focal adhesion contacts (cell-substrate interactions that enable the migrating cell to transmit force) to either surrounding cells or the ECM, a process aided by reversed pH gradient of cancer cells [272, 273].

The migration and invasion of cells into tissue is also dependent on the degradation of the ECM. This degradation is mediated by the secretion of proteinases and the activity of matrix metalloproteinases (MMPs) (reviewed in [274]). Acidic pHe values lead to the increased secretion of proteinases and MMPs, thereby further aiding invasion and migration [275]. The acid-mediated invasion hypothesis is one of the mechanisms through which cancer cells are thought to invade (reviewed in [225]). In this model, acidosis of the tumour microenvironment causes the breakdown of normal tissue surrounding the tumour. The tumour itself, however, is able to cope with the low pHe values as a result of the expression and/or activation of

pH regulating proteins, with the cells of the tumour undergoing greater levels of migration on exposure to the acidic microenvironment.

1.13.2 pH and proliferation/apoptosis

Proliferating cells go through the cell cycle, which is made up of the Gap 1 phase (G1 phase; cells increase in size and prepare to duplicate DNA), the Synthesis phase (S phase; DNA replication occurs), the Gap 2 phase (G2; any repair needed is carried out and the cell prepares for mitosis), and mitosis (M phase; the cell divides into 2 daughter cells) (reviewed in ref [276]). Entry into each of the phases is regulated by cell-cycle checkpoints, controlled by the cyclin-dependent kinase (Cdk) proteins bound to proteins called cyclins (reviewed in [277]). More alkaline pHi values have been demonstrated to contribute to an increase in the rate of cell proliferation through increasing the proportion of cells entering the S phase [278] and G2/M phases of the cell cycle [279], with more acidic pHi values delaying entry into the G2/M phase [279]. While intracellular alkalinisation seems to be a common feature in proliferative processes, the role of pH in cell death is not as clear. Cytosolic acidification seems to be a common feature of apoptosis, indicating that acidic pHi may have a permissive role in the apoptotic cascade [280]. For example, the cytochrome C-mediated activation of caspases (proteins that have an essential role to play in apoptosis) is much more efficient in acidic pH compared to neutral cytosolic pH conditions [281].

1.13.3 pH and irradiation

pH can affect the responsiveness of cells to irradiation. Investigations carried out in the 1980s showed that cells cultured in acidic media were more resistant to the effects of irradiation [282-284], with other work showing that acidic pHe values reduce the fixation of radiation damage [285]. Studies have shown that acidic pHe values can lead to the inhibition of radiation-induced apoptosis in cells, with an increase in radiation-induced apoptosis observed in cells exposed to a more alkaline pH [286, 287]. Altered cell cycle progression in acidic environments is also thought to contribute to resistance to irradiation. The G2 checkpoint before entry into the M

phase, or the G2/M phase arrest, enables cells to repair any DNA damage before mitosis (reviewed in [288]). One study showed that radiation-induced G2/M-phase arrest was delayed in colorectal cancer cells cultured in medium with a pH of 6.6, compared to cells cultured in pH 7.5 medium [289]. This elongation of the G2 phase after irradiation in cells present in acidic conditions allows a greater amount of time for the DNA damage repair, thereby decreasing the proportion of cells that undergo mitotic death, and thus increasing radiation-resistance [289].

1.13.4 pH and drug treatment

In addition to affecting radiotherapy responses, the reversed pH gradient of cancer cells also has an influence on the effectiveness of chemotherapeutics (reviewed in [215, 290]). Drugs display acidic, basic and neutral properties. For pharmacological agents that are either weak acids or weak bases, the amount of ionization is dependent on pH (reviewed in [290]). Some of the drugs used in chemotherapy are weak bases (examples include Doxorubicin [Adriamycin] and Daunorubicin [Cerubidin]) [291], which are protonated in the acidic extracellular environments of cancer cells, changing them from a neutral to a charged species. The differing ratios of charged and neutral species can influence drug distribution both intracellularly and extracellularly, and also within different subcellular compartments with varying pH values, with charged agents having lower rates of diffusion through cell membranes (reviewed in [215, 290]). Because chemotherapeutics such as doxorubicin have intracellular targets [292], this inhibits some drugs from reaching their targets, thereby leading to increased resistance to chemotherapy treatment.

Conversely, the more alkaline pHi of cancer cells leads to a large proportion of weak base chemotherapeutics being present in a neutral form intracellularly, which can lead to increased diffusion of drug out of the cell. The increased concentration of basic drugs in the acidic organelles of cancer cells, which also inhibits drugs from reaching their target, is another mechanism of chemotherapy resistance [293]. The opposite situation is the case in normal cells, where pH gradients lead to higher concentrations of the anti-cancer agents being found intracellularly, increasing the likelihood of toxic effects (reviewed in [215]). Several studies conducted *in vitro*

[293-295] and *in vivo* [295, 296] have shown that these pH effects do occur and that drug efficacy is affected as a result. In addition to affecting drug distribution through changing the passive diffusion of drugs, the reversed pH of cancer cells may also influence drug effectivity through modifying the active efflux of drugs. It is thought that the acidic pHe of cancers may lead to the activation of multidrug transporters such as P-glycoprotein [297, 298], and the breast cancer resistant protein ABCG2 [299], which may contribute to multidrug resistance in some cancers.

1.14 Targeting the pH regulation of cancer cells

Given the influence of the reversed pH gradient on cancer cell biology (see sections 1.13.1 and 1.13.2) and resistance to therapy (see sections 1.13.3 and 1.13.4), interference with the pH regulation mechanisms of cancer cells is one possible approach to improve patient outcomes. Targeting the proteins responsible for the control of pH in cancer cells is a mechanism that is not exploited by any of the traditional anti-cancer drugs.

1.14.1 CAIX inhibition

The role of CAIX in cancer progression is well recognised (reviewed in [237, 300, 301]), and it is an established marker of poor prognosis across a wide variety of cancers [302-305], including breast cancer [306, 307]. However, CAIX has great potential as a target for cancer therapies as a result of its limited expression in normal tissues within the body (see section 1.10.1), suggesting that limited drug toxicity should be expected when targeting this molecule. Evidence of this comes from mouse studies where knockout of CAIX led to little abnormality, other than gastric hyperplasia [308]. The majority of cancer deaths result from metastasis (see section 1.13.1). The recognition of CAIX as a target for metastatic disease [309, 310], in addition to the extracellular catalytic domain of CAIX facilitating access to drug treatment [311], has led to considerable interest in CAIX as a target for cancer therapy.

There has been much work conducted on the development of inhibitors targeting tumour-associated carbonic anhydrases (reviewed in [222, 311-313]), with 2 main

approaches used to target CAIX in particular. One such approach is the use of CAIX-specific monoclonal antibodies, which can exhibit anti-cancer effects through the induction of antibody-mediated cellular cytotoxicity [314]. Some of these agents have already been tested in humans. Phase I and phase II clinical trials with the CAIX-specific antibody Girentuximab (cG250) demonstrated that this antibody led to disease stabilisation either alone or in combination with IL-2 treatment, and was well tolerated in patients with advanced renal cell carcinoma [315, 316]. However, a phase III trial conducted in patients suffering from non-metastatic renal cell carcinoma did not show any improvement in disease-free survival with this antibody (NCT00087022).

Monoclonal antibodies can also be used to target the delivery of therapeutic compounds. cG250 labelled with Lutetium 177, a β-emitting radionucleotide, is an example of one such compound that has been tested in humans. Phase I clinical trials carried out using cG250 labelled with Lutetium 177 showed this compound to be safe and well-tolerated [317]. A phase II study demonstrated that ^{177}Lu-cG250 led to disease stabilisation in patients with advanced renal cell carcinoma [318]. However, other studies using monoclonal antibodies targeting CAIX have not produced such positive results, with a phase I clinical trial involving the use of a novel CAIX monoclonal antibody conjugated to the microtubule inhibitor MMAE (monomethyl auristatin E) terminated due to patient safety [311].

The development of small molecule inhibitors of carbonic anhydrases represents another approach to target CAIX in cancer therapy [311]. The sulphamates are one class of small molecule inhibitors that have been established (figure 9A and B) [222, 312]. These carbonic anhydrase inhibitors (CAIs) act by binding to the catalytic Zn^{2+} ion present in the active site of the protein [222, 312], blocking its function and inhibiting the carbonic anhydrase enzymes from catalysing the extracellular hydration reaction of CO_2. Many of these pharmacological agents were specifically designed to inhibit the tumour-associated isoforms of the carbonic anhydrase proteins, with some dually inhibiting both CAIX and CAXII (reviewed in [319]). Nitroimidazole-based CAIX inhibitors, such as DTP348, have also been developed

for use in combination with radiotherapy [320] (figure 9C). The sulphamide component of these molecules inhibits CAIX, while the 5-nitroimidazole moiety acts as a radio-sensitizer through mimicking O_2. The purpose of these compounds is to selectively target hypoxic cancer cells, thus improving the effects of radiotherapy. A selection of these small molecule inhibitors have also been tested in clinical trials. SLC-0111 is one such compound for which phase I clinical trials are currently underway (NCT02215850), with DTP-348 due to enter Phase I trials (NCT02216669) after beneficial effects seen in combination with irradiation [320] and doxorubicin [321] *in vivo*.

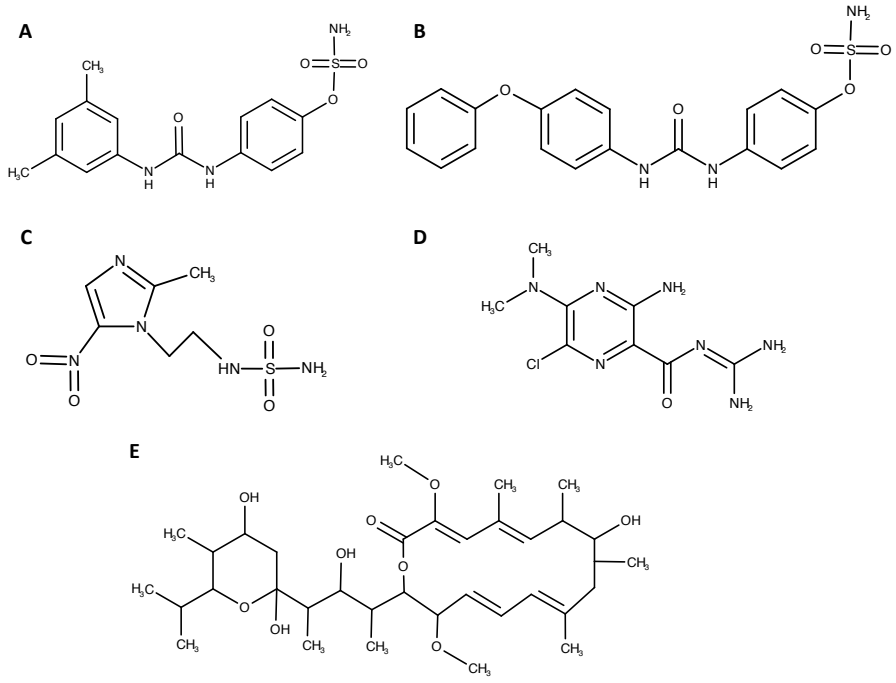

Figure 9: Drug structures.

Structures of the sulphamate CAIX inhibitors S4 (A) and FC9403A (B), the nitroimidazole based sulphamide CAIX inhibitor DTP348 (C), the NHE1 inhibitor DMA (D), and the V-ATPase inhibitor bafilomycin A1 (E), are shown.

1.14.2 NHE1 inhibition

Despite the ubiquitous expression of NHE1 in cells all around the body, this protein has been firmly connected to the malignant transformation of cells and cancer progression [225, 322, 323], with many studies observing increased activity/expression of this protein in cancer cells compared to normal cells in the body (see section 1.11).

As a result of the importance of NHE1 in many different physiological processes, numerous inhibitors of NHE1 have been developed (reviewed in [241, 322, 324]). Many of these compounds are modifications of amiloride, the original drug shown to inhibit NHE1 activity. However, while NHE1 was the isoform most sensitive to amiloride, this drug also affected NHE2 [325] and NHE5 [326] isoforms as well. Using the basic structure of amiloride, inhibitors with increased specificity for NHE1, such as Dimethylamiloride (DMA) (figure 9D), were designed. Studies conducted into the mechanism of inhibition have shown that amiloride-type compounds are partly competitive with the binding of Na^+, suggesting that drug binding involves the Na^+ binding site, or an area nearby [241].

In vivo studies exhibit the potential of NHE1 inhibitors in the treatment of cancer, with compounds of the amiloride series shown to inhibit the development of mutagen-induced lesions in animals, reducing the size of xenografts and suppressing metastases (reviewed in [327]). While there are clinical trials assessing the effects of the NHE1 inhibitor cariporide in a cardiological setting (reviewed in [328]), the anti-cancer effects of NHE1 inhibition have not been assessed in humans. Because of the widespread expression of NHE1 in multiple cell types throughout the body, the selective targeting of the NHE1 protein present on cancer cells represents more of a challenge than that of CAIX. However, it has been hypothesised that the increased basal activity of NHE1 proteins in tumours compared to the NHE1 present in normal tissues should facilitate the use of future NHE1 inhibitors in human trials to assess their anti-tumour effects [323]. One possible approach that may decrease the toxicity of NHE1 inhibitors is the conjugation of either peptides or amino acids to NHE1 inhibitors, producing a prodrug that could be activated by proteases present in the tumour microenvironment [329, 330].

1.14.3 V-ATPase inhibition

As with NHE1, V-ATPase has also been associated with cancer despite its widespread expression in normal tissues of the body [225, 331-333], with studies connecting V-ATPase to multidrug resistant mechanisms [266, 334] and cancer cell

invasion [260, 335, 336]. The first inhibitor specific for V-ATPase identified was bafilomycin A1 (figure 9E). This compound was originally isolated from species of the Streptomyces bacteria in the 1980s [337], and was synthesised for the first time in 1997 [338]. This compound inhibits V-ATPase by binding to both subunits a and c of the V_0 domain of the V-ATPase complex [339-342], impeding the helical swivelling of the protein, and thereby blocking proton transport (reviewed in [239]). In addition to preventing proton transport through V-ATPase, bafilomycin A1 has also been shown to have ionophoric properties, leading to the transport of potassium across the inner mitochondrial membrane, causing mitochondrial damage [343].

Similar to NHE1, the targeting of V-ATPase within humans represents more of a challenge than the pharmacological inhibition of the tumour-associated carbonic anhydrases due to the multitude of roles V-ATPase has within normal cells (see section 1.12). Proton pump inhibitors (PPIs) such as esomeprazole and omeprazole, in addition to the targeting of H^+/K^+ ATPases, can inhibit V-ATPase activity, thereby giving them potential use in the treatment of cancer [344, 345]. These compounds are prodrugs that are activated in acidic conditions, and may provide less toxicity by targeting the acidic microenvironment of tumours [222]. Proton pump inhibitors such as these have been used in humans for acid related diseases with negligible side effects (reviewed in [346]).

Various clinical trials have been carried out assessing the effects of PPIs on the treatment of cancer. Proton pump inhibitors have been reported to reduce the risk of neoplastic progression in patients with Barrett's oesophagus [347]. A number of studies have assessed the combination of PPIs with other treatment modalities. A Phase II trial showed that esomeprazole increased the sensitivity of osteosarcoma to neo-adjuvant chemotherapy, as identified through the visualisation of increased tumour necrosis, without any significant increase in toxicity [348]. A veterinary Phase I/II trial in canines and felines with tumours exhibiting resistance to chemotherapy showed the benefits of combining high doses of PPIs with chemotherapy for tumour treatment [349]. A pilot clinical trial investigating the effects of combining either docetaxel or cisplatin with esomeprazole in metastatic

breast cancer has reported the improved effects of chemotherapy with no escalation of toxicity [350].

1.15 Cancer cell models

Many different models are used in cancer research to analyse the expression of cancer-related proteins or the therapeutic effects of newly developed drugs. Cancer cell lines are intrinsic to many of the 2D and 3D cancer models used (reviewed in [351-353]). In terms of breast cancer, a cell line panel can represent the major breast cancer subtypes, while 3D modelling can examine compounds in a system that includes both O_2 and pH gradients. The testing of pharmacological compounds on fresh untreated patient tissue derived from biopsies allows for the effect of the heterogeneity of tumour tissue and the presence of stromal cells in the experimental set up [354, 355]. *In vivo* studies can also be pursued by using cancer cell lines transplanted into mice (reviewed in [352, 356]). However, because all models of human breast cancer developed to date are imperfect, with both advantages and disadvantages to each model system, the soundest experimental approach is to use multiple systems for the initial phase of drug testing [356].

1.15.1 2D cell culture

The use of cell lines cultured in 2D is the most practical approach for assessing target protein expression or measuring the therapeutic effects of anti-cancer compounds. However, 2D cell culture represents a very simple model system that does not reflect the *in vivo* tumour environment, as cancer cells cultured in 2D exhibit extensive variation in morphology, proliferation, signalling and gene expression when compared to cells cultured in 3D (reviewed in [357]). Also, many experiments investigating breast cancer culture cells at 20% O_2, while studies have shown that the O_2 tensions of cells in both normal breast tissue and cancerous tissue are actually much lower (see section 1.7.2). Discrepancies in O_2 conditions between 2D cell culture and O_2 tensions *in vivo* can be partially resolved through using cell culture incubators that have the capacity to produce O_2 concentrations that are more representative of physiological levels. However, while these systems enable the

analysis of gene/protein expression or drug response at a particular O_2 tension, they do not enable simultaneous analysis across the range of O_2 tensions that occur in tumours *in vivo*. In 2010 it was estimated that more than 70% of cancer researchers relied on 2D cell culture experiments to produce results [358]. Some believe that an over-reliance on 2D cell culture alone for the testing of new anti-cancer compounds may affect the choice of lead compounds for later *in vivo* studies, which could contribute to failure at the later stages of drug development [357, 359]. These failures are damaging to pharmaceutical companies, and ultimately affect patient treatment. The use of cancer cell models that simulate the *in vivo* tumour microenvironment in pre-clinical tests has the potential to help researchers identify compounds that are more likely to pass clinical trials [357, 359].

1.15.2 3D models

The value of 3D cultures in experimental research is obvious as experiments with these models show better correlation with results from *in vivo* studies (reviewed in [357]). To reproduce the *in vivo* situation more accurately, numerous 3D culture systems have been developed [360]. The multicellular tumour spheroid model is one that is extensively used. There are many different ways to produce spheroids for use in 3D assays [360-363], one of which is the spinner flask method. This involves placing a suspension of cells in media into a flask that is constantly stirred. As a result of the constant motion, the cells do not adhere to the surfaces of the flask, but instead aggregate together to form spheroids. The spinner flask method of spheroid formation leads to the production of a large number of spheroids in a short time frame [360-363]. These spheroids exhibit 3D cell-cell interactions and, if of a large enough size, develop gradients of O_2, nutrients and catabolites (reviewed in [364]). Cells located in the outer rim of the spheroid have an ample supply of O_2 and nutrients, mimicking the proliferative cancer cells present next to capillaries in the body. The levels of both O_2 and nutrients are limited in cells further away from the outer rim of the spheroid. These cells mirror hypoxic cancer cells *in vivo* that are distant from the vasculature, with apoptotic/necrotic areas evident in the centre of the spheroids (reviewed in [364]) (figure 10).

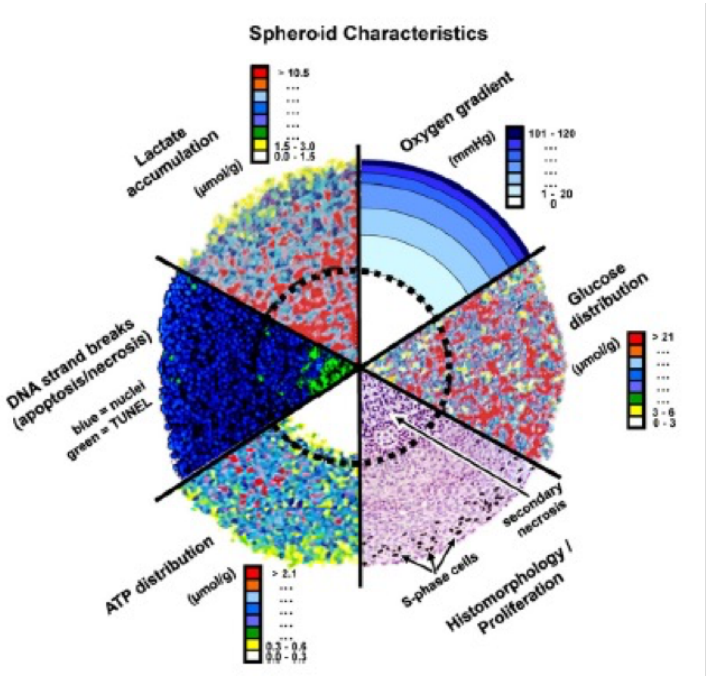

Figure 10: Multicellular tumour spheroid characteristics.

Spheroids re-create many different aspects of the in vivo tumour microenvironment, including hypoxia and acidosis, which leads to the creation of necrotic, peri-necrotic and hypoxic areas within the spheroid. The proliferative and metabolic gradients found within cancers are also present in spheroids. The spheroid model enables the analysis of the effects of a drug in the context of diffusion gradients and adhesion and tight junction barriers. Heterogeneous cancer cell populations are present within the spheroids, with some cells in the normoxic layer undergoing proliferation, while at the core of the spheroid there are non-cycling/dead cells, with hypoxic cells present in between these two layers. This image is taken from [364], and is a combination of spheroid sections analysed by the tunnel assay, autoradiography, probing with oxygen microelectordes, and bioluminescence imaging.

1.15.3 3D invasion models

The invasion and migration of cancer cells from the primary tumour to other parts of the body (metastasis) is the main cause of patient mortality [270]. As a result, studies assessing the anti-metastatic ability of potential cancer drugs are of the upmost importance. There are many different methods for analysing the effects of pharmacological inhibitors on cancer cell invasion and migration [365]. The use of spheroids embedded into a 3D extracellular matrix (ECM, a collection of extracellular molecules secreted by cells that provides structural and biochemical support) is one such method used. This experimental set-up closely mimics that which occurs *in vivo*, with invasion occurring from clusters of cells with established cell-cell interactions into the ECM [365]. A range of different ECM gels can be used

in these experiments. For studies conducted in breast cancer, the use of collagen type I further re-creates the *in vivo* conditions as there is a high proportion of this protein present within breast cancer stroma in the body [366].

1.15.4 Patient-derived material

The reconstruction of the 3D tumour environment of cancers through the use of models such as spheroids goes some way to reproducing the pathobiology of cancer. However, as with any cancer cell model, there are problems with the spheroid model described. One disadvantage encountered with spheroid invasion assays concerns the cancer cell lines used in these experiments. Many researchers use cell lines that represent certain sub-types of cancer. However, studies have shown that cancer cell lines cultured for extended periods *in vitro* can lose some of the biological traits of the cancer from which they derived, meaning that they may no longer represent the primary cancer from which they originated [367, 368]. 3D invasion assays conducted with primary tissue derived from human patients, cultured in a similar manner to that of spheroids in 3D [354, 355], do not encounter this problem. The analysis of the effects of pharmacological inhibitors on human tumour explants, which contain cells usually found within the cancer stroma in addition to the tumour cells [369], represent an improvement over the spheroid invasion assays, allowing the analysis of anti-cancer agents on heterogeneous cancer material and varying tumour sub-types. However, the cell culture environment is unable to totally re-create the complex multicellular and cell-extracellular matrix interactions that occur *in vivo* that contribute to the major aspects of breast cancer biology [352].

1.15.5 *In vivo* systems

The growth of human breast cancer cell lines in immunocompromised mice as xenografts allows the investigation of the effects of anti-cancer agents in an *in vivo* environment. Xenografts represent a model that is frequently used in breast cancer research (reviewed in [352, 356]). There are many advantages in the use of mice in cancer research, as they enable the testing of anti-cancer compounds in a model that re-creates some features of the human tumour micro-environment, including stromal and vasculature elements, along with relative ease of measurements of the effects of

drug treatment in this environment (reviewed in [356]). However, these strengths are counterbalanced by various limitations. The deficiencies associated with human cancer cell lines represents one such drawback (already discussed in section 1.15.4). The immune system is thought to play a key role in cancer progression [370, 371], and the use of immunodeficient mice therefore makes it impossible to precisely model tumourigenesis. Therefore, as with all of the models discussed so far, xenografts remain only an approximation of breast cancer disease.

1.16 Aims

The abnormal regulation of H^+ ions in both normoxic and hypoxic cancer cells, leading to a reversed pH gradient in these cells when compared to normal cells, is a phenomenon that is considered to be one of the most distinctive characteristics of cancer [269]. This feature of tumour cells, however, has only undergone limited exploitation in the treatment of cancer to date. The targeting of pH regulating proteins, implicated in the initiation and/or regulation of the reversed pH gradient in cancer cells, could result in more effective therapies that target tumour cells more selectively, causing less toxicity, leading to an overall improvement in cancer treatment.

Low O_2 conditions have been shown to lead to the increased expression of both the tumour-associated carbonic anhydrases (section 1.10) and NHE1 (section 1.11). While little has been published relating hypoxia/HIF to V-ATPase expression (section 1.12), some hypothesise that, due to its importance in pH regulation, hypoxia may have some part to play in the regulation of V-ATPase [261]. Studies also indicate that the activity of both CAIX and NHE1 is similarly affected by changes in O_2 concentration, with increased levels of activity recorded in hypoxic conditions [254, 256, 372-374]. With these studies in mind, we hypothesised that inhibitors targeting the tumour-associated carbonic anhydrases, NHE1 and V-ATPase would be more effective under hypoxic conditions. Based on this hypothesis and rationale, the aim of this project was to assess the therapeutic effects of inhibitors targeting these pH regulating proteins on cancer cell proliferation and

invasion, comparing their effects on cancer cells present in both aerobic and hypoxic conditions.

While prior studies have exhibited the inhibitory effects of targeting these pH regulating proteins separately, a comparison of the effects of targeting these proteins within one study in differing O_2 conditions has not previously been performed. Initial experiments were conducted in 2D, before moving into 3D, using models that more realistically re-create the *in vivo* tumour microenvironment (figure 11).

For the initial stage of the project, we sought to investigate the expression levels of the tumour-associated carbonic anhydrases, NHE1 and V-ATPase in different breast cancer cell lines, in order to assess the expression of these target proteins in various O_2 conditions in the 2D and 3D cancer cell models employed in this project. Experiments comparing the effects of inhibitors targeting each of the pH regulating proteins on both cancer cell number in 2D, and cancer cell invasion in 3D using multicellular tumour spheroids, were also carried out in both aerobic and hypoxic conditions to evaluate the effects of oxygenation on the response of the cells to treatment, while also enabling a direct comparison of the anti-cancer effects of these inhibitors to each other. pH has been shown to have a role in cancer cell radio-resistance (section 1.13.3); experiments comparing the effects of combining drugs targeting the 3 pH regulating proteins with irradiation were also carried out. Further work was then performed with the agents identified as having the most promise. Additional invasion assays were conducted with explant tissue derived from human patients, a model that more realistically re-creates the *in vivo* tumour microenvironment (section 1.15.4). Lastly, the effects of inhibitors targeting the pH regulating mechanisms of cancer cells were assessed using *in vivo* mouse breast cancer models.

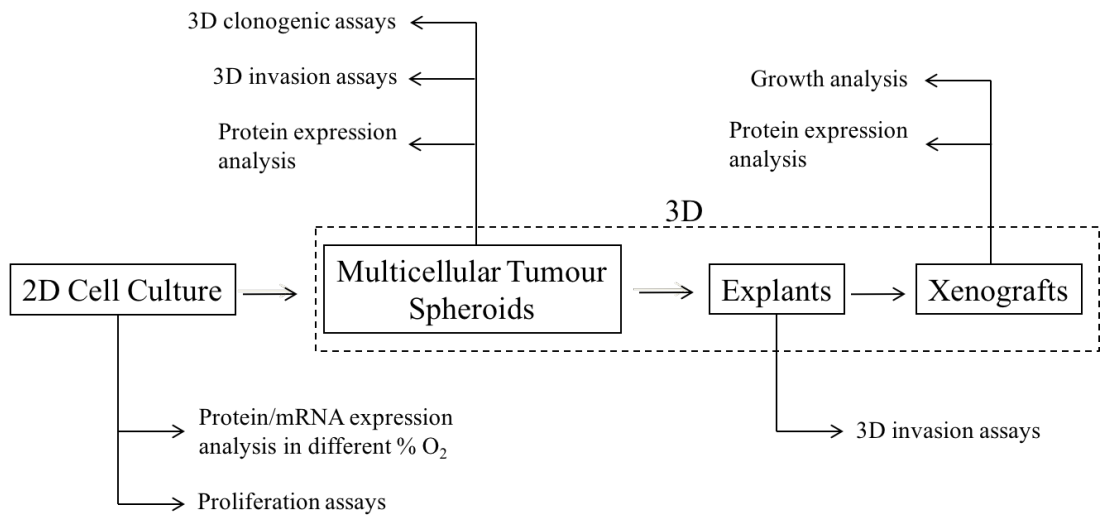

Figure 11. Project outline.

2 Chapter 2: Materials and Methods

2.1 Cell Culture

The breast cancer cell lines MCF-7, MDA-MB-231 and HBL-100 were chosen for this study due to their ability to form compact spheroids for 3D cell culture studies, in addition to their differing molecular classification and traits (see table 2). These breast cancer cells were acquired from either American Type Culture Collection (ATCC) or Public Health England (PHE, Salisbury, UK). The stocks of cells were authenticated by short tandem repeat (STR) profiling, undertaken by PHE in December 2014. Mycoplasma testing was performed within the lab by Helen Caldwell, with samples also sent to the IGMM for analysis at routine intervals.

All cells were incubated at 37°C in a humidified atmosphere containing 5% CO_2. Cells were cultured in Dulbecco's Modified Eagle Medium (DMEM, Gibco) supplemented with 10% heat-inactivated fetal calf serum (PAA) and 50 U ml^{-1} penicillin and 50 mg ml^{-1} streptomycin. Cells were grown to confluence with intermittent medium changes and harvested by incubation with trypsin/EDTA (ethylene-diamine-tetra-acetic acid) solution. New stocks of cells were obtained after 30 passages from STR authenticated stocks.

Cell line	Origin	Classification	Description
MCF-7	Pleural effusion of patient with adenocarcinoma	Luminal A	$ER^+/PR^+/HER2^-$
MDA-MB-231	Pleural effusion of patient with adenocarcinoma	Basal B	$ER^-/PR^-/HER2^-$
HBL-100	Milk from healthy nursing mother	Basal B	$ER^-/PR^-/HER2^-$ Harbours SV40 genome

Table 2. Breast cancer cell lines studied.

The effect of targeting the tumour associated carbonic anhydrases IX and XII, NHE1 and V-ATPase, in addition to the expression levels of target proteins and mRNA, was assessed in 3 cancer cell lines with varying molecular classification and traits [375, 376].

Aerobic cells were cultured in atmospheric oxygen conditions (20% O_2) in an incubator. Cells were cultured in lower oxygen concentrations using a hypoxic chamber (Whitley H35 hypoxystation); these cells were maintained at 0.5%, 2% or 7% O_2 and 5% CO_2, balanced with N_2, for up to 72h. Cells were also cultured in the hypoxic chamber for over 10 weeks at 0.5% O_2. The pre-gassing of media, PBS and tissue culture plastics was performed for the experiments conducted on the hypoxic cells, with these materials placed into the hypoxystation 24h before use to allow the O_2 levels to equilibrate.

2.2 Pharmacological inhibitors

The NHE1 inhibitor DMA (5-(N,N-Dimethyl)amiloride hydrochloride) was purchased from Sigma. The CAIX inhibitors were gifted from Claudiu Supuran of the University of Florence. The V-ATPase inhibitor bafilomycin A1 was purchased from Wako Pure Chemical Industries, Ltd. DMA was re-suspended in sterile water, while both the CAIX and V-ATPase inhibitors were dissolved in DMSO.

2.3 Sulforhodamine B (SRB) assays

The Sulforhodamine B (SRB) assay was established in 1990 as a new approach for anticancer drug screening [377]. This method relies on the capacity of the SRB protein dye to bind to the basic amino acids of fixed proteins electrostatically in a pH-dependent manner [377-379]. Because this is a rapid and inexpensive method to use, SRB assays are frequently used to assess the effects of drugs on cancer cell number, and have previously been used to test compounds that are chemically similar to one another in pre-clinical drug development studies [380]. This method was used to assess and compare the effects of drugs targeting CAIX, NHE1 and V-ATPase on cancer cell number in differing O_2 conditions.

Cells were fixed post-treatment with 50 µl/well of 25% TCA (trichloroacetic acid, Sigma) for 1h at 4°C, and washed with H_20 (10x washes). The fixed cells were stained with 50 µl/well of SRB dye solution (Sigma) for 30 minutes, and the SRB washed off with 1% glacial acetic acid (VWR) (4x washes). The protein-bound SRB

was solubilised using 150 µl of Tris buffer solution (Sigma). Optical density (OD) was measured at 540 nM on a plate reader (BP 800 Biohit), and IC_{50} values were calculated on Excel using the Excel package Fit Designer.

Due to the differential effects of O_2 concentration on the growth rate of cells, differing numbers of cells were seeded depending on the culturing conditions. 500 cells were seeded per well for the MCF-7 and HBL-100 cell lines, while 700 cells were seeded per well for the MDA-MB-231 cells cultured in 20% O_2. 2000 and 4000 cells were seeded for the acute and chronic hypoxic cells respectively. If the optical density (OD) values measured are below 3.0, the relationship between OD and cell number is linear. However, if the OD values are greater than 3.0, then there is a risk that saturation may be occurring. Each of these seeding densities led to OD values below 3 by the end of the 120h drug treatment in the differing O_2 conditions (Figure 12).

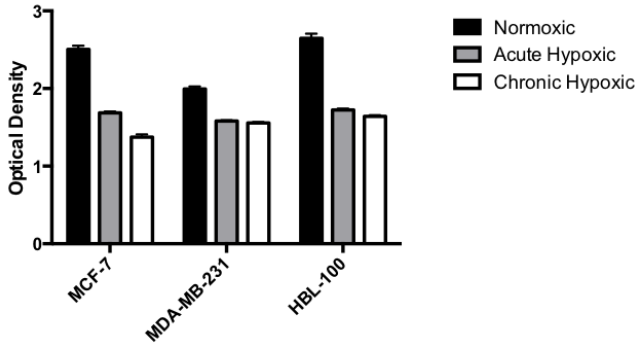

Figure 12. Optical density (OD) values from the 3 cell lines cultured in differing O_2 conditions indicate the cell seeding numbers used led to a linear relationship between cell number and the OD values obtained.

Readings from control cells 120h after initial drug treatment. In 20% O_2 conditions, 500 MCF-7/HBL-100 and 700 MDA-MB-231 cells were seeded per well. 2000 cells were seeded per well for the acute hypoxic cells cultured in 0.5% O_2, while 4000 cells were seeded per well for the chronic hypoxic cells cultured in 0.5% O_2 conditions.

2.4 Knockdown of FIH-1 in MCF-7 cells using siRNA

There are different methods available to researchers to silence genes in order to study gene or protein function. RNA interference is a natural mechanism present within the cell that suppresses gene expression, and can be exploited to specifically inhibit the

function of target genes [381]. To investigate the effects of FIH-1 on CAIX expression in MCF-7 cells, short interfering RNA (siRNA) was used to reduce factor inhibiting HIF-1 (FIH-1) protein expression levels.

Solutions of 4 siRNAs targeting FIH-1 (Dharmacon, L-004073-03), individual siRNAs targeting FIH-1 (Dharmacon, L-004073-19, L-004073-20, L-004073-20, L-004073-22) and scrambled siRNA (Dharmacon, [D-01810-01-20]) were prepared using the protocols outlined [382], and siRNA transfection was carried out using the recommended protocols [383]. Briefly, 150,000 MCF-7 cells were seeded into the wells of a 6-well plate for the low O_2 experiments, and 50,000 MCF-7 cells seeded per well for the cobalt chloride ($CoCl_2$) experiments. Transfection was performed 24h after seeding using 50 nM concentrations of siRNA with Dharmafect transfection reagent 1 (Dharmacon, T-2001-03). The cells were incubated for 48h, before the transfection/siRNA + DMEM solution was removed from each well and replaced with DMEM containing FCS. These cells were cultured for a further 72h before lysate acquisition. In the aerobic MCF-7 $CoCl_2$ experiments, 400 μM $CoCl_2$ was added at 24h intervals after the removal of the transfection/siRNA + DMEM solution, with lysates acquired every 24h up to 72h after the initial $CoCl_2$ treatment.

2.5 Protein detection in cell lines

Western blotting is a technique widely used by researchers to detect and quantify the levels of specific proteins from a complex mixture of proteins isolated from cells [384]. This method was used to detect and quantify the levels of proteins acquired from both whole-cell and nuclear/cytoplasmic lysates obtained from the 3 breast cancer cell lines.

2.5.1 Whole cell lysate acquisition

At the time of lysate acquisition, the cells were washed with ice-cold PBS and incubated for 10 mins on ice with 400 μl of lysis buffer [5 mM EGTA (Sigma) pH 8.5, 50 mM Tris (Sigma) pH 7.5 and 150 mM NaCl (Sigma)] containing 100 μl phosphatase inhibitor cocktail 2 (Sigma), 100 μl phospahatase inhibitor cocktail 3

(Sigma), one complete protease inhibitor tablet (Roche), 50 µl aprotinin (Sigma) and 1% Triton X-100 (Sigma). Samples were spun at 13,000 g at 4°C for 6 mins. The supernatant was isolated and stored at -80°C.

2.5.2 Nuclear/cytoplasmic lysate acquisition

At the time of lysate acquisition the cells were washed with ice-cold PBS, 1 ml of PBS was added, and the cells released from the plate using a cell scraper. The PBS/cell solution was spun at 4°C at 13,000 rpm for 1 min, the supernatant was discarded and the pellet was re-suspended in 0.4 ml of lysis buffer [10 mM HEPES pH 7.8 (Sigma), 10 mM KCl (Sigma), 2 mM $MgCl_2$ (Sigma), 0.1 mM EDTA (Sigma)]. The lysates were left on ice for 15 mins, after which 15 µl of IGEPAL CA-630 (Sigma) solution was added. The samples were mixed by vortexing and were then spun at 13,000 rpm for 1 min. The resulting supernatant was the cytoplasmic fraction. 50 µl of a solution made up of 50 mM HEPES pH 7.8, 50 mM KCl, 300 mM NaCl (Sigma), 0.1 mM EDTA and 10% sterile glycerol (VWR) was then added, and the samples were placed into a rotating table and slowly spun at 4°C. After 20 mins, the samples were spun at 13,000 rpm for 5 mins at 4°C. The supernatant was the nucleic fraction. The samples were stored at -80°C.

2.5.3 Bicinchoninic acid (BCA) protein assay

BCA assays were carried out to determine the protein concentrations of the lysates obtained. An 8-point standard curve was created using a 1 mg/ml protein standard (Sigma, P0914). A 1:50 dilution of copper (II) sulphate (Sigma, C2284) in BCA solution (Sigma, B9643) was made up as the assay reagent. 5 µl of the lysate samples were diluted 1:10 in distilled water in separate 12 x 75mm borosilicate glass tubes (Fisherbrand, 14-961-26), and 1 ml of the assay reagent was added to each of these. All the samples were vortexed and incubated at 60°C for 15 mins. 200 µl of the standards and samples were pipetted into the wells of a 96-well plate in duplicate, and the plate was read at 540 nm using a microplate reader (Biohit BP800).

2.5.4 SDS polyacrylamide gel electrophoresis

Cell lysates (40 μg for whole cell samples, 10 μg for nuclear/cytoplasmic samples) prepared in 4x Laemmli sample buffer (Bio Rad) were denatured by placing into a heating block at 60°C for 60 mins. Samples were electrochemically separated by sodium dodecyl sulphate polyacrylamide gel electrophoresis (SDS-PAGE) with either the vertical electrophoresis systems Bio-Rad Mini-PROTEAN ® 3 or the Bio-Rad Protean II xi cell, using a resolving gel made up of acrylamide, 1M Tris pH 8.85 (Sigma), 10% SDS (Sigma), and dH_2O. The stacking gel consisted of 3.6% acrylamide (Severn Biotech Ltd), 0.375M Tris pH 6.8, 10% SDS and dH_2O. Polymerization was initiated by adding TEMED (Bio Rad) and 10% APS (ammonium persulphate) (GE Healthcare Life Sciences). Samples were loaded into the wells alongside a pre-stained protein marker broad range (Cell Signaling), and electrochemically resolved in running buffer (192 mM Glycine (Sigma), 25 mM Tris, 0.1% (w/v) SDS) at 100V for the stacking gel and 180V for the resolving gel.

2.5.5 Western blotting

The resolved proteins were electrophoretically transferred onto an Immobilon-P transfer membrane (Millipore) at 100V for 90 mins at 4°C (for the whole cell lysates protein transfer was performed at 30V overnight). The membranes were blocked for 1 hour at 4°C with blocking buffer solution (PBS and Li-Cor Odyssey Blocking Buffer) and probed overnight with primary antibody (dilutions are listed in tables 3 and 4). The membranes were washed twice with PBS-Tween20 (a 1:1000 solution of Tween20 (Sigma) and PBS), and incubated with fluorescently labelled secondary antibodies [IRDye 800CW (Li-Cor, 926-32210), IRDye 680LT (Li-Cor, 926-68021), 1:10,000 dilution] for 45 mins. The membranes were washed and placed on filter paper to dry before scanning using a Li-Cor odyssey scanner. The expression levels of the proteins were analysed using Image Studio Lite (Li-Cor), with the signal of the target proteins in each lysate sample was corrected for loading control.

Primary antibody	Working dilution	Source	Supplier/Cat No.
ATP6V1A polyclonal antibody (A01)	1:2,000	Mouse	Abnova/H00000523-A01
Purified mouse anti NHE1	1:1,000	Mouse	BD/611774
Purified mouse anti-human HIF-1α	1:250	Mouse	BD/610958
HIF-2 α antibody	1:1,000	Rabbit	Novus Biologicals/NB100-122
Carbonic anhydrase IX antibody, clone m75	1:6,000	Mouse	Bioscience Slovakia
FIH-1/HIF-1AN antibody	1:1,000	Rabbit	Novus Biologicals/NB100-428
Anti-MMP14 antibody [EP1264Y]	1:4,000	Rabbit	Abcam/ab51074
Cleaved PARP (Asp 214)(19F4)	1:8,000	Mouse	Cell signaling/9546

Table 3. Primary antibodies used in western blots to detect target protein expression.

Primary antibody	Working dilution	Source	Supplier/Cat No.
Anti-β actin antibody	1:8,000	Rabbit	Abcam/ab8227
α-Tubulin antibody	1:10,000	Mouse	Abcam/ab7291
Anti-Lamin B1 antibody [EPR8985(B)]	1:2,500	Rabbit	Abcam/ab133741
Anti-TATA binding protein TBP antibody	1:2,500	Mouse	Abcam/ab51841

Table 4. Primary antibodies used in western blots to detect proteins used as loading controls.

2.6 RNA processing, microarray analysis and data analysis

Both the RNA extraction and RNA amplification were carried out in collaboration with Arran Turnbull, Ed Jarman, Chrysi Xintaropoulou and Carlos Martinez.

RNA extraction was carried out using the *RNeasy Mini Kit* from Qiagen as per the manufacturers instructions [385]. RNA was reverse transcribed, amplified and labelled using the *Illumina ® TotalPrep™ RNA Amplification Kit* (Ambion)[386].

Samples were sent to Hologic Ltd (Manchester, UK), where the RNA was hybridized to whole genome HumanHT-12 v4 Illumina BeadChips, and the arrays were scanned with an Illumina iScan. Hologic Ltd provided the raw microarray scan result files. These raw gene expression files were filtered with Illumina probe detection P-value, and were log2-transformed and quantile-normalised with lumi Bioconductor.

2.7 Multicellular Tumour Spheroids

2.7.1 Multicellular tumour spheroid formation

Different cancer cell models have been developed to replicate the *in vivo* tumour microenvironment, with multicellular tumour spheroids representing one such model that is extensively used [360]. To produce these spheroids, single cell suspensions obtained from cancer cell lines grown in flasks as 2D monolayer cultures were transferred into a sterile spinner flask (VWR) containing a magnetic stirrer rod. The spinner flask was placed onto a Cellspin stirrer (Integra Biosciences), which was present inside a humidified incubator set at 5% CO_2 at 37°C.

2.7.2 Hypoxyprobe labelling and fixing of spheroids

Hypoxyprobe-1, a compound which has previously been used for the detection of hypoxic areas within different cancer models [387-390], was used to identify hypoxic regions within spheroids. The spheroids were transferred into 60 mm petri dishes and incubated with 100 μM hypoxyprobe for 1h before fixation with 4% formaldehyde.

2.7.3 Immunohistochemistry

The fixed spheroids were embedded, cut and mounted on glass slides. Sections were de-waxed in xylene and rehydrated in alcohol and water before antigen retrieval using a NaCitrate solution [0.1M citric acid (Sigma), 0.1M NaCitrate (Sigma)]. Slides were washed with PBS/Tween20, incubated in 3% H_2O_2 solution (Dako) and washed again before the addition of Total Protein Block (Dako). The sections were incubated for 1h with primary antibody diluted in antibody diluent (Dako, see table 5 for dilutions), followed with 30 mins in Envision Labelled Polymer (Dako) and 10

mins with DAB and substrate buffer (Dako, 1:50 dilution), with washes performed in between each step using PBS/Tween20. The sections were counterstained in hematoxylin for 1 min and brought through graded alcohols to xylene, and were then mounted in DPX mountant. Images of the sections were taken using Nanozoomer (Hamamatsu).

Primary antibody	Working dilution	Supplier/Cat No.
Hypoxyprobe antibody	1:500 – 1:8,000	Hypoxyprobe/HP1-100
Carbonic anhydrase IX antibody clone m75	1:1,000	Bioscience Slovakia
Human carbonic anhydrase XII/CA12 antibody	1:50	R and D systems/MAB2190
Purified mouse anti-NHE1	1:400	BD Biosciences/611774
FIH-1/HIF-AN antibody	1:1000	Novus Biologicals/NB100-428
Anti-MMP14 antibody	1:250	Abcam/ab51074
Human carbonic anhydrase XII/CA12 antibody	1:50	R and D systems/MAB2190
ATP6V1A monoclonal antibody (M02)	1:6,000	Abnova/H00000523-M02
Anti-human Ki67 antigen, clone MIB-1	1:300	Dako/M7240
Cleaved caspase-3	1:300	Cell signaling/9661S

Table 5. Antibodies used in immunohistochemistry.

2.7.4 Analysis of spheroid immunohistochemical staining

Developments in image acquisition technology and image analysis software have led to the increased use of computer-assisted image analysis of IHC staining [391]. The image analysis software Definiens has been shown to be a powerful tool for the analysis of protein expression levels in IHC-stained tissue [392]. Definiens Architect XD 64 Tissue Studio 4.1 was used to analyse target protein expression within the normoxic and hypoxic areas of spheroids.

The image analysis was conducted using the different 'cellular analysis actions' available in this software. The cellular analysis action performed was dependent on the location of staining (either nuclear, plasma membrane or intracellular). For each of the analyses conducted, the hypoxyprobe stained spheroids acted as a guide to determine the normoxic and hypoxic regions within each spheroid. Overall, 4 different methods of analysis were carried out.

The cellular analysis action ‘marker area detection’ was used to give the % area of caspase 3 staining. The first step in this analysis was to select the normoxic (blue region) and hypoxic (orange region) areas of the spheroids, using the hypoxyprobe-stained spheroid images as a guide (figure 13A, number 1). The analysis was then performed using the settings indicated in figure 13. The marker threshold value (represents the threshold of the IHC stain, with any objects above this threshold labelled as positive brown staining) was set to 0.2. The threshold hematoxylin stain is used to detect nuclei, with any objects above the threshold hematoxylin value classified as nuclei. Since caspase 3 staining was the only staining of interest here, this was set to the maximum value, preventing the detection of any nuclei. The minimum area was set to 1, to try and ensure that all areas of positive caspase 3 staining were detected. Yellow areas represent regions with caspase 3 positive staining detected (figure 13A).

Using the settings indicated in figure 13B, the cellular analysis action ‘nucleus detection’ (distinguishes and classifies IHC-stained nuclei and nuclei stained with hematoxylin, giving the overall % of nuclei present with brown staining) was used to assess Ki67 staining, with any nuclei having an IHC threshold above 0.2 labelled as Ki67 positive.

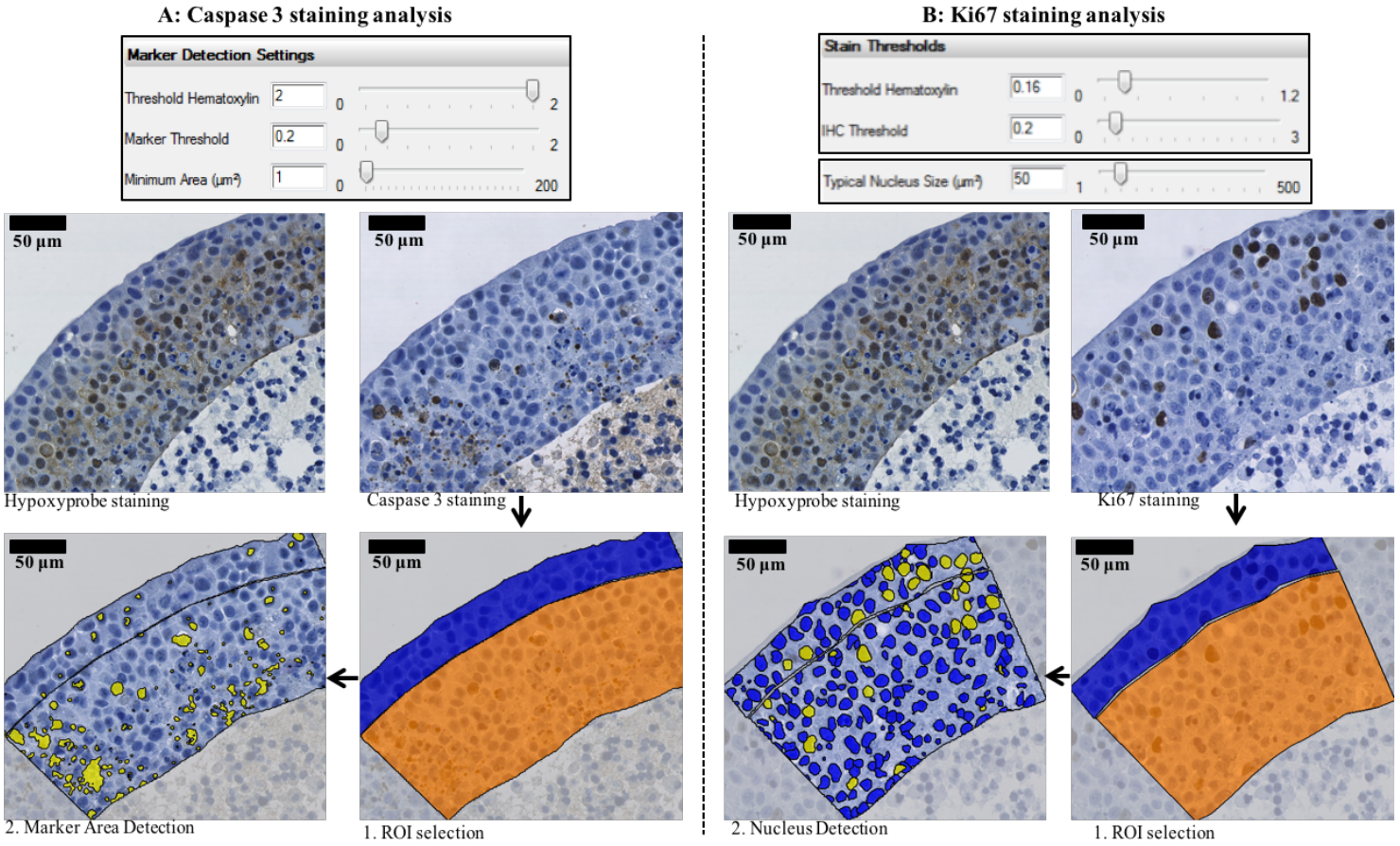

Figure 13. Caspase 3 and Ki67 Definiens analysis.

The settings used to determine the % area of caspase 3 staining (A) and the % of Ki67-positive nuclei (B) are shown, in addition to screen shots taken during the analysis

A number of different cellular analysis actions were combined to analyse the proteins that were present on the plasma membranes of cells. For CAIX, CAXII, NHE1 and MMP14 (all of which exhibited plasma membrane staining in spheroids of some of the cell lines), the same set of cellular analysis actions were used.

Using CAIX staining within HBL-100 spheroids as an example (figure 14A), the following analysis was carried out. Firstly, regions encompassing the normoxic and hypoxic areas were selected using the hypoxyprobe stained spheroids as a guide (figure 14A, number 1), followed by the nucleus detection action to detect the nuclei (figure 14A, number 2). The 'membranes and cells' cellular analysis action was then used (figure 14A, number 3), which simulates a cell body using the presence of the nuclei and the presence of plasma membrane staining. The same settings were used for this analysis for all of the different plasma membrane proteins analysed (figure 16A). The IHC threshold was set to 0 to include all areas for membrane detection, enabling regions without plasma membrane staining to be included in the analysis (figure 16A). Finally, the 'cell classification' cellular analysis action was carried out (figure 14A, number 4). This analysis sub-classified each cell based on plasma membrane marker intensity (white, no plasma membrane staining; yellow, low intensity plasma membrane staining; orange, medium intensity plasma membrane staining; red, high intensity of plasma membrane staining), giving the % of cells that had been identified within each subgroup.

This same set of cellular analysis actions was carried out for CAXII (figure 14B), NHE1 (figure 15A) and MMP14 (figure 15B) plasma membrane staining analysis. While the membranes and cells settings remained the same for each analysis (figure 16A), the settings used for the cell classification analysis varied with the target protein analysed (figure 16B).

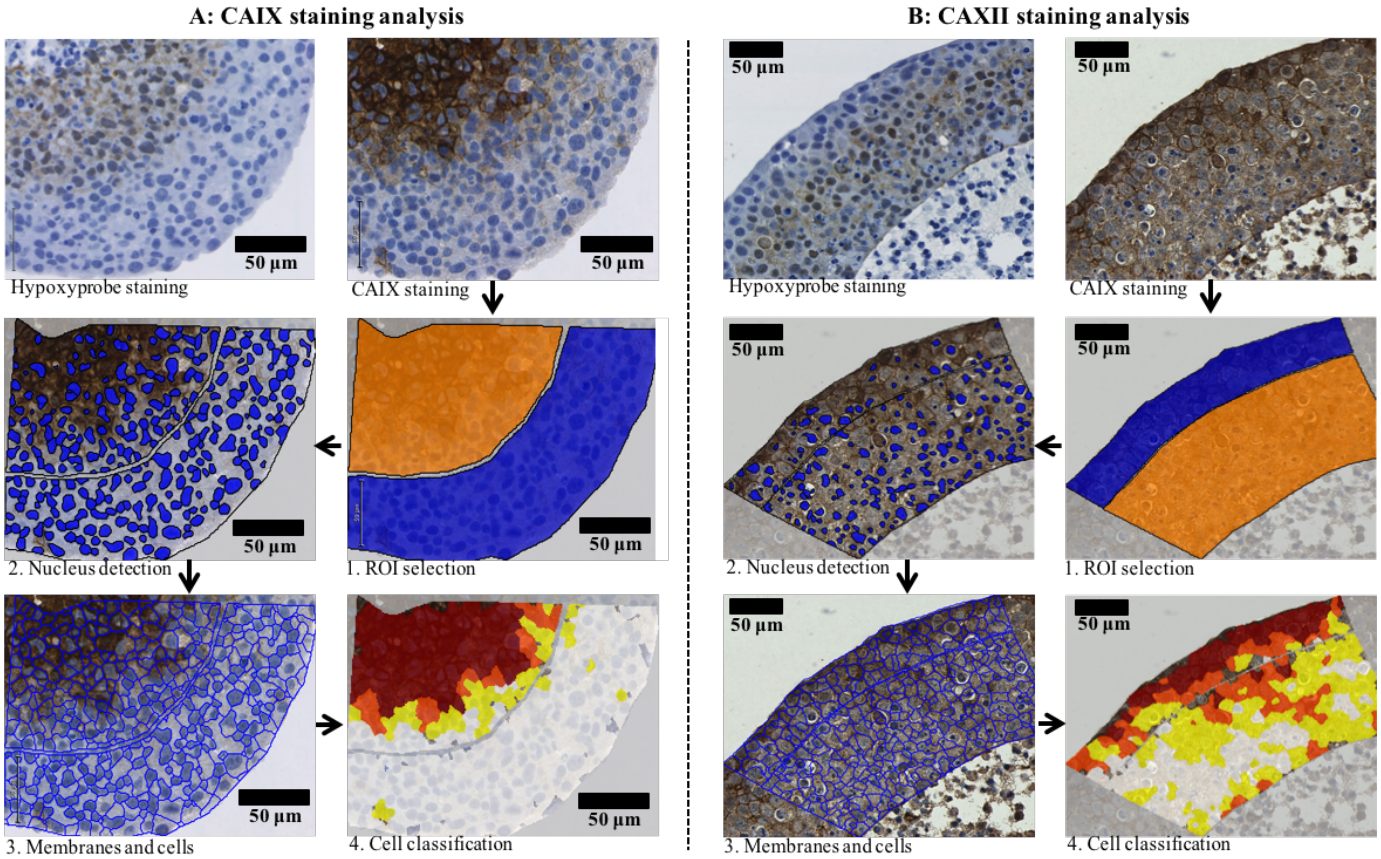

Figure 14. Plasma membrane CAIX and CAXII staining analysis.

Screenshots taken during plasma membrane CAIX (A) and CAXII (B) staining analysis, showing the region of interest selection (1), nucleus detection cellular analysis (2), membranes and cells cellular analysis (3), and cell classification cellular analysis (4). The screenshots showing the CAIX analysis have been rotated.

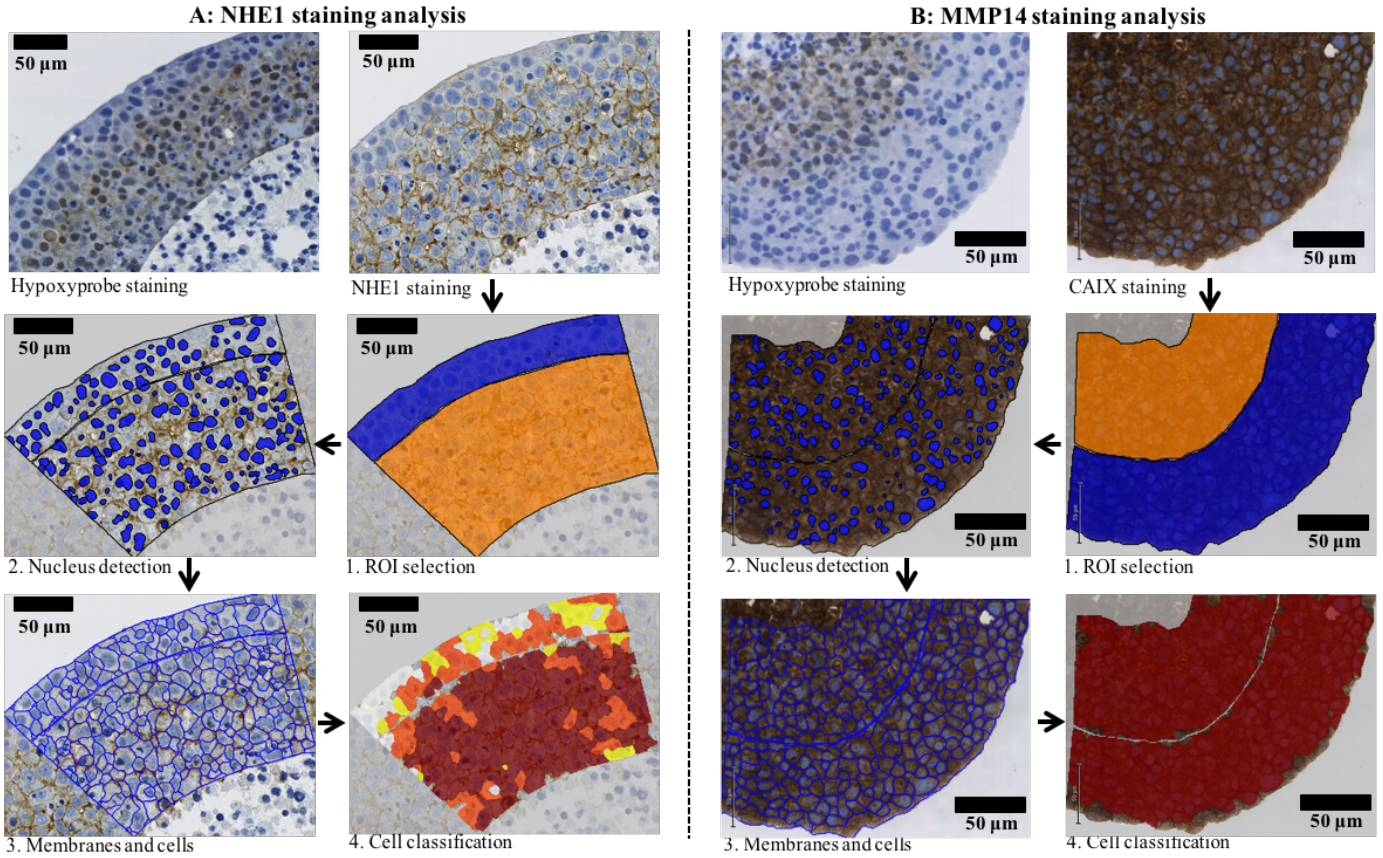

Figure 15. Plasma membrane NHE1 and MMP14 staining analysis.

Screenshots taken during plasma membrane NHE1 (A) and MMP14 (B) staining analysis, showing the region of interest selection (1), nucleus detection cellular analysis (2), membranes and cells cellular analysis (3), and cell classification cellular analysis (4). The screenshots showing the MMP14 analysis have been rotated.

A. Membranes and cells settings

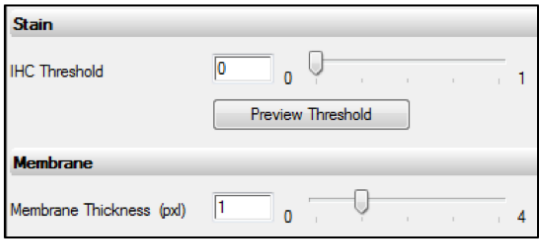

B. Cell classification settings

CAIX

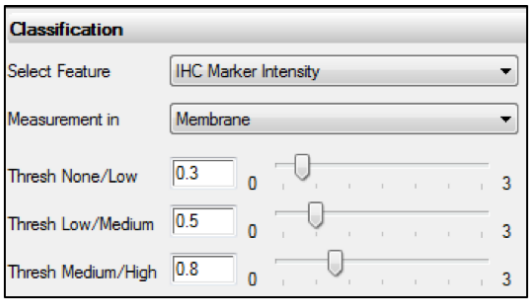

CAXII

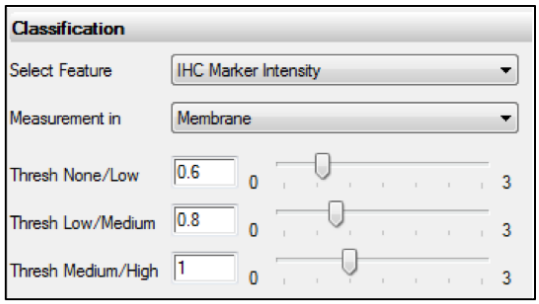

NHE1

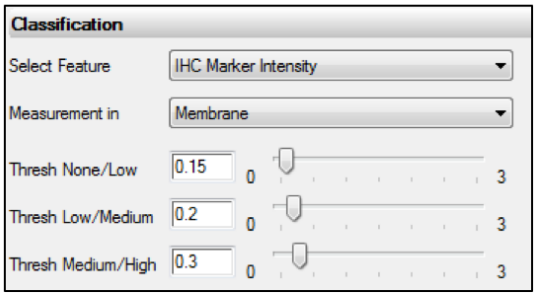

MMP14

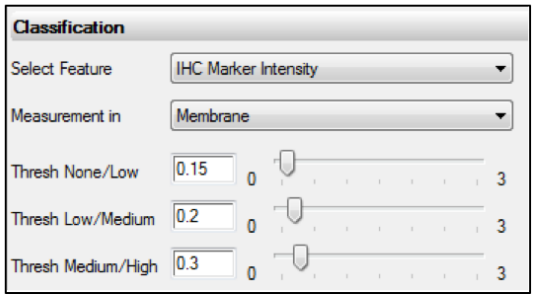

Figure 16. Settings used for the analysis of plasma membrane protein staining.

The membranes and cells cellular analysis settings (A) shown were used for each of the different plasma membrane proteins analysed. The cell classification settings employed varied with the protein analysed (B).

Intracellular localisation of proteins was also evident with some of the staining performed. A number of different cellular analysis actions were combined to measure intracellular protein expression levels. Using MMP14 staining in MCF-7 spheroids as an example (figure 18A), the following analysis was performed. Regions encompassing the normoxic and hypoxic regions of the spheroids were selected, and the nucleus detection cellular analysis action was carried out to detect the presence of nuclei (figure 18A, number 2). The 'cell simulation' cellular analysis action, which simulates a cell based on the presence of nuclei, was then performed (figure 18A, number 3). The simulation mode 'grow from nuclei' was chosen, in which cells grow from the nuclei to a maximum distance set by the user. The cell classification cellular analysis action was performed after this (figure 18A, number 4), which sub-classified each cell based on the intracellular staining intensity (white, no intracellular staining; yellow, low intensity intracellular staining; orange, medium intensity intracellular staining; red, high intensity intracellular staining).

This same set of analyses was carried out for CAXII staining analysis in MDA-MB-231 and HBL-100 spheroids (figure 18B, showing the analysis within HBL-100 spheroids), which exhibited intracellular staining of CAXII. The same cell classification settings were used for both MMP14 and CAXII analysis (figure 17).

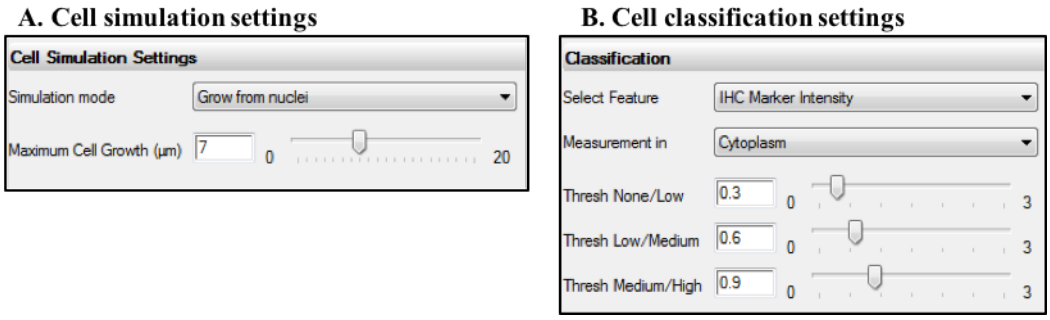

Figure 17. Settings used for the analysis of intracellular protein staining.

The cell simulation settings (A) and cell classification (B) settings were the same for the analysis of intracellular MMP14 and CAXII staining.

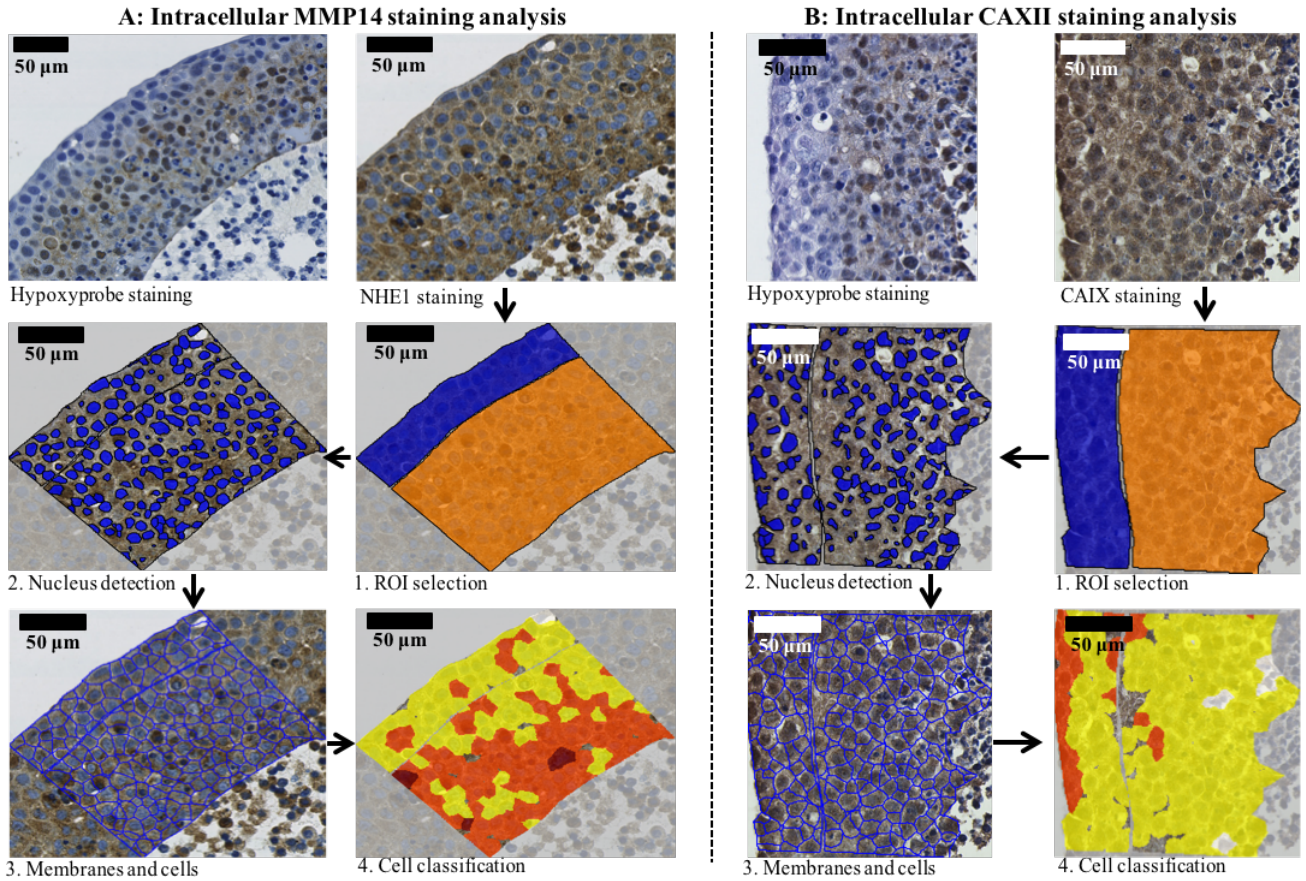

Figure 18. Intracellular MMP14 and CAXII staining analysis.

Screenshots taken during intracellular MMP14 (A) and CAXII (B) staining analysis, showing the region of interest selection (1), nucleus detection cellular analysis (2), membranes and cells cellular analysis (3), and cell classification cellular analysis.

2.8 3D invasion assays

2.8.1 Multicellular tumour spheroid invasion assays

The effect of inhibiting the pH regulating proteins of cancer cells on invasion was analysed through 3D invasion assays, using spheroids produced from each of the cancer cell lines. This assay is advantageous because the movement of cells through a 3D matrix closely mimics invasion *in vivo*, with invasion occurring from clusters of cells with established cell-cell interactions [365].

A collagen gel was created on ice by mixing 1:1000 filtered acetic acid, cell matrix type 1-A (pH 3.0, 3 mg/ml, Alphalabs), 0.22 M NaOH (Sigma), FCS, and 10x DMEM (Sigma) at concentrations of 45%, 25%, 10%, 10%, and 10% respectively. The CAIX, NHE1 and V-ATPase inhibitors were added to the collagen mix at the desired concentrations. Spheroids were taken up into the collagen, and the spheroid + collagen mix was pipetted into the wells of a 24-well plate, with the plate placed into the incubator for 1h to allow collagen polymerisation. A p200 pipette tip was used to release the collagen gel, and DMEM +/- drug added to each well. Images of the spheroids were taken by phase contrast microscopy (Axiovert S100, x2.5 objective).

MDA-MB-231 invasion was measured using a macro developed by Matthew Pearson, the Light Microscopy Application Specialist from the IGMM imaging facility (figure 19). This macro firstly processes the image to find the edges and highlights the cells using morphological filters, which improves the identification of cells by intensity thresholding. This thresholding can be altered if the auto step is not accurate. There are 3 readings given after the analysis; the total area, the spheroid area, and the invasive area alone. However, since the spheroid and invasion area alone measurements were not always accurate, the total area was the only measurement used for each spheroid (figure 19). While this macro worked well for the analysis of the MDA-MB-231 spheroids, it had trouble accurately measuring the HBL-100 spheroid areas at 72h. As a result, the HBL-100 spheroid areas were measured manually using the freehand selection tool in Fiji (figure 19).

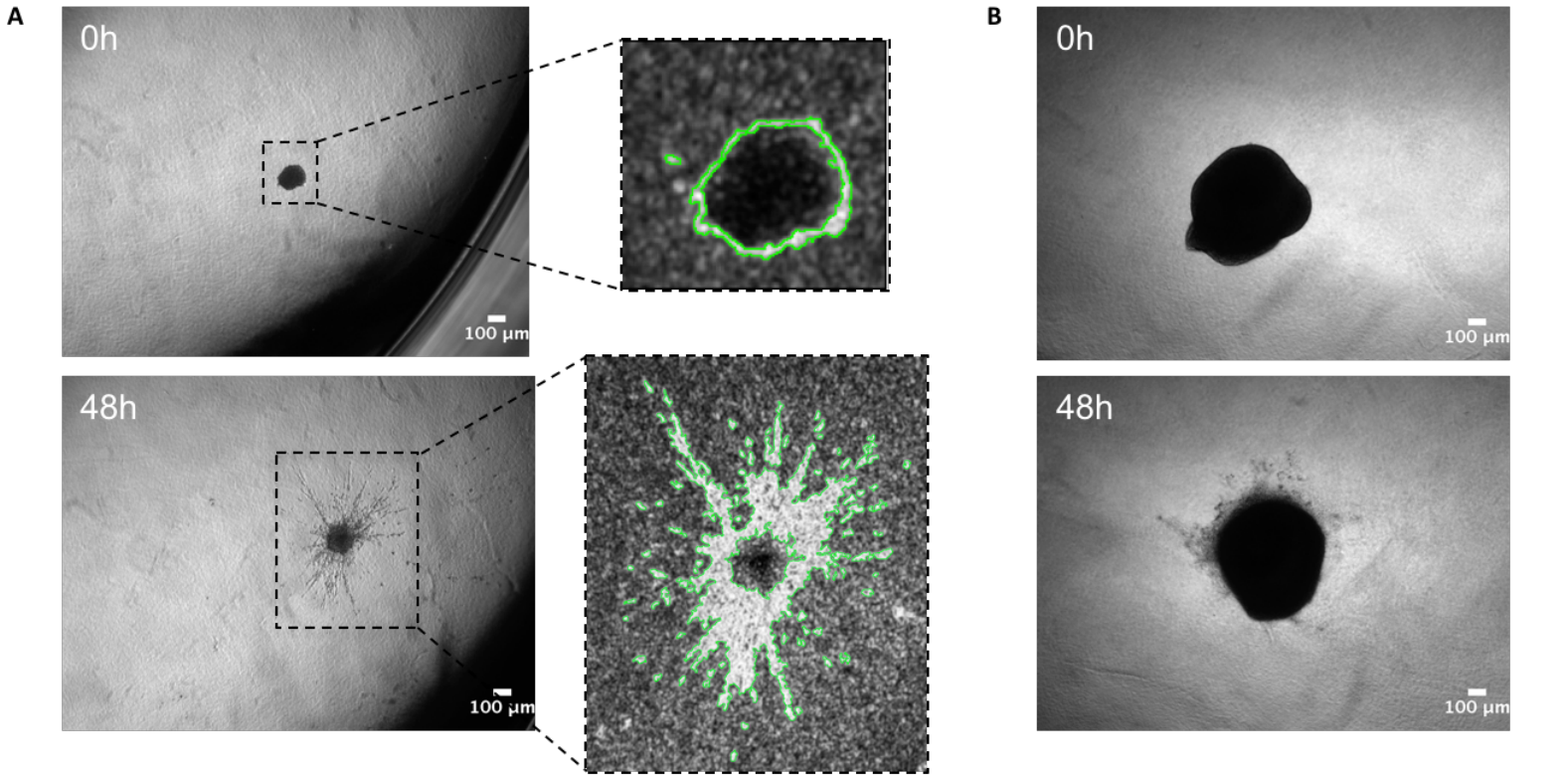

Total area 0h	Total area 48h	% invasion
5802	47810	824.0261979

Total area 0h	Total area 48h	% invasion
95893	158538	165.3280219

Figure 19. Spheroid invasion measurement.

The effect of drugs targeting pH regulators on MDA-MB-231 (A) and HBL-100 (B) spheroid invasion was measured using FIJI. Images show 1uM S4-treated MDA-MB-231 and control HBL-100 spheroids cultured in 20% O_2. MDA-MB-231 spheroid invasion was measured using a macro developed by Matthew Pearson, while HBL-100 invasion was measured manually using the freehand selection tool in FIJI.

2.9 3D invasion assays with explant tissue derived from human patients

These experiments were carried out in collaboration with Carol Ward. The collection of breast cancer biopsy material was given local ethical approval from the Lothian Tissue Governance Committee (10/S1402/33). Informed consent for the collection of tissue and its use was acquired from patient's prior to use. The breast tumour biopsy tissue was cut into 1 mm^3 pieces using a sterile scalpel on a sterilised surface. The method used is the same as outlined in section 2.8.5, however MEGM complete media (Lonza, Switzerland) was used instead of DMEM culture media in these experiments. Images were acquired and the media replaced every 5 days for 15 days overall. For the reversal of invasion experiments the explants were left to invade for 15 days before the first drug treatment, after which they were left to invade for 10 further days. % invasion was quantified in collaboration with Carol Ward using the freehand selection tool in Image J.

2.10 3D clonogenic assays

The Faxitron RX-650 was used to irradiate MDA-MB-231 spheroids. Dosimetry checks were conducted once a year by Alan Doig and Sanker Andiappa of the NHS Medical Physics Department, Western General Hospital. The dose-rate [mGy/s] was measured using an Innovision Dosimeter 35050A and 150cc Ion chamber 96020C. The Faxitron RX-650 used had no extra filtration, with x-rays passing through a 1.6 mm beryllium window. The spheroids used in these experiments had been cultured in a spinner flask for 1 week before use. The warm-up procedure was carried out for the Faxitron. Once completed, the spheroids were transferred from the spinner flask into petri dishes. The petri dish was placed onto the glass on the centre of the shelf, which turned at 2 RPM (revolutions per minute) to ensure uniform dosing. The distance from the focal spot of the x-ray tube to the cells (FSD) was 40.6 cm. The 0.5 Gy dose was given with the voltage set to 130 kV (kilovolts) for 30 seconds. Directly after irradiation, the spheroids were collected and placed into a universal, and a single cell suspension was made by syringing the media + spheroids through a fine bore needle. The suspension was centrifuged and the media discarded. The cell pellet

was re-suspended in 1 ml of DMEM, and the number of cells was counted twice to ensure an accurate cell count. 1,000 cells were placed into a new plate, with or without the drug. The cells were cultured at 20% O_2 for 1 week to allow colony formation. After 1 week, the media was removed and the cells were stained with 1,9-dimethyl-methylene blue zinc chloride double salt (Sigma, 341088). The plates were placed on a rocker and left for 45 mins to ensure all of the colonies were stained. The plates were then washed 3 times with H_2O and left to dry. Only colonies of 50 cells or over were counted.

2.11 Xenograft studies

These experiments were carried out in collaboration with Simon Langdon and Edward Jarman. Simon Langdon carried out the mice work, while myself and Edward Jarman performed the IHC staining and analysis. MDA-MB-231 tumour fragments were inserted subcutaneously into the flanks of adult nude mice. The tumours were grown to a diameter of 4-6 mm. A 90% tumour uptake efficiency was recorded. The mice were treated after 1 month of growth. There were 3 groups overall; control, FC9398A-treated and DTP348-treated, with 10 mice per group. 25 mg/kg/day of FC9398A and 10 mg/kg/day of DTP348 were given in saline via the intraperitoneal route from day 0 until day 4. Callipers were used to quantify tumour size, with measurements carried out 3 times a week. The volume of each of the tumours was calculated using the formula $\pi/6$ x width^2 x length. Relative tumour volume was worked out by dividing the volume of the tumour on day t (Vt) by the volume of the tumour on day 0 (V0), and then multiplying by 100. 10 days after the completion of treatment, the tumour tissue was taken out and fixed in formalin, embedded in paraffin, and sections cut. CAIX and Ki67 expression levels were analysed after immunohistochemistry was performed (section 2.7.3). For the Ki67 analysis, the percentage of Ki67 positive cells was measured in ten fields of xenograft section. For CAIX expression level analysis, the percentage area of CAIX positive cells was analysed using Image J.

3 Chapter 3: Expression analysis and pharmacological targeting of the tumour-associated carbonic anhydrases, NHE1 and V-ATPase

3.1 Introduction

The tumour-associated carbonic anhydrases CAIX and CAXII, NHE1 and V-ATPase have each been strongly linked to cancer cell survival and tumour progression (section 1.14). The reversed pH gradient of cancer cells, formed in part from these pH regulating proteins, has a large effect on cancer cell biology, influencing both the proliferation (section 1.13.2) and invasive potential (section 1.13.1) of cancer cells. While previous studies have exhibited the inhibitory effects of targeting these pH regulating proteins on cancer cell proliferation [310, 355, 393-397] and invasion [260, 310, 335, 355, 373, 398-400], a comparison of the effects of targeting these proteins within one study has not previously been performed.

The first stage of this project sought to investigate inhibitors targeting these pH regulatory molecules, assessing and comparing their inhibitory effects on cancer cell number and invasion in both aerobic and hypoxic conditions, evaluating their effects in differing O_2 conditions and identifying the most promising agent for further analysis. DMA and bafilomycin A1 were the inhibitors chosen to target NHE1 and V-ATPase respectively, with previous studies showing that both of these drugs have high selectivity for their target molecules [401, 402]. The carbonic anhydrase inhibitors used within this chapter were novel small molecule inhibitors of the sulphamate class (see section 1.14.1), developed by Fabrizio Carta of the University of Florence. These inhibitors have been shown to target the tumour-associated carbonic anhydrases IX and XII at low nM concentrations, while having much less activity against the other carbonic anhydrase isoforms not linked with cancer [310, 393].

As well as influencing cancer cell proliferation and invasion, pH has also been shown to affect the responsiveness of cells to irradiation (section 1.13.3). Previous studies have exhibited the radio-sensitisation potential of targeting CAIX [320, 403,

404] and V-ATPase [405]. While little has been published to date on the effects of combining irradiation with the inhibition of NHE1, the targeting of this pH regulator has been hypothesised as a possible mechanism to increase the effectiveness of radiotherapy [328]. The exact mechanism through which irradiation and drugs that target the pH regulation proteins of cancer cells might combine is not known. One way through which radiotherapy achieves its therapeutic effect is through the induction of apoptosis [406]. Acidic pHi is thought to have a permissive role in the apoptotic cascade (section 1.13.2); it is believed that pH regulating proteins such as the tumour-associated carbonic anhydrases may be protecting cancer cells through their capacity to maintain an alkaline pHi [404], and that the combination of irradiation with drugs targeting the pH regulation mechanisms of cancer cells may increase the extent of radiation-induced apoptosis occurring in the cells [403]. With this in mind, we hypothesised that the treatment of cancer cells post-irradiation with drugs that target the pH regulation proteins would sensitise these cells to radiotherapy through the induction of increased levels of apoptosis, and lead to a lower survival fraction when compared against either treatment alone. 3D clonogenic assays, comparing the effects of inhibitors targeting the tumour-associated carbonic anhydrases, NHE1 and V-ATPase in combination with irradiation, were carried out to test this hypothesis.

Studies have shown that the expression of the tumour-associated carbonic anhydrases and NHE1 are influenced by low O_2 concentrations (section 1.10). Even though the link between V-ATPase expression and hypoxia is not as evident, there are some who believe that hypoxia may also have a role in the regulation of V-ATPase [261]. Because the expression levels of the pH regulatory proteins in differing O_2 conditions were hypothesised to affect the response of cells to drug treatment, the initial experiments carried out within this Chapter assessed the expression of the 3 pH regulatory proteins in 2D, in a range of O_2 concentrations that have been shown to occur *in vivo* (section 1.7.2). Further expression analysis was also carried out using multicellular tumour spheroids, a 3D model system that more accurately re-creates the *in vivo* tumour environment (section 1.15.2), to assess whether similar expression patterns were also observed in 3D.

3.2 Results

3.2.1 2D protein and mRNA analysis shows that, of the 3 pH regulatory proteins analysed, the expression levels of the tumour-associated carbonic anhydrases are the most sensitive to changes in O_2 concentration

The preliminary experiments performed investigated the protein and mRNA expression levels of the pH regulatory proteins CAIX, NHE1 and V-ATPase in MCF-7, MDA-MB-231 and HBL-100 cancer cells cultured in a 2D environment in differing O_2 concentrations. The expression levels of HIF-1α and HIF-2α, transcription factors that enable hypoxic cancer cells to survival in low O_2 conditions [112], were also assessed.

HIF-1α, HIF-2α and CAIX protein expression levels were evaluated in the initial experiments conducted. Protein expression was measured in acute hypoxic cancer cells cultured for 24h, 48h and 72h in both 2% and 0.5% O_2 conditions, in addition to cancer cells cultured in 7% O_2 at the same time points. Protein expression levels within these cells were compared against cells cultured in 20% O_2 conditions for 24h (aerobic cells). To assess the effects of longer periods of hypoxia on protein expression, western blot analysis was also performed on lysates acquired from cells that had been cultured for 10 weeks in 0.5% O_2 conditions (chronic hypoxia). Further, the effect of re-oxygenation on target protein expression was also analysed in chronically hypoxic cancer cells that were re-oxygenated in 20% O_2 for 1 and 3 weeks before lysate acquisition.

Two bands were identified for HIF-1α (figure 20A, figure 21A and figure 22A), with changes in the intensity levels of these bands found to be similar in each of the cell lines cultured in the different O_2 concentrations (figures 20B-C, figure 21B-C, figure 22B-C). While increases in HIF-1α protein expression were seen in the 3 cell lines cultured in 2% and 7% O_2, significant increases in HIF-1α levels were only observed in the HBL-100 cell line at 2% O_2 (figure 22B-C). Although significantly higher levels of HIF-1α were observed in all 3 cell lines cultured in acute and chronic hypoxic conditions, the intensity of both the upper and lower bands was seen to

decrease by the 72h time point in 0.5% O_2 conditions in MCF-7 (figure 20B-C) and HBL-100 (figure 22B-C) cells.

HIF-2α expression was more variable between the cell lines in comparison to the results observed for HIF-1α. Hypoxic induction of HIF-2α was evident in two of the cell lines, with significant increases in HIF-2α levels detected in 0.5% O_2 concentrations in MDA-MB-231 cells (figure 21A and D), and in both 2% and 0.5% O_2 conditions in the HBL-100 cell line (figure 22A and D). Longer incubation times in 0.5% O_2 appeared to lead to a decrease in the levels of HIF-2α in both of these cell lines (figure 21D, figure 22D). There was no visible induction of HIF-2α seen in MCF-7 cells at any of the different O_2 percentages tested (figure 20A and D).

Because CAIX is a HIF-1α inducible protein [132], westerns were performed to analyse CAIX protein levels in the differing O_2 concentrations to assess the relationship between HIF-1α and CAIX within the 3 breast cancer cell lines. The CAIX protein levels observed varied despite the presence of similar amounts of HIF-1α in each of the cell lines. Significant increases in CAIX protein levels were observed in both acute and chronically hypoxic MDA-MB-231 (figure 21A and E) and HBL-100 (figure 22A and E) cells cultured in 0.5% O_2, with significant increases in CAIX protein expression also detected in the HBL-100 cells cultured in 2% O_2 conditions (figure 22E). Out of the 3 cell lines, CAIX expression levels within MCF-7 cells were the least responsive to hypoxic induction (figure 20A and E). Despite the presence of significantly higher levels of HIF-1α, no significant increase in CAIX expression was seen within MCF-7 cells in acute hypoxic conditions (24-72h in 0.5% O_2). Only chronically hypoxic MCF-7 cells exhibited a significant increase in CAIX expression (figure 20A and E). In each of the cell lines studied, re-oxygenation of the chronic hypoxic cells led to a reversion of CAIX protein intensities to levels that were similar to those of the aerobic cells (figure 20E, figure 21E, figure 22E), suggesting that the changes in expression of this protein observed in the chronic hypoxic cells are reversible and temporary.

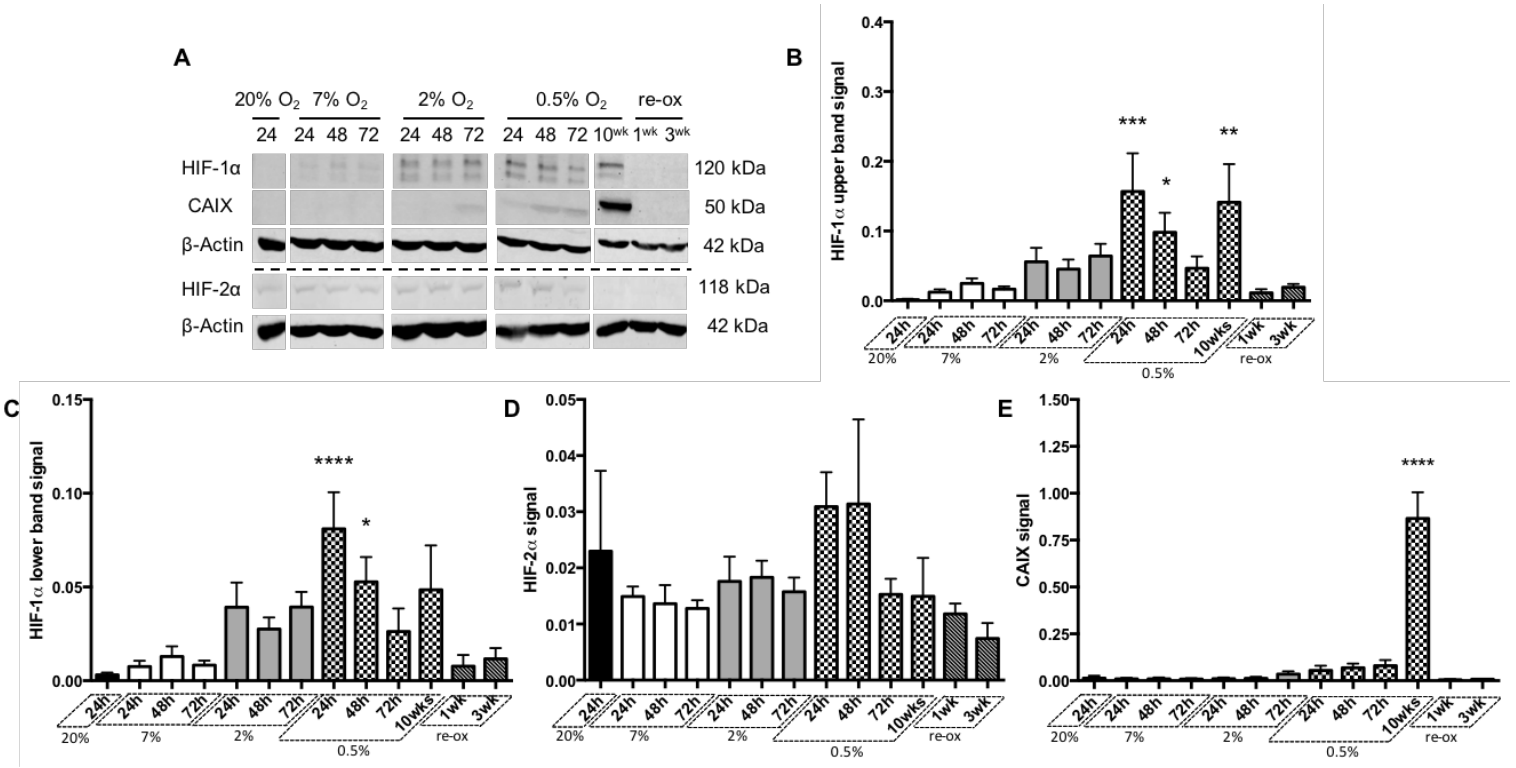

Figure 20. HIF-1α and CAIX protein expression are increased in MCF-7 cells in lower O_2 percentages, while no induction of HIF-2α is evident in this cancer cell line in hypoxic conditions.

*(A) Western blotting was performed to analyse the protein expression of HIF-1α, HIF-2α and CAIX in cells cultured in differing oxygen concentrations (20% O_2, 7% O_2, 2% O_2 and 0.5% O_2) for 24, 48 and 72h. Whole-cell lysates were also acquired from cells that had been present in 0.5% O_2 for 10 weeks, along with chronic hypoxic cells that were re-oxygenated for 1-3 weeks before lysate acquisition (re-ox). β-Actin used as the loading control. (B-E) Graphs show the densitometry measurements of HIF-1α (B, upper band. C, lower band), HIF-2α (D), and CAIX (E). Data expressed as mean ± SEM (n = 3 for the 10 week and re-ox samples, n = 4 for the rest of the samples). * $P \leq 0.05$, ** $P \leq 0.01$, *** $P \leq 0.001$, **** $P \leq 0.0001$ (One-way ANOVA followed by Dunnett's multiple comparison test performed, comparing each sample to the 20% O_2 group).*

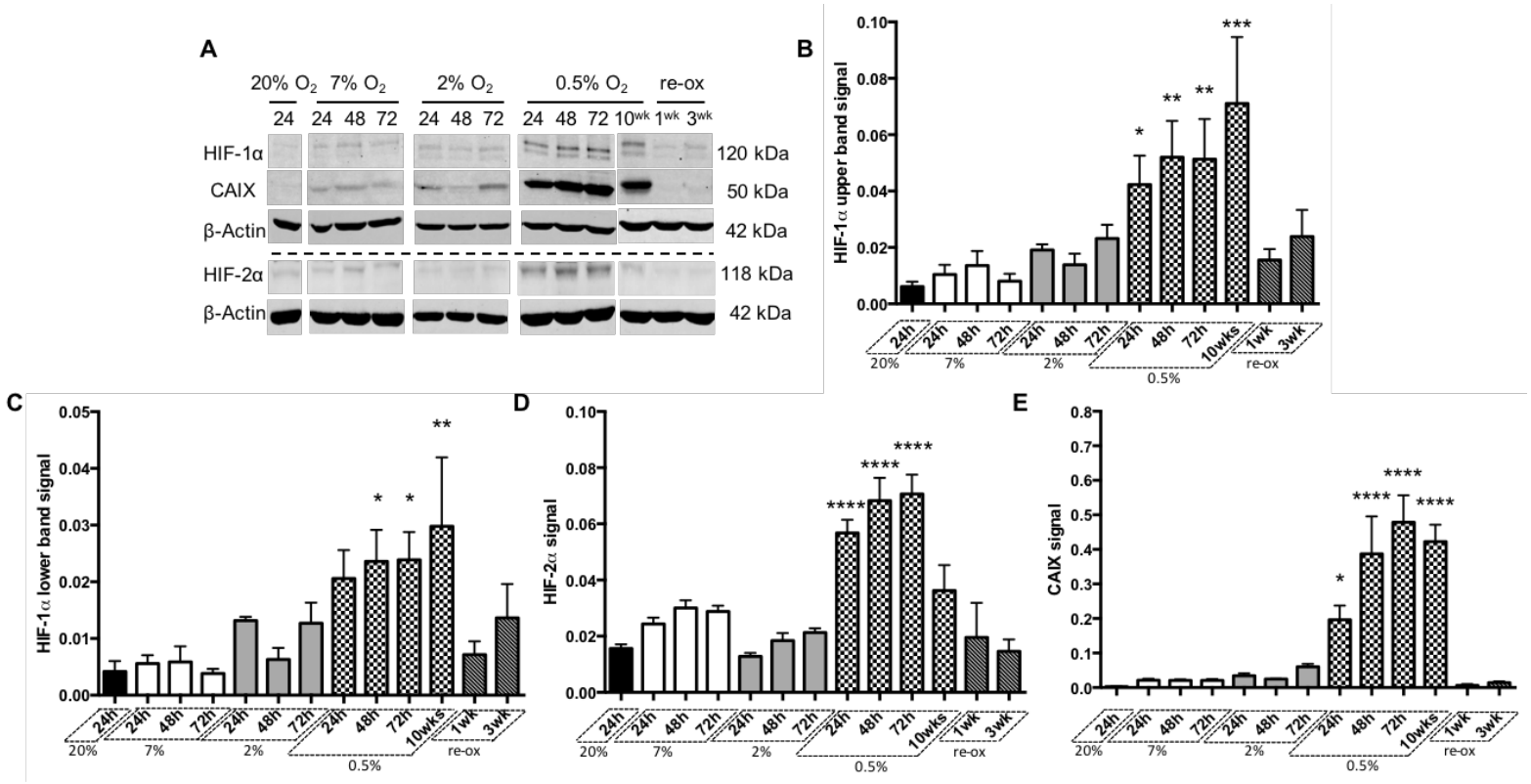

Figure 21. HIF-1α, HIF-2α and CAIX protein expression are increased in MDA-MB-231 cells in lower O_2 conditions.

*(A) Western blotting was performed to analyse the protein expression of HIF-1α, HIF-2α and CAIX in cells cultured in differing oxygen concentrations (20% O_2, 7% O_2, 2% O_2 and 0.5% O_2) for 24, 48 and 72h. Whole-cell lysates were also acquired from cells that had been present in 0.5% O_2 for 10 weeks, along with chronic hypoxic cells that were re-oxygenated for 1-3 weeks before lysate acquisition (re-ox). β-Actin used as the loading control. (B-E) Graphs show the densitometry measurements of HIF-1α (B, upper band. C, lower band), HIF-2α (D), and CAIX (E). Data expressed as mean ± SEM (n = 3 for the 10 week and re-ox samples, n = 4 for the rest of the samples). * P ≤ 0.05, ** P ≤ 0.01, *** P ≤ 0.001, **** P ≤ 0.0001 (One-way ANOVA followed by Dunnett's multiple comparison test performed, comparing each sample to the 20% O_2 group).*

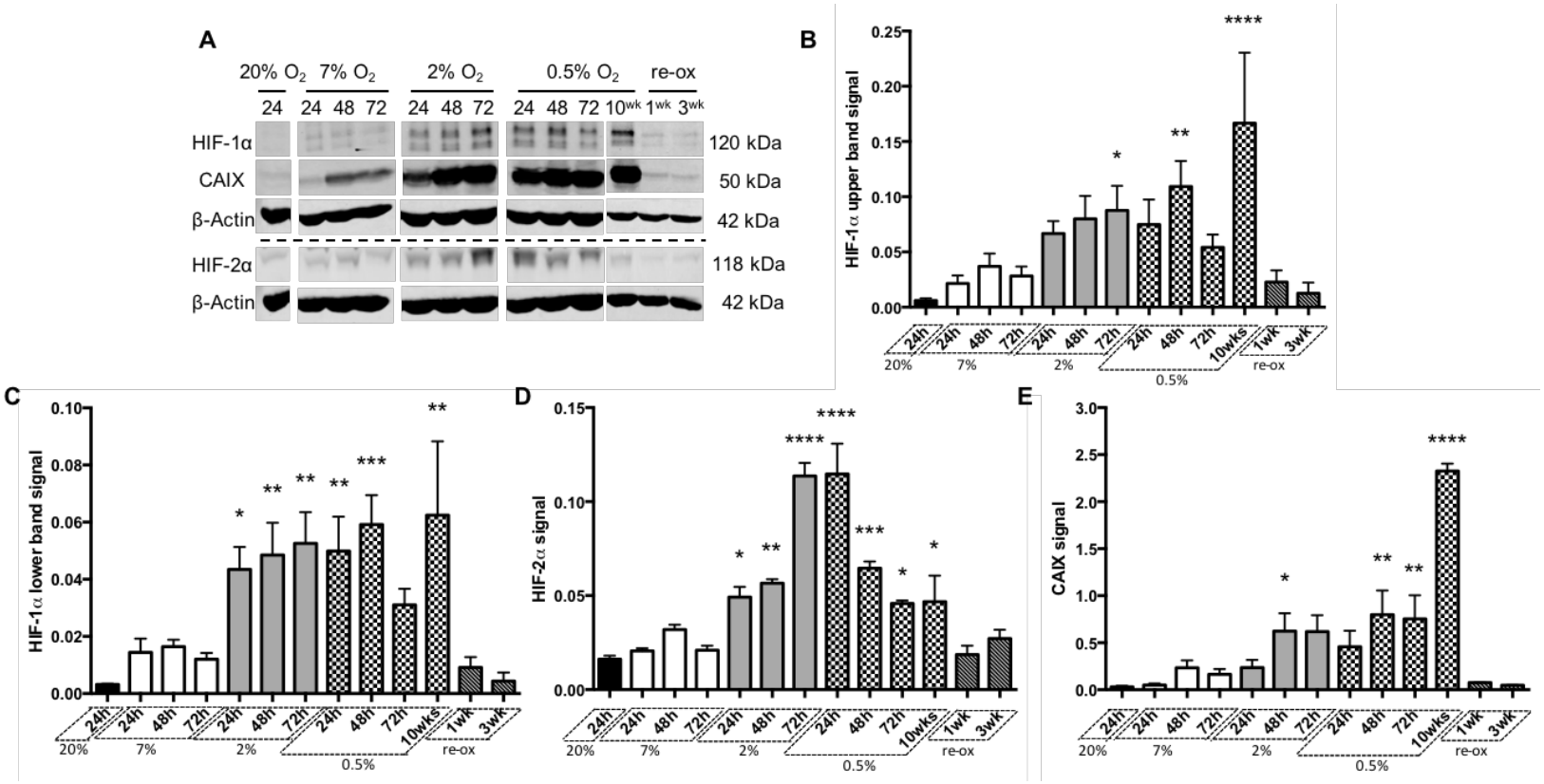

Figure 22. HIF-1α, HIF-2α and CAIX protein expression are increased in HBL-100 cells cultured in lower O_2 conditions.

*(A) Western blotting was performed to analyse the protein expression of HIF-1α, HIF-2α and CAIX in cells cultured in differing oxygen concentrations (20% O_2, 7% O_2, 2% O_2 and 0.5% O_2) for 24, 48 and 72h. Whole-cell lysates were also acquired from cells that had been present in 0.5% O_2 for 10 weeks, along with chronic hypoxic cells that were re-oxygenated for 1-3 weeks before lysate acquisition (re-ox). β-Actin used as the loading control. (B-E) Graphs show the densitometry measurements of HIF-1α (B, upper band. C, lower band), HIF-2α (D), and CAIX (E). Data expressed as mean ± SEM (n = 3 for the 10 week and re-ox samples, n = 4 for the rest of the samples). * $P \leq 0.05$, ** $P \leq 0.01$, *** $P \leq 0.001$, **** $P \leq 0.0001$ (One-way ANOVA followed by Dunnett's multiple comparison test performed, comparing each sample to the 20% O_2 group)*

In addition to the evaluation of target protein expression through western blots, expression analysis was also performed assessing the levels of target mRNAs in the 3 breast cancer cell lines by microarray analysis. mRNA levels were evaluated in hypoxic cells cultured in 0.5% O_2 for 24h (acute hypoxic cells), along with cells cultured in 0.5% O_2 conditions for 10 weeks (chronically hypoxic cells), with aerobic cells present in 20% O_2 conditions for 24h acting as the controls. Initial analysis assessed the mRNA levels of HIF-1α, HIF-2α, CAIX and CAXII.

No significant increases in either HIF-1α (figure 23A) or HIF-2α (figure 23B) mRNA levels were detected in the acute hypoxic or chronically hypoxic cells compared to the aerobic cells in any of the cell lines. The CAIX mRNA results largely mirrored those seen in the protein expression analysis, with CAIX mRNA levels significantly increased in the acute hypoxic and chronically hypoxic MDA-MB-231 (figure 23C-D) and HBL-100 (figure 23C) cancer cells. Although there were similar levels of HIF-1α observed in each of the cell lines, there was no significant increase in CAIX mRNA levels in hypoxic MCF-7 cells (figure 23C-D). Overall, the CAIX protein and mRNA expression results suggested that there were differences in the control of CAIX expression between the 3 cell lines.

The mRNA levels of CAXII, another tumour-associated carbonic anhydrase isoform whose expression levels have been shown to be influenced by hypoxia [242, 243], were also assessed, with varying results were observed between the 3 cell lines. High levels of CAXII mRNA were detected in MCF-7 cells cultured in 20% O_2 conditions, with a significant down-regulation in the levels of CAXII mRNA seen in both acute and chronic hypoxic conditions when compared against aerobic MCF-7 cells (figure 23E). These results differed to those seen in the MDA-MB-231 and HBL-100 cell lines, which exhibited 20-fold and 22-fold lower levels of CAXII mRNA respectively in 20% O_2 conditions compared to aerobic MCF-7 cells (figure 23E). While hypoxic conditions led to significant decreases in the levels of CAXII mRNA in MCF-7 cells, both MDA-MB-231 and HBL-100 cell lines had significantly up-regulated levels of CAXII mRNA levels in acute and chronic

hypoxia (figure 23E-F). Both CAIX and CAXII play similar roles in pH regulation within cells. The relative lack of CAIX mRNA and protein in MCF-7 cells compared to the 2 other cell lines may be explained by the increased amount of CAXII in these cells.

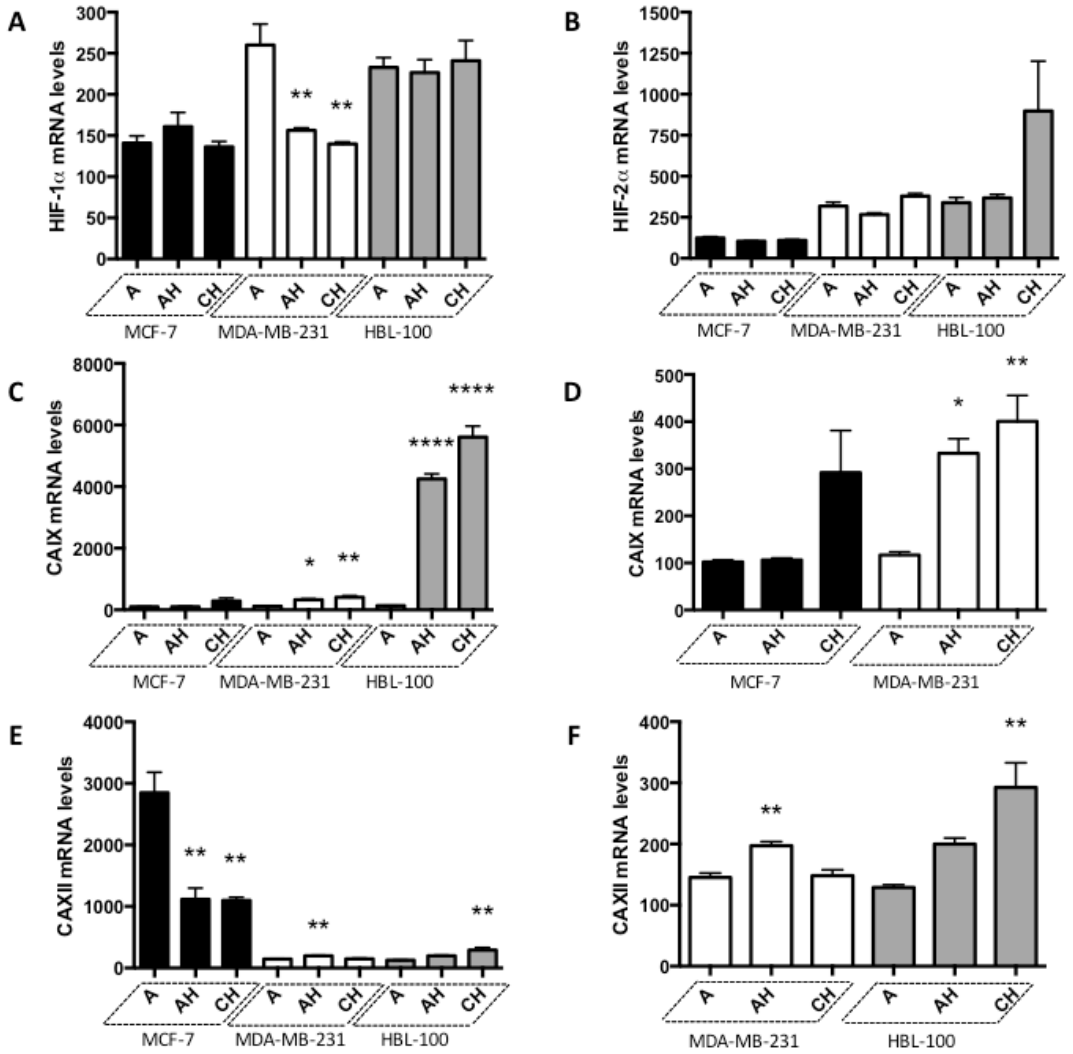

Figure 23. CAIX and CAXII mRNA levels exhibit a varying response to changes in O_2 conditions between the 3 cell lines, while HIF-1α and HIF-2α mRNA levels are much more consistent.

*HIF1α (A), HIF-2α (B), CAIX (C and D [D without HBL-100 data]) and CAXII (E and F [F without MCF-7 data]) mRNA levels were analysed in the 3 breast cancer cell lines cultured in 20% O_2 (aerobic, A), 0.5% O_2 for 24h (AH) and 0.5% O_2 for 10 weeks (CH). Data expressed as mean ± SEM (n=3). * $P \leq 0.05$, ** $P \leq 0.01$, **** $P \leq 0.0001$ (One-way ANOVA followed by Dunnett's multiple comparison test performed, comparing each sample to the 20% O_2 group within each cell line).*

Na^+-H^+ exchanger 1 protein and mRNA expression was also analysed in the 3 breast cancer cell lines cultured in differing O_2 conditions. In contrast to the CAIX expression results, NHE1 protein and mRNA expression was relatively constant across the 3 cancer cell lines (figure 24). No significant changes in NHE1 expression levels were observed in either MDA-MB-231 (figure 24C) or HBL-100 (figure 24D) cells at any time point in the different O_2 conditions. MCF-7 cells were the only cell line to show any significant change in NHE1 protein levels, with a significant increase in NHE1 protein quantity detected in MCF-7 cells cultured for 10 weeks in 0.5% O_2 conditions (figure 24B). NHE1 mRNA levels were quite stable between the differing conditions in the 3 cancer cell lines, with a small decrease in NHE1 mRNA levels observed in chronic hypoxic HBL-100 cancer cells the only significant change detected (figure 24E).

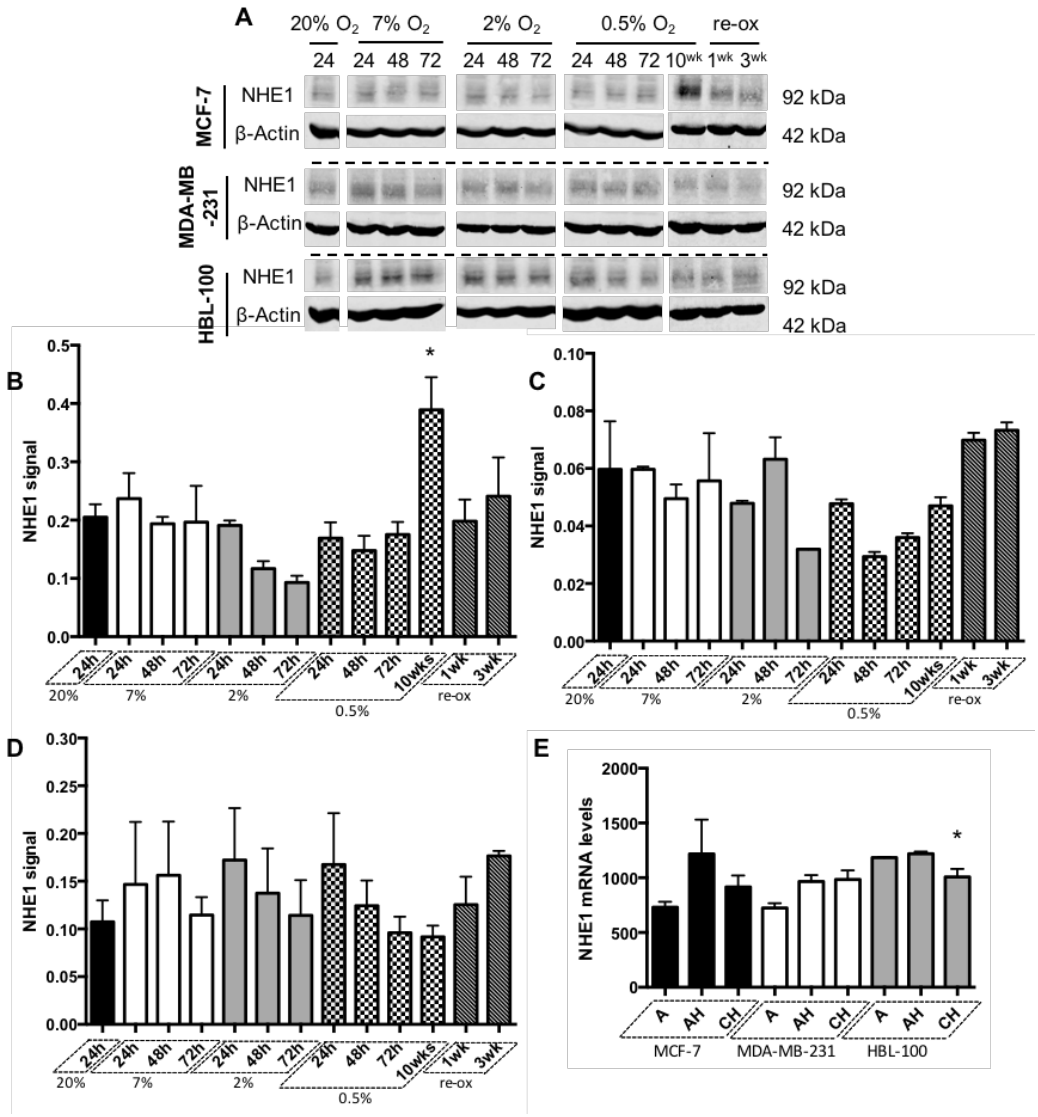

Figure 24. NHE1 protein and mRNA expression levels are relatively constant in the 3 cell lines cultured in differing O_2 concentrations.

*(A) Western blotting was performed to analyse the protein expression of NHE1 in MCF-7, MDA-MB-231 and HBL-100 cells cultured in differing oxygen concentrations (20% O_2, 7% O_2, 2% O_2 and 0.5% O_2) for 24, 48 and 72h, Whole-cell lysates were also acquired from cells that had been present in 0.5% O_2 for 10 weeks, along with chronic hypoxic cells that were re-oxygenated for 1-3 weeks before lysate acquisition (re-ox). β-Actin used as the loading control. (B-D) Graphs show the densitometry measurements of NHE1 in MCF-7 (B), MDA-MB-231 (C) and HBL-100 (D) cells lines. Data expressed as mean ± SEM (n = 2) * P ≤ 0.05 (One-way ANOVA followed by Dunnett's multiple comparison test performed, comparing each sample to the 20% O_2 group). (E) NHE1 mRNA levels were analysed in the 3 breast cancer cell lines cultured in 20% O_2 (aerobic, A), 0.5% O_2 for 24h (AH) and 0.5% O_2 for 10 weeks (CH). Data expressed as mean ± SEM (n=3). * P ≤ 0.05 (One-way ANOVA followed by Dunnett's multiple comparison test performed, comparing each sample to the 20% O_2 group within each cell line).*

Vacuolar H^+-ATPases are made up of a peripheral domain (V_1) and an integral domain (V_0), each consisting of many different subunits (see section 1.12). To analyse the overall protein expression levels of V-ATPase within the 3 cancer cell lines in the varying O_2 conditions, an antibody targeting the ATP6V1A subunit, present in the peripheral V1 domain of the complex, was used. Similar to the NHE1 expression results obtained, V-ATPase protein expression was seen to be relatively steady in each of the 3 cancer cell lines cultured in the differing O_2 conditions, with many of the samples present in low O_2 concentrations having similar levels of V-ATPase protein to the cells cultured in 20% O_2 conditions (figure 25A-D).

The mRNA levels of the ATP61VA subunit targeted in the protein expression analysis, in addition to the subunits ATP6V0A3 and ATP6V0A4 (both of which have been linked to the directing of the V-ATPase complex to the plasma membrane of cells [400]) were also assessed (figure 25E-G). While the mRNA quantities of the ATP6V1A subunit were found to decrease under hypoxic conditions in each of the cell lines (figure 25E), the expression levels of the ATP6V0A3 (figure 25F) and ATP6V0A4 (figure 25G) were much more constant across the different O_2 concentrations, with an increase in the levels of the ATP6V0A4 subunit within chronically hypoxic MDA-MB-231 cells the only significant change detected (figure 25G).

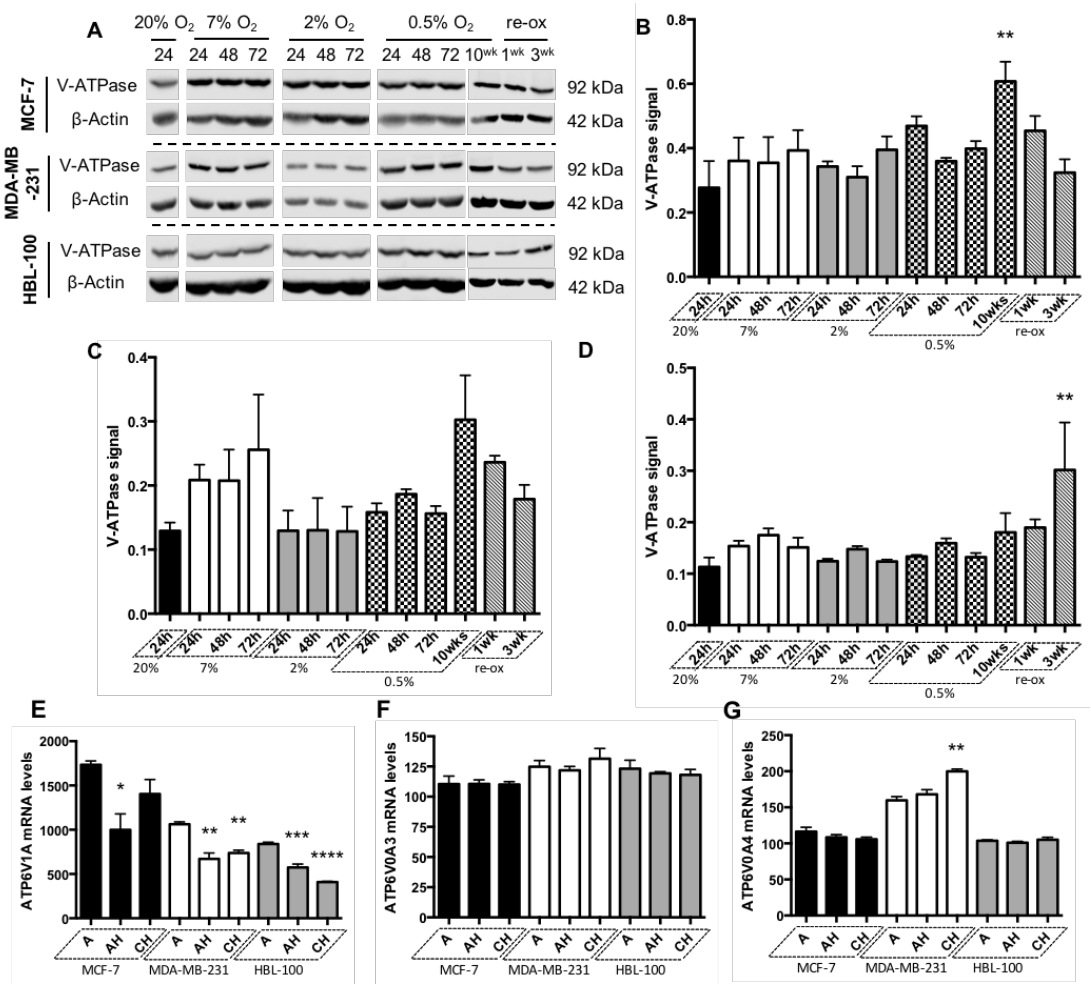

Figure 25. V-ATPase protein and mRNA subunit expression levels are relatively constant in the 3 cell lines cultured in differing O_2 conditions.

*(A-D) Cells were placed into differing oxygen concentrations (20% O_2, 7% O_2, 2% O_2 and 0.5% O_2), and total protein was extracted from the cells at 24, 48 and 72h. Whole-cell lysates were also acquired from cells that had been present in 0.5% O_2 for 10 weeks, along with chronic hypoxic cells that were re-oxygenated for 1-3 weeks before lysate acquisition (re-ox). Western blotting was performed to detect the expression of V-ATPase, with β-Actin used as the loading control. (B-D) Graphs show the densitometry measurements of V-ATPase protein levels within the MCF-7 (B), MDA-MB-231 (C) and HBL-100 (D) cell lines. Data expressed as mean ± SEM (n = 3). ** P ≤ 0.01 (One-way ANOVA followed by Dunnett's multiple comparison test performed, comparing each sample to the 20% O_2 group). (E-G) ATP6V1A (E), ATP6V0A3 (F) and ATP6V0A4 (G) subunit mRNA levels were analysed in cells cultured in 20% O_2 (aerobic, A), 0.5% O_2 for 24h (AH) and 0.5% O_2 for 10 weeks (CH). Data expressed as mean ± SEM (n=3). * P ≤ 0.05, ** P ≤ 0.01, *** P ≤ 0.001 and **** P ≤ 0.0001 (One-way ANOVA followed by Dunnett's multiple comparison test performed, comparing each sample to the 20% O_2 group within each cell line).*

3.2.2 3D expression analysis indicates that, of the 3 pH regulatory proteins analysed, the tumour-associated carbonic anhydrases are the most sensitive changes in O_2 conditions

2D expression analysis showed that both CAIX protein and mRNA expression, along with CAXII mRNA levels, were differentially regulated between the 3 cell lines in various O_2 concentrations, while both NHE1 and V-ATPase protein and mRNA expression levels were much more constant across the different O_2 conditions. Further expression analysis was conducted to investigate whether the same pattern of expression occurred in 3D, studying the protein expression levels of each of these targets in multicellular tumour spheroids of the 3 cancer cell lines.

Hypoxyprobe was used to reveal the presence of hypoxic areas within spheroids. Viable regions outside of the central necrotic cores showed extensive hypoxyprobe staining within both MCF-7 (figure 26) and HBL-100 (figure 28) spheroids, with hypoxic areas forming several cell diameters in from the outside edge of the spheroids. MDA-MB-231 spheroids also exhibited the formation of hypoxic areas (figure 27). However, the hypoxyprobe staining was much more restricted within these MDA-MB-231 spheroids in comparison to the spheroids of the other cell lines, with the presence of hypoxic areas evident only in certain regions (figure 27).

Using the hypoxyprobe staining to delineate the normoxic and hypoxic areas within spheroids of each of the cell lines, quantitative evaluation of CAIX (figure 29), CAXII (figure 30) and NHE1 (figure 31) protein expression was carried out, measuring the levels of these proteins in the normoxic and hypoxic areas of spheroids from each of the 3 breast cancer cell lines. Of those cells recognised as having positive staining, the % of cells with low, medium or high intensity levels of staining within the normoxic and hypoxic areas was measured. This analysis was performed with Definiens Architect XD 64 Tissue Studio 4.1 (see section 2.7.4).

Plasma membrane staining of CAIX was evident in spheroids of each of the 3 cancer cell lines (figures 26-28). However, as was already seen in the 2D expression analysis performed, the extent of CAIX expression again varied greatly between the

cell lines. Cells within MCF-7 spheroids had the lowest levels of CAIX (figure 29A), with no CAIX expressing cells detected within the normoxic areas of these spheroids, and only 0.1% of cells in the hypoxic regions expressing a low intensity level of CAIX (figure 29A). The % of cells detected as CAIX positive was higher in the HBL-100 spheroids in comparison to the MCF-7 spheroids (figure 29A), with over 60% of cells within the hypoxic regions of these spheroids exhibiting CAIX staining. The majority of cells within the hypoxic regions of HBL-100 spheroids were labelled as having high intensity levels of CAIX (figure 29A). MDA-MB-231 spheroids exhibited the highest levels of CAIX expressing cells out of all the cell lines (figure 29A). Nearly 100% of the cells within the hypoxic regions were recognised as CAIX-positive, with only 9% of cells within the normoxic region labelled as negative for CAIX expression (figure 29A). Cells within the normoxic and hypoxic regions of the MDA-MB-231 spheroids were seen to have similar intensity levels of CAIX protein expression (figure 29B).

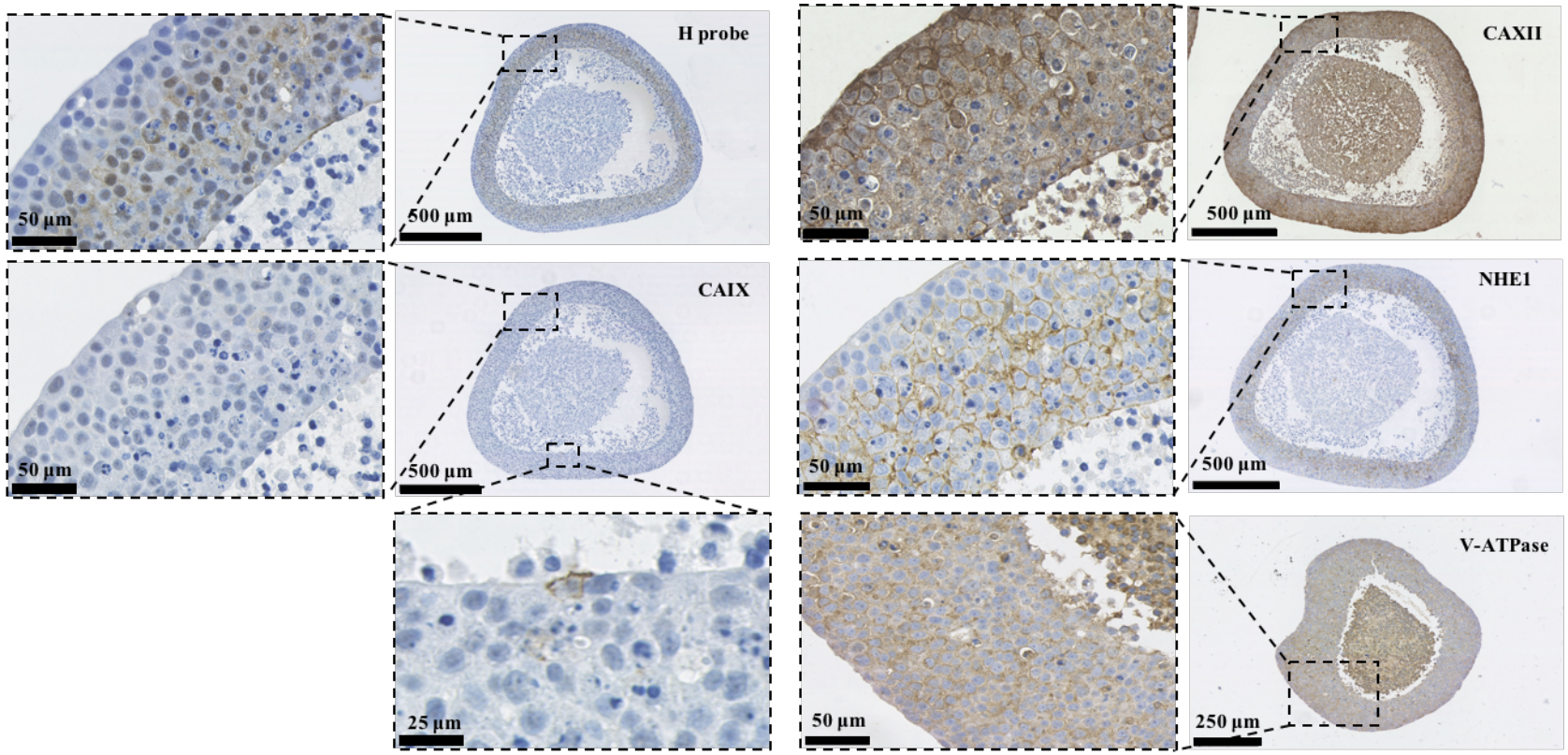

Figure 26. Large changes in the plasma membrane expression of CAXII and NHE1 are evident within the different regions of MCF-7 spheroids, while V-ATPase and CAIX expression is much more consistent.

Images show hypoxyprobe (H probe), CAIX, CAXII, NHE1 and V-ATPase staining within MCF-7 spheroids that were allowed to form for a week before fixation.

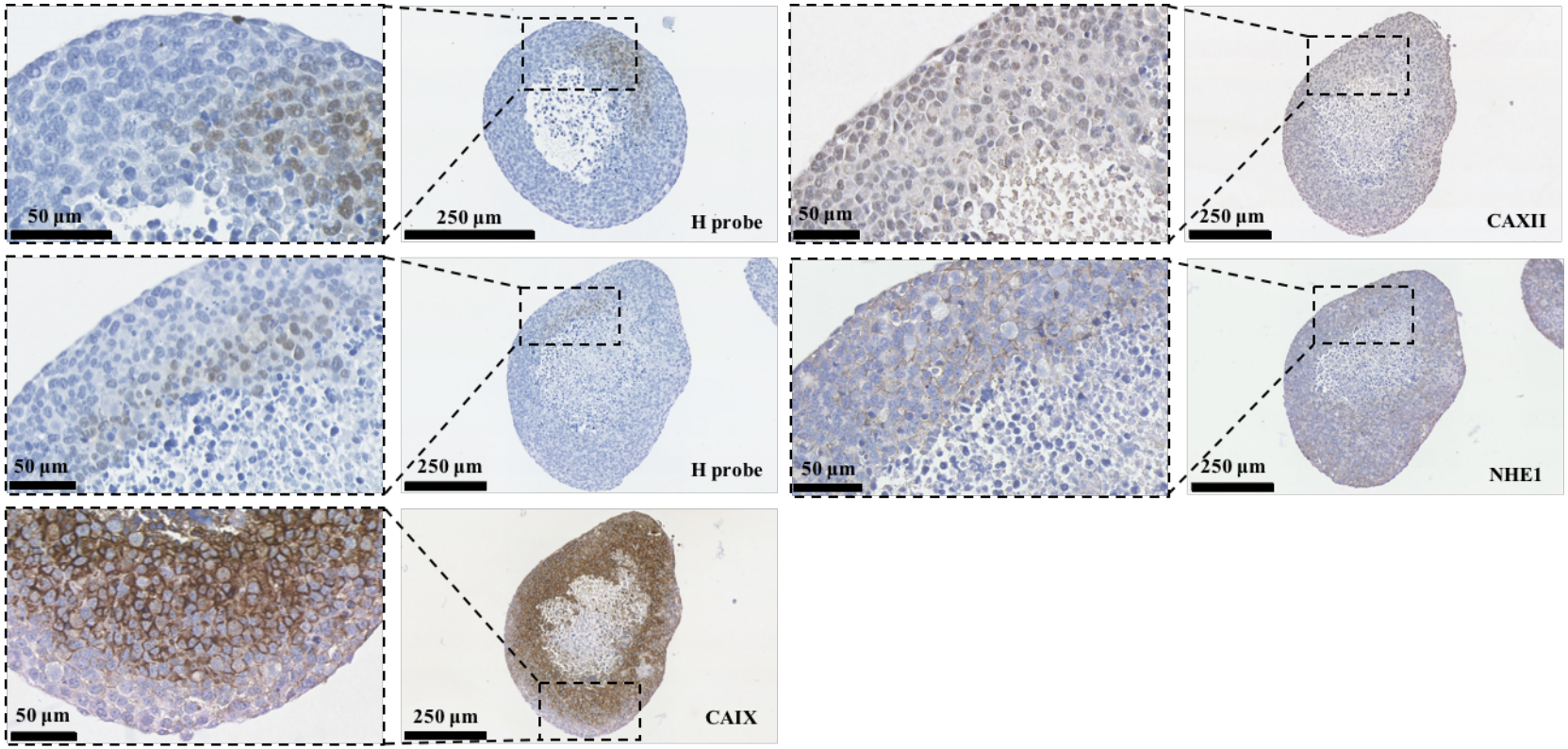

Figure 27. MDA-MB-231 spheroids exhibit large amounts of CAIX staining, with no plasma membrane staining of CAXII evident. NHE1 protein expression is also more consistent across the different regions of these spheroids.

Images show hypoxyprobe (H probe), CAIX, CAXII and NHE1 staining within MDA-MB-231 spheroids that were allowed to form for a week before fixation.

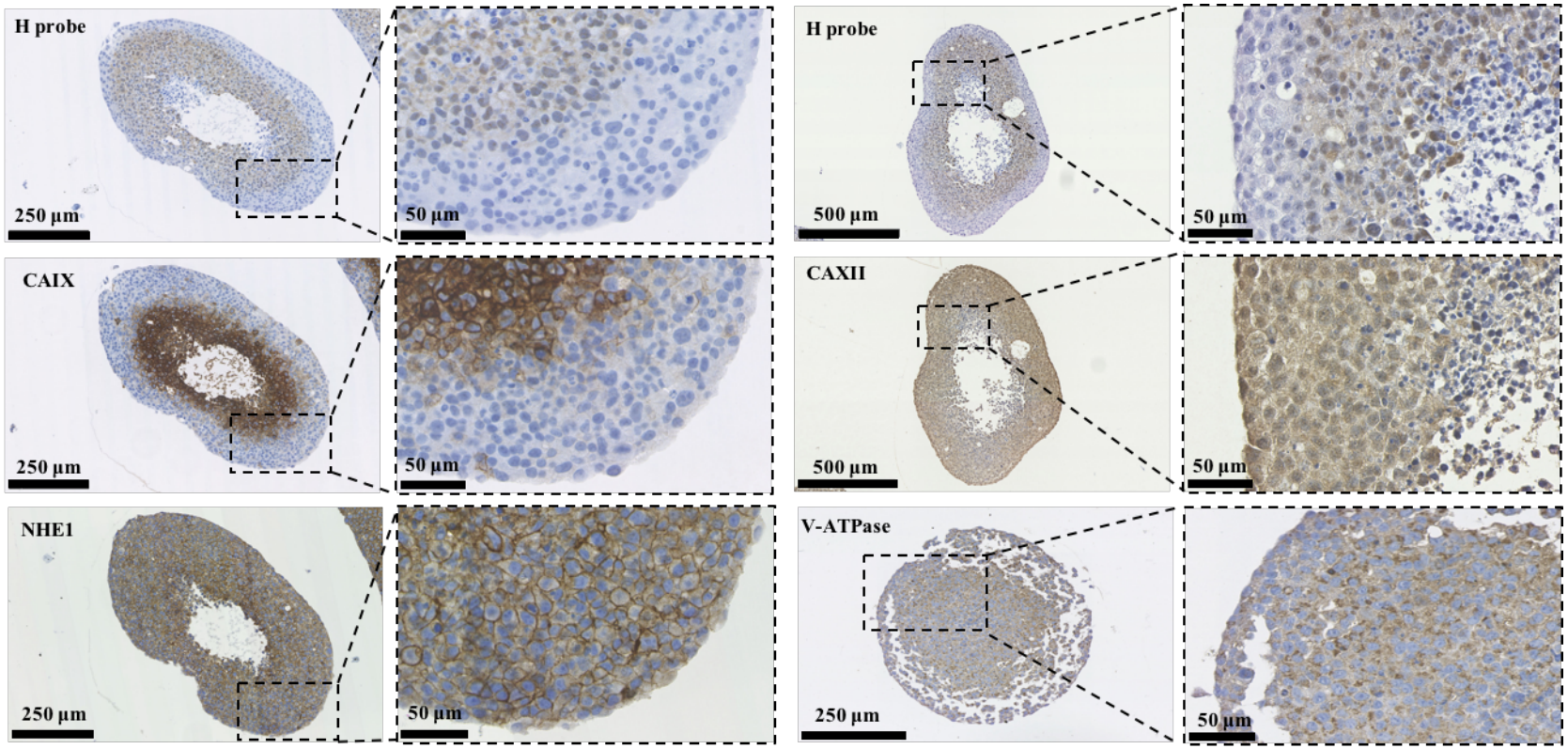

Figure 28. While no plasma membrane CAXII expression is present in HBL-100 spheroids, marked expression of plasma membrane CAIX and NHE1 is observed, with CAIX expression showing evident hypoxic induction. V-ATPase protein expression is seen to be much more consistent in the different regions.

Images show hypoxyprobe (H probe), CAIX, CAXII, NHE1 and V-ATPase staining within HBL-100 spheroids that were allowed to form for a week before fixation.

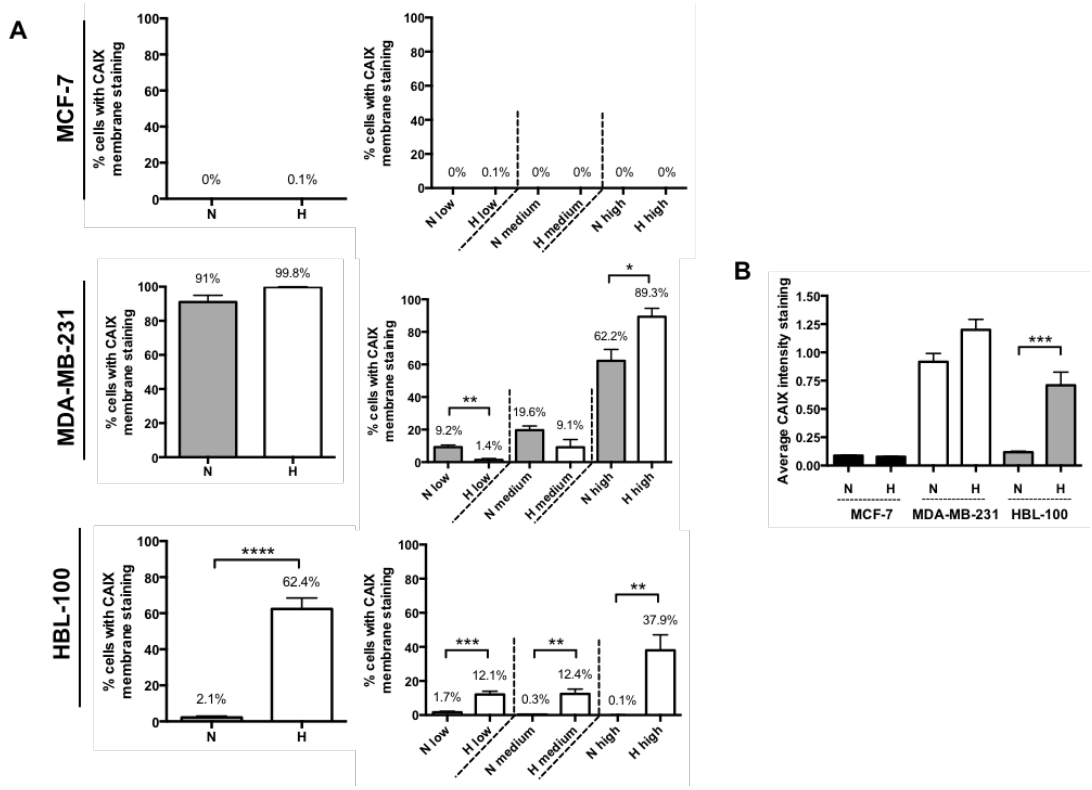

Figure 29. Definiens analysis indicates that the 3D expression of CAIX differs between the 3 cell lines.

*(A) Graphs on the left show the % of cells within the normoxic (N) and hypoxic (H) regions of spheroids that expressed CAIX. Graphs on the right show the % of cells within the normoxic and hypoxic areas that had low, medium, and high intensity levels of CAIX staining. (B) Average intensity of CAIX membrane staining detected within the normoxic and hypoxic areas of spheroids of each cell line. Data expressed as mean ± SEM (n = at least 3 for each cell line). *P≤0.05, **P≤0.01, ***P≤0.001 and ****P≤0.0001 (Unpaired t-tests performed).*

Quantitative analysis of CAXII expression levels between spheroids of the different cell lines was also carried out. However, in contrast to CAIX, the localisation of CAXII expression differed between the cell lines. Plasma membrane CAXII staining was evident in cells within MCF-7 spheroids (figure 26), while intracellular CAXII staining was observed in spheroids of the MDA-MB-231 (figure 27) and HBL-100 (figure 28) cell lines. This difference in CAXII localisation led to varying methods of analysis being carried out between the cell lines (see section 2.7.4).

Similar to observations from the 2D mRNA analysis (figure 23), hypoxia led to a down-regulation of CAXII protein expression in MCF-7 spheroids, with a significantly higher % of cells exhibiting plasma membrane CAXII staining present in the normoxic areas (figure 30A). The majority (58.2%) of cells within the

normoxic regions had high intensity levels of CAXII staining, while in the hypoxic areas only 18% of cells were labelled as such (figure 30A). The overall intensity of plasma membrane CAXII expression was also higher in the MCF-7 cells within the normoxic regions compared to the cells within the hypoxic regions (figure 30A). Quantitative analysis indicated that regional differences in the expression levels of CAXII were present in HBL-100 spheroids, with an increased intensity of CAXII staining detected within the normoxic areas of HBL-100 spheroids (figure 30B). No such variations in intracellular CAXII staining were seen within the different regions of the MDA-MB-231 spheroids (figure 30B).

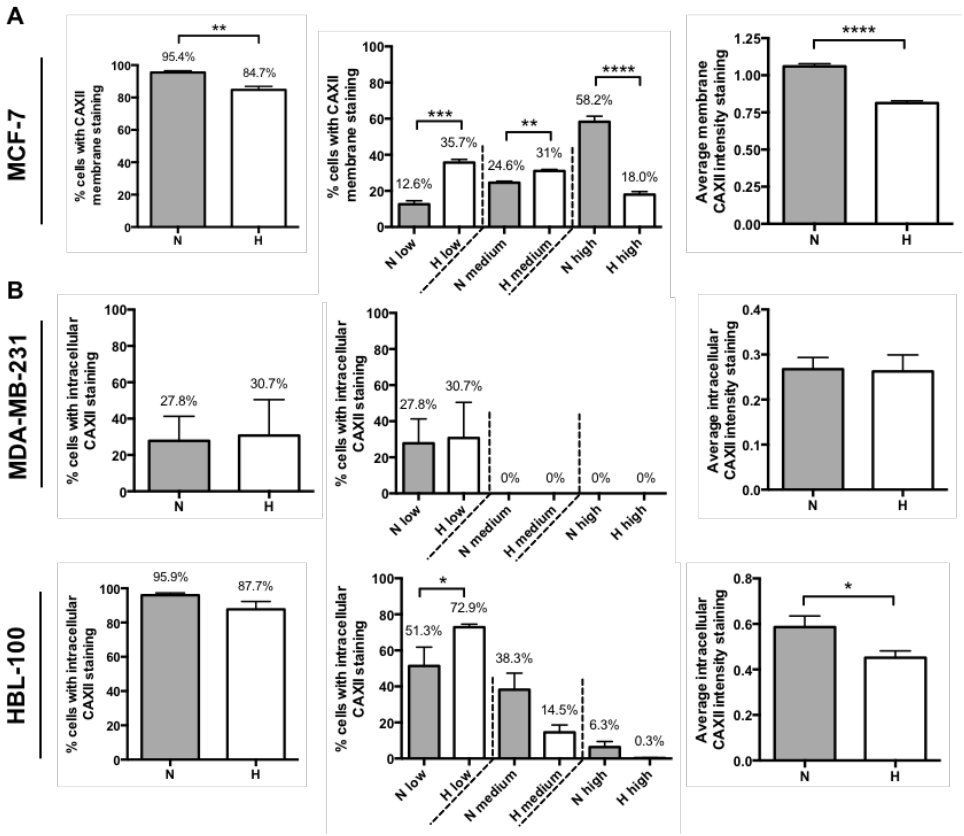

Figure 30. Definiens analysis reveals the presence of regional differences in the expression of CAXII within MCF-7 and HBL-100 spheroids.

*Definiens analysis showing the levels of plasma membrane CAXII within MCF-7 spheroids (A) and intracellular CAXII staining within MDA-MB-231 and HBL-100 spheroids (B). The graphs on the left show the % of cells within the normoxic and hypoxic regions that exhibited CAXII staining. The graphs in the center show the % of cells within the normoxic and hypoxic areas that had low, medium, and high intensity levels of CAXII staining. The graphs on the right show the average intensity of CAXII staining detected within the normoxic and hypoxic areas of the spheroids. Data expressed as mean ± SEM (n = 4). *P≤0.05, **P≤0.01, ***P≤0.001 and ****P≤0.0001 (Unpaired t-tests performed).*

2D analysis showed that NHE1 protein expression was relatively consistent across the different cell lines cultured in various O_2 conditions, with only chronic hypoxic MCF-7 cells exhibiting a significant increase in NHE1 protein levels (figure 24). Additional analysis carried out in 3D showed that large variations in NHE1 protein expression levels were evident within the different regions of the MCF-7 spheroids (figures 26 and 31A). Only 35.5% of cells within the normoxic regions of the MCF-7 spheroids expressed NHE1, while 88.5% of cells within the hypoxic regions were labelled as having NHE1 plasma membrane staining (figure 31A). In contrast to the normoxic areas, the majority of cells within the hypoxic region were labelled as having high intensity levels of NHE1 staining (figure 31A). The NHE1 expression patterns within MDA-MB-231 and HBL-100 spheroids did not show as much evidence of hypoxic induction as was seen in the MCF-7 spheroids (figure 31A). Of the 3 cell lines, HBL-100 spheroids had the largest number of NHE1-expressing cells, with nearly 100% of cells within both normoxic and hypoxic regions labelled as NHE1-positive and having high intensity levels of NHE1 staining (figure 31A). An analysis of the average intensity staining of NHE1-positive cells within the normoxic and hypoxic regions of each of the spheroids indicated that HBL-100 cells expressed the highest levels of NHE1 protein out of the 3 cell lines (figure 31B).

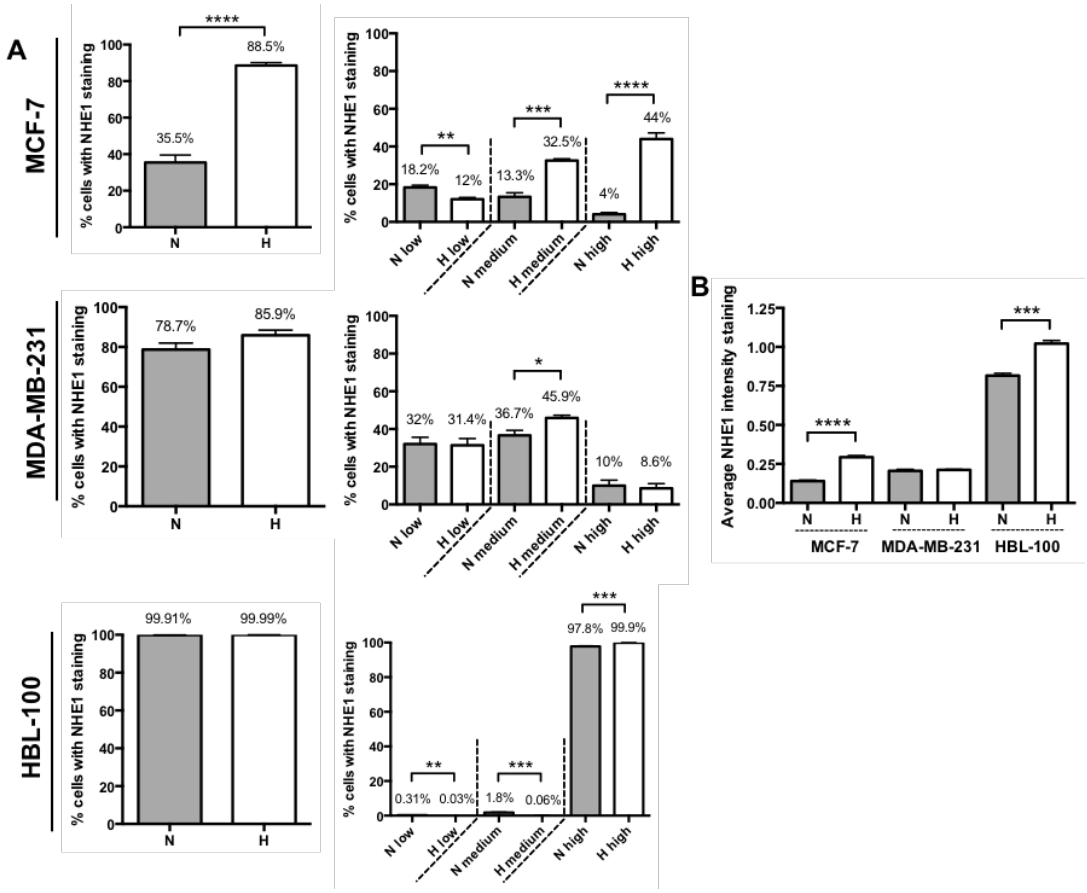

Figure 31. MCF-7 spheroids exhibit the largest regional changes in NHE1 protein expression of the 3 cell lines.

*(A) Graphs on the left show the % of cells within the normoxic and hypoxic regions of spheroids that exhibited NHE1 staining. Graphs on the right show the % of cells within the normoxic and hypoxic areas that had low, medium, and high intensity levels of NHE1 staining. (B) Average intensity of NHE1 staining detected within the normoxic and hypoxic areas of spheroids of each cell line. Data expressed as mean ± SEM (n = at least 3 for each cell line). *P≤0.05, **P≤0.01, ***P≤0.001 and ****P≤0.0001 (Unpaired t-tests performed).*

Preliminary experiments performed, testing different dilutions of V-ATPase antibody in IHC, showed that V-ATPase protein expression levels were similar in the different regions of both MCF-7 (figure 26) and HBL-100 (figure 28) spheroids. Further IHC was carried out, with the intention of assessing V-ATPase protein expression levels in spheroids that had been treated with hypoxyprobe, using the hypoxyprobe staining to demarcate the normoxic and hypoxic areas of the spheroids However, despite repeated attempts, the V-ATPase antibody failed to produce any positive staining in the hypoxyprobe stained spheroids. As a result, no quantitative analysis of V-ATPase protein expression in 3D was carried out.

Spheroids re-create different aspects of the *in vivo* tumour microenvironment, mimicking the heterogeneous cancer cell populations that occur within tumours, with proliferative cells present in the normoxic layer, and non-cycling or apoptotic cells present in the hypoxic regions (see section 1.15.2). The pH regulating proteins, through their role in the control of pH, support cancer cell survival (see sections 1.10 - 1.12). Quantitative analysis was carried out to assess whether the differential expression of the pH regulating proteins observed between the cell lines in 3D had any effect on cell viability, comparing the expression levels of Ki67 and caspase 3 in the normoxic and hypoxic regions of spheroids.

Hypoxic regions of MCF-7 spheroids had significantly lower percentages of cycling cells (as indicated by Ki67) in comparison to the normoxic areas (figures 32A and 33), while also exhibiting significantly increased levels of apoptosis, as analysed through caspase 3 staining (figures 32B and 33). The proliferative and cell death gradients that appeared within MCF-7 spheroids were not present within MDA-MB-231 spheroids, which exhibited no significant differences in either proliferation (figure 32A) or apoptosis (figure 32B) between the normoxic and hypoxic areas of the spheroids. Cells within the hypoxic regions of HBL-100 spheroids exhibited a similar proliferation index to the normoxic cells (figures 32A and 34). However, a small significant increase in caspase 3 staining was observed in the hypoxic areas of HBL-100 spheroids (figure 32B).

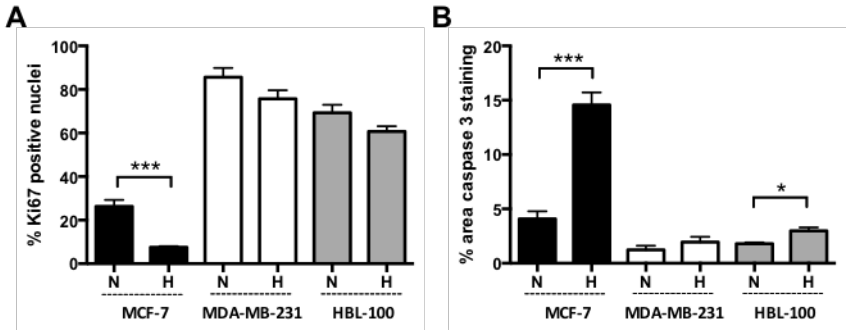

Figure 32. The presence of proliferative and cell death gradients are observed within spheroids of the MCF-7 cell line.

*Analysis of the % of Ki67 positive cells (A) and the % area of caspase 3 staining (B) within the normoxic and hypoxic regions of spheroids of the 3 cancer cell lines. Data expressed as mean ± SEM (n = at least 3). ***P≤0.001 (Unpaired t-tests performed).*

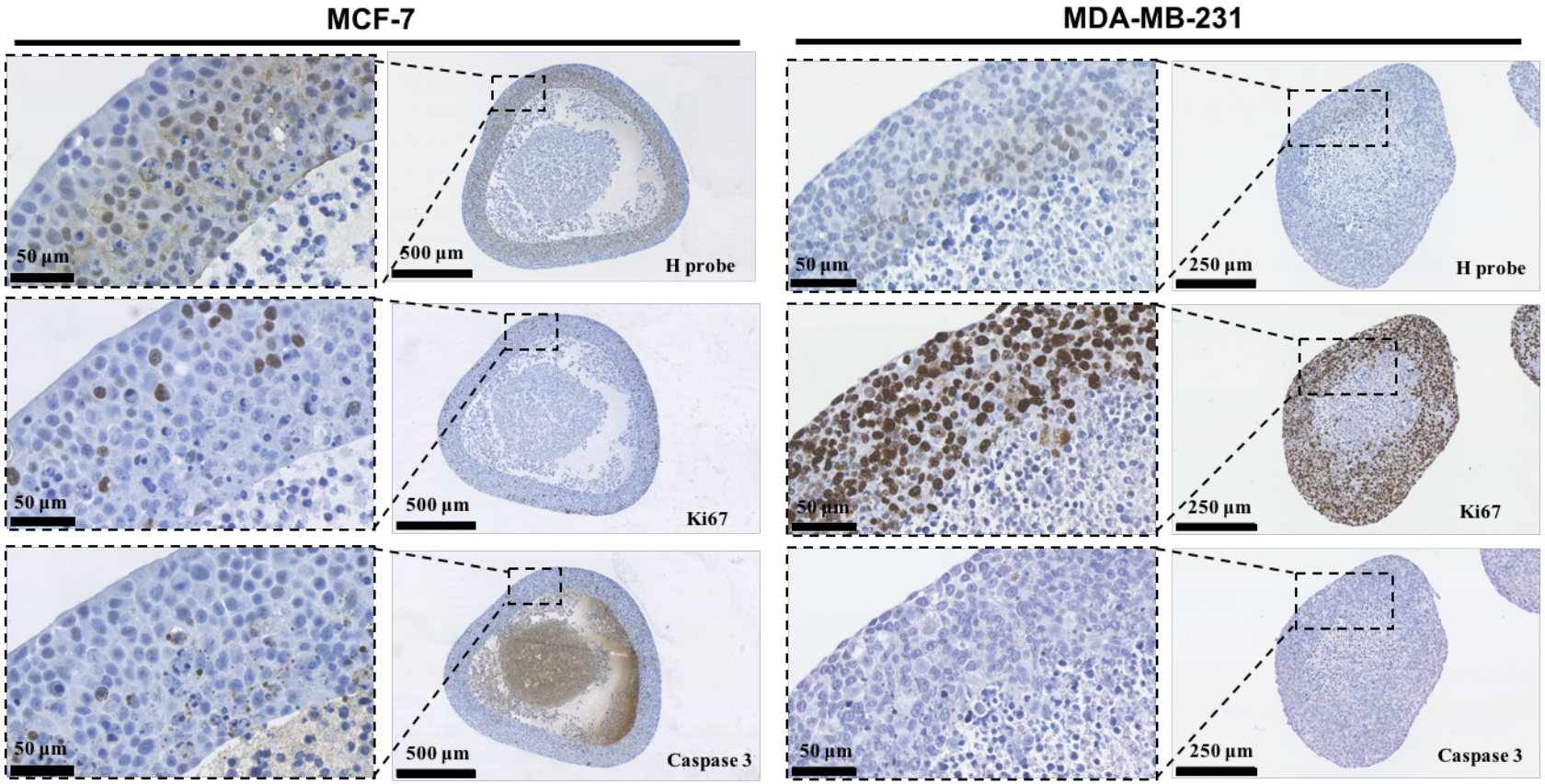

Figure 33. Ki67 and caspase 3 staining show evidence of the proliferative and cell death gradients present within spheroids of the MCF-7 cell line.

Images show hypoxyprobe (H probe), Ki67 and caspase 3 staining within MCF-7 and MDA-MB-231 spheroids that were allowed to form for a week before fixation

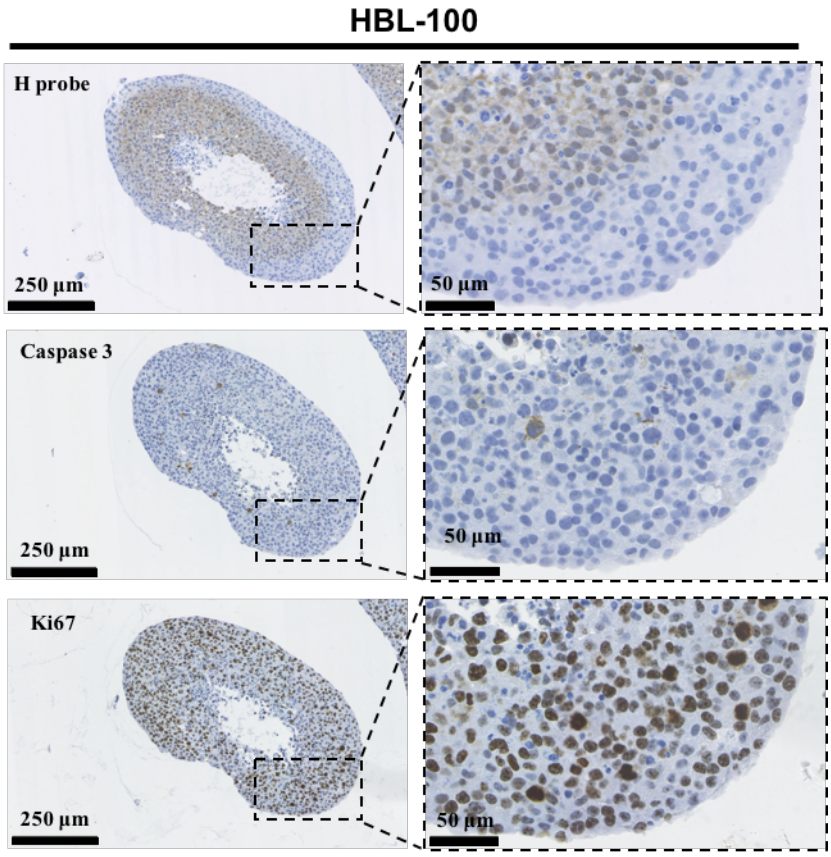

Figure 34. Extensive Ki67 staining observed in all regions of the HBL-100 spheroids, with caspase 3 staining present within the hypoxic areas of these spheroids.

Images show hypoxyprobe (H probe), Ki67 and caspase 3 staining within HBL-100 spheroids that were allowed to form for a week before fixation.

3.2.3 Changes in O_2 concentration alters the effects of inhibitors targeting the tumour-associated carbonic anhydrases and NHE1 on cancer cell number

SRB assays were performed to investigate the effects of inhibitors targeting the tumour-associated carbonic anhydrases, NHE1 and V-ATPase on cancer cell number, comparing the sensitivity of aerobic, acute hypoxic and chronic hypoxic cells to drug treatment. Cells in each of these conditions were treated with the inhibitors for 24-120h. The acute hypoxic cells were cultured at 0.5% O_2 for 24h prior to drug-treatment to allow them to adapt to the low O_2 conditions, while the chronic hypoxic cells had been cultured for over 21 weeks in 0.5% O_2 conditions before the assay. Both acute and chronic hypoxic cancer cells were kept in 0.5% O_2 conditions throughout the experiment. The intensity readings procured from the SRB assays (figures 35 – 43 left column) were used to produce graphs showing the effect of pH inhibition on cancer cell number, with the control cell intensity readings representing 100% cell number (figures 35 – 43 middle column). The data from these graphs were then used to produce IC_{50} values (half maximal inhibitory concentration) for reduction in cell number in response to drug treatment (figures 35 – 43 right column).

Treatment with the carbonic anhydrase inhibitor led to a reduction in cell number in all 3 of the cell lines cultured in aerobic conditions (figure 35). 30 and 100 μM concentrations of S4 had large effects on intensity readings in the MCF-7 and MDA-MB-231 cell lines (figure 35 left column), leading to sizeable reductions in cell number in comparison to the un-treated cells (figure 35 middle column). HBL-100 cells were more resistant to the effects of S4 treatment in comparison to both the MCF-7 and MDA-MB-231 cells, as reflected in the IC_{50} values obtained for each of the cell lines (figure 35 right column). While concentrations of S4 were able to reduce MCF-7 and MDA-MB-231 cell number by 50%, no concentration of inhibitor used had the same effect on the HBL-100 cell line in aerobic conditions.

Acute hypoxic cells were more resistant to the effects of S4 compared to aerobic cells (figure 36). The 30 μM and 100 μM drug concentrations, which were leading to

significant reductions in cell number in aerobic MCF-7 and MDA-MB-231 cells, had less influence on intensity readings in the acute hypoxic cells (figure 36 left column), with acute hypoxic HBL-100 cells displaying a near complete resistance to S4 treatment (figure 36 left column). The augmented resistance of the acute hypoxic cells in comparison to the aerobic cells was supported by the IC_{50} values obtained. While drug treatment was able to reduce cell number by 50% in the aerobic MCF-7 and MDA-MB-231 cells (figure 35 right column), most of the drug concentrations used did not lead to the same effect in acute hypoxic conditions (figure 36 right column).

The results for the chronically hypoxic cells were more similar to the results obtained with the aerobic cells (figure 37). Higher concentrations of S4 had a sizeable effect on the intensity readings of both MCF-7 and MDA-MB-231 cells (figure 37 left column), leading to large reductions in cell number when compared against the un-treated cells (figure 37 middle column). Comparable IC_{50} values were obtained for the aerobic (figure 35 right column) and chronic hypoxic (figure 37 right column) cells.

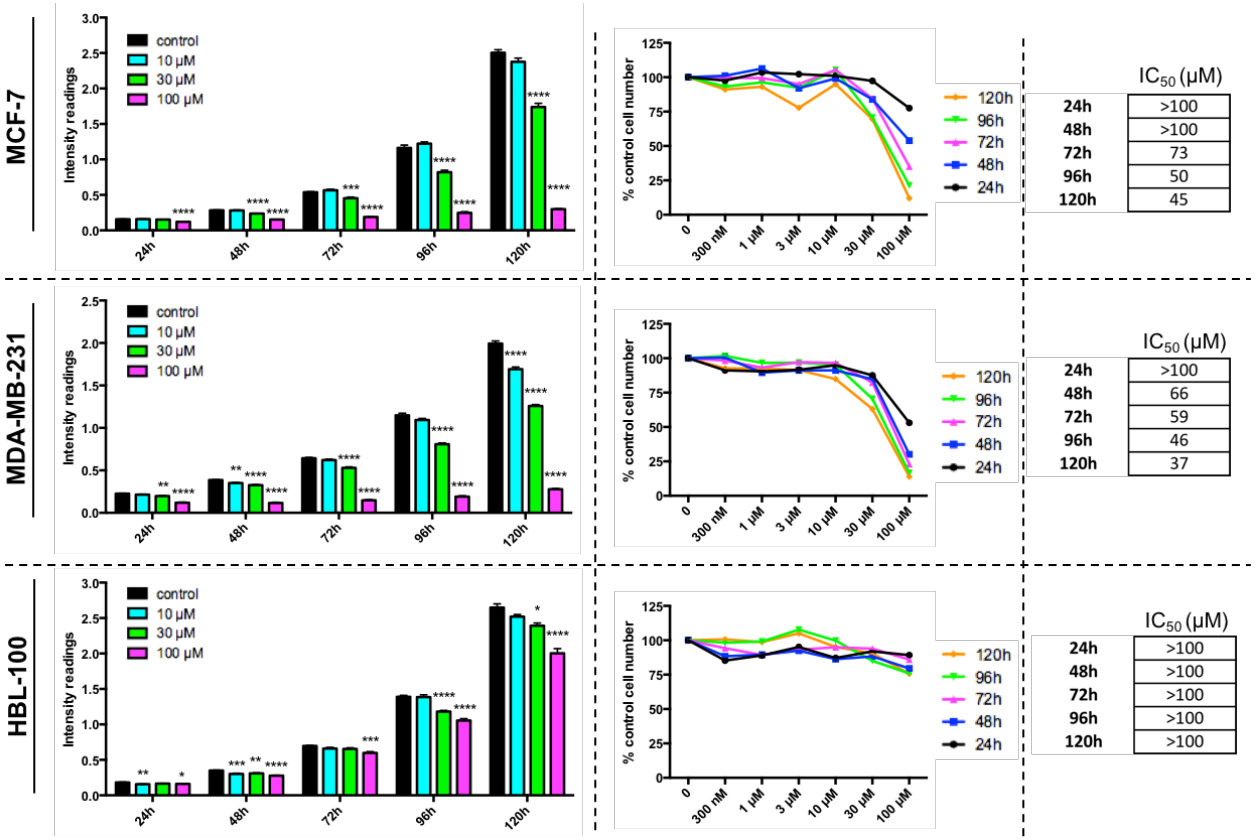

Figure 35: Reductions in cell number indicate that aerobic MCF-7 and MDA-MB-231 cells are sensitive to S4.

*Left column: The effects of S4 on the intensity readings of aerobic cancer cells, in comparison to un-treated cells. Data expressed as mean ± SEM (n=6). *P≤0.05, **P≤0.01, ***P≤0.001 and ****P≤0.0001 (One-way ANOVA followed by Dunnett's multiple comparison test performed, comparing only the values within each time point). Middle column: The effects of S4 on aerobic cancer cell number, with each drug-treated intensity reading given as a percentage of the control intensity readings at that time point. Right column: The IC_{50} values (µM) for S4 in each of the aerobic cell lines. These values were produced using the data from the middle column.*

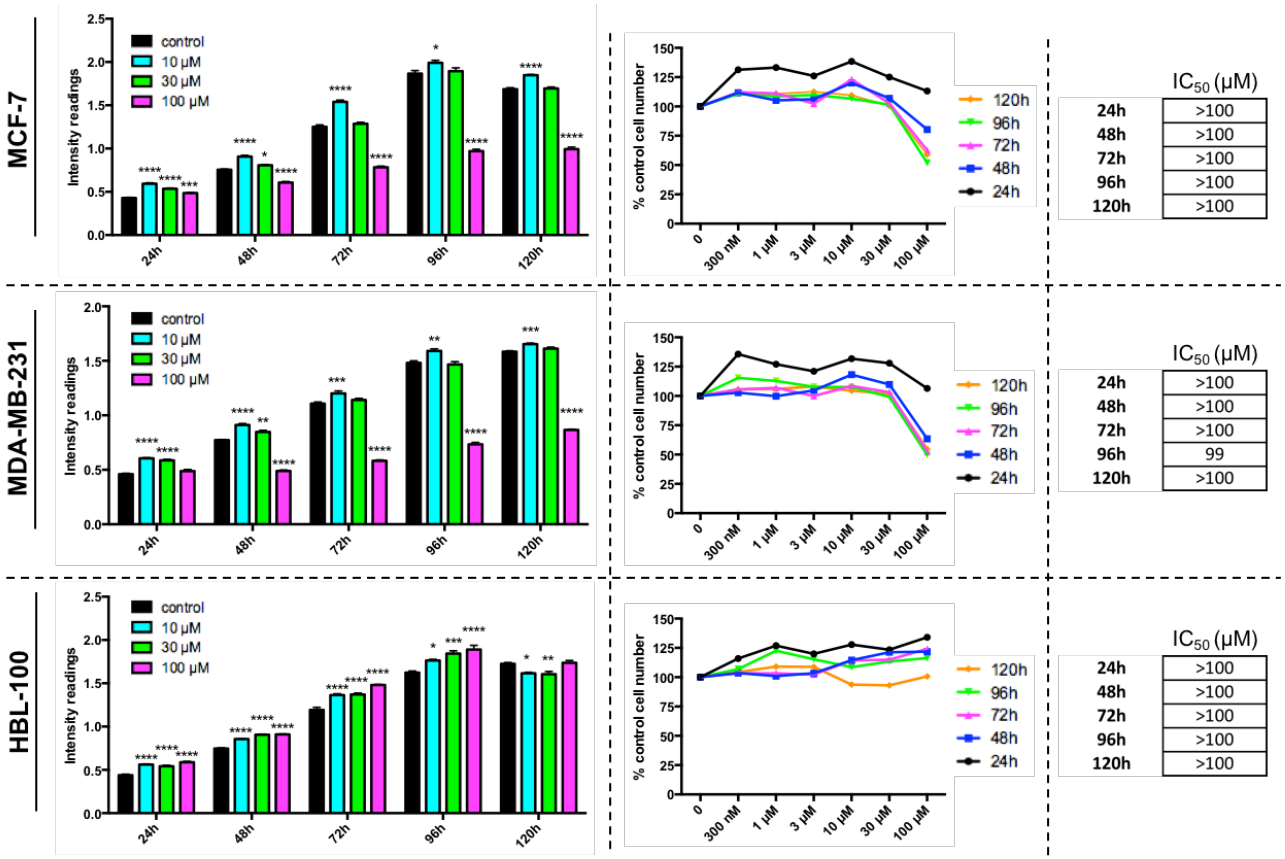

Figure 36: Acute hypoxic cells are more resistant to the effects of S4 on cancer cell number.

*Left column: The effects of S4 on the intensity readings of acute hypoxic cancer cells, compared to un-treated cells. Data expressed as mean ± SEM (n=6). *P≤0.05, **P≤0.01, ***P≤0.001 and ****P≤0.0001 (One-way ANOVA followed by Dunnett's multiple comparison test performed, comparing only the values within each time point). Middle column: The effects of S4 on acute hypoxic cancer cell number, with each drug-treated intensity reading given as a percentage of the control intensity readings at that time point. Right column: The IC_{50} values (µM) for S4 in each of the acute hypoxic cell lines. These values were produced using the data from the middle column.*

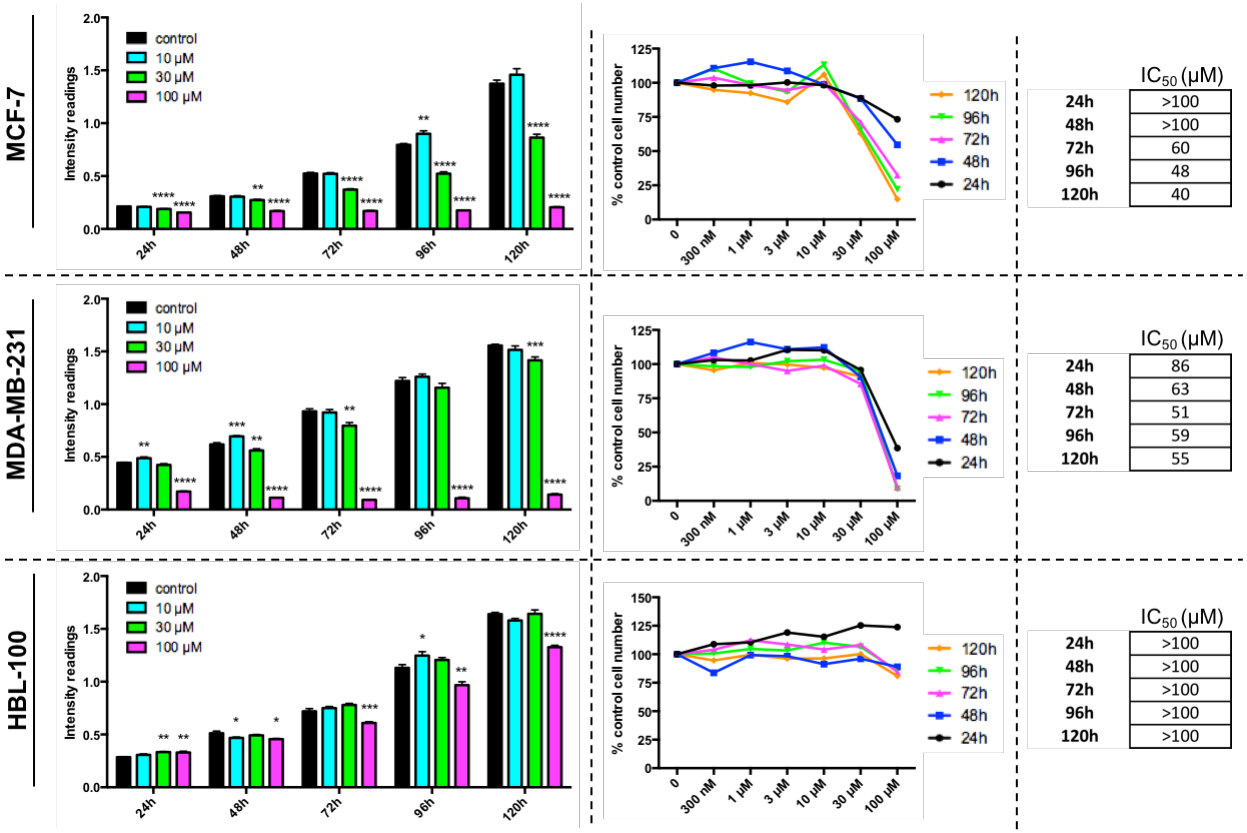

Figure 37: Chronic hypoxic cells appear to be re-sensitised to the effects of S4 on cancer cell number.

*Left column: The effects of S4 on the intensity readings of chronic hypoxic cancer cells. Data expressed as mean ± SEM (n=6). *P≤0.05, **P≤0.01, ***P≤0.001 and ****P≤0.0001 (One-way ANOVA followed by Dunnett's multiple comparison test performed, comparing only the values within each time point). Middle column: The effects of S4 on chronic hypoxic cancer cell number, with each drug-treated intensity reading given as a percentage of the control intensity readings at that time point. Right column: The IC_{50} values (µM) for S4 in each of the chronic hypoxic cell lines produced using the data in the middle column.*

In contrast to the carbonic anhydrase inhibitor S4, DMA treatment had a large effect on the cell number of all 3 cancer cell lines cultured in aerobic conditions (figure 38). DMA concentrations over 10 μM had the largest influence on cell number in 20% O_2 conditions, with higher concentrations causing a significant reduction in the intensity values obtained after only 24h of treatment (figure 38 left column). MCF-7 cells seemed to be the most sensitive to the effects of NHE1 inhibition in aerobic conditions out of all the cell lines, with MCF-7 cells requiring the lowest concentration of drug to reduce cell number by 50% at the later time points (figure 38 right column).

DMA also influenced acute hypoxic cancer cell number (figure 39). However, while 30 μM DMA had a large effect on intensity values in the experiments conducted in 20% O_2 conditions (figure 38 left column), each of the acute hypoxic cell lines were more resistant to the effects of 30 μM treatment (figure 39 left column). This observation, in addition to the increased IC_{50} values observed with the acute hypoxic cells (figure 39 right column) compared to the aerobic cells (figure 38 right column), suggested that acute hypoxic cells were more resistant to the effects of NHE1 inhibition.

Overall, lower IC_{50} values were obtained in the chronic hypoxic MCF-7 and HBL-100 cells (figure 40 right column) compared to the acute hypoxic cells (figure 39 right column), suggesting these chronic hypoxic cell lines may have re-sensitised to DMA treatment. The chronically hypoxic MDA-MB-231 cells, however, seemed to be more resistant to drug treatment than the 2 other cell lines, exhibiting similar IC_{50} values (figure 40 right column) to the acute hypoxic MDA-MB-231 cancer cells (figure 39 right column).

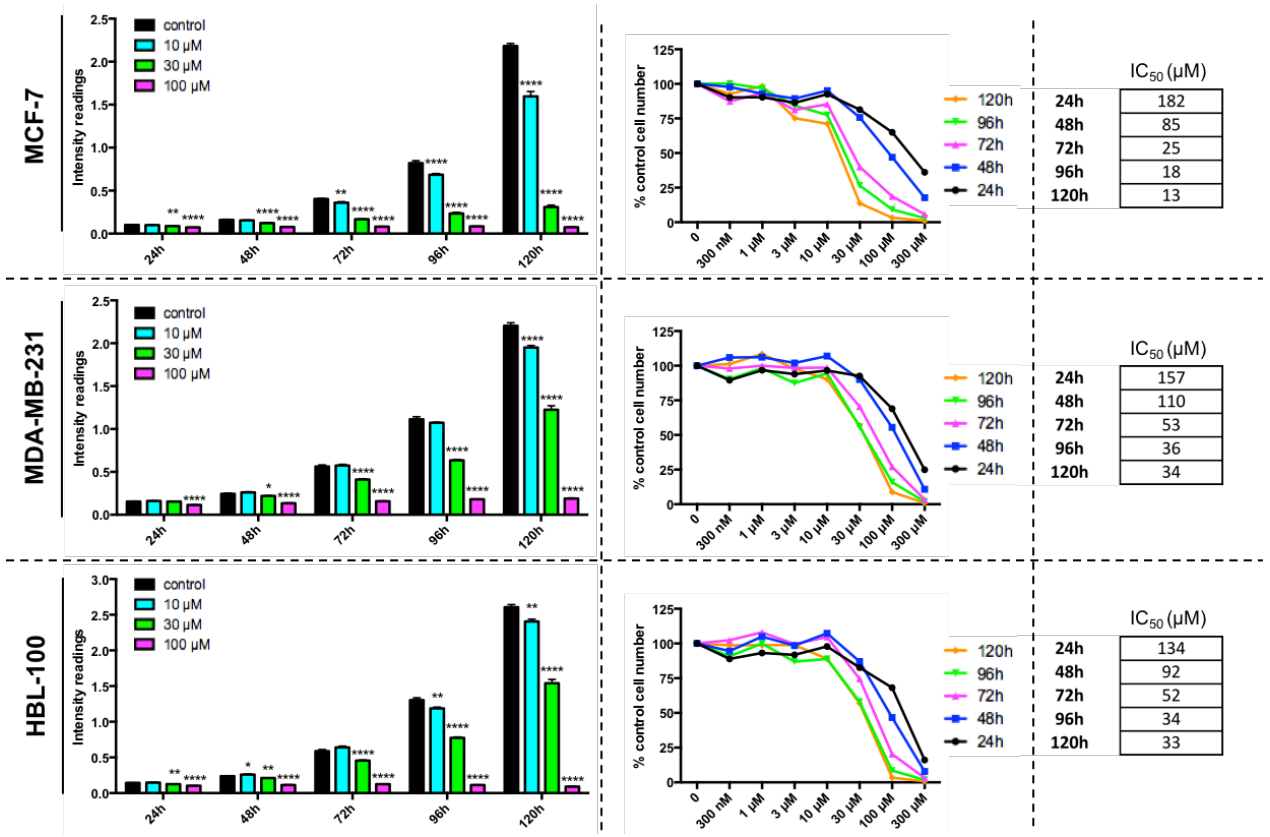

Figure 38. Each of the cancer cell lines exhibit sensitivity to the effects of DMA on cell number in aerobic conditions.

*Left column: The effects of DMA on the intensity readings of aerobic cancer cells, in comparison to un-treated cells. Data expressed as mean ± SEM (n=6). *P≤0.05, **P≤0.01 and ****P≤0.0001 (One-way ANOVA followed by Dunnett's multiple comparison test performed, comparing only the values within each time point). Middle column: The effects of DMA on aerobic cancer cell number, with each drug-treated intensity reading given as a percentage of the control intensity reading at that time point. Right column: The IC_{50} values (µM) for DMA in each of the aerobic cell lines. These values were produced using the data from the middle column.*

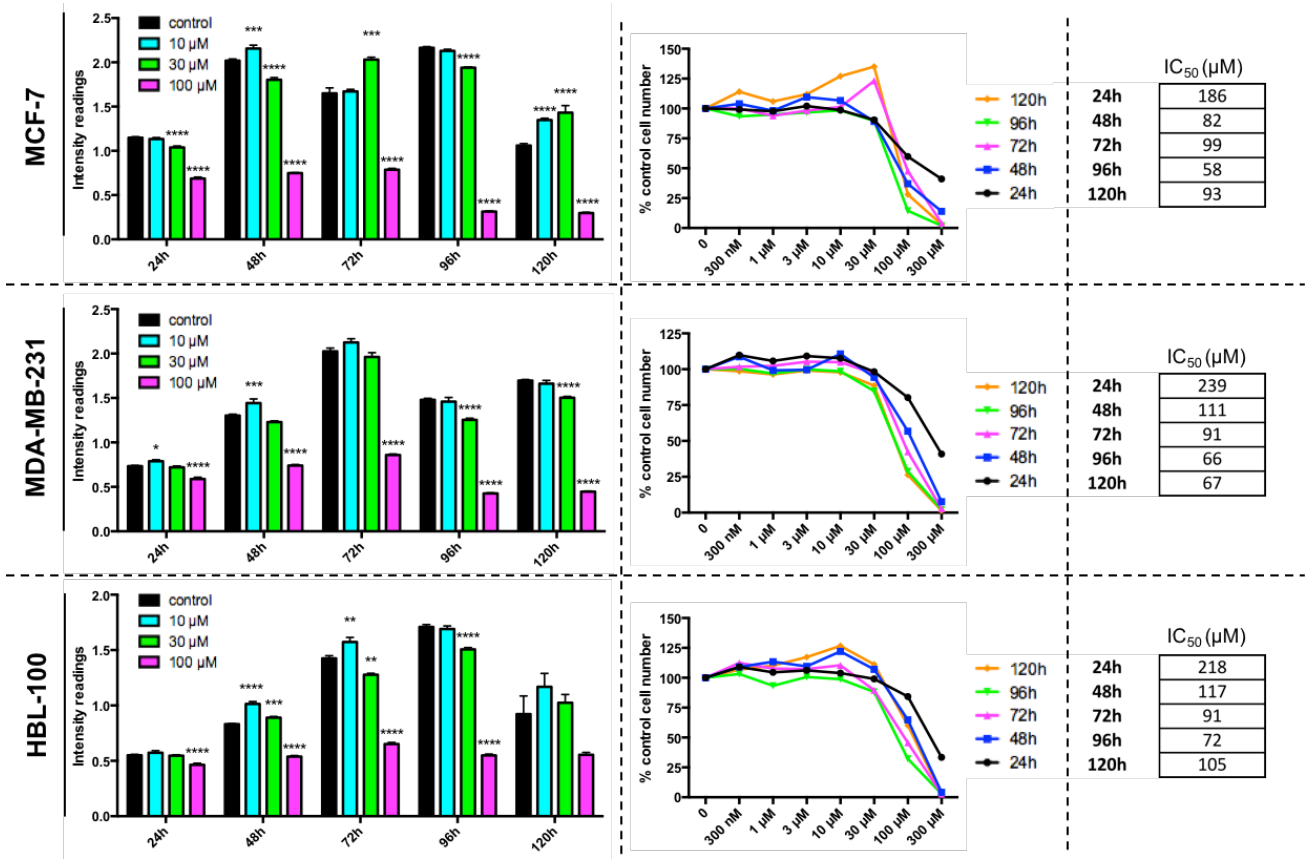

Figure 39. Acute hypoxic cancer cells show a slightly increased resistance to the effects of DMA on cancer cell number.

*Left column: The effects of DMA on the intensity readings of acute hypoxic cancer cells, compared to un-treated cells. Data expressed as mean ± SEM (n=6). *P≤0.05, **P≤0.01, ***P≤0.001 and ****P≤0.0001 (One-way ANOVA followed by Dunnett's multiple comparison test performed, comparing only the values within each time point). Middle column: The effects of DMA on acute hypoxic cancer cell number, with each drug-treated intensity reading given as a percentage of the control intensity reading at that time point. Right column: The IC_{50} values (µM) for DMA in each of the acute hypoxic cell lines. These values were produced using the data from the middle column.*

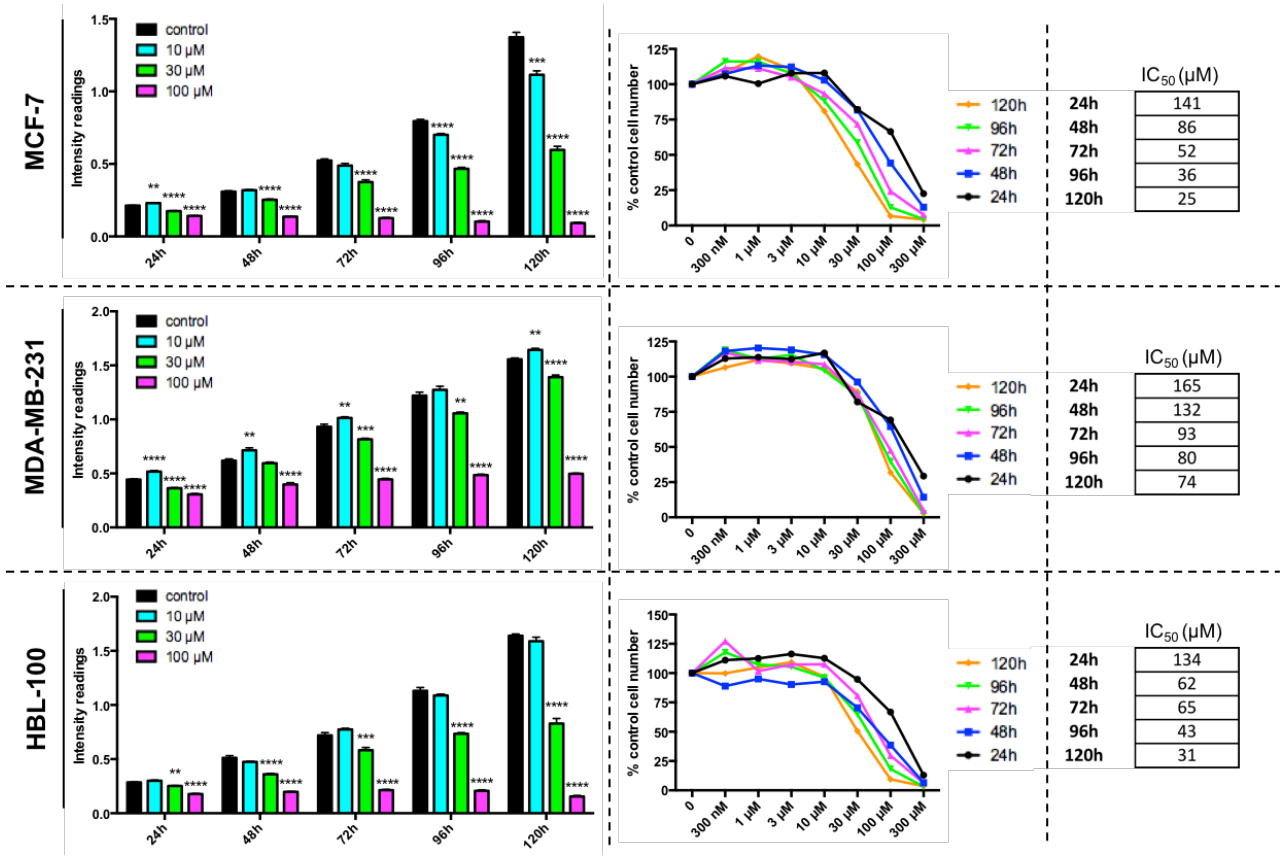

Figure 40. Chronic hypoxic MCF-7 and HBL-100 cells are re-sensitised to DMA treatment.

*Left column: The effects of DMA on the intensity readings of chronic hypoxic cancer cells, in comparison to un-treated cells. Data expressed as mean ± SEM (n=6). **P≤0.01, ***P≤0.001 and ****P≤0.0001 (One-way ANOVA followed by Dunnett's multiple comparison test performed, comparing only the values within each time point). Middle column: The effects of DMA on chronic hypoxic cancer cell number, with each drug-treated intensity reading given as a percentage of the control intensity reading at that time point. Right column: The IC_{50} values (µM) for DMA in each of the chronic hypoxic cell lines produced using the data in the middle column.*

Of the 3 drugs tested, the V-ATPase inhibitor bafilomycin A1 was the most potent, with nM concentrations of this drug causing significant reductions in cancer cell number in each of the conditions tested (figures 41 – 43). However, while the highest concentrations of the NHE1 inhibitor DMA tested exerted large effects on cancer cell number after only 24h of treatment (figures 38 – 40), the effect of bafilomycin A1 on cancer cell number was more delayed. 24h treatment with the concentrations of bafilomycin A1 tested had no large effect on cancer cell number in aerobic conditions (figure 41). By 48h treatment, higher concentrations of bafilomycin A1 had reduced cell number by around 25% in each of the cancer cell lines, with 72h of treatment with the V-ATPase inhibitor required to reduce cell number by over 50% (figure 41 middle and right columns). MCF-7 and MDA-MB-231 cells treated with 3 nM of inhibitor between the 24-120h time points had intensity values similar to that of the un-treated cells at 24h (figure 41 left column), indicating that cells treated with this concentration of drug were not exhibiting any increase in cell number compared to the control cells at 24h, possibly as a result of bafilomycin A1 treatment inhibiting the proliferation of these cells. In contrast, concentrations of bafilomycin A1 over 3 nM were leading to decreased intensity values compared to the 24h control cells as treatment time increased (figure 41 left column), indicating that these higher concentrations of bafilomycin A1 were leading to reduced cell numbers within the wells, possibly through the induction of cell death.

The results observed in the acute (figure 42) and chronic (figure 43) hypoxic cancer cells were comparable to those seen in the aerobic cells, with similar IC_{50} values obtained in these cells and the aerobic cells, suggesting that the culturing conditions did not influence the response of cells to bafilomycin A1 treatment.

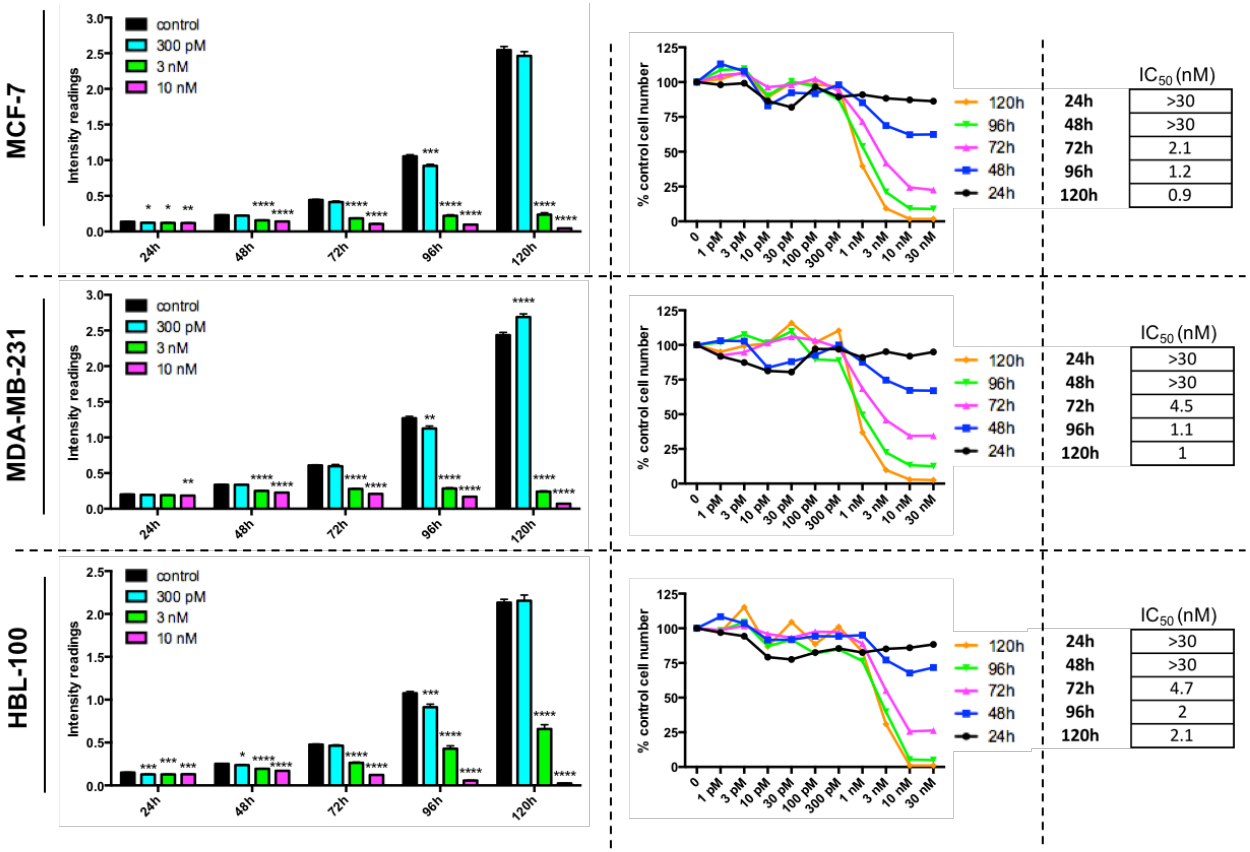

Figure 41. Nanomolar concentrations of bafilomycin A1 are required to reduce aerobic cancer cell number.

*Left column: The effects of bafilomycin A1 on the intensity readings of aerobic cancer cells, in comparison to un-treated cells. Data expressed as mean ± SEM (n=6). *P≤0.05, **P≤0.01, ***P≤0.001 and ****P≤0.0001 (One-way ANOVA followed by Dunnett's multiple comparison test performed, comparing only the values within each time point). Middle column: The effects of bafilomycin A1 on aerobic cancer cell number, with each drug-treated intensity reading given as a percentage of the control intensity readings at that time point. Right column: The IC_{50} values (nM) for bafilomycin A1 in each of the aerobic cell lines. These values were produced using the data from the middle column.*

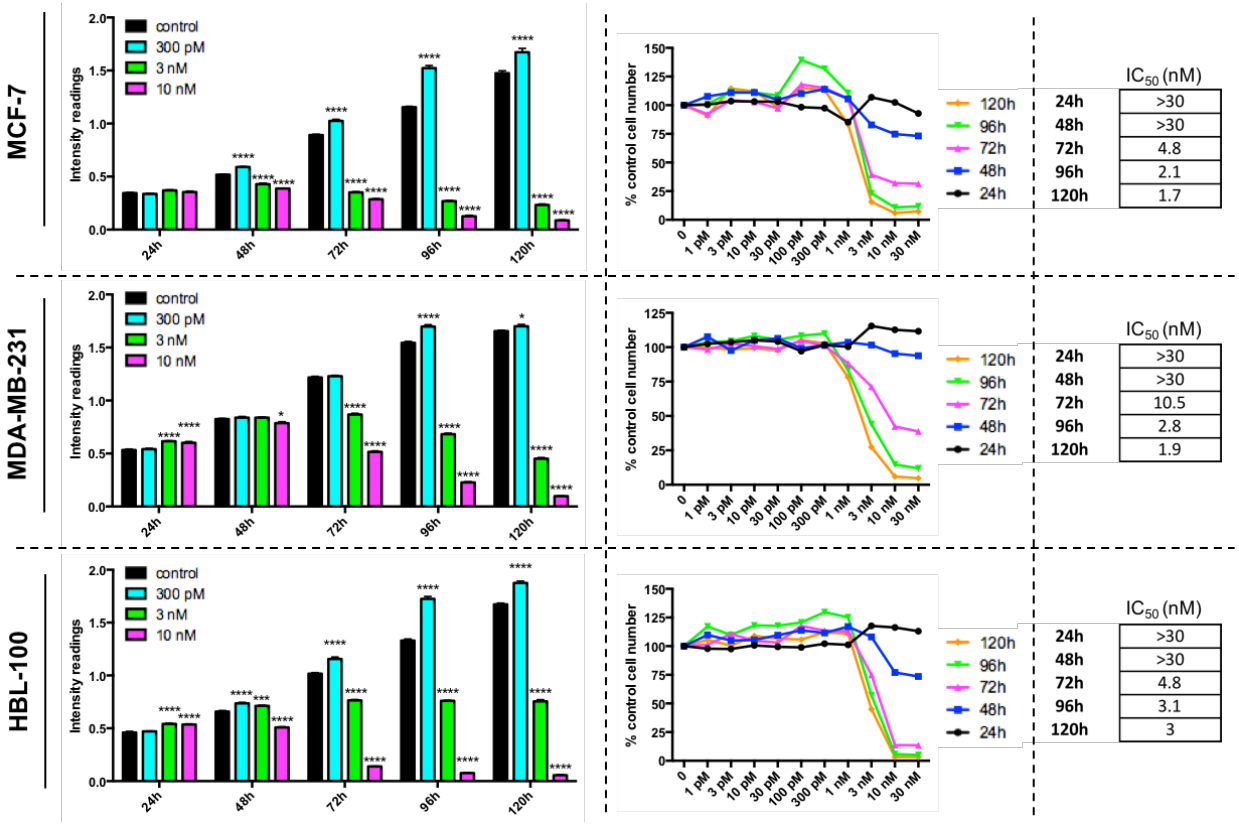

Figure 42. Acute hypoxic cancer cells show a similar sensitivity to the effects of bafilomycin A1 on cell number compared to aerobic cancer cells.

*Left column: The effects of bafilomycin A1 on the intensity readings of acute hypoxic cancer cells, compared to un-treated cells. Data expressed as mean ± SEM (n=6). *P≤0.05, ***P≤0.001 and ****P≤0.0001 (One-way ANOVA followed by Dunnett's multiple comparison test performed, comparing only the values within each time point). Middle column: The effects of bafilomycin A1 on acute hypoxic cancer cell number, with each drug-treated intensity reading given as a percentage of the control intensity readings at that time point. Right column: The IC_{50} values (nM) for bafilomycin A1 in each of the acute hypoxic cell lines. These values were produced using the data from the middle column.*

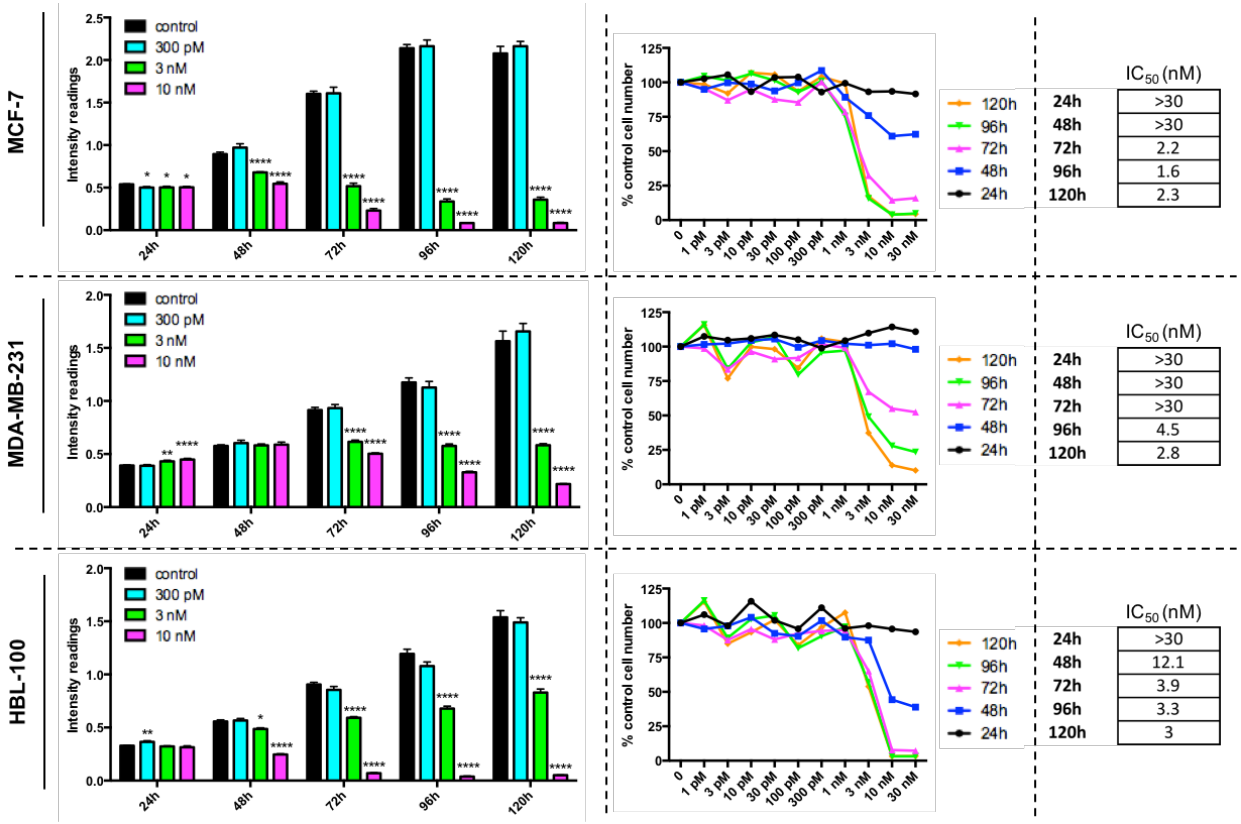

Figure 43. Chronic hypoxic cancer cells show a similar sensitivity to the effects of bafilomycin A1 on cell number compared to cells cultured in both aerobic and acute hypoxic conditions.

*Left column: The effects of bafilomycin A1 on the intensity readings of chronic hypoxic cancer cells, in comparison to un-treated cells. Data expressed as mean ± SEM (n=6). *P≤0.05, **P≤0.01, and ****P≤0.0001 (One-way ANOVA followed by Dunnett's multiple comparison test performed, comparing only the values within each time point). Middle column: The effects of bafilomycin A1 on chronic hypoxic cancer cell number, with each drug-treated intensity reading given as a percentage of the control intensity readings at that time point. Right column: The IC_{50} values (nM) for bafilomycin A1 in each of the chronic hypoxic cell lines produced using the data in the middle column.*

3.2.4 Preliminary experiments indicate that inhibitors targeting the tumour-associated carbonic anhydrases reduce the invasion of cells from MDA-MB-231 spheroids

3D invasion assays were carried out to compare the effects of inhibitors targeting the tumour-associated carbonic anhydrases, NHE1 and V-ATPase on cancer cell invasion (figure 44). For these experiments, spheroids were placed into collagen type 1, the major component of breast stroma within the body [366]. Spheroids produced from both MDA-MB-231 and HBL-100 cells were used in this analysis, as cells from spheroids of these cell lines exhibited the capacity to invade into collagen (figure 19). MCF-7 spheroids, however, were not used, as they were non-invasive. For these experiments, the MDA-MB-231 and HBL-100 spheroids were left to invade for 48h and 72h respectively in either aerobic or hypoxic (0.5% O_2) conditions.

100 μM concentrations of S4 significantly reduced the % of cells invading into collagen from MDA-MB-231 spheroids cultured in both 20% O_2 and 0.5% O_2 conditions (figure 44). However, while S4 also seemed to have an effect on the invasion of cancer cells from HBL-100 spheroids, reducing the % of invading cells in hypoxic conditions at higher concentrations, carbonic anhydrase inhibition did not lead to any significant reduction in invasion from HBL-100 spheroids cultured in either aerobic or hypoxic conditions.

NHE1 and V-ATPase inhibition had little impact on invasion, with no significant decrease in the % of invading cells observed in drug-treated MDA-MB-231 and HBL-100 spheroids cultured in either aerobic or hypoxic conditions (figure 44). In fact, certain concentrations of both of the NHE1 and V-ATPase inhibitors were seen to lead to a significant increase in the amount of invasion.

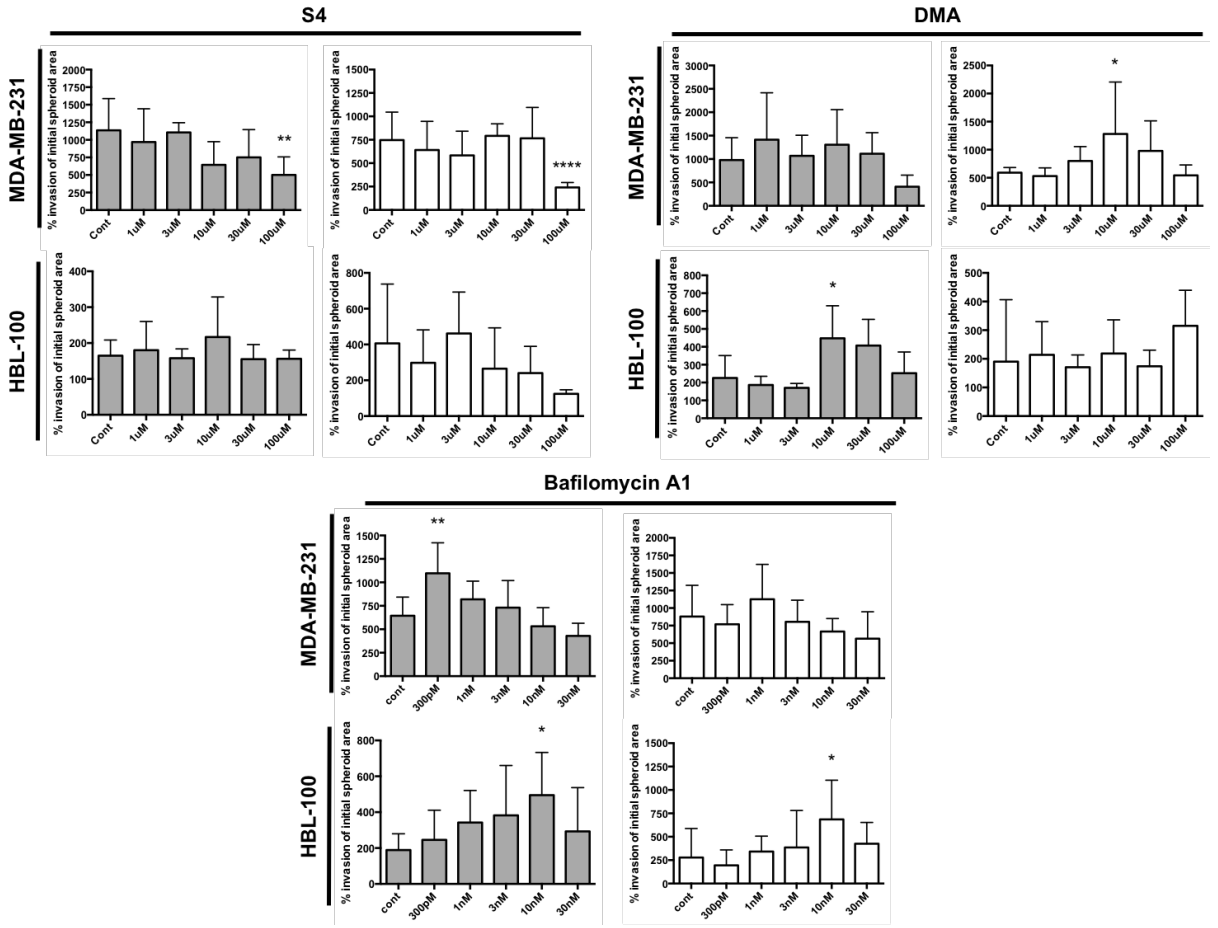

Figure 44. Preliminary invasion assays conducted with inhibitors targeting the 3 pH regulating proteins indicate that S4 reduces the invasion of cells from MDA-MB-231 spheroids cultured in both 20% and 0.5% O_2 conditions.

See next page for figure legend.

Figure 44. Preliminary invasion assays conducted with inhibitors targeting the 3 pH regulating proteins indicate that S4 reduces the invasion of cells from MDA-MB-231 spheroids cultured in both 20% and 0.5% O_2 conditions.

*The effect of S4, DMA and bafilomycin A1 on cancer cell invasion from MDA-MB-231 and HBL-100 spheroids cultured in 20% O_2 (grey bars) and 0.5% O_2 (white bars) conditions was analysed in 3D invasion assays. Data expressed as mean ± SD (at least 4 technical replicates were present for each drug concentration). * $P \leq 0.05$, ** $P \leq 0.01$, **** $P \leq 0.0001$ (One-way ANOVA followed by Dunnett's multiple comparison test performed).*

IHC was carried out in order to assess CAIX and NHE1 expression levels within invading spheroids present in collagen. This experiment was performed with un-treated HBL-100 spheroids placed into collagen type 1 and left to invade for 24h (figure 45A) and 48h (figure 45B) in 20% O_2 conditions. While the pattern of NHE1 protein expression was similar to that already shown (figure 28), the expression of CAIX within these collagen embedded spheroids differed from that previously observed. Whereas the preceding analysis of CAIX expression in HBL-100 spheroids showed CAIX expression to be strongest in the central hypoxic regions of the spheroid (figure 28), invading HBL-100 spheroids embedded in collagen for 24h (figure 45A) and 48h (figure 45B) exhibited strong CAIX expression in cells at the outer rim of the spheroids, in addition to the high levels of CAIX present in the more central cells. The isolation of MDA-MB-231 spheroids for IHC proved more problematic than that of the HBL-100 spheroids. As a result, no IHC was performed on the MDA-MB-231 spheroids embedded in collagen.

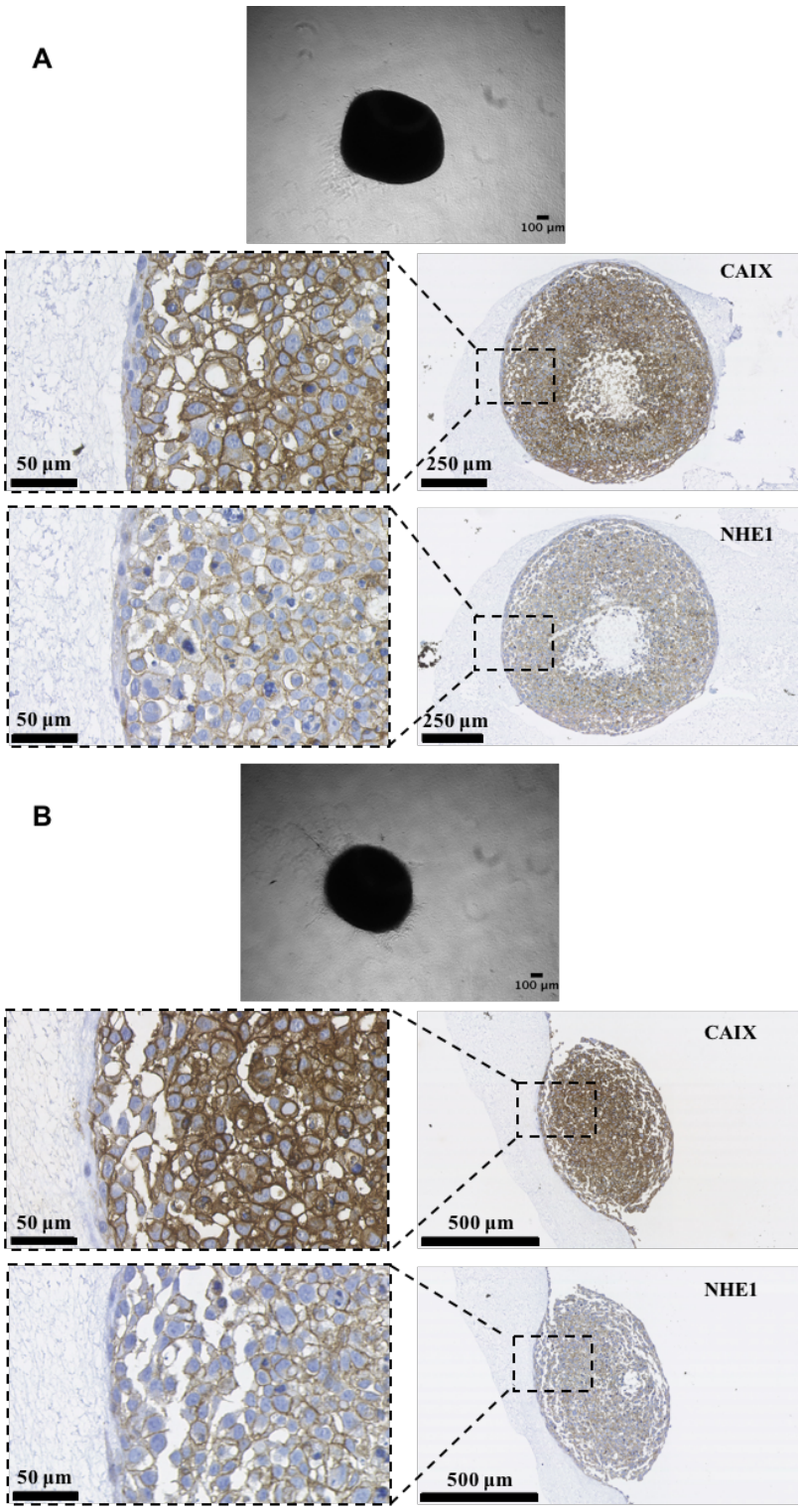

Figure 45. CAIX and NHE1 expression within HBL-100 spheroids present in collagen type 1. The CAIX expression results indicate that the spheroids cultured in 20% O_2 conditions may be hypoxic.

IHC assessing CAIX and NHE1 expression was performed on HBL-100 spheroids that were placed into collagen and left to invade for 24h (A) and 48h (B) without the addition of any S4. Images of the spheroids present in collagen before fixation are also shown.

3.2.5 Preliminary clonogenic assays suggest that inhibitors targeting the tumour-associated carbonic anhydrases and NHE1 have potential to combine with irradiation.

3D clonogenic assays were carried out with MDA-MB-231 spheroids to compare the effects of inhibitors targeting the tumour associated carbonic anhydrases, NHE1 and V-ATPase on their ability to combine effectively with irradiation, and lead to significantly reduced colony numbers when compared to either irradiation or drug treatment alone.

S4 and FC9403A (another carbonic anhydrase inhibitor previously shown to have potency in experiments carried out within the laboratory [355]) were the 2 carbonic anhydrase inhibitors tested in these clonogenic assays, along with the NHE1 inhibitor DMA and the V-ATPase inhibitor bafilomycin A1 (figure 46). Concentrations of these inhibitors that were previously shown to not have large effects on cancer cell number (section 3.2.3) were chosen for these assays.

The results from these experiments suggested that both FC9403A (figure 46A) and DMA (figure 46C) may have the ability to combine with irradiation, with the combination of drug and 0.5 Gy leading to a significant reduction in the survival fraction of MDA-MB-231 cells when compared against either treatment alone. However, while positive results were observed with both of these inhibitors, no significant reduction in survival fraction was observed in the MDA-MB-231 cells treated with a combination of S4/bafilomycin A1 and 0.5 Gy compared to either treatment alone (figure 46B and D), indicating that no effective combination was occurring.

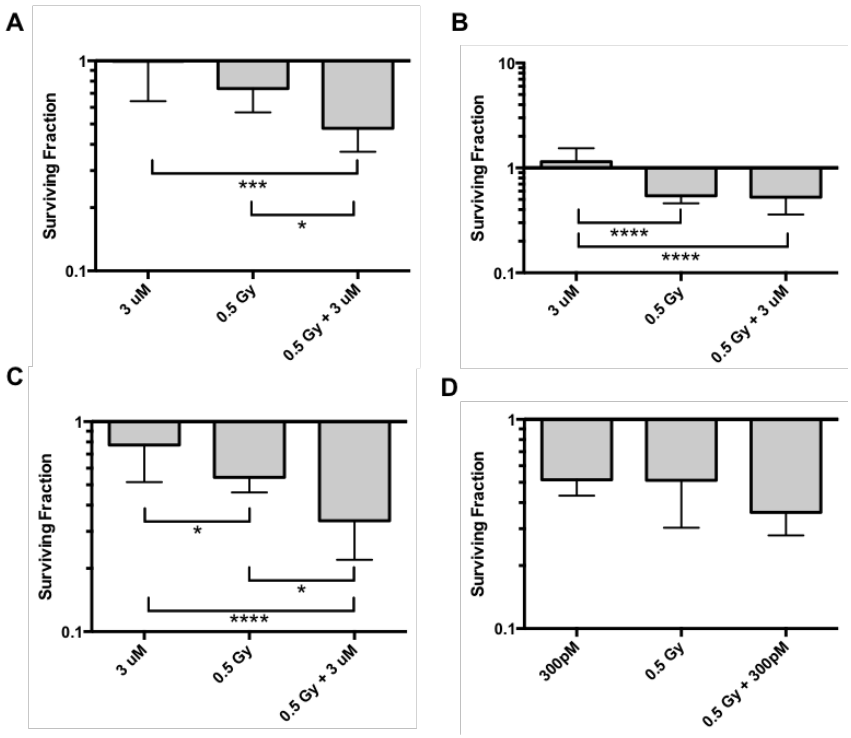

Figure 46. 3D clonogenic assays performed with MDA-MB-231 spheroids suggest that inhibitors targeting the tumour-associated carbonic anhydrases and NHE1 have potential to combine with irradiation.

3D clonogenic assay assessing the effect of the carbonic anhydrase inhibitors FC9403A (A) and S4 (B), the NHE1 inhibitor DMA (C), and the V-ATPase inhibitor bafilomycin A1 (D) on MDA-MB-231 surviving fraction, either alone or in combination with 0.5 Gy irradiation. Plating efficiencies calculated for each of the experiments were 0.083 (FC9403A), 0.115 (S4 and DMA), and 0.112 (bafilomycin A1). Data expressed as mean ± SD (n=8-11) $P \leq 0.05$, *** $P \leq 0.001$, **** $P \leq 0.0001$ [Kruskal-Wallis test (A) and one-way ANOVA followed by Tukey's multiple comparison test (B-C) performed].*

3.3 Discussion

The abnormal regulation of H^+ ions within cancer cells is thought to be one of the most distinctive characteristics of cancer [269]. The carbonic anhydrases CAIX and CAXII, NHE1 and V-ATPase are pH regulating proteins that have been linked with cancer (see section 1.14). In addition to an assessment of the expression levels of these proteins in differing O_2 concentrations, the work described in this chapter compared the effects of inhibitors targeting these molecules on cancer cell number and invasion in 2D and 3D culture models in both aerobic and hypoxic conditions, in addition to the effects of combining these inhibitors with irradiation in clonogenic assays. These assays were carried out in order to distinguish the most promising agent for further analysis.

Initial experiments assessed the expression of the pH regulatory proteins in differing O_2 conditions in both 2D and 3D culture systems. The expression levels of the hypoxia inducible factors, crucial mediators of the response of hypoxic tumour cells to low O_2 concentrations [122], were also analysed to indicate the extent of hypoxia within the cells cultured in 2D. Hypoxyprobe, a compound that is reduced in cells when O_2 concentration is 1.3% or less [407], forming a covalent bond with the thiol groups of proteins, was used to detect the presence of hypoxic areas within the spheroids. Hypoxyprobe has been used before for the detection of hypoxic areas within multicellular tumour spheroids [408, 409].

The 2D expression analysis results observed with HIF-1α were consistent with expectation, with significantly increased levels of HIF-1α protein present in each of the cell lines cultured in the lower percentage O_2 conditions (figures 20 – 22). Two bands were identified for HIF-1α in each of the cell lines. Numerous published studies have reported the presence of two bands in western blots when analysing HIF-1α protein levels [410-415], with some suggesting that the presence of the two bands results from HIF-1α phosphorylation [410, 412, 413, 415]. Previous work has indicated that HIF-1α and HIF-2α are stabilised at different O_2 concentrations and have varying temporal responses to hypoxia, with HIF-1α reported to respond preferentially to acute hypoxic conditions in neuroblastoma cells [416], while HIF-

2α has been shown to accumulate gradually over time in less severe O_2 concentrations in both neuroblastoma and cervical cancer cell lines [416, 417]. However, a differential response in HIF-1α and HIF-2α stabilisation in hypoxic conditions was not observed in the western blots performed here, with significant increases in the levels of HIF-2α detected within MDA-MB-231 cells cultured in 0.5% O_2 conditions, and HBL-100 cells exposed to both 2% and 0.5% O_2 concentrations, mirroring the results observed with HIF-1α in these cell lines (figures 21 and 22). Both HIF-1α and HIF-2α mRNA levels were much more consistent across the different O_2 conditions in the 3 cell lines compared to the protein levels (figure 23). These results were expected, as the O_2-dependent regulation of the HIF pathway is known to be controlled primarily at the post-transcriptional level [112].

The expected hypoxyprobe staining was observed in the multicellular tumour spheroids produced from the MCF-7 (figure 26) and HBL-100 (figure 28) cell lines. Hypoxic areas were evident in the more central areas of the spheroids from these cell lines, with the cells present in the outer rim lacking any positive staining. However, the staining of the MDA-MB-231 spheroids (figure 27) differed to that of the other two cell lines, with only certain areas of the spheroid surrounding the necrotic core exhibiting hypoxyprobe staining. The reason for the observation of such selective staining is unknown. Some positive staining was also seen in areas near the outer edge of the spheroids. A previous study has shown the detection of hypoxyprobe staining within normoxic MDA-MB-231 cells overexpressing cytochrome p450 reductase [418]. The positive staining in some of the MDA-MB-231 cells near the outer edges of the MDA-MB-231 spheroids may be evidence of the presence of cells with increased levels of this enzyme.

Of the pH regulatory proteins analysed, the expression levels of tumour-associated carbonic anhydrases were the most sensitive to changes in O_2 concentrations. CAIX expression is induced by hypoxia and HIF-1 [132, 242]. However, CAIX protein expression in the 2D and 3D cell culture models differed considerably between the 3 cancer cell lines, despite the observation of similar levels of HIF-1α and hypoxyprobe staining in each of the cell lines in the lower O_2 concentrations. CAIX

mRNA (figure 23) and protein (figures 20 and 26) expression within the MCF-7 cell line was the least responsive to low O_2 conditions, while significant increases in CAIX expression were evident within the MDA-MB-231 and HBL-100 cell lines in hypoxia in both 2D (figures 21–23) and 3D (figures 27–29). Further work, presented in Chapter 4, investigated the possible mechanisms leading to the varying expression of CAIX protein observed between the 3 cell lines.

CAXII expression was also shown to be modulated by changes in O_2 concentrations. Similar to the CAIX expression, differing results were observed between the 3 cell lines. Comparable levels of CAXII mRNA were detected in the MDA-MB-231 and HBL-100 cells, with a small significant increase in the levels of CAXII mRNA detected in hypoxic conditions in both cell lines. Aerobic MCF-7 cells exhibited the highest levels of CAXII mRNA out of all the samples analysed, with a significant decrease in the levels of CAXII mRNA observed in hypoxic conditions with the MCF-7 cells (figure 23). CAXII protein expression within the MCF-7 spheroids produced similar results, with a significant decrease in the levels of CAXII protein detected in the hypoxic regions (figure 30A). Other studies have demonstrated the presence of an inverse relationship between the expression of the different carbonic anhydrase isoforms, with the reduction of CAIX protein levels through shRNA previously shown to lead to increased CAXII mRNA [419, 420] and protein [420] expression. These observations have led some investigators to hypothesise that the different carbonic anhydrase isoforms might communicate in a network which has yet to be fully resolved [419]. Although no significant induction of CAIX protein was observed within acute hypoxic MCF-7 cells in 2D, or within the hypoxic areas of MCF-7 spheroids, the up-regulation of other carbonic anhydrase isoforms not assessed in the 2D or 3D analysis performed may help explain why CAXII protein and mRNA levels were reduced in low O_2 conditions in this cell line.

While plasma membrane expression of CAXII was detected within the cells of the MCF-7 spheroids, intracellular CAXII staining was observed within the spheroids of the MDA-MB-231 and HBL-100 cell lines (figures 27 and 28). Both plasma membrane and intracellular localisation of CAXII staining has been shown before in

IHC performed on human breast cancer tissue [421], with intracellular CAXII also seen within MDA-MB-231 cells in other studies as well [231]. The lack of plasma membrane CAXII in the MDA-MB-231 and HBL-100 spheroids suggests that, at least in 3D, this isoform is unlikely to be involved in the control of pHi within cells of these cell lines.

NHE1 mRNA and protein expression levels were observed to be quite constant in the different O_2 concentrations tested in 2D cell culture (figure 24). 3D expression analysis indicated that the hypoxic areas within MCF-7 spheroids displayed a significantly higher percentage of NHE1-positive cells compared to the normoxic regions, with the intensity of NHE1 staining also increased in the hypoxic areas (figure 31). While previous work conducted in other cell lines has shown NHE1 expression to be regulated by hypoxia and HIF-1 (see section 1.11), other studies assessing NHE1 protein expression in MCF-7 spheroids did not observe any regional variation in NHE1 expression levels [422, 423]. However, within those studies protein expression was analysed in spheroids that were allowed to form for 1, 15 and 30 days [422], or for 9 days [423], whereas the spheroids used in this study were only allowed to form for 1 week before fixation. The differing times at which NHE1 expression was assessed within the spheroids may have contributed to the variation in the results observed. With reports indicating that NHE1 expression within certain cell types is controlled by HIF-1 [254], it is interesting that the NHE1 protein within the MCF-7 cell line was the most responsive to low O_2 concentrations, as this cell line exhibited the lowest level of CAIX (another protein reported to be controlled by HIF-1 signalling [132, 242]) mRNA and protein expression out of the 3 cell lines. As such, it is probable that mechanisms other than hypoxia and HIF-1α stabilisation also control NHE1 expression within this cell line. pH has been shown to lead to changes in the expression levels of NHE1 in some cell types [424]. However, acidic pH was found to lead to decreased NHE1 expression levels in this study. Therefore, acidosis in the hypoxic areas of the MCF-7 spheroids is unlikely to be the cause of the increased NHE1 protein expression observed.

[425]Of the 3 different pH regulatory proteins analysed, the 2D protein expression analysis showed that V-ATPase expression was the most stable across the different O_2 concentrations analysed (figure 25A–D). An analysis of V-ATPase expression in 3D was also attempted, however, quantification of V-ATPase expression levels was not possible due to problems encountered with the antibody. Nonetheless, the preliminary experiments presented similar results to the 2D expression analysis, with no obvious difference in V-ATPase protein expression observed in the different areas of the spheroids analysed (figures 26 and 28). The observations were in line with the expected results, as little work has been published to date associating hypoxia or HIF to changes in V-ATPase expression levels.

Studies suggest that V-ATPase subunit composition controls the targeting of V-ATPase to different cellular compartments, with both the ATP6V0A3 and ATP6V0A4 subunits connected to the targeting of V-ATPase to the plasma membrane of breast cancer cells [400]. mRNA analysis indicated that there was no change in the expression levels of the ATP6V0A3 subunit in hypoxia in any of the cell lines (figure 25F). However, significantly increased levels of the ATP6V0A4 subunit were detected in the chronically hypoxic MDA-MB-231 cells (figure 25G). These results suggest that hypoxia may increase the levels of V-ATPase targeted to the cell surface within the MDA-MB-231 cell line, where it could contribute to the invasion of cells through the increased acidification of the extracellular microenvironment. This would help account for the increased capacity this cell line exhibits to migrate and invade in hypoxic conditions [426, 427]. Therefore, while no large changes in V-ATPase protein expression levels were observed in the differing O_2 conditions, hypoxia may instead influence the localisation of V-ATPase complexes within the cell. Further work assessing the effects of hypoxia on ATP6V0A3 and ATP6V0A4 subunit expression and V-ATPase localisation is merited.

Both CAIX and CAXII support cancer cell survival as a result of their function in controlling pH levels within the cells (section 1.15.2). Studies have revealed the contribution of CAIX to the control of pH within multicellular tumour spheroids,

with spheroids lacking CAIX protein shown to have increased levels of acidity at their core [428]. Knockdown of CAIX within a colon cancer cell line was also demonstrated to reduce Ki67 staining within the hypoxic areas of spheroids formed from this cell line [429]. IHC was performed assessing Ki67 and cleaved caspase 3 staining within spheroids (figures 33–34) to investigate whether there was any association between the different expression patterns of both CAIX and CAXII observed between the cell lines, and proliferation and apoptosis. The normoxic and hypoxic areas of both MDA-MB-231 and HBL-100 spheroids exhibited similar levels of Ki67 (figure 32A). However, large differences were detected between cells present in the normoxic and hypoxic regions of MCF-7 spheroids, with significantly lower levels of proliferative cells present in the hypoxic areas of MCF-7 spheroids (figure 32A). The lower levels of CAIX protein present in the hypoxic areas of MCF-7 spheroids, combined with the down-regulation in CAXII protein observed, may have contributed to these results, as the hypoxic MCF-7 cells may have been less able to control their pH compared to the cells present within the hypoxic areas of the MDA-MB-231 and HBL-100 spheroids, which exhibited high expression levels of CAIX.

IHC staining assessing cleaved caspase 3 staining indicated that cells within the hypoxic areas of both the MCF-7 and HBL-100 spheroids were undergoing significantly increased levels of apoptosis compared to the normoxic cells (figure 32B). However, the observation of cleaved caspase 3 staining within MCF-7 spheroids was abnormal, as it has previously been reported that the MCF-7 cell line does not express caspase 3 [430-432]. With these studies in mind, tests should have been performed prior to the IHC experiments to ensure the specificity of the antibodies used. Additionally, to prevent any potential inaccuracies with the thresholding of staining, and to improve the validity of the IHC analysis performed, the image analysis conducted should have also been carried out by a second investigator blinded to the initial work.

SRB assays were performed to compare the effects of inhibitors targeting the tumour-associated carbonic anhydrases (figures 35–37), NHE1 (figures 38–40) and

V-ATPase (figures 41–43) on aerobic, acute hypoxic and chronic hypoxic cancer cell number. Targeting each of the pH regulating proteins led to a reduction in cancer cell number, in agreement with previous studies [310, 355, 393-397]. However, culturing conditions had an unexpected effect on the response of the cancer cells to DMA and S4, with the acute hypoxic cells exhibiting increased resistance to drug treatment. While no increase in NHE1 protein expression levels were observed in any of the cell lines cultured in acute hypoxic conditions in 2D, the higher CAIX expression levels observed in low O_2 conditions were expected to lead to an increased sensitivity to S4 treatment, as the raised expression levels might have meant an increased dependency on this protein for the control of pH within the cell. In addition to stimulating CAIX expression, hypoxia has also been shown to lead to the increased activity of both CAIX and NHE1 (section 1.16). Therefore, it is possible that increased CAIX protein expression, in addition to the increased activity of CAIX and NHE1, may actually contribute to the increased resistance of the acute hypoxic cells to drug treatment, meaning that higher concentrations of inhibitors are required to exert an effect on these cells.

Both MCF-7 and MDA-MB-231 cell lines were sensitive to S4 treatment in aerobic conditions. The observation of high levels of CAXII mRNA in the aerobic MCF-7 cells in 2D cell culture, in addition to the plasma membrane CAXII observed in cells within the normoxic regions of MCF-7 spheroids, may help explain the sensitivity of these cells to S4 in high O_2 conditions. However, this pattern of CAXII expression was not observed within the MDA-MB-231 cell line present in 20% O_2 conditions. Previous studies have shown that over-confluence can lead to CAIX expression in cells [242, 433]. Therefore, it is possible that the effects of S4 observed on MDA-MB-231 cancer cell number were due to the over-confluence of cells within the wells. As a result of the observation of similar levels of NHE1 protein expression in each of the cell lines in aerobic conditions in 2D cell culture, the reduction in cancer cell number observed with DMA in 20% O_2 was not surprising.

In contrast to the acute hypoxic cancer cells, the response of chronic hypoxic cancer cells to S4 and DMA treatment was more similar to that seen in the aerobic cells,

suggesting that the chronic hypoxic cells had re-sensitised to drug treatment. The S4 results were again unexpected, taking into account the response of acute hypoxic cells to this agent, as the chronic hypoxic cells also had much increased levels of CAIX compared to the aerobic cells. The chronic hypoxic cells had been cultured in 0.5% O_2 conditions for 20 weeks before treatment. The presence of the cells in such harsh culturing conditions for an extended period of time may have meant that the cells were more sensitive to both carbonic anhydrase and NHE1 inhibition.

In comparison to the results presented with the carbonic anhydrase and NHE1 inhibitors, the response observed with the V-ATPase inhibitor bafilomycin A1 was similar between each of the cell lines, with no noticeable change in the SRB results in either the acute or chronic hypoxic cells. V-ATPase inhibition was seen to have more potent effects on cancer cell number compared to the other inhibitors, with low nM concentrations required to reduce cell number by over 50% in each of the cell lines. The low IC_{50} values obtained for V-ATPase possibly reflect the diverse roles played by V-ATPase in the cell that are critical for cell function [239]. While the effects of the carbonic anhydrase and NHE1 inhibitors on cancer cell number were observed after only 24h treatment, the effects of bafilomycin A1 were delayed, with reductions in cell number only seen after 48 and 72h of treatment. One mechanism through which V-ATPase inhibition is thought to affect cancer cells is through the induction of apoptosis [395, 396, 434, 435], with the damage of cellular mitochondria [395, 396], or the increases in lysosomal pH leading to lysosomal dysfunction [435], possibly contributing to cell death. The induction of apoptosis within these studies was only detected 48 or 72h after Bafilomycin A1 addition [396, 434], perhaps explaining why a reduction in cell number was only observed after 48h treatment in each of the cell lines used in this study.

Many of the processes underlying tumour cell migration and invasion are dependent on pH (see section 1.13.1), with each of the pH regulating proteins analysed within this study linked to invasion. 3D collagen invasion assays were conducted with both MDA-MB-231 and HBL-100 spheroids to compare the abilities of S4, DMA and bafilomycin A1 to affect cancer cell invasion. To test the hypothesis that cells

present in hypoxic conditions would be more sensitive to the effects of drug treatment, due to increased target protein expression/activity, these experiments were carried out with spheroids cultured in either 20% O_2 or 0.5% O_2 conditions. However, IHC analysis of the collagen-embedded HBL-100 spheroids cultured in 20% O_2 conditions showed CAIX staining in the cells at the outer rim of the spheroids (figure 45), rather than in the central hypoxic regions alone, as observed in the previous expression analysis conducted with spheroids of this cell line (figure 28). The collagen used in the experiments may have inhibited O_2 from reaching the cells at the edges of the spheroid. Therefore, while these experiments were carried out with spheroids cultured in 20% and 0.5% O_2 conditions, it is possible that all of the cells within the spheroids cultured in the differing O_2 concentrations were hypoxic.

S4 was shown to reduce the % of invading cells from MDA-MB-231 spheroids present in both aerobic and hypoxic conditions (figure 44). Other studies, testing the effects of S4 on the MDA-MB-231 cell line, have also produced similar results, displaying the inhibitory effects of S4 treatment on the 2D migration [310] and 3D invasion [355], with S4 shown to retain its anti-metastatic effects *in vivo* [310]. In contrast, the spheroids treated with DMA and bafilomycin A1 did not exhibit any reduction in cancer cell invasion (figure 44). In fact, an increase in invasion was observed at certain concentrations for both of these inhibitors. Previous studies have already exhibited the anti-invasive effects resulting from the inhibition of both NHE1 [373, 398, 399] and V-ATPase [260, 335, 400]; therefore, the increases in invasion observed were surprising. However, because these results are only from one independent experiment with a number of technical replicates, repeat experiments are required testing the effects of these inhibitors on cancer cell invasion.

In retrospect, the presence of additional experimental controls in both the SRB and 3D invasion assays were required. Positive controls that are known to reduce cancer cell number, as well as the use of inhibitors that have been proven to reduce the invasion of cancer cells, would have increased confidence in the accuracy and validity of the results obtained from these experiments. Additionally, the passage

window of the cells used in some of the experiments was beyond that which is recommended [436]. New stocks of cells should have been obtained after 10 passages to prevent any changes that can result from the subculturing of cells [437].

The induction of apoptosis is one mechanism through which radiotherapy achieves its therapeutic effect [406]. Because acidic pHi is thought to have a permissive role in the induction of apoptosis [280], we hypothesised that the treatment of cancer cells post-irradiation with agents that target the pH regulating proteins of cancer cells would lead to increased levels of apoptosis within these cells, thereby sensitising them to irradiation. 3D clonogenic assays were conducted with MDA-MB-231 spheroids to directly compare the effects of S4, DMA and bafilomycin A1, and their potential to combine effectively with irradiation (figure 46). FC9403A, another novel carbonic anhydrase inhibitor synthesised by Fabrizio Carta of the University of Florence, was also used in these studies (figure 46). The spheroids in these experiments were irradiated with 0.5 Gy, dissociated, and then plated with or without the presence of drug. The results of these experiments suggested that both FC9403A and DMA have the potential to combine with irradiation, with a combination of drug and 0.5 Gy leading to a significant reduction in the survival fraction of MDA-MB-231 cells when compared against either treatment alone. There are different methods available to analyse and study the effects of combining therapies, assessing whether the combinatorial effects are additive, synergistic, or antagonistic (reviewed in [438] and [439]). Further work is required to investigate which combinatorial effects were observed.

While these experiments did present some positive results with two of the inhibitors tested, there were a number of issues with the experimental design. The plating efficiency of the control cells used in these experiments was much lower than that reported for other cancer cell lines [440]. The method of spheroid dissociation used (through repeated syringing) likely contributed to this, and any repeat experiments should use other methods, apart from mechanical dissociation, that have previously been employed in other studies [441-443]. Additionally, the cells were left for 7 days after irradiation before fixation. Even though this amount of time was sufficient for

colonies of 50 cells to form, longer periods of incubation before fixation would have been more appropriate [444], to ensure all cells who had the potential to form colonies were counted. Furthermore, while 0.5 Gy was used in the experiments conducted here, supplementary experiments should also test the effects of combining more clinically relevant doses of irradiation (such as 2 Gy) with each of the inhibitors. Lastly, experiments assessing a different sequence of treatments would also be beneficial. For the clonogenic assays conducted, the spheroids were first irradiated, and then treated with the different inhibitors after the cells were plated. While this sequence of treatments has been performed before, and shown the radiosensitisation effects of inhibiting V-ATPase [405], additional experiments performing drug treatment before irradiation, such as that carried out in other studies [320, 403], would also be beneficial.

4 Chapter 4: Further investigation of CAIX expression in 2D and 3D cancer models

4.1 Introduction

CAIX expression is induced by HIF-1α [132, 242]. However, despite the presence of similar levels of HIF-1α in each of the cancer cell lines cultured in the lower O_2 concentrations, CAIX protein expression levels were higher in the hypoxic MDA-MB-231 and HBL-100 cell lines compared to the MCF-7 cell line, which only exhibited a significant increase in CAIX protein expression levels under more severe hypoxic conditions (section 3.2.1). The 2D mRNA (figure 23) and 3D protein (section 3.2.2) expression analysis illustrated similar results.

This chapter details further expression analysis carried out in the 3 cancer cell lines that was performed to investigate why, despite the presence of similar levels of HIF-1α, CAIX expression differed between the cell lines. For HIF-1α to have an effect on gene expression, it must be present in the nucleus of the cells, where it can bind to HREs and induce the expression of target genes. Experiments conducted in Chapter 3 analysed HIF-1α levels in whole-cell lysates produced from the 3 breast cancer cell lines. While these experiments measured total cellular HIF-1α expression, they did not give an indication of the levels of transcriptionally active HIF-1α present within the nucleus of the cells. Therefore, to assess nuclear levels of HIF-1α, and to relate these levels to the quantities of CAIX, expression analysis was conducted in 2D using nuclear and cytoplasmic lysates acquired from each of the cancer cell lines cultured in either aerobic or hypoxic conditions. To further examine the relationship between HIF-1α and CAIX expression, additional work was also carried out evaluating the levels of both HIF-1α and CAIX in aerobic cancer cells treated with cobalt chloride ($CoCl_2$), a chemical that prevents the proteasomal degradation of the HIF-α subunits in high O_2 concentrations by occupying the VHL-binding domain [445].

While PHD proteins have a major role to play in the regulation of HIF-1α signalling, through controlling the degradation of HIF-1α (see section 1.8.2), FIH-1 is another

protein present in cells that inhibits HIF-1α signalling by hydroxylating the C-TAD of HIF-1α, thus impeding the binding of the transcriptional co-activators p300/CBP [130, 133]. Although PHD proteins are inactivated in low O_2 concentrations, studies have shown that FIH-1 retains it's activity in hypoxia [132], with more severe hypoxic conditions leading to the inactivation of FIH-1 [131]. Further work shown in this chapter presents the results from experiments conducted with siRNA targeting FIH-1, which was used to investigate whether increased levels or activity of FIH-1 were responsible for the low CAIX expression levels observed in acute hypoxic MCF-7 cells.

Other methods of FIH-1 inactivation, apart from inhibition due to more severe hypoxic conditions, have also been demonstrated. Mint3 has been shown to bind FIH-1, preventing FIH-1 from hydroxylating the C-TAD of HIF-1α, thus enhancing HIF-1α activity [446]. Membrane type-1 matrix metalloproteinase (MMP14), a protease present in the plasma membrane of cells which promotes invasion [447], has been linked to this inhibition of FIH-1, as studies have shown that MMP14 mediates the binding of FIH-1 to Mint3 [448] (figure 47). MMP14 is produced in cells in a latent form (60 kDa) that requires activation (reviewed in [449]). Cleavage of the latent form takes place in the Golgi network through the action of a protease called Furin, a protein that has the ability to also bind Mint3 [450]. Furin cleaves latent MMP14, leading to the production of active MMP14 (57 kDa), which is transported to the plasma membrane (reviewed in [449]). It is during the process of latent MMP14 cleavage by Furin that MMP14 is thought to bring FIH-1 and Mint3 together, leading to the suppression of FIH-1 activity [448]. Further processing of MMP14 can also occur. Auto-catalytic cleavage of active MMP14 present on the plasma membrane of cells can take place, leading to the generation of an inactive membrane tethered 44 kDa protein and a soluble 18 kDa inactive fragment (reviewed in [449]).

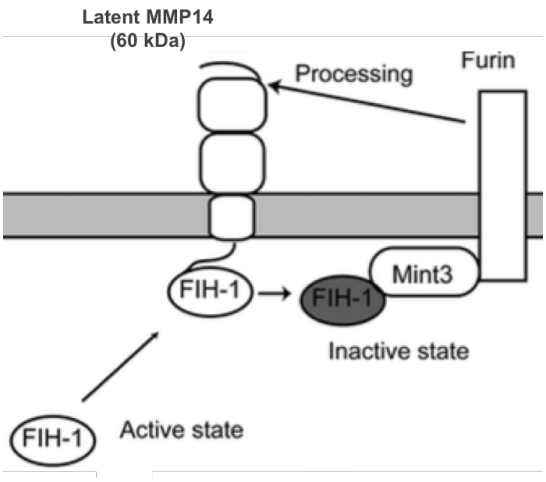

Figure 47. The proposed role of MMP14 in the inactivation of FIH-1.

Latent MMP14 is cleaved by Furin, leading to the binding of FIH-1 and Mint3, and the suppression of FIH-1 activity. Image adapted from [448].

Various studies have shown that both MDA-MB-231 [451, 452] and HBL-100 [453] cells express MMP14, while MCF-7 cells do not [451-453], with MMP14 expression shown to be modulated by HIF-2α [454]. To investigate whether the differential expression of MMP14 may also be contributing to the CAIX expression results observed in Chapter 3, analysis of MMP14 expression within the 3 cancer cell lines was also carried out in both 2D and 3D.

4.2 Results

4.2.1 Analysis of nuclear and cytoplasmic lysate samples indicates that CAIX expression differs between the 3 cell lines despite the presence of similar levels of nuclear HIF-1α in aerobic and hypoxic conditions

Nuclear and cytoplasmic lysates were acquired to assess the levels of HIF-1α and HIF-2α within the nuclei of MCF-7, MDA-MB-231 and HBL-100 cell lines, in addition to the protein levels of CAIX. These lysates were obtained from cells cultured in aerobic (24h in 20% O_2), acute hypoxic (24-72h 0.5% O_2) and chronic hypoxic (16 weeks in 0.5% O_2) conditions.

The results from the western blots assessing nuclear HIF-1α and HIF-2α levels were comparable to those seen in section 3.2.1. As in the whole-cell lysates, two bands were present for HIF-1α in each of the cancer cell lines cultured in both acute hypoxic and chronic hypoxic conditions, with increased band intensities observed in the lower O_2 conditions (figure 48A). Large increases in HIF-2α proteins levels were again evident within the MDA-MB-231 and HBL-100 cell lines cultured in hypoxic conditions (figure 48A). Similar to the whole-cell lysates analysed in section 3.2.1, CAIX expression within both the MDA-MB-231 and HBL-100 cell lines was more responsive to hypoxic induction compared to the MCF-7 cells, which exhibited the lowest levels of CAIX out of the 3 cell lines (figure 48A and B). Chronic hypoxic MCF-7 cells again displayed an increase in CAIX levels compared to the aerobic cells. However, in this experiment there were also significantly increased levels of CAIX protein evident within 48h and 72h acute hypoxic MCF-7 cells, in addition to the chronic hypoxic MCF-7 cells (figure 48A and B).

While quantification of CAIX protein levels was performed in the cytoplasmic lysates obtained from the 3 cell lines, this same analysis was not possible for either HIF-1α or HIF-2α due to problems encountered with expression of the loading controls. As the duration of hypoxic incubation increased, the levels of the nuclear loading control proteins Lamin B1 and TATA seemed to decrease, a problem that was not observed with the cytoplasmic loading control β-Actin (figure 48A). This

was especially noticeable within the HBL-100 cell line (figure 48C). This reduction in loading control levels at the later time points meant that the protein levels of HIF-1α and HIF-2α could not be accurately quantified.

Experiments were conducted to investigate why the levels of the nuclear loading controls were reduced in the hypoxic conditions (figure 48D). It was reasoned that there were two likely explanations for the drop in loading control levels; (i) either the slower proliferation rate of the hypoxic cells was leading to less cells being present at the time of lysate acquisition, and this was affecting the nuclear loading levels, or (ii) the expression levels of both Lamin B1 and TATA were being affected by the incubation of the cells in hypoxic conditions. To investigate this, additional nuclear lysates of HBL-100 cells cultured in 20% O_2 and 0.5% O_2 were obtained. The HBL-100 cell line was chosen for this analysis, as the presence of reduced levels of loading control in hypoxic conditions was the most obvious within this cell line. Two of the samples were produced as before, without counting of either the aerobic or hypoxic cells before lysate acquisition. In the other two samples cultured in the same conditions, the cells were counted before lysate acquisition to ensure the same number of cells were present. As can be seen in figure 48D, equal cell number at the time of lysate acquisition led to nuclear loading control levels of similar intensity in cells cultured in both 20% O_2 and 0.5% O_2 conditions. However, when the same numbers of cells were not present at the time of lysate acquisition, the levels of loading control were reduced in the cells cultured in hypoxic conditions. As a consequence of these results, cell numbers were counted prior to lysates acquisition in future experiments involving nuclear lysates in an effort to produce samples with equal loading control levels.

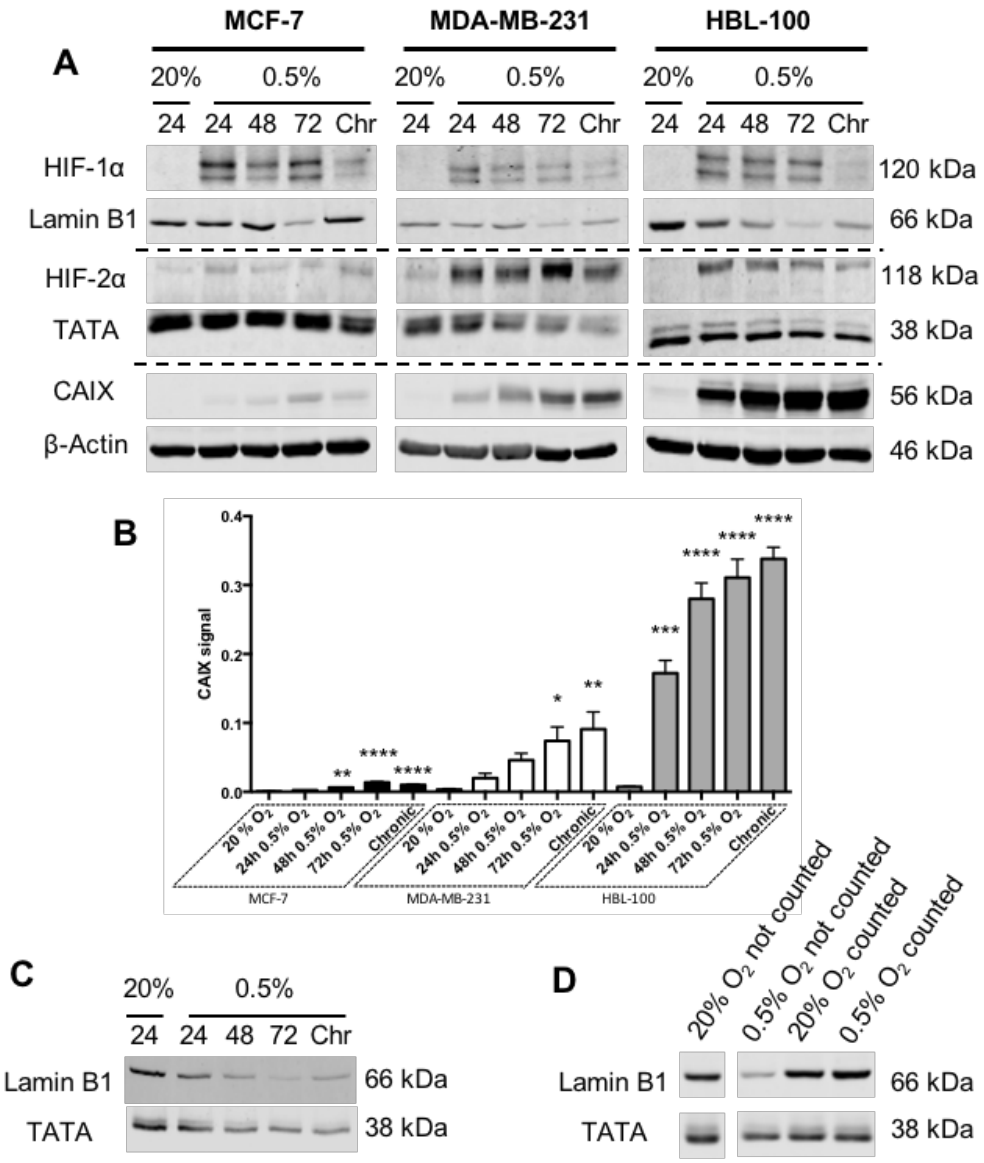

Figure 48. CAIX protein expression differs between the 3 cell lines cultured in hypoxic conditions, despite the presence of similar levels of HIF-1α within the nuclei of the cells.

*(A) Nuclear and cytoplasmic proteins were extracted from aerobic cells and acute hypoxic cells that had been cultured in 0.5% O_2 conditions for 24, 48 and 72h, in addition to cells that had spent 16 weeks in 0.5% O_2 conditions (Chr). Western blotting was performed to detect the nuclear levels of HIF-1α and HIF-2α, along with the cytoplasmic levels of CAIX. Lamin B1, TATA and β-Actin were used as the loading controls. (B) Densitometry measurements of CAIX levels. Data expressed as mean ± SEM (n = 3). * P ≤ 0.05, ** P ≤ 0.01, *** P ≤ 0.001, **** P ≤ 0.0001 (One-way ANOVA followed by Dunnett's multiple comparison test performed, comparing each sample to the 20% O_2 group). (C) Western blotting performed to detect the levels of Lamin B1 and TATA in nuclear lysates acquired from HBL-100 cells cultured in differing O_2 conditions. (D) Nuclear lysates acquired from HBL-100 cells cultured for 72h in either 20% or 0.5% O_2 conditions. Samples in which the cells were counted to ensure equal cell numbers were present prior to lysate acquisition are labelled.*

To further analyse the relationship between HIF-1α and CAIX in the 3 cell lines, additional experiments were carried out assessing their protein and mRNA levels in aerobic cells treated with $CoCl_2$, a chemical that prevents the proteasomal degradation of HIF-1α in high O_2 concentrations. Untreated cells present in 20% O_2 conditions were used as controls. An analysis of HIF-2α levels within $CoCl_2$-treated cells was also carried out.

Two bands were again identified for HIF-1α in each of the aerobic cancer cell lines treated with $CoCl_2$ (figure 49A-C). Out of all the time points analysed, the largest amount of stabilised HIF-1α was detected in the 5h $CoCl_2$-treated cells (figure 49A-C). A large significant increase in the levels of both HIF-1α bands was seen at this time point in each of the cell lines, with decreased HIF-1α protein levels observed at the later time points. The stabilisation of HIF-2α due to $CoCl_2$ treatment was not as apparent as that observed for HIF-1α, with only small increases in the levels of HIF-2α detected in the $CoCl_2$-treated MDA-MB-231 and HBL-100 cells (figure 49A). Differing results were observed in the mRNA analysis performed. While no significant changes were detected in the mRNA levels of HIF-1α after $CoCl_2$ addition in any of the cell lines (figure 49E), $CoCl_2$ treatment led to significantly increased levels of HIF-2α in the MDA-MB-231 and HBL-100 cell lines (figure 49F).

Induction of CAIX protein expression was evident in both MDA-MB-231 and HBL-100 cells treated with $CoCl_2$ (figure 49A and D). HBL-100 cells exhibited higher CAIX protein expression levels out of the two cell lines, and were the only cell line to show an induction of CAIX mRNA levels after $CoCl_2$ treatment (figure 49G). Despite the presence of similar levels of HIF-1α in the $CoCl_2$-treated MCF-7 cells compared to the other cell lines, no CAIX band was visible in the $CoCl_2$-treated MCF-7 cells (figure 49A and D).

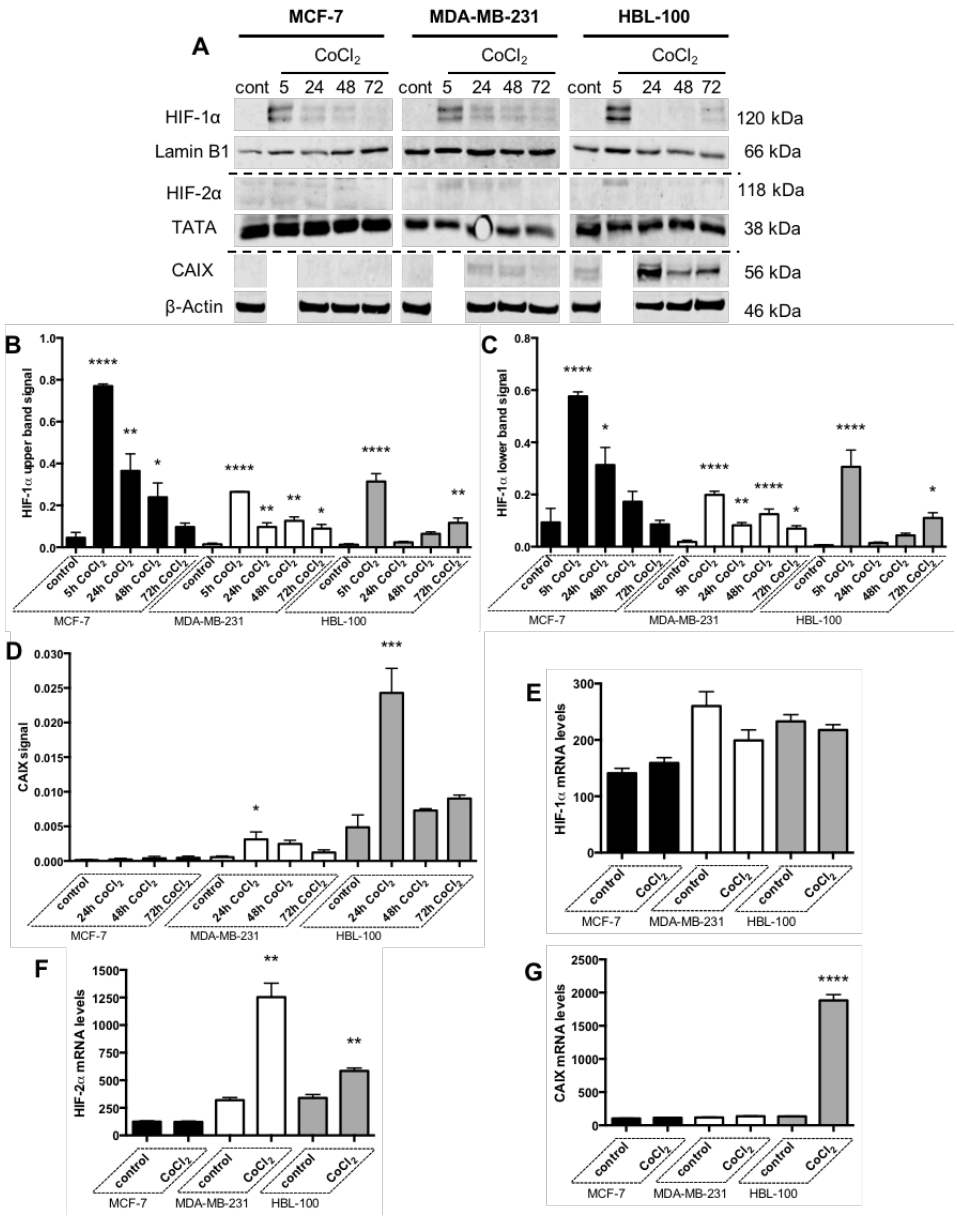

Figure 49. HIF-1α stabilisation due to $CoCl_2$ treatment leads to differing CAIX expression between the cell lines.

*The protein (A-D) and mRNA (E-G) expression levels of HIF-1α, HIF-2α and CAIX in aerobic cancer cells treated with 400 μM $CoCl_2$ for the indicated time points, with un-treated aerobic cells cultured in 20% O_2 conditions acting as the controls. (A) Western blots performed assessing the protein expression levels of HIF-1α, HIF-2α and CAIX. (B-D) Densitometry measurements of the upper (B) and lower (C) HIF-1α bands, in addition to CAIX (D). Data expressed as mean ± SEM (n = 5 for the nuclear control, 24/48/72h MCF-7 and MDA-MB-231 lysates. n = 4 for the nuclear control, 24/48/72h HBL-100 lysates. n = 2 for the 5h $CoCl_2$ nuclear lysates. n = 3 for the 5h $CoCl_2$ cytoplasmic lysates). * P ≤ 0.05, ** P ≤ 0.01, *** P ≤ 0.001, **** P ≤ 0.0001 (One-way ANOVA followed by Dunnett's multiple comparison test performed, comparing each sample to control group). (E-G) mRNA levels of HIF-1α (E), HIF-2α (F) and CAIX (G). Data expressed as mean ± SEM (n=3). ** P ≤ 0.01, **** P ≤ 0.0001 (Unpaired t-test, comparing each $CoCl_2$ sample to the 20% O_2 group within each cell line).*

4.2.2 2D expression analysis indicates that the protein expression of FIH-1 and MMP14 varies between the 3 cell lines

The protein and mRNA expression analysis conducted so far has shown that CAIX expression differs between the 3 cell lines, with hypoxic and $CoCl_2$-treated MCF-7 cells expressing much lower levels of CAIX in comparison to the two other cell lines. The observation of similar levels of nuclear HIF-1α in each of the 3 cancer cell lines indicated that this variation in CAIX expression was not due to any disparity in HIF-1α levels. Further analysis was conducted, assessing the protein expression levels of FIH-1 and MMP14 in each of the cancer cell lines, to investigate whether the differential expression of these proteins might explain the variation in CAIX expression observed (figure 50). Protein expression levels were analysed in cells cultured in aerobic (24h in 20% O_2), acute hypoxic (24-72h in 0.5% O_2) and chronic hypoxic (16 weeks in 0.5% O_2) conditions. An antibody targeting the extracellular domain of MMP14, which is released after autocatalysis of the active plasma membrane MMP14 as a soluble 18 kDa protein, was used to identify the presence of MMP14 in the western blots performed.

FIH-1 protein was detected in each of the 3 cancer cell lines (figure 50A). The culturing of cells in hypoxic conditions did not lead to any changes in the levels of FIH-1 (figure 50C). Out of the 3 cell lines, MCF-7 cells exhibited the highest expression levels of FIH-1 (figure 50C). Greater variation in MMP14 protein expression was observed between the 3 cancer cell lines (figure 50B). Both latent (60 kDa) and active (57 kDa) MMP14 were observed in MDA-MB-231 and HBL-100 cells cultured in aerobic and hypoxic conditions (figure 50B). Culture conditions had no significant effect on MMP14 expression within these two cell lines, although HBL-100 cells were seen to have increased amounts of the active 57 kDa MMP14 compared to MDA-MB-231 cells (figure 50D). Neither the latent (60 kDa) nor the active form (57 kDa) of MMP14 protein was detected within the MCF-7 cells (figure 50B). The mRNA analysis showed small significant changes in FIH-1 mRNA levels within the different culture conditions in both MCF-7 and MDA-MB-231 cells (figure 50E). MMP14 mRNA expression levels were constant in all 3 cell lines in the

differing conditions, with MCF-7 cells exhibiting comparable levels of MMP14 mRNA to the other two cell lines (figure 50F).

The mRNA analysis (figure 50F) showed that the absence of MMP14 protein (figure 50B) in MCF-7 cells was not due to a lack of gene transcription within these cells. A possible explanation for the lack of MMP14 protein detection within the western blot analysis, despite the presence of MMP14 mRNA within the cells, could be that the MMP14 mRNA present within MCF-7 cells is not translated into protein. However, the antibody used in the western blots binds to the extracellular portion of the MMP14 protein. This part of the protein is released after autocatalysis of MMP14, and would not be collected in the lysates used in this analysis. Therefore, the possibility that MCF-7 cells were expressing MMP14, but that this MMP14 was not detected with the antibody used, cannot be excluded.

The results presented thus far suggest a possible hypothesis to explain the lower CAIX expression levels observed within the acute hypoxic and $CoCl_2$-treated MCF-7 cells in comparison to the 2 other cell lines cultured in the same conditions. A combination of high FIH-1 protein levels in the MCF-7 cell line, combined with the lack of any MMP14 protein detected in the westerns performed, could be leading to higher levels of active FIH-1 in the MCF-7 cells. The greater levels of active FIH-1 in the MCF-7 cell line could be causing the increased hydroxylation of the HIF-1α C-TAD in these cells, thus inhibiting the binding of the co-activator p300/CBP to HIF-1α. Only partial HIF signalling would occur in these cells, thereby giving rise to lower levels of CAIX expression in the $CoCl_2$-treated and acute hypoxic MCF-7 cells. In contrast, MDA-MB-231 and HBL-100 cells displayed lower levels of FIH-1 protein in comparison to the MCF-7 cells, with the existence of MMP14 protein also detected in the western blots performed. The presence of MMP14 may be leading to the inhibition the FIH-1 within these 2 cell lines, enabling the binding of p300/CBP to the stabilised HIF-1α in the acute hypoxic and $CoCl_2$-treated cells, resulting in full HIF signalling and CAIX expression within these cell lines.

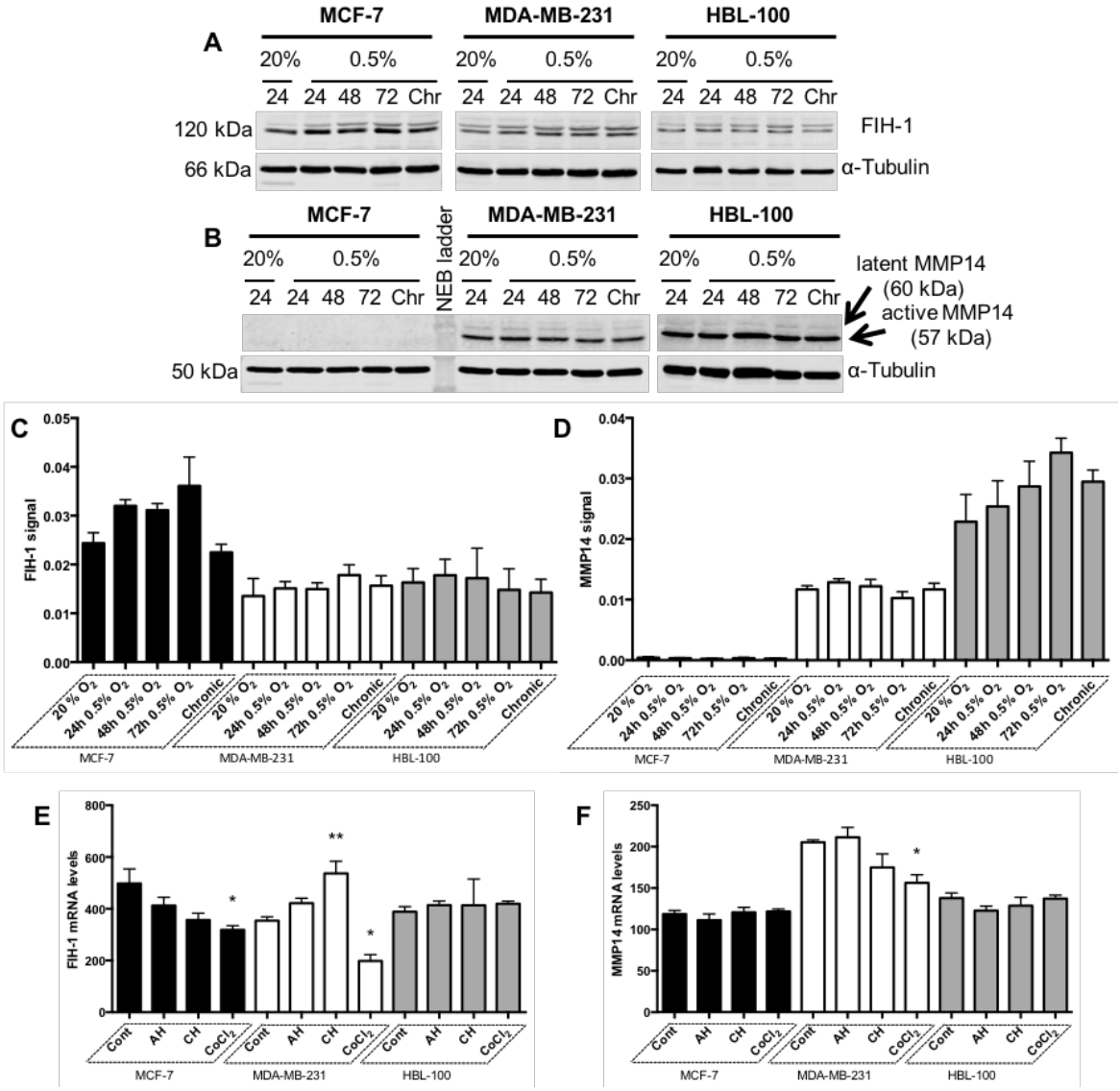

Figure 50. Western Blots indicate that MMP14 protein expression differs between the 3 cell lines despite the presence of similar levels of MMP14 mRNA. FIH-1 protein expression is unchanged across the different O_2 conditions.

*(A-D) Cytoplasmic proteins were extracted from the 3 cell lines cultured in in either aerobic or acute hypoxic conditions at the indicated time points, with cytoplasmic lysates also acquired from cells that had spent 16 weeks in 0.5% O_2 conditions (Chr). Western blotting was performed to detect FIH-1 (A, lower band) and MMP14 (B), with α-Tubulin acting as a loading control. Densitometry measurements of FIH-1 (C) and MMP14 (D) protein expression levels are also shown. (E-F) FIH-1 (E) and MMP14 (F) mRNA levels in cells cultured in 20% O_2 (cont), 0.5% O_2 for 24h (AH) and 0.5% O_2 for 10 weeks (CH). mRNA levels were also analysed in aerobic cells treated with 400 μM $CoCl_2$ for 24h. Data expressed as mean ± SEM (n = 3). * $P \leq 0.05$, ** $P \leq 0.01$ (One-way ANOVA followed by Dunnett's multiple comparison test, comparing each sample to the 20% O_2 group within the same cell line).*

4.2.3 FIH-1 contributes to the low levels of CAIX observed within the MCF-7 cell line

Experiments conducted in section 4.2.2 suggested that increased levels of active FIH-1 might have been the cause of the low CAIX expression levels seen within the acute hypoxic MCF-7 cells (see sections 3.2.1 and 4.2.1). siRNA targeting FIH-1 was used to investigate whether this was the case. MCF-7 cells were cultured in 0.5% O_2 conditions for 24h prior to siRNA addition, and were treated with either single siRNAs targeting FIH-1 (19-22), or a mixture of 4 siRNAs (pool). MCF-7 cells cultured in 0.5% O_2 conditions and treated with transfection reagent alone (mock) acted as the control in these initial experiments.

Each concentration of the pool of siRNAs tested led to a reduction in the levels of FIH-1 protein (bottom band) within the acute hypoxic MCF-7 cells compared to the mock control sample (figure 51A). The single siRNA 21 caused the largest reduction in FIH-1 protein levels of the 4 single siRNAs tested. A corresponding increase in CAIX protein levels was observed within the samples that exhibited the largest decrease in FIH-1 protein levels, with increased CAIX protein expression observed in the cells treated with the pool of siRNA and siRNA 21 (figure 51A).

Repeat experiments were performed to confirm these results (figure 51B). MCF-7 cells were again cultured in 0.5% O_2 conditions for 24h prior to treatment with either a pool of siRNAs at a concentration of 50 nM, or a single siRNA (21) at the same concentration. Hypoxic MCF-7 cells treated with scrambled siRNA (scrambled) and cells treated with transfection reagent alone (mock) acted as the controls, in addition to acute hypoxic MCF-7 cells that received no treatment (control). Both the pool and the single siRNA targeting FIH-1 reduced FIH-1 protein expression levels within the acute hypoxic MCF-7 cells compared to each of the controls (figures 51B and C). The CAIX protein expression levels within the pool and single siRNA-treated samples were increased in comparison to each of the control samples (figure 51B and D).

Previous work showed that HIF-1α stabilisation as a result of $CoCl_2$ treatment did not lead to CAIX expression within MCF-7 cells, whereas CAIX protein expression was observed in both the MDA-MB-231 and HBL-100 cell lines (figure 49). siRNA targeting FIH-1 was used to investigate whether reducing the levels of FIH-1 in $CoCl_2$-treated MCF-7 cells led to CAIX expression within this cell line (figure 51E-G). MCF-7 cells cultured in 20% O_2 conditions were treated with a pool of siRNAs, with $CoCl_2$ added 48h after the initial siRNA treatment. The duration of $CoCl_2$ treatment ranged from 24-72h. Aerobic MCF-7 cells that received siRNA alone, in addition to un-treated MCF-7 cells cultured in 20% O_2 conditions, acted as the controls.

Both the aerobic MCF-7 cells that received siRNA alone, and the cells that were given a combination of siRNA and $CoCl_2$, exhibited decreased FIH-1 protein levels in comparison to the control cells (figure 51E and F). While no increase in CAIX protein levels was observed within the cells that were treated with siRNA alone, a strong induction of CAIX protein expression was observed within MCF-7 cells that received a combination of both siRNA and $CoCl_2$, with the highest intensity CAIX protein bands observed after 48h and 72h $CoCl_2$ treatment (figure 51E and G).

Weak CAIX expression was also observed within the un-treated cells (figure 51E and G). Transfection of siRNA into cells causes a small amount of cell death. To counteract this effect, and to ensure that an adequate number of cells were present at the time of lysate acquisition, high numbers of cells were seeded per well. The same numbers of cells were seeded per well for each of the different treatments within this experiment. While this cell seeding number led to sufficient cell numbers in the wells that received siRNA, the control wells, which did not receive any transfection reagent, had too many cells at the time of lysate acquisition and were over-confluent. Previous studies have shown that over-confluence can lead to CAIX expression in cells [242, 455]. The presence of too many cells within the control wells may explain the presence of the CAIX band in the untreated cells.

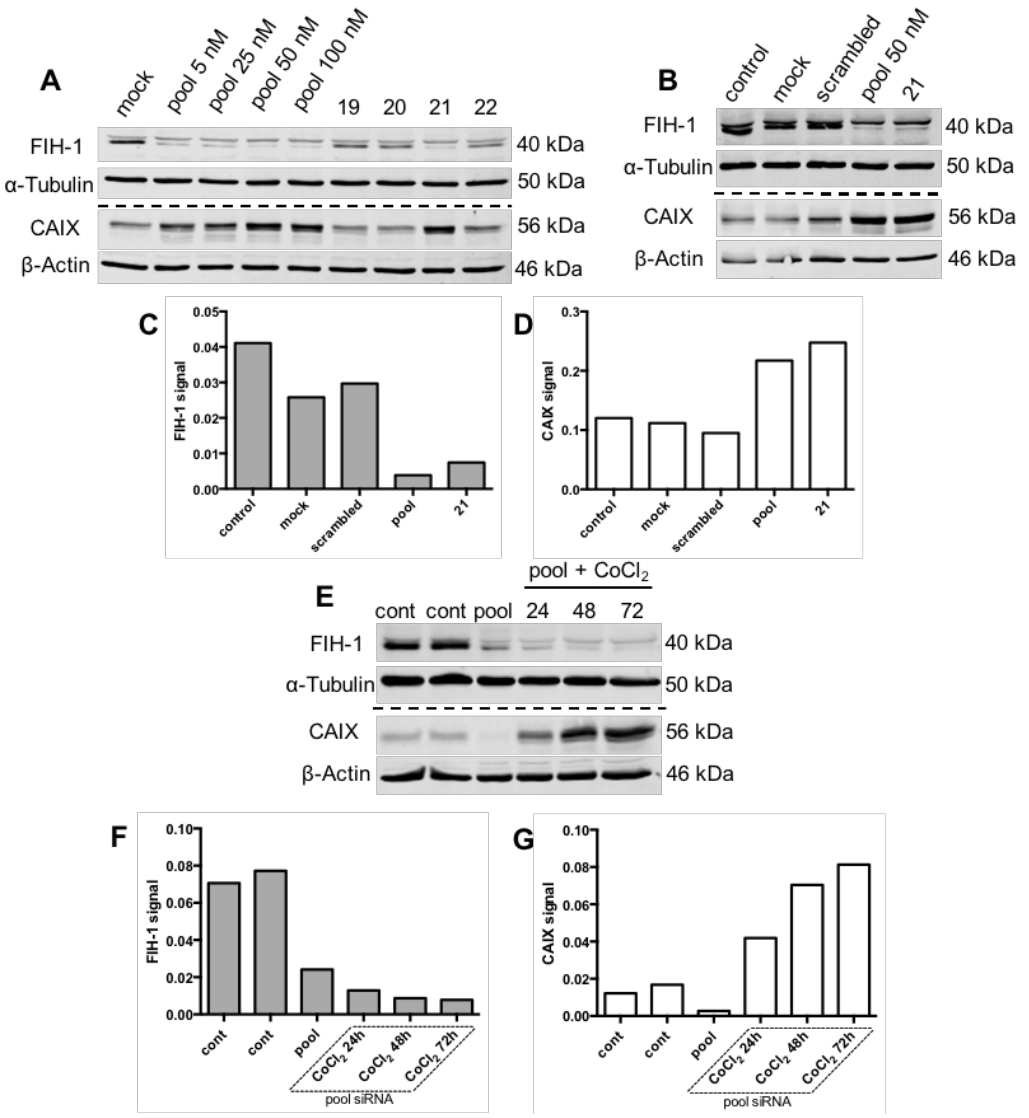

Figure 51. siRNA targeting FIH-1 leads to increased CAIX expression in hypoxic and $CoCl_2$-treated MCF-7 cells.

(A) MCF-7 cells cultured in 0.5% O_2 conditions for 24h were treated with either a mixture of 4 siRNAs targeting FIH-1 (pool), or individual siRNAs targeting FIH-1 (19, 20, 20 and 22. 50nM concentration used). Cells treated with transfection reagent alone (mock) acted as the control. Cytoplasmic lysates were acquired 120h after the initial siRNA treatment, and western blots were performed to assess the protein expression of FIH-1 (lower band) and CAIX. α-Tubulin and β-Actin acted as the loading controls. (B) Repeat of the experiment conducted in (A), with the addition of hypoxic MCF-7 cells that received scrambled siRNA (50 nM), along with the presence of an un-treated hypoxic control. (C-D) Densitometry measurements of the FIH-1 (C) and CAIX (D) bands shown in (B). (E) MCF-7 cells cultured in 20% O_2 conditions were treated with a mixture of 4 siRNAs targeting FIH-1 (pool, 50nM concentration used) and 400 μM $CoCl_2$. Aerobic MCF-7 cells that did not receive either siRNA or $CoCl_2$ (cont), and cells that were treated with siRNA alone (pool), acted as the controls. Western blots assessed the expression of FIH-1 and CAIX in cytoplasmic lysates acquired. α-Tubulin and β-Actin acted as the loading controls. (F-G) Densitometry measurements of the FIH-1 (F) and CAIX (G) bands shown in (E).

4.2.4 3D expression analysis indicates that each of the cancer cell lines may produce MMP14, but that the processing of this protein may differ between the cell lines

The 2D expression analysis presented above showed that the 3 cancer cell lines expressed comparable levels of FIH-1, with both FIH-1 protein and mRNA detected within each of the cancer cell lines. However, MMP14 expression differed. While similar levels of MMP14 mRNA were seen in each of the cell lines, no MMP14 protein was observed within the MCF-7 cells cultured in 2D (see section 4.2.2). Further analysis was conducted in 3D, investigating MMP14 and FIH-1 protein expression within spheroids of each of the cancer cell lines (figure 52). The same MMP14 antibody used in the 2D analysis, which binds to the extracellular portion of the MMP14 protein that is released after autocatalysis, was used to analyse MMP14 expression in 3D. Quantitative analysis of protein expression was carried out using Definiens Architect XD 64 Tissue Studio 4.1 (figure 53A and B).

As in the 2D analysis, MMP14 protein expression again differed between the 3 cancer cell lines. Plasma membrane expression of MMP14 was detected within both MDA-MB-231 and HBL-100 spheroids (figure 52). The pattern of expression differed slightly between the two cell lines, with a lower % of MDA-MB-231 cells exhibiting plasma membrane staining compared to the HBL-100 cells, which also exhibited an increased intensity of staining (figure 53B). The analysis with the Definiens software indicated that hypoxia may have caused a slight induction in MMP14 expression within the HBL-100 spheroids, with a greater percentage of cells within the hypoxic areas of these spheroids labelled as having a high intensity of MMP14 staining (figure 53B).

MMP14 protein expression was also detected within the MCF-7 spheroids. However, in contrast to both the MDA-MB-231 and HBL-100 spheroids, no plasma membrane MMP14 staining was detected within the MCF-7 spheroids (figure 52). The Definiens analysis indicated that the MCF-7 protein expression differed in the various regions of the MCF-7 spheroids, with significant increases in the intensity of staining observed in the hypoxic areas (figure 53A). These results show that, at least

when cultured in 3D, MCF-7 cells do express MMP14 protein. However, in contrast to MDA-MB-231 and HBL-100 spheroids, the MMP14 protein in cells within MCF-7 spheroids may autocatalyse. This may have led to the formation of an inactive membrane-tethered protein, in addition to an 18 kDa soluble protein, which is perhaps the form being detected with the antibody used.

Tissue inhibitor of metalloproteinases-2 (TIMP-2) is a protein that has been shown to regulate the autocatalysis of plasma membrane MMP14, with lower levels of TIMP-2 linked to the increased degradation of MMP14 [456]. Analysis of the levels of TIMP-2 mRNA in each of the cell lines was carried out to see if the decreased expression of TIMP-2 within the MCF-7 cell line might explain the positive, non-membranous staining detected within the MCF-7 spheroids, possibly present due to the autocatalysis of plasma membrane MMP14 within this cell line. However, similar levels of TIMP-2 mRNA were present in both the MCF-7 and HBL-100 cell lines (figure 53C).

IHC assessing FIH-1 protein expression was also carried out in spheroids of each of the 3 cancer cell lines. As in the 2D expression analysis, FIH-1 protein was detected in all of the cell lines, with both nuclear and cytoplasmic localisation of FIH-1 evident in each of the spheroids (figure 52). While an increased proportion of nuclear staining may have been present within the cells of MCF-7 and MDA-MB-231 spheroids, the nuclear and cytoplasmic FIH-1 staining within HBL-100 spheroids appeared to be very similar. Attempts were made to quantify the nuclear and cytoplasmic staining of FIH-1 within the spheroids; however, this analysis was precluded as a result of the large amount of FIH-1 staining present.

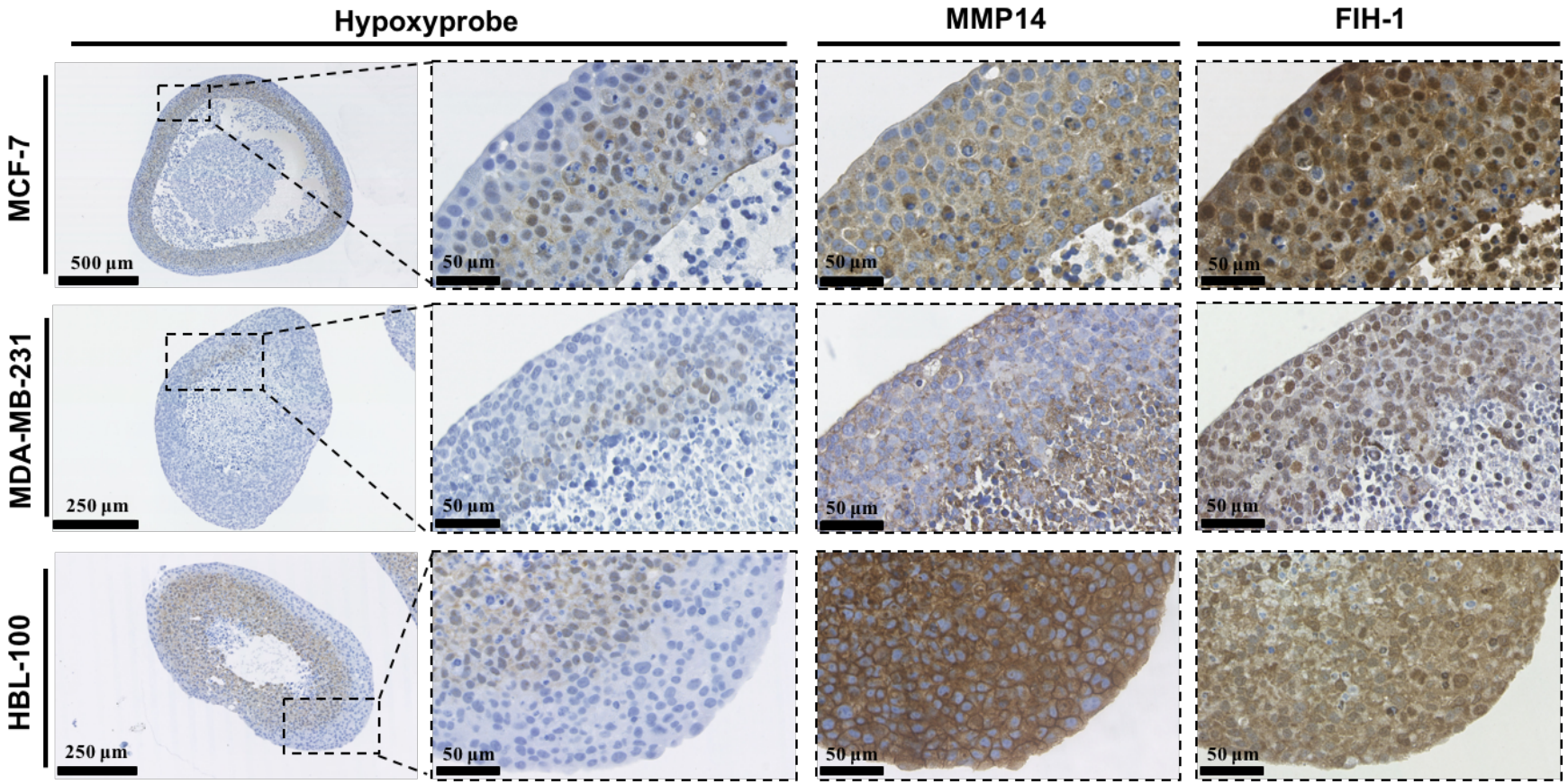

Figure 52. MMP14 and FIH-1 protein expression differ within spheroids of the 3 cancer cell lines.

Hypoxyprobe, MMP14 and FIH-1 staining within spheroids of the 3 cell lines that were allowed to form for a week before fixation.

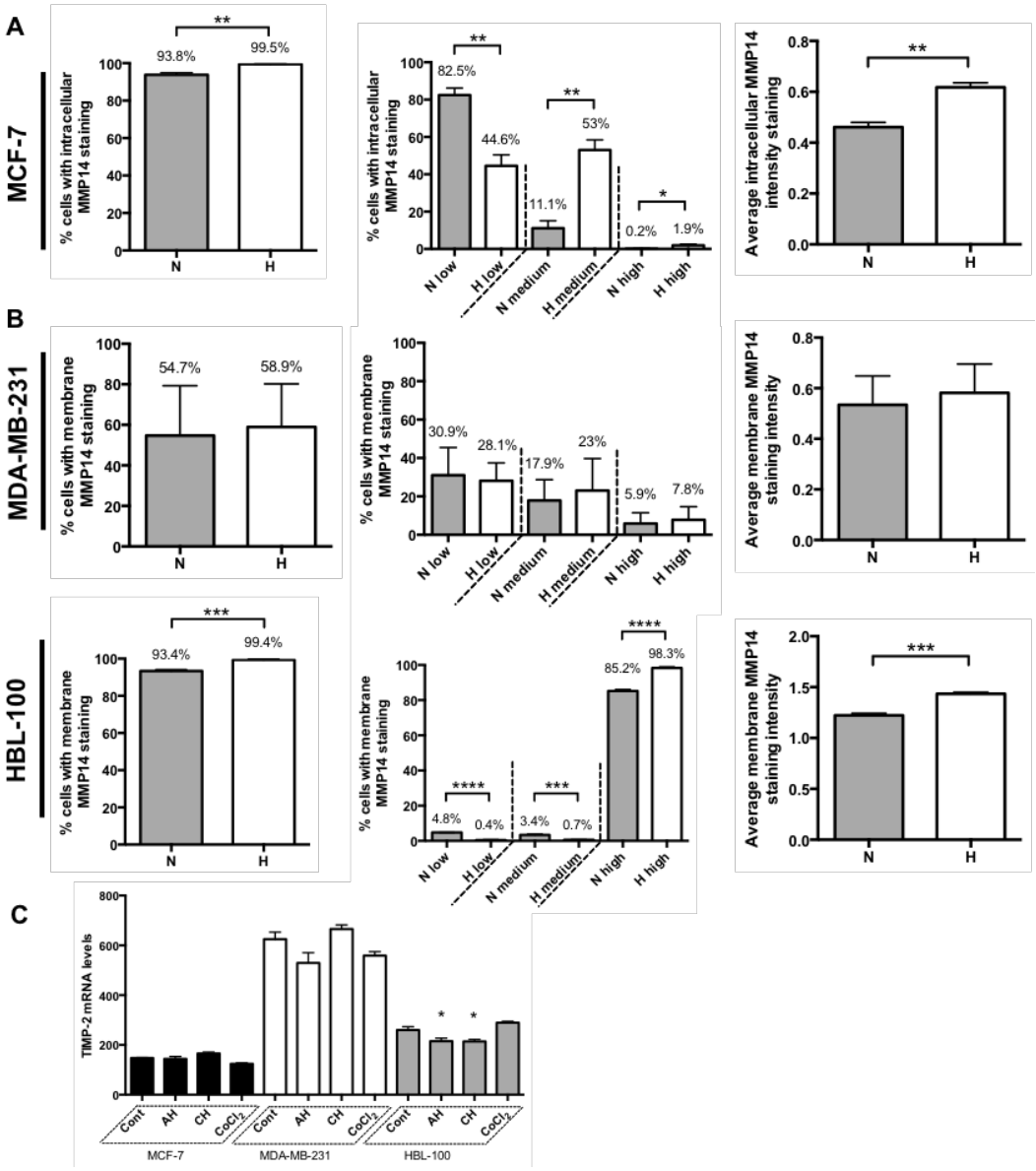

Figure 53. Definiens analysis indicates that MMP14 expression is induced in the hypoxic areas of MCF-7 and HBL-100 spheroids, while mRNA analysis shows the presence of similar levels of TIMP-2 mRNA in the 3 cell lines.

*Definiens analysis showing the levels of intracellular MMP14 within MCF-7 spheroids (A) and plasma membrane MMP14 staining within MDA-MB-231 and HBL-100 spheroids (B). The graphs on the left show the % of cells within the normoxic and hypoxic regions that exhibited MMP14 staining. The graphs in the centre show the % of cells within the normoxic and hypoxic areas that had low, medium, and high intensity levels of MMP14 staining. The graphs on the right show the average intensity of MMP14 staining detected within the normoxic and hypoxic areas of the spheroids. Data expressed as mean ± SEM (n = 3). *P≤0.05, **P≤0.01, ***P≤0.001 and ****P≤0.0001 (Unpaired t-tests performed). (C) TIMP-2 mRNA levels in cells cultured in 20% O_2 (cont), 0.5% O_2 for 24h (AH) and 0.5% O_2 for 10 weeks (CH). mRNA levels were also analysed in aerobic cells treated with 400 µM $CoCl_2$ for 24h. Data expressed as mean ± SEM (n = 3). * P ≤ 0.05 (One-way ANOVA followed by Dunnett's multiple comparison test, comparing each sample to the 20% O_2 group within the same cell line).*

The initial 2D expression analysis conducted on the whole-cell lysates showed that CAIX protein expression levels were increased in the chronic hypoxic MCF-7 cells in comparison to the acute hypoxic cancer cells (see section 3.2.1). More severe hypoxic conditions have been shown to inhibit FIH-1 activity [131], with the work presented in section 4.2.3 displaying the inhibitory role FIH-1 has on CAIX expression in hypoxic MCF-7 cells. Only small amounts of CAIX expression were observed within the hypoxic areas of MCF-7 spheroids that were allowed to form for 1 week (figure 26). Further IHC was performed on MCF-7 spheroids cultured for 2 and 3 weeks before fixation, to investigate whether longer periods of hypoxia might lead to higher CAIX expression levels within the hypoxic areas of these spheroids due to FIH-1 inhibition (figure 54). IHC analysis did not reveal any positive hypoxyprobe staining in the MCF-7 spheroids left for 2 or 3 weeks in spinner flasks before fixation, indicating that no hypoxic cells were present in these spheroids. No CAIX-positive cells were detected within these spheroids.

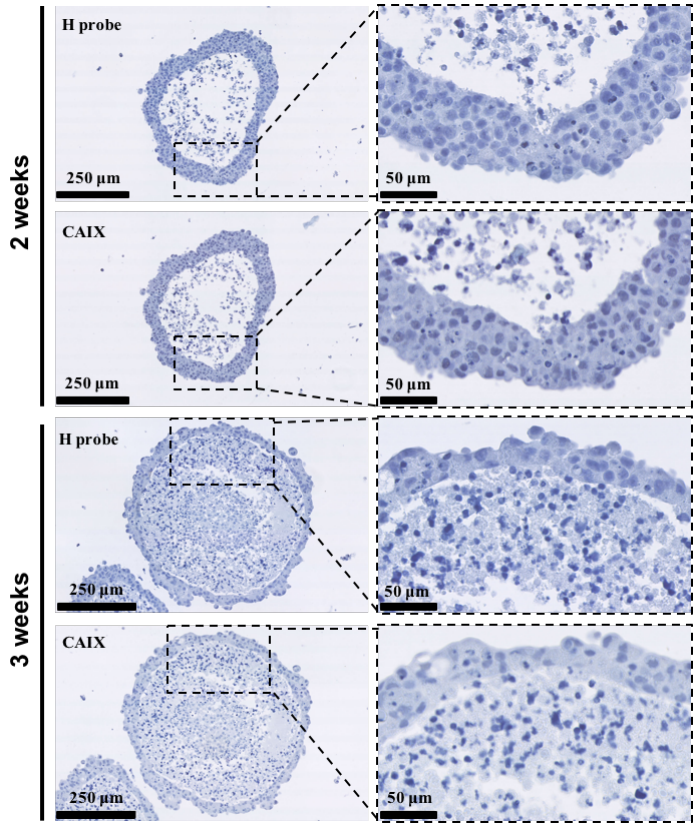

Figure 54. MCF-7 spheroids cultured for 2 and 3 weeks do not exhibit hypoxyprobe or CAIX staining.

Hypoxyprobe (H probe) and CAIX staining within MCF-7 spheroids that were allowed to form for 2 and 3 weeks before fixation.

4.3 Discussion

The results from Chapter 3 showed that the level of CAIX expression varied markedly between the 3 cancer cell lines in differing O_2 conditions, with MCF-7 cells exhibiting the lowest induction of CAIX in hypoxia. The work presented in this chapter was performed to investigate why CAIX expression levels differed between the 3 cell lines.

The control of the transport of transcription factors into the nucleus of cells is one mechanism through which cells can regulate transcriptional activity (reviewed in [457]). Studies have shown that both the HIF-1α and HIF-2α subunits interact with nuclear transport receptors [458], with the extent of nuclear localisation of HIF-1α after hypoxia demonstrated to be cell line dependent [459]. Therefore, a difference in the nucleocytoplasmic shuttling of HIF-1α between the cell lines was one possible mechanism to explain the differences in CAIX expression observed in Chapter 3. However, while this prior expression analysis displayed the levels of the total HIF-1α protein levels, it did not give an indication of the levels of HIF-1α present in the nucleus, which may have differed between the 3 cell lines, and possibly explained the differential CAIX expression observed. Initial experiments conducted in this Chapter assessed the nuclear levels of HIF-1α in cells cultured in 0.5% O_2 conditions, relating the levels of nuclear HIF-1α to CAIX expression (figure 48). This analysis was also performed with $CoCl_2$-treated cells (figure 49). Comparable HIF-1α levels were observed in each of the nuclear lysates produced from the 3 cell lines when cultured in 0.5% O_2 conditions. $CoCl_2$ treatment also led to the detection of similar levels of nuclear HIF-1α in each of the cell lines. However, a pattern of CAIX expression similar to that already observed in Chapter 3 was seen here, with MCF-7 cells again exhibiting the lowest levels of CAIX out of the 3 cell lines. The results from these experiments indicated that the variation in CAIX expression observed between the cell lines was not due to differences in the nucleocytoplasmic shuttling of HIF-1α.

Further analysis was conducted, assessing whether the expression of FIH-1 (a negative regulator of HIF-1α transcriptional activity [129, 130]) and MMP14 (reported to inhibit FIH-1 activity [section 4.1.1]) were contributing to the varying CAIX expression between the 3 cell lines. The initial analysis conducted in 2D suggested that the differing CAIX expression may have been due to a lack of MMP14 protein in the MCF-7 cells (figure 50B), possibly contributing to increased levels of active FIH-1 in this cell line compared to the MDA-MB-231 and HBL-100 cells, with the addition of siRNA to both hypoxic and $CoCl_2$-treated MCF-7 cells leading to increased CAIX protein expression levels (figure 51). While the 2D expression analysis indicated that a lack of MMP14 protein in MCF-7 cells may have been contributing to increased levels of active FIH-1 in this cell line, the 3D expression analysis showed the presence of positive staining within the MCF-7 spheroids, with non-plasma membrane staining detected within the MCF-7 spheroids (figure 52). In contrast to the 2D protein expression analysis conducted here (figure 50B), and the results from other studies assessing MMP14 protein expression through Western Blots [451, 452], this positive staining detected in the 3D analysis indicated that MCF-7 cells may actually be producing MMP14 protein, but that the active 57 kDa MMP14 produced may autocatalyse, leading to the formation of a soluble form released from the MCF-7 cells that was detected in the spheroids, but not in the 2D analysis. Further experiments are required to investigate if soluble MMP14 is present in conditioned media, to confirm the expression of the MMP14 protein in the MCF-7 cell line in 2D

Sakamoto et al reported that MMP14 contributes to FIH-1 inhibition through mediating the binding of Mint3 to FIH-1, hypothesising that this inhibition occurs during the cleavage of latent MMP14 (60 kDa) into active MMP14 (57 kDa) [448] (figure 47). The detection of similar levels of MMP14 mRNA in MCF-7 cells compared to the other cell lines, in addition to the MMP14 staining detected within MCF-7 spheroids, indicates that MCF-7 cells may actually express MMP14 protein, and that this cleavage may occur in these cells too. If this is the case, and the mechanism of FIH-1 inhibition by MMP14 put forward by Sakamoto et al is correct, then MMP14 should contribute to the inhibition of FIH-1 in MCF-7 cells. Therefore,

MMP14 may not be the cause of the differing CAIX expression results observed between the 3 cell lines. Further experiments, possibly involving the reduction in MMP14 protein translation through the use of siRNA in each of the cell lines, are required to investigate what role MMP14 has in the expression of CAIX within these 3 cell lines.

If the staining within the MCF-7 spheroids is from detection of the soluble form of MMP14, released through autocatalysis of the plasma membrane form, then what processes are leading to higher rates of MMP14 autocatalysis within the MCF-7 cells compared to the other cell lines? Tissue inhibitor of metalloproteinases-2 (TIMP-2) is a protein that has been shown to regulate the degradation of active 57 kDa MMP14 present on the plasma membranes of cells, with lower levels of TIMP-2 demonstrated to lead to increased autocatalysis of the active MMP14 [456]. A prior study indicated that MCF-7 cells have low levels of TIMP-2 mRNA [460]. To investigate if low levels of TIMP-2 within MCF-7 cells may be the cause of the differential MMP14 expression results observed, mRNA analysis of the levels of TIMP-2 in each of the cell lines was performed. Similar levels of TIMP-2 were found within both the MCF-7 and HBL-100 cell lines (figure 53C), indicating that differences in the levels of TIMP-2 are unlikely to explain the variation in MMP14 processing between the cell lines. Further experiments, assessing the protein expression levels of TIMP-2 in each of the cell lines, are required.

Definiens analysis of MMP14 expression indicated that the staining intensity of the MMP14 antibody was significantly higher in the hypoxic areas of the MCF-7 and HBL-100 spheroids (figure 53A and B). Studies have indicated that MMP14 expression can be regulated by hypoxia. A functional HIF-binding site has been identified in the proximal promoter of MMP14, with MMP14 gene expression controlled by HIF-2α [454], possibly explaining the increased levels of MMP14 present detected in the hypoxic regions with the setting used.

Varying localization of FIH-1 protein was evident between the spheroids of the cell lines. While high amounts of FIH-1 staining were observed within both the cytoplasm and nuclei of HBL-100 spheroids, an increased nuclear localization was

evident within the MCF-7 and MDA-MB-231 spheroids (figure 52). Previous studies have shown FIH-1 to have distinct subcellular localization patterns within breast cancer tissue, with FIH-1 expression found to be either exclusively nuclear, exclusively cytoplasmic, or both nuclear and cytoplasmic [461, 462]. The 3D CAIX expression analysis conducted in Chapter 3 showed MDA-MB-231 spheroids to have the highest CAIX expression levels out of the 3 cell lines. However, this increased CAIX expression in 3D may not be explained by the FIH-1 localisation staining presented here, as the study by Tan et al found nuclear FIH-1 expression to be inversely correlated with CAIX expression levels, with exclusive cytoplasmic FIH-1 expression associated with CAIX expression [462].

There are other negative regulators of HIF-1α transcriptional activity, apart from FIH-1, present within the cell that may be contributing to the CAIX expression results observed. CBP/p300 Interacting Transactivator With Glu/Asp Rich Carboxy-Terminal Domain 2 (CITED2) is one such protein that has been shown to compete with HIF-1α for binding to p300/CBP, thereby inhibiting HIF-1 signalling [463-465]. Additional experiments investigating the expression levels of CITED2 are required to examine whether the varying levels of this protein may be contributing to the CAIX expression results observed.

5 Chapter 5: Further testing of the novel carbonic anhydrase inhibitors in pre-clinical cancer models

5.1 Introduction

The experiments presented in section 3.2.3 showed that carbonic anhydrase inhibition had a significant effect on cancer cell number. Inhibition of carbonic anhydrase protein function, or a decline in carbonic anhydrase protein levels as a result of drug treatment, resulting in the loss of pH regulating capabilities within the cancer cells and thus affecting cell survival, might help explain how S4 treatment produced this effect. Cytosolic acidification is thought to have a permissive role in the apoptotic cascade, with caspase activation shown to be more efficient in acidic pHi conditions (see section 1.13.2). Poly (ADP-ribose) polymerase (PARP) is a protein involved in DNA damage repair [466], with PARP cleavage seen in cells undergoing apoptosis [467]. Initial work presented in this chapter investigated the effect of S4 treatment on both CAIX and cleaved PARP expression, examining whether drug treatment was affecting the levels of either of these protein in hypoxic cancer cells. NHE1 and V-ATPase protein expression levels were also assessed, to ascertain whether drug-treated cancer cells expressed higher levels of these pH regulating proteins in an attempt to adapt to inhibition of the carbonic anhydrases.

The 3D invasion assays conducted in section 3.2.4 showed that S4 significantly inhibited the invasion of cells from MDA-MB-231 spheroids into collagen type 1. However, as already discussed in section 1.15.4, there are disadvantages to the use of spheroids in such assays. 3D invasion assays conducted with explant tissue derived from treatment naive biopsy specimens from human patients represents an improvement over this spheroid model, enabling the testing of pharmacological compounds on heterogeneous tumour material containing cells usually found within the cancer stroma (see section 1.15.4). Further work presented in this chapter examined the effects of carbonic anhydrase inhibition on the invasion of cells from explant tissue. S4, FC9403A and FC9398A were the compounds tested in these experiments.

Lastly, MDA-MB-231 xenografts were used to assess whether the carbonic anhydrase inhibitors retained their effects *in vivo*. Pharmacokinetic data (personal communication - Simon Langdon) indicated that two carbonic anhydrase inhibitors previously used within the laboratory, FC9398A and DTP348, had better *in vivo* stability than the other compounds, with positive results already reported in HT-29 colorectal xenografts [320, 468]. Therefore, these compounds were used in *in vivo* experiments to characterise (i) the influence of carbonic anhydrase inhibition on the growth of MDA-MB-231 xenografts in a murine model, and (ii) the effects of these novel inhibitors on proliferation and CAIX protein expression levels within these xenografts.

.

5.2 Results

5.2.1 S4 treatment leads to the reduction of CAIX protein levels and induces apoptosis within acute hypoxic cancer cells

Whole-cell lysates of MCF-7, MDA-MB-231 and HBL-100 cell lines treated with S4 were acquired to investigate the effects of carbonic anhydrase inhibition on the protein expression levels of CAIX and PARP. Cells were cultured in 0.5% O_2 conditions for 24h to allow them to adapt to hypoxic conditions, after which they were treated with 10, 30 and 100 μM concentrations of S4 for 24, 48 and 72h. Un-treated cells present in 0.5% O_2 conditions acted as controls.

Initial experiments showed that S4 treatment led to a reduction in CAIX protein levels within hypoxic MCF-7 cells (figure 55A). The highest concentration of S4 tested (100 μM) caused a reduction in the expression of CAIX at 24 and 48h, with each of the concentrations used producing this effect in the 72h-treated cells (figure 55A). Repeat experiments were performed with the MCF-7 cells without the inclusion of 100 μM S4 at 48 and 72h (figure 55B), as S4 treatment at this concentration was affecting loading control values at these time points, possibly due to the reduction of cell number at this drug concentration. These experiments showed that S4 significantly reduced the levels of CAIX protein in hypoxic MCF-7 cells (figure 55B). Hypoxic MDA-MB-231 cells were less responsive to S4 treatment in comparison to the MCF-7 cell line, with only 100 μM concentrations of S4 causing a reduction in CAIX protein levels within this cell line (figure 55A). As with the MCF-7 cells, repeat experiments were again performed. However, because higher concentrations of S4 were having effects on loading control levels at the later time points, repeat experiments were only conducted with the 24h treated cells (figure 55C). While 100 μM concentrations of S4 were again shown to reduce CAIX intensity values within hypoxic MDA-MB-231 cells, this reduction in CAIX protein levels was not found to be significant when compared to the control cells (figure 55C). Out of the 3 cell lines, hypoxic HBL-100 cells exhibited the greatest resistance to S4 treatment (figure 55A). No concentration of drug used had any effect on CAIX expression levels within this cell line at any of the time points analysed.

Using an antibody that identifies the presence of both full length and cleaved PARP, westerns were performed to investigate if cleaved PARP could be detected in any of the drug-treated hypoxic cells, thereby showing that carbonic anhydrase inhibition could induce apoptosis (figure 55D). PARP expression was observed in the MCF-7 cell line at each time point analysed. Bands corresponding to both full length and cleaved PARP were seen in each of the MCF-7 samples at the 72h time point, with stronger cleaved-PARP bands observed in the 10 and 30 μM-treated cells in comparison to the control cells, indicating that S4 treatment was leading to increased levels of apoptosis in hypoxic MCF-7 cells (figure 55D). While full length PARP expression was observed in both MDA-MB-231 and HBL-100 cells at each of the time points analysed, no cleaved PARP band was evident in these cell lines (figure 55D).

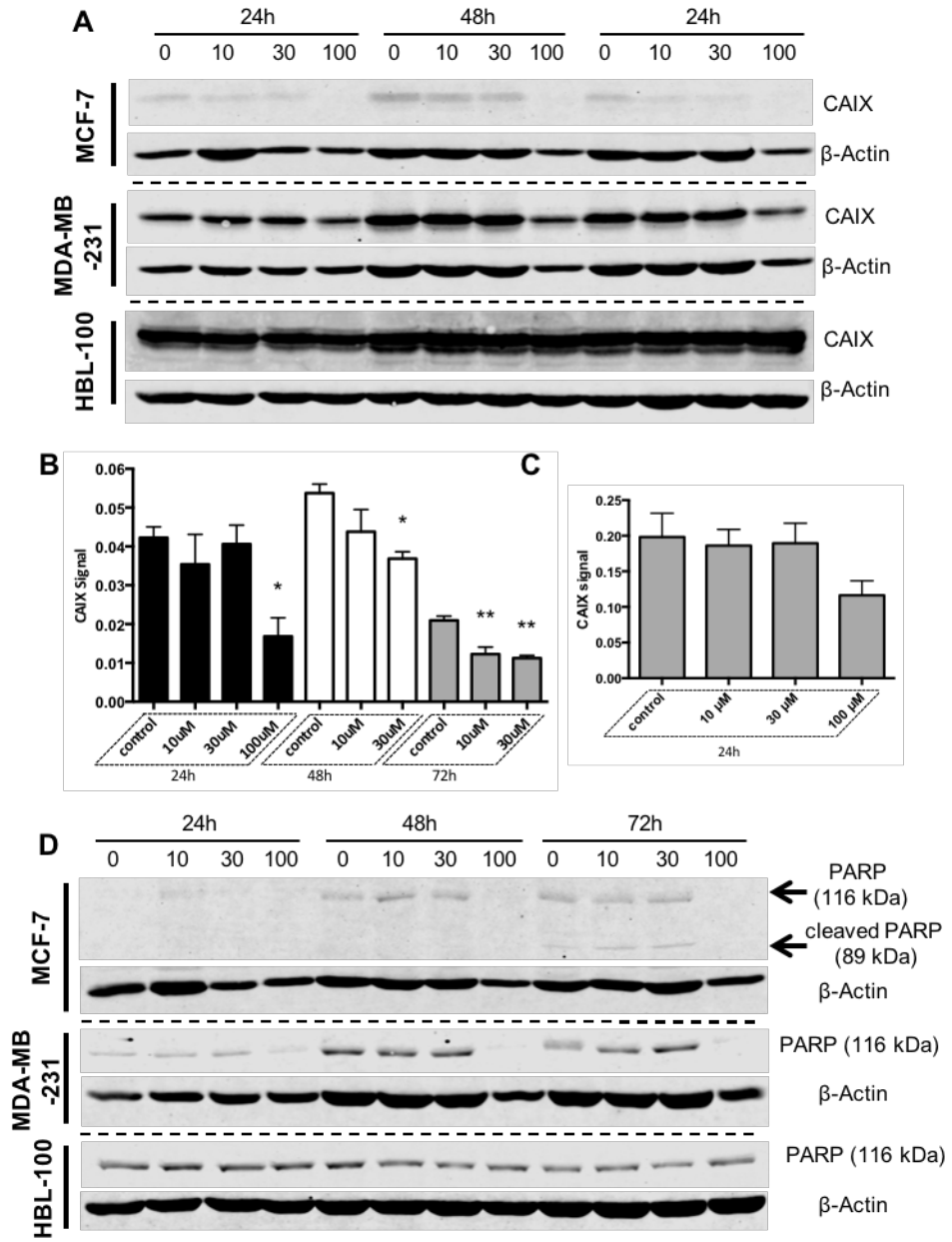

Figure 55. While S4 leads to reduced CAIX protein levels and increased levels of cleaved PARP in MCF-7 cells, the other cell lines were more resistant to treatment.

*MCF-7, MDA-MB-231 and HBL-100 cells were cultured in 0.5% O_2 conditions for 24h, after which they were treated with 10, 30 and 100 μM concentrations of S4 for 24, 48 and 72h. Untreated cells cultured in 0.5% O_2 conditions acted as the controls. Western blotting was performed to detect CAIX (A), PARP (D) and cleaved PARP (D), with β-Actin used as the loading control. (B/C) Densitometry measurements of CAIX protein levels in S4-treated MCF-7 (B) and MDA-MB-231 cells (C). Data expressed as mean ± SEM (n = 3). *P≤0.05, **P≤0.01 (One-way ANOVA followed by Dunnett's multiple comparison test performed, comparing only values within each time point).*

2D expression analysis was also conducted assessing the levels of the pH regulating proteins NHE1 (figure 56A) and V-ATPase (figure 56B) in hypoxic cancer cells treated with S4, to investigate whether the drug-treated cells were up-regulating the levels of other pH regulating proteins to help them adapt to the inhibition of the carbonic anhydrases. No consistent differences in the expression levels of either NHE1 (figure 56A) or V-ATPase (figure 56B) were observed in the drug-treated cells in comparison to the control cells at any time point, indicating that S4 treatment was not leading to an up-regulation of either NHE1 or V-ATPase protein.

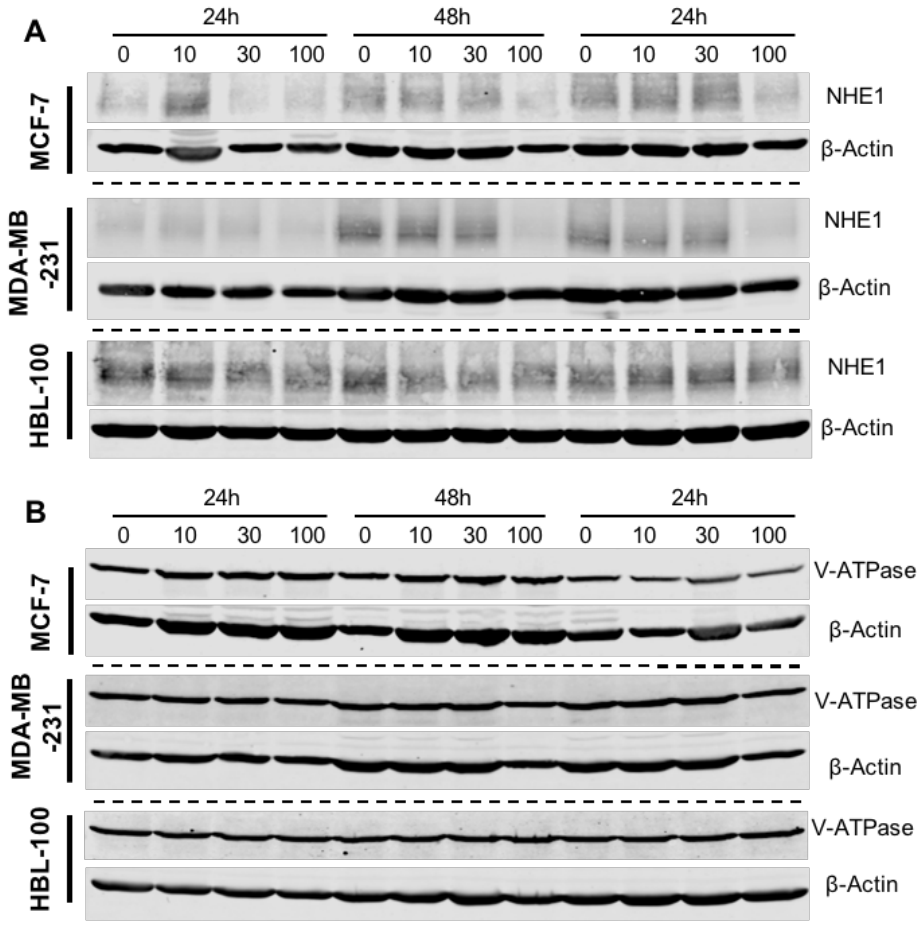

Figure 56. S4 treatment does not induce either NHE1 or V-ATPase expression in hypoxic cancer cells.

MCF-7, MDA-MB-231 and HBL-100 cells were cultured in 0.5% O_2 conditions for 24h, after which they were treated with the 10, 30 and 100 μM concentrations of S4 for 24, 48, and 72h. Untreated cells cultured in 0.5% O_2 conditions acted as the controls. Western blotting was performed to detect NHE1 (A) and V-ATPase (B), with β-Actin used as the loading control.

5.2.2 Tumour-associated carbonic anhydrase inhibition reduces the invasion of cells from explant tissue derived from human patients

The experimental work presented in this section was performed in collaboration with Dr Carol Ward, with both Dr Carol Ward and myself carrying out the experimental work and performing the image analysis.

3D invasion assays were carried out with 3 carbonic anhydrase inhibitors (S4, FC9403A and FC9398A), testing their effects on the invasion of cells from explant tissue derived from human patients into collagen type 1. Briefly, tumour tissue was cut into 1 mm^3 pieces, placed into collagen, and left to invade for 15 days overall, with photos of the explants taken every 5 days. Representative images from an experiment carried out with FC9403A are shown in figure 57, where higher concentrations of the carbonic anhydrase inhibitor can be seen reducing the number of cells invading into the collagen.

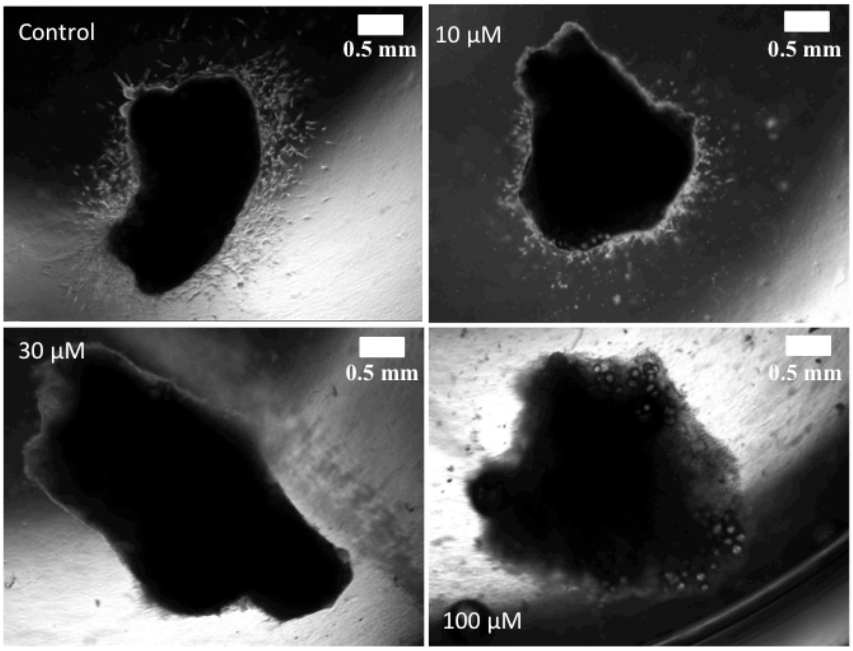

Figure 57. Representative images from a 3D invasion assay conducted with explant tissue derived from human patients treated with FC9403A.

Representative images taken from an invasion assay conducted with explant tissue placed into collagen type 1 and treated with FC9403A. These images were acquired after 5 days of treatment.

In the initial analysis performed, the influence of drug treatment on invasion was examined by the effects of the compounds on the areas of the explant tissue, as measured through ImageJ. Explant areas were measured at 0, 5, 10 and 15 days. The areas of the explants at 5, 10 and 15 days were compared to the area at day 0, with the % increase in area giving an indication of the amount of invasion that had occurred. Figure 58 displays pooled data from 26 different biopsy specimens, with the % invasion of un-treated samples shown. Ten days after being placed into collagen, un-treated explants exhibited a significantly increased area in comparison to the tissues at day 0.

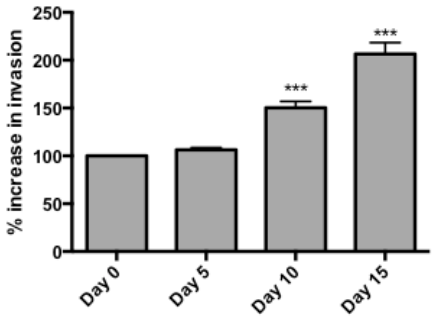

Figure 58. Control explant invasion analysed through the measurement of explant area.

*Invasion measured by increased area compared to day 0 explant size. Data pooled from 26 separate biopsy samples. Data expressed as mean ± SEM. *** P ≤ 0.001 (One-way ANOVA followed by Tukey's multiple comparison test).*

Figure 59 presents the data from each of the carbonic anhydrase inhibitors tested. Higher concentrations of S4 had an effect on explant invasion, with 30 and 100 μM concentrations causing a significant reduction in the % area of the explants after 10 and 15 days of treatment compared to the un-treated explants at the same time points (figure 59A). Similar results were seen with the 2 other carbonic anhydrase inhibitors tested, FC9403A (figure 59B) and FC9398A (figure 59C). FC9403A was the most potent of the 3 drugs, with 3 and 10 μM, in addition to 30 and 100 μM concentrations, leading to a significant reduction in the % area of the explants compared to the controls (figure 59B).

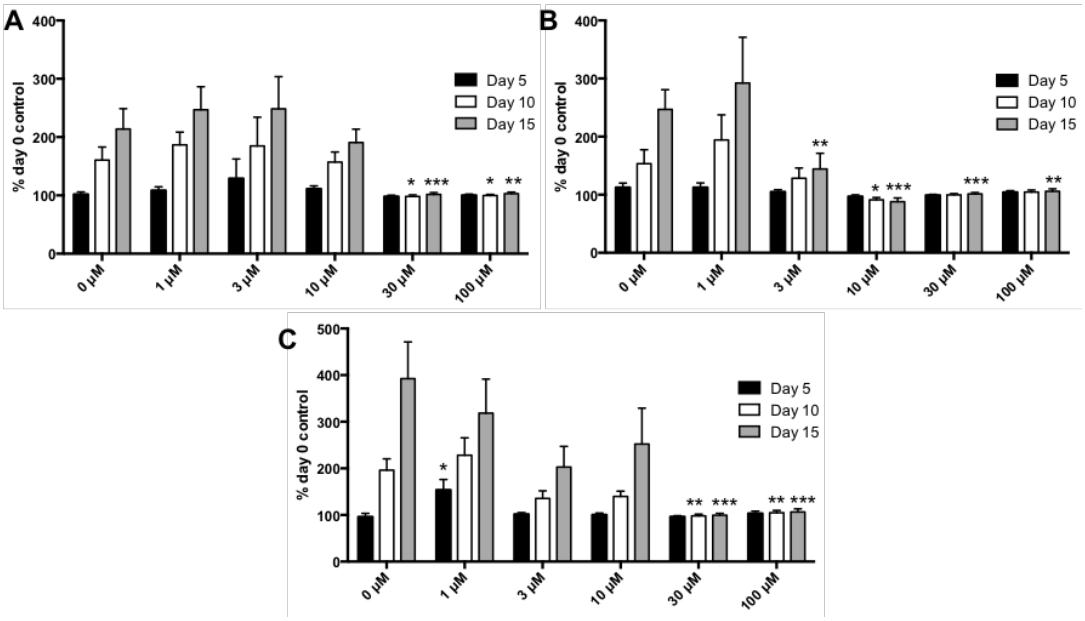

Figure 59. The carbonic anhydrase inhibitors S4, FC9398A and FC9403A significantly reduce the invasion of cells from explant tissue.

*% invasion of collagen-embedded explants treated with S4 (A), FC9403A (B) and FC9398A (C). Explants were cultured for 15 days overall with images taken every 5 days. The areas of the explants at 5, 10 and 15 days were compared against the area at day 0, with the % increase in area giving an indication of the amount of invasion that had occurred. Data expressed as mean ± SEM (n=8). * P ≤ 0.05, ** P ≤ 0.01, *** P ≤ 0.001 (One-way ANOVA followed by Tukey's multiple comparison test).*

Even though the explants showed invasive capabilities, some also exhibited regression in size after drug treatment. If explant area were the only criteria used to measure the effects of carbonic anhydrase inhibition on invasion, then many of the explants would have been considered non-invasive. Therefore, to ensure that the effects of the carbonic anhydrase inhibitors on explant invasion were analysed accurately, another method was also used. This involved recording only whether an explant was invasive or non-invasive, without taking explant area into account. With this method, it was observed that after 5 days there was a significant increase in the percentage of invasive explants (figure 60A). Using this method of analysis, the effects of drug treatment after 15 days of explant invasion was analysed. Similar results were observed to those presented in figure 59. Significant reductions in the % of explants that had invaded after 15 days were seen with higher concentrations of each of S4 (figure 60B), FC9403A (figure 60C) and FC9398A (figure 60D). Again, FC9403A was shown to be the more potent of the 3 carbonic anhydrase inhibitors,

with 30 and 100 μM concentrations of this drug completely preventing the invasion of cells from the explant tissue (figure 60C).

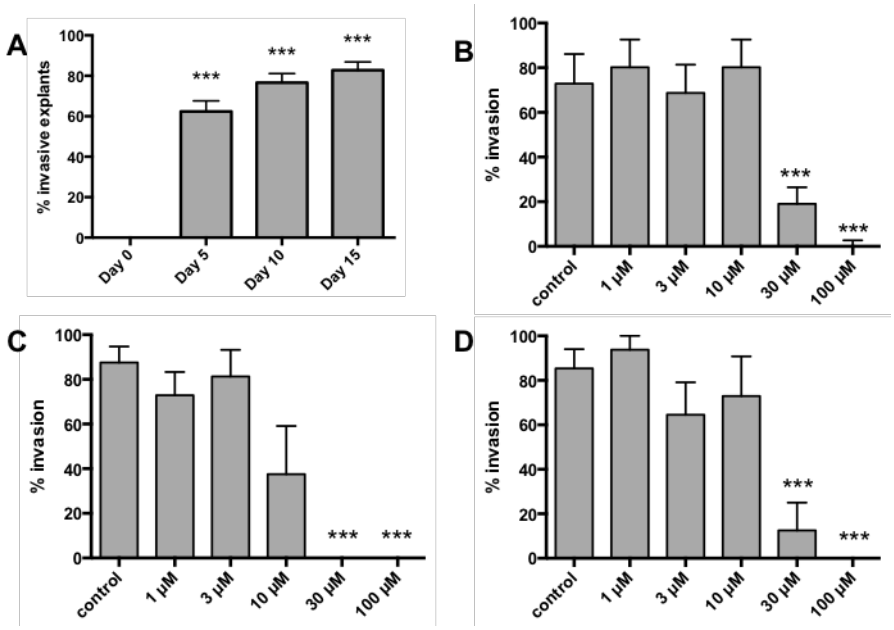

Figure 60. Carbonic anhydrase inhibitors significantly reduce the invasion of cells from explant tissue.

*(A) Percentage of un-treated explants invading over 15 days. Data expressed as mean ± SEM (n=230). (B-D) The % of explants showing invasive morphology in explant tissue after 15 days of S4 (B), FC9403A (C) and FC9398A (D) treatment. Data expressed as mean ± SEM (n=8). *** P ≤ 0.001 (One-way ANOVA followed by Tukey's multiple comparison test)*

Lastly, experiments were conducted to assess whether the 3 carbonic anhydrase inhibitors had any effect on established invasion (figure 61), with drug addition carried out after the explants had been left to invade for 15 days. 30 μM drug concentrations were chosen for these experiments, as this concentration had previously been shown to significantly reduce the invasion of cells from explant tissues. Initial measurements of the areas of the explants were conducted after 15 days of invasion (day 0 control measurements), with further measurements taken 5 and 10 days after the start of treatment. The areas of the drug-treated explants after 5 and 10 days of treatment were compared against the day 0 control explants to assess whether any reversal of invasion, identified through a significant reduction in area, had occurred. Explant areas after 5 and 10 days of drug treatment were also compared to the control explants at the same time points, to examine whether the drugs were affecting any continued explant invasion.

No reversal of invasion was observed in the S4-treated explants over the treatment period (figure 61A). However, after 10 days the S4-treated explants had significantly different areas to both the day 0 and day 10 controls, indicating that even though invasive growth was continuing in these treated explants, it was continuing at a reduced rate in comparison to the un-treated explants (figure 61A). FC9398A-treated explants also did not exhibit any reversal of invasion (figure 61C). However, addition of this compound prevented any further invasion from occurring, as no significant differences were observed in the areas of the day 5 and day 10 treated explants in comparison to the day 0 explants (figure 61C). The results observed with FC9403A indicated that treatment with this compound reversed the invasion that had occurred over the 15 days prior to treatment, with the day 5 and day 10 treated explants having significantly reduced areas in comparison to the day 0 controls (figure 61B). Day 5 and day 10 FC9403A-treated explants also had significantly decreased areas compared to the day 5 and day 10 controls (figure 61B).

For the reversal of invasion experiments presented in figure 61A-C, separate biopsy tissue had been used for each of the 3 carbonic anhydrase inhibitors. Due to the heterogeneous nature of the biopsy tissue, an additional experiment was carried out testing the 3 compounds using explant tissue from the same biopsy tissue, employing the same treatment schedule as was used before (figure 61D). Treatment with both S4 and FC9398A for 5 and 10 days led to significantly reduced areas in comparison to the controls at the same time points, indicating that these compounds had prevented any further invasion from occurring (figure 61D). However, no reversal of invasion was seen with these compounds. As was the case in figure 61B, FC9403A treatment again led to a significant decrease in area of the explants after 5 and 10 days treatment compared to the day 0 controls (figure 61D), indicating that this compound had caused a reversal of the invasive front.

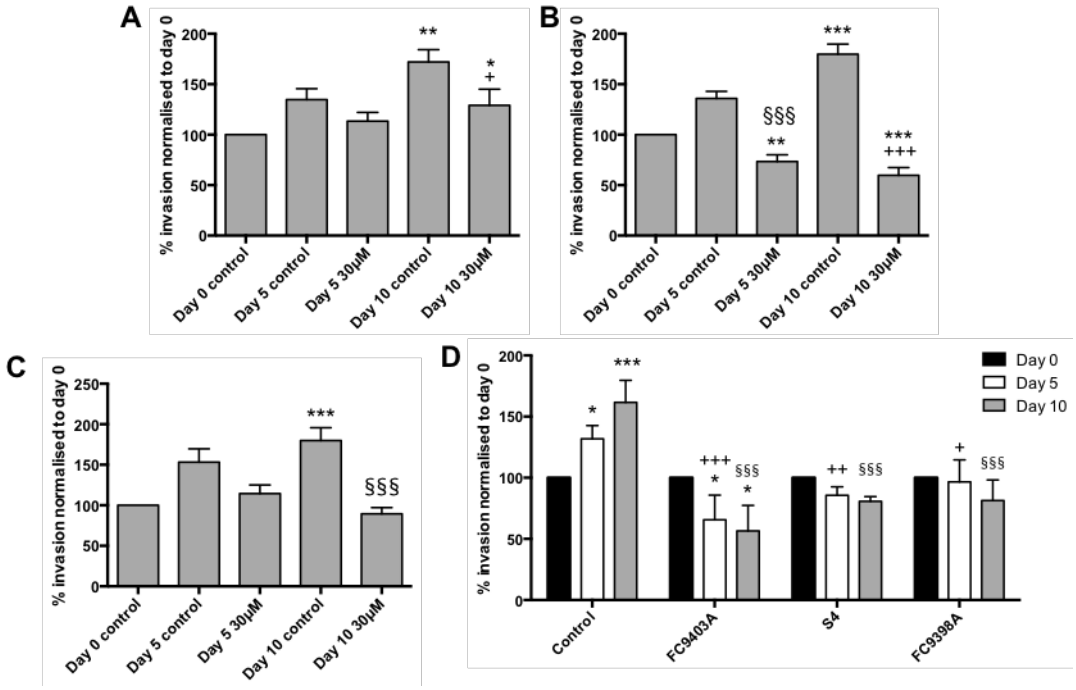

Figure 61. Of the 3 inhibitors tested, FC9403A is the only one to lead to the reversal of established invasion.

*(A-C) The effects of S4 (A), FC9403A (B) and FC9398A (C) on the reversal of invasion. Explant were left to invade into collagen for 15 days, after which they were treated with 30 µM of the carbonic anhydrase inhibitors. (A) Data shown as mean ± SEM (n=10-13). * P ≤ 0.05, ** P ≤ 0.01 compared to day 0 control. + P ≤ 0.05 compared to day 10 control. (B) Data shown as mean ± SEM (n=10-13). ** P ≤ 0.01, *** P ≤ 0.001 compared to day 0 control. §§§ P ≤ 0.001 compared to day 5 control. +++ P ≤ 0.001 compared to day 10 control. (C) Data shown as mean ± SEM (n=10). *** P ≤ 0.001 compared to day 0 control. §§§ P ≤ 0.001 compared to day 10 control. (D) Comparing the effects of S4, FC9403A and FC9398A on the reversal of invasion using the same biopsy tissue. Explants were left to invade for 15 days before treatment with 30 µM of the carbonic anhydrase inhibitors. Data expressed as mean ± SEM (n=3). * P ≤ 0.05, *** P ≤ 0.001 compared to day 0 control. ++ P ≤ 0.01, +++ P ≤ 0.001 compared to day 5 control. §§§ P ≤ 0.001 compared to day 10 control. (One-way ANOVA followed by Tukey's multiple comparison test).*

5.2.3 *In vivo* experiments with MDA-MB-231 xenografts suggest that tumour-associated carbonic anhydrase inhibitors may lead to diminished tumour growth through reducing the proliferation rate of cancer cells

The work performed in this section, investigating whether the carbonic anhydrase inhibitors could retain their effects *in vivo* by analysing their effects on MDA-MB-231 xenografts, was carried out in collaboration with Dr Simon Langdon and Edward Jarman. Dr Simon Langdon performed the *in vivo* work, while myself and Ed Jarman performed the IHC staining and analysis.

The influence of 2 carbonic anhydrase inhibitors, FC9398A and DTP348, on the growth of MDA-MB-231 tumours within mice was examined. Briefly, mice were given the carbonic anhydrase inhibitors via the intraperitoneal route from days 0 to day 4. Tumour size was measured 3 times a week, and the relative tumour volume was calculated for each individual tumour. Differences in the growth of the drug-treated tumours were observed, with both FC9398A and DTP348-treated mice exhibiting significantly lower tumour volumes compared to the controls (figure 63A). These significant differences in tumour volume were observed in the measurements taken during the treatment period at days 2 and 4, and also at day 7.

The tumours were removed and fixed 14 days after the initial treatment. IHC was performed to investigate whether drug treatment was having any effect on either proliferation or CAIX expression levels within the tumours, with proliferation measured by analysing Ki67 staining (representative images of the IHC performed shown in figure 62). Even though both compounds significantly reduced the growth of tumours within mice, only DTP348 treatment led to a significant reduction in the percentage of Ki67 expressing cells in comparison to the controls (figure 63B). Neither DTP348 nor FC9398A had any significant effect on the % area of CAIX expression within the xenografts (figure 63C).

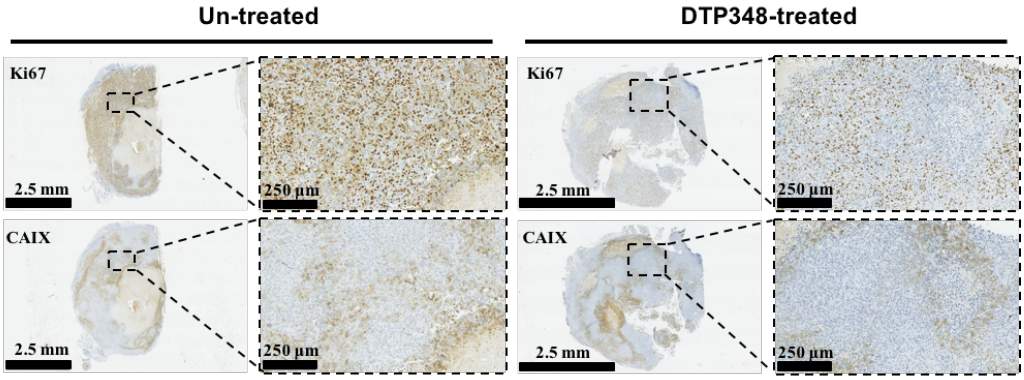

Figure 62. Representative images showing Ki67 and CAIX IHC in MDA-MB-231 xenografts.

Representative images of Ki67 and CAIX staining within control and DTP348-treated xenografts.

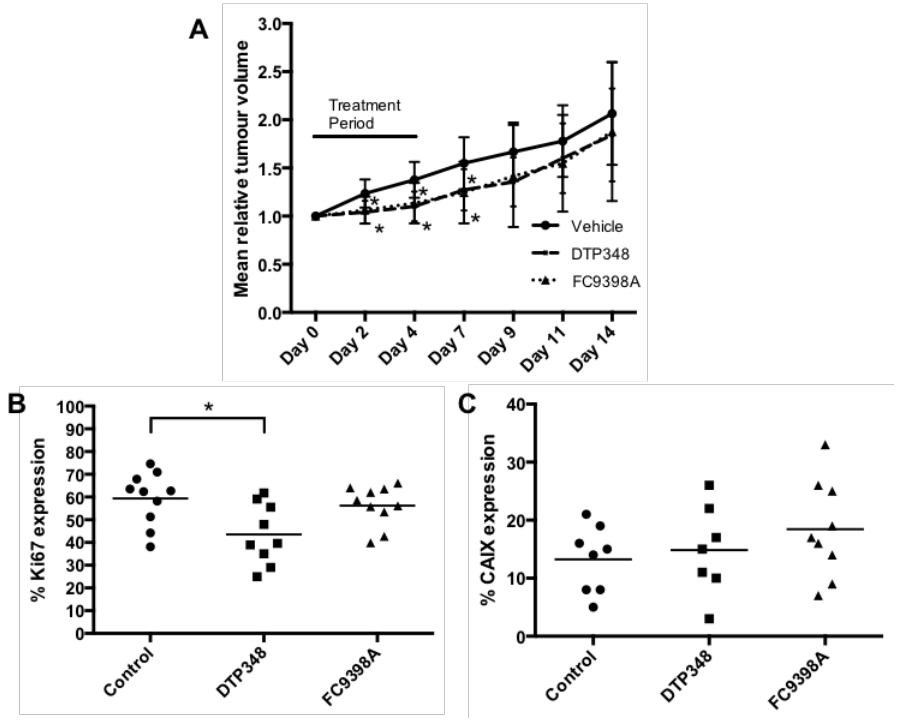

Figure 63. DTP348 and FC9398A-treated xenografts exhibit significantly reduced volumes compared to control explants, with DTP348 also leading to lower Ki67 expression, while CAIX expression is unaffected by treatment.

*(A) The effects of DTP348 and FC9398A on the relative mean tumour volume of MDA-MB-231 tumours was analysed. 25 mg/kg/day of FC9398A and 10 mg/kg/day of DTP348 were given in saline via the intraperitoneal route from day 0 until day 4. Relative tumour volume was calculated, with measurements taken 3 times a week. Data expressed as mean ± SD (n=10). * P ≤ 0.05 (Related t-tests comparing against the control on each day). (B/C) The % of Ki67-positive cells (B) and the % area of CAIX-positive cells (C) were analysed in both drug-treated and control xenografts that had been fixed 14 days after the initial treatment. Data expressed as mean ± SD (n=10). * P ≤ 0.05 (Mann-Whitney test, comparing the control group to the treated group).*

5.3 Discussion

Of the 3 different pH inhibitory compounds tested within Chapter 3, the carbonic anhydrase inhibitor S4 produced the most promising results. This Chapter focused on additional experiments carried out with novel inhibitors targeting the tumour-associated carbonic anhydrases.

The initial work presented assessed the effects of the carbonic anhydrase inhibitor S4 on the protein expression levels of CAIX and cleaved PARP, an indicator of apoptotic cell death [467], within the 3 cell lines cultured in acute hypoxic conditions. MCF-7 cells were the only cell line to show a significant reduction in CAIX protein levels due to drug treatment, with increased PARP cleavage also detected within this cell line (figure 55). Studies have indicated that plasma membrane CAIX can undergo shedding, wherein the extracellular domain of the protein is released from the plasma membrane through proteolytic cleavage [469]. CAIX shedding is thought to regulate the distribution, abundance and function of CAIX, and is believed to be a regulated process that responds to differing stimuli (reviewed in [470]). CAIX ectodomain shedding has been shown to be induced in cells treated with cytotoxic drugs, and is thought to be a consequence of apoptosis [471]. The observation of increased cleaved PARP expression in MCF-7 cells, in combination with the significant decrease in CAIX protein expression levels detected, possibly as a result of the increased shedding of CAIX, may signify the occurrence of higher levels of apoptosis in the acute hypoxic MCF-7 cells treated with S4.

Previous studies have shown that carbonic anhydrase inhibition can impede the pH regulating capabilities of cancer cells *in vitro* [320, 468]. Because cytosolic acidification is believed to have a permissive role in apoptosis (see section 1.13.2), the reduced CAIX expression levels after S4 treatment may be hindering the capability of MCF-7 cells to control pH, possibly contributing to increased apoptosis in the acute hypoxic MCF-7 cells. In contrast, no significant changes in CAIX expression were observed within the MDA-MB-231 or HBL-100 cell lines, with no cleaved PARP detected within these cell lines either. The higher protein expression

levels of CAIX within these two cell lines compared to the MCF-7 cell line in acute hypoxic conditions might have contributed to the results observed. Higher concentrations of S4 may therefore be required to observe the same effect in these two cell lines. Further work is required to assess the mechanism through which S4 is leading to reduced CAIX protein levels in the MCF-7 cell line.

Prior studies, performed with colorectal carcinoma cell lines [472] and a mouse laryngeal tumour model [473], have also shown that S4 treatment can affect CAIX protein levels. However, S4 treatment was found to produce varying effects on CAIX protein levels in these investigations. In the study by Hektoen et al, the effect of S4 treatment on CAIX expression was cell line dependent, with the decreased CAIX protein levels observed in one cell line attributed to the increased shedding of the CAIX ectodomain from the surface of the cell, while higher CAIX protein expression levels were observed in another cell line after S4 addition [472]. In the study by Meijer et al, CAIX ectodomain shedding was demonstrated to decrease after S4 treatment [473]. Metalloproteinases have been shown to be involved in the process of CAIX shedding [469]. Because prior studies indicated that sulphonamide-based inhibitors can inhibit metalloproteinases in addition to the carbonic anhydrases [474], some hypothesise that treatment with carbonic anhydrase inhibitors may lead to decreased rates of shedding due to the inhibition of the metalloproteinases [472]. However, while this may help explain the increased levels of CAIX protein observed after S4 treatment in some studies, it does not explain why S4 addition is leading to the lower CAIX levels observed here.

Tests performed in Chapter 3 indicated that S4 had the ability to affect the invasion of cells from MDA-MB-231 spheroids. Additional experiments were carried out in this Chapter, assessing the effect of carbonic anhydrase inhibition on the invasion of cells from explant tissue derived from treatment naïve biopsy specimens. The novel carbonic anhydrase inhibitors S4, FC9403A and FC9398A were tested in these experiments, and were all shown to significantly reduce the invasion of cells from explant tissue into collagen type 1 (figure 59 and 60), whilst also having a significant effect on established invasion (figure 61). Because experiments indicated that S4

treatment may be causing cell death (figure 55), it was recognised that the effects of the carbonic anhydrase inhibitors on the invasion of cancer cells may have been partly down to the induction of cell death, especially at the higher concentrations used. Because of this, each piece of explant tissue utilised in the invasion assays was fixed for IHC analysis, in order to assess the expression of markers for cell death. However, this analysis was prevented due to the small size of the sections obtained, which detached from the slides during the antigen retrieval process.

Studies have shown that tumour grafts from patients suffering from breast cancer that are cultured in mice re-create the metastatic potential and pathology of the different breast cancer classifications [475]. Others have also reported the use of explant tissue derived from human patients, showing that the explants retain the different histological markers of the original tumour, such as ER and HER2 positivity, in addition to the proliferation indices [476]. These explants were also shown to inform the outcomes of therapeutic response to a cyclin dependent kinase 4 (CDK4) inhibitor [476], exhibiting the value of this preclinical model in the testing of pharmacological compounds. The tumour explant tissue used within this study also preserves different aspects of the original cancer pathophysiology, while also enabling the effect of stromal elements [which have a role to play in cancer cell invasion (reviewed in [477])] on drug response to be investigated. Biopsies from the different breast cancer subtypes were used within this study; the potency of the carbonic anhydrase inhibitors exhibited suggests that these compounds may be able to affect the invasion of cells from different types of breast cancer.

The last section of this Chapter assessed the *in vivo* effects of 2 carbonic anhydrase inhibitors on MDA-MB-231 xenografts. The statistical analysis conducted indicated that the mean relative tumour volumes of the mice treated with the inhibitors were significantly lower than that of the un-treated mice, with the tumours of the DTP348-treated mice also exhibiting significantly decreased levels of Ki67 staining compared to the controls (figure 63). While these results suggested that carbonic anhydrase inhibition may be leading to diminished tumour growth through reducing the proliferation rate of the cancer cells, the biological significance of the growth assay

results must be questioned, as the mean relative tumour volumes of the drug-treated mice were quite similar to those of the un-treated mice at each of the measurements taken. Analysis of CAIX expression was also conducted, the results of which indicated that drug treatment had no effect on CAIX protein expression levels. However, this expression analysis was performed on tissue that had been fixed ten days after drug treatment had ended. Different results may have produced had the analysis been performed on tissue that had been fixed immediately after the cessation of treatment.

Various studies have shown the importance of CAIX in the growth of tumours within mice, with knock down of CAIX observed to significantly decrease tumour growth in xenografts produced from colon carcinoma cell lines [429] and the MDA-MB-231 cell line [307]. Others have also reported the testing of carbonic anhydrase inhibitors *in vivo*, but with varying results. While DTP348 has been described to reduce the growth rate of HT-29 tumours [320], S4 did not have an effect on the growth of tumours derived from either a breast [310] or a transglottic laryngeal squamous cell carcinoma cell line [473].

6 Chapter 6: Conclusion

6.1 Summary

While previous studies have investigated the effects of targeting the tumour-associated carbonic anhydrases, NHE1 and V-ATPase separately, a direct comparison of the effects of targeting these proteins within one study has not previously been carried out. The aim of this project was to compare the therapeutic effect of inhibitors targeting these 3 pH regulatory molecules on breast cancer proliferation and invasion, in addition to assessing the effects of combining these inhibitors with irradiation, with experiments conducted using both 2D and 3D cancer models. Low O_2 conditions have been shown to lead to the increased expression of both the tumour-associated carbonic anhydrases and NHE1, while some believe hypoxia may also have a role in V-ATPase expression. Additionally, increased levels of activity have been reported for CAIX and NHE1 in reduced O_2 concentrations. Due to this increased expression and/or activity in low O_2 conditions, we hypothesised that agents targeting these pH regulators might be more effective in hypoxic conditions.

The initial experiments performed investigated the expression of the pH regulatory proteins in the differing O_2 concentrations that have been shown to occur *in vivo,* to assess the expression of these proteins in the cancer cell lines used within this study in both 2D and 3D cancer cell models. While NHE1 and V-ATPase expression was seen to be relatively consistent in the varying O_2 concentrations, the expression of the HIF-1α inducible CAIX was seen to be markedly increased in the 3 breast cancer cell lines in low O_2 conditions, in agreement with other studies. However, despite the presence of similar levels of HIF-1α between the 3 cell lines, the extent of CAIX expression varied, with MCF-7 cells exhibiting the lowest levels of CAIX mRNA and protein.

Further experiments were performed, assessing the expression of FIH-1 (a negative regulator of HIF-1α [129, 130]) and MMP14 (reported to inhibit FIH-1 [448]), to investigate whether the expression levels of these proteins might explain the

variation in CAIX expression seen. The initial analysis conducted in 2D suggested that increased levels of active FIH-1 within the MCF-7 cells, possibly due to a lack of MMP14 protein in this cell line, may have been the reason for the lower levels of CAIX observed within these cells. However, the 3D analysis performed indicated that the MCF-7 cells may actually express MMP14 protein.

SRB assays were carried out to investigate the effects of targeting the pH regulating proteins on cancer cell number, with these experiments conducted using aerobic, acute hypoxic and chronic hypoxic cancer cells. Due to the increased CAIX protein expression levels observed in cells cultured in hypoxic conditions, in addition to the increased activity of the pH regulatory proteins reported in low O_2 conditions, we hypothesized that the hypoxic cancer cells might be more sensitive to treatment with inhibitors targeting each of these proteins. Contrary to the expected results, acute hypoxic cells treated with inhibitors targeting the tumour-associated carbonic anhydrases and NHE1 actually showed increased resistance to drug treatment.

Invasion assays, conducted with spheroids cultured in both 20% O_2 and 0.5% O_2 conditions, suggested that carbonic anhydrase inhibitors had the most potential of all the agents tested to reduce cancer cell invasion. Preliminary experiments were also carried out assessing the ability of drugs targeting the tumour-associated carbonic anhydrases, NHE1 and V-ATPase to combine with irradiation. These clonogenic assays indicated that inhibitors targeting both the tumour-associated carbonic anhydrases and NHE1 have potential to combine effectively with irradiation.

The positive results observed with the novel carbonic anhydrase inhibitors led to additional testing with these agents. The treatment of hypoxic cancer cells with S4 was shown to lead to a significant reduction in CAIX protein levels, in addition to increased cleaved PARP expression, suggesting that drug treatment was leading to higher levels of apoptosis within hypoxic cancer cells. Further 3D invasion assays demonstrated the ability of the novel carbonic anhydrase inhibitors to inhibit the invasion of cells from explant tissue derived from human patients, with significant effects observed in all of the breast cancer subtypes assessed. The carbonic

anhydrase inhibitors were also shown to have anti-cancer effects in an *in vivo* model, significantly reducing the growth and proliferation of tumours within mice.

6.2 Future work

Further experiments are required to investigate possible reasons for the differential CAIX expression patterns observed between the 3 cancer cell lines studied. While the initial 2D expression analysis performed indicated that the low levels of CAIX within MCF-7 cells were consistent with an increased activity of FIH-1, possibly due to a lack of MMP14 protein within this cell line, the 3D expression analysis suggested that the MCF-7 cells may produce the MMP14 protein.

Further work is required to ascertain whether MCF-7 cells cultured in 2D express MMP14 protein, and, if so, whether the MMP14 protein auto-catalyses within this cell line. Additional experiments, employing siRNA targeting MMP14, are also required to assess the function of this protein in the control of CAIX expression. If the role of MMP14 in FIH-1 inhibition discussed by Sakamoto et al is correct [448], then the reduction of MMP14 protein expression would be expected to lead to decreased CAIX expression levels in each of the cancer cell lines. Additionally, while CAIX expression was analysed in each of the cell lines in the differing O_2 conditions, further experiments assessing the expression levels of other C-TAD sensitive genes that rely on FIH-1 inhibition for expression apart from CAIX, such as hexokinase-2 [478], would increase the confidence in the results obtained. Aside from FIH-1, there are other negative regulators of HIF-1α transcriptional activity, such as CITED2, that may be influencing the CAIX expression observed in the 3 cell lines (section 4.3). The expression levels of proteins such as CITED2 should also be analysed to assess whether differing expression levels of this protein may be contributing to the CAIX expression patterns observed.

The treatment of cancer usually involves a combination of the different therapies described in section 1.5. While treatment with each of the tumour-associated carbonic anhydrase, NHE1 and V-ATPase inhibitors alone produced anti-cancer effects, the potential benefit of combining irradiation with inhibitors targeting the pH

regulating proteins of cancer cells was shown in the preliminary clonogenic assays conducted. However, there were several issues with the experimental design. Further work, incorporating the changes suggested in section 3.3, should be performed to more accurately analyse the effects of combining each of the inhibitors with clinically relevant doses of irradiation.

In addition to combining inhibitors targeting the pH regulation mechanisms of cancer cells with irradiation, there are other possible combinations that were not tested. One possible strategy would be to combine agents that target pH regulating proteins with compounds currently used in the clinic [330]. The reversed pH of cancer cells has been shown to influence the effectiveness of chemotherapy (see section 1.13.4). While studies have shown the chemomodulatory properties of drugs targeting CAIX, leading to the improved effectiveness of certain chemotherapeutics [479], others have produced mixed results [480], indicating that further work is required before combining these pH inhibitors with more standard treatment modalities [480]. Therefore, further experiments with the agents used in this study in combination with chemotherapeutic agents are merited.

We hypothesised that hypoxic cancer cells might be more sensitive to the effects of drugs targeting the pH regulatory molecules of cancer cells, due to the increased expression and/or activity of the pH regulatory proteins in low O_2 conditions. However, acute hypoxic cells exhibited an increased resistance to drug treatment. It may be the case that the increased expression/activity in hypoxic conditions is actually leading to the enhanced resistance of cells to treatment. Another possible strategy for combination treatment involves the use of a ‘cocktail’ of inhibitors targeting the different pH regulatory proteins that are linked to pH control within cancer cells [330]. A recent study in melanoma cells showed that the combination of PPIs, which have the ability to target V-ATPases, with carbonic anhydrase inhibitors was more effective than treatment with either agent alone [481]. As a result of the increased protein expression/activity in hypoxic conditions, combinations of ‘cocktails’ of inhibitors targeting the different pH regulatory proteins may be required to achieve the same effect as seen with single agent treatment in the aerobic

cancer cells. Therefore, future experiments assessing the effects of combining inhibitors targeting the different pH regulating proteins of hypoxic breast cancer cells are merited. In addition to assessing the effect of combining 'cocktails' of drugs that target different pH regulatory proteins, experiments evaluating the effects of combining compounds that target the same pH regulatory protein are also worthy of investigation. Experiments involving the use of multiple tumour associated carbonic anhydrase inhibitors, for example, would be hypothesised to have greater effects on cancer cells than single agent treatment alone.

Many of the different processes involved in the migration and invasion of cancer cells are dependent on pH (section 1.13.1), with each of the pH regulating proteins analysed in this study connected with the invasion of breast cancer cells. The preliminary 3D invasion assays conducted showed that S4 was the only drug to negatively affect tumour cell invasion, while the NHE1 and V-ATPase inhibitors, which have previously been shown to reduce the invasive potential of cancer cells (section 3.3), were seen to lead to increased amounts of invasion at certain concentrations. Because these results are from one independent experiment including a number of technical replicates, further experimentation is needed to suitably compare the anti-invasive effects of the inhibitors against one another, with the use of an agent that has been proven to reduce the invasive capabilities of cancer cells also included as an additional experimental control.

Studies show that MMP14 increases the invasive ability of cells, with this protein demonstrated to have a role in the invasion of cancer cells into collagen type 1 [482]. Reports also indicate that CAIX interacts with MMP14, leading to the localisation of these proteins in the invadopodia of invading cells, where CAIX is thought to promote the ability of MMP14 to break down collagen type 1 during the process of invasion [483]. High levels of plasma membrane MMP14 protein were observed in spheroids of both the MDA-MB-231 and HBL-100 cell lines (section 4.2.4). Experiments assessing the combination of tumour-associated carbonic anhydrase inhibitors with a selective MMP14 inhibitor are warranted in any future invasion

assays carried out, and would be hypothesised to have a greater effect on cancer cell invasion than single agent treatment alone.

Further invasion assays exhibited the ability of the novel carbonic anhydrase inhibitors tested to affect the invasion of cells from explant tissue derived from human patients, with significant effects observed in all of the different breast cancer subtypes tested. However, the anti-invasive effects of the 3 inhibitors analysed were not shown to be equal, with FC9403A observed to be the most potent of the inhibitors tested. Similarly, in the preliminary 3D clonogenic assays carried out, FC9403A was observed to have more potential in combining with irradiation than S4 at the dose tested. Additional work with these novel inhibitors is required to investigate why these differences in activity were observed, and may give an idea of the structural alterations in these compounds that led to these differences, which could be incorporated into any future inhibitors produced.

The novel carbonic anhydrase inhibitors used within this study inhibit the tumour-associated carbonic anhydrases CAIX and CAXII at nM concentrations [310, 393]. However, treatment with S4 had an effect on aerobic MCF-7 cancer cell number (section 3.2.3). These cells were shown to express elevated levels of CAXII mRNA and protein in high O_2 concentrations in the 2D (section 3.2.1) and 3D (section 3.2.2) analyses performed, indicating that the carbonic anhydrase inhibitors may be affecting cell number by targeting CAXII within these cells. Hypoxic incubation was shown to lead to decreased levels of CAXII mRNA in the MCF-7 cell line (section 3.2.1). Other studies have demonstrated the presence of an inverse relationship between the expression of CAIX and CAXII [419, 420], which has led some investigators to hypothesise that the various carbonic anhydrase isoforms present in the cell might communicate in a network that has yet to be resolved [419]. Further work investigating the expression of the different carbonic anhydrase isoforms within MCF-7 cells is merited to assess whether such a network exists within this cell line, and, if it is present, the mechanisms through which it functions. The use of inhibitors that target both CAIX and CAXII may be useful if such a network does exist, and could lead to carbonic anhydrase inhibition affecting cancer cells present

in both the normoxic and hypoxic areas of patient tumours, thereby increasing the effectiveness of drug treatment.

While anti-cancer effects were observed with DMA and bafilomycin A1 in the experiments conducted in this study, there are other more recently developed inhibitors that target NHE1 and V-ATPase. Cariporide is one such NHE1 inhibitor that is believed to have potential in the treatment of cancer (reviewed in [328]). Studies conducted with PPIs such as esomeprazole and omeprazole show the potential of drugs such as these to inhibit the proliferation [484] and invasion [485] of cancer cells, while also exhibiting the ability to induce apoptosis [486-488]. A direct comparison of more recently developed inhibitors such as Cariporide and PPIs, alongside the novel tumour-associated carbonic anhydrases inhibitors, would be beneficial in any future work conducted.

Experiments carried out with the novel carbonic anhydrase inhibitors in MDA-MB-231 xenografts indicated that carbonic anhydrase inhibition may be reducing tumour growth *in vivo* through a reduction in the proliferation rate of cancer cells, without having any effect on CAIX expression levels. However, as outlined in section 5.3, while the growth assay results obtained were statistically significant, the biological significance of these must be questioned, as the mean relative tumour volumes of the drug-treated mice were very similar to those of the control mice. Repeat xenograft experiments are required to more accurately assess the effects of carbonic anhydrase inhibition on both tumour growth and CAIX expression, with the expression analysis conducted on tissue that has been fixed immediately after treatments have finished, rather than 10 days after treatment has concluded, as was the case in this study.

6.3 Final remarks

In agreement with previous studies employing drugs that target the pH regulating proteins of cancer cells, the results reported here show the potential of agents that inhibit the pH regulation mechanisms of cancer cells in the treatment of breast cancer. Of the different drugs analysed, the novel tumour-associated carbonic anhydrase inhibitors represented the compounds with the most promise.

7 References

1. *GLOBOCAN 2012: Estimated cancer incidence, mortality and prevalence worldwide in 2012*. [cited 2016 11th August]; Available from: http://globocan.iarc.fr/old/FactSheets/cancers/breast-new.asp.
2. *CRUK. Breast cancer statistics*. [cited 2016 11th August]; Available from: http://www.cancerresearchuk.org/health-professional/cancer-statistics/statistics-by-cancer-type/breast-cancer.
3. Hortobagyi, G.N., et al., *The Global Breast Cancer Burden: Variations in Epidemiology and Survival.* Clinical Breast Cancer, 2005. **6**(5): p. 391-401.
4. Tao, Z., et al., *Breast Cancer: Epidemiology and Etiology.* Cell Biochemistry and Biophysics, 2014. **72**(2): p. 333-338.
5. Hanahan, D. and R.A. Weinberg, *The Hallmarks of Cancer.* Cell, 2000. **100**(1): p. 57-70.
6. Hanahan, D. and Robert A. Weinberg, *Hallmarks of Cancer: The Next Generation.* Cell, 2011. **144**(5): p. 646-674.
7. Geddes, D., *Inside the Lactating Breast: The Latest Anatomy Research.* Journal of Midwifery & Women's Health, 2007. **52**(6): p. 556-563.
8. Hassiotou, F. and D. Geddes, *Anatomy of the human mammary gland: Current status of knowledge.* Clinical Anatomy, 2013. **26**(1): p. 29-48.
9. *American Cancer Soceity*. [cited 2016 11th August]; Available from: http://mstage.qa.cancer.org/healthy/findcancerearly/womenshealth/non-cancerousbreastconditions/non-cancerous-breast-conditions-normal-breast-tissue.
10. *CRUK. Types of cancer*. [cited 2016 11th August]; Available from: http://www.cancerresearchuk.org/about-cancer/what-is-cancer/how-cancer-starts/types-of-cancer - main).
11. Malhotra, G.K., et al., *Histological, molecular and functional subtypes of breast cancers.* Cancer Biology & Therapy, 2014. **10**(10): p. 955-960.
12. Li, C.I., D.J. Uribe, and J.R. Daling, *Clinical characteristics of different histologic types of breast cancer.* Br J Cancer, 2005. **93**(9): p. 1046-52.
13. Singletary, S.E. and J.L. Connolly, *Breast cancer staging: working with the sixth edition of the AJCC Cancer Staging Manual.* CA Cancer J Clin, 2006. **56**(1): p. 37-47; quiz 50-1.
14. Bloom, H.J.G. and W.W. Richardson, *Histological Grading and Prognosis in Breast Cancer: A Study of 1409 Cases of which 359 have been Followed for 15 Years.* British Journal of Cancer, 1957. **11**(3): p. 359-377.
15. Elston, C.W. and I.O. Ellis, *Pathological prognostic factors in breast cancer. I. The value of histological grade in breast cancer: experience from a large study with long-term follow-up.* Histopathology, 1991. **19**(5): p. 403-10.
16. Rakha, E.A., et al., *Breast cancer prognostic classification in the molecular era: the role of histological grade.* Breast Cancer Res, 2010. **12**(4): p. 207.
17. Haybittle Jl Fau - Blamey, R.W., et al., *A prognostic index in primary breast cancer.* 1982(0007-0920 (Print)).
18. Blamey, R.W., et al., *Survival of invasive breast cancer according to the Nottingham Prognostic Index in cases diagnosed in 1990-1999.* 2007(0959-8049 (Print)).

19. Dai, X., et al., *Breast cancer intrinsic subtype classification, clinical use and future trends.* American Journal of Cancer Research, 2015. **5**(10): p. 2929-2943.
20. Allison, K.H., *Molecular pathology of breast cancer: what a pathologist needs to know.* Am J Clin Pathol, 2012. **138**(6): p. 770-80.
21. Prat, A., et al., *Clinical implications of the intrinsic molecular subtypes of breast cancer.* Breast, 2015. **24 Suppl 2**: p. S26-35.
22. Harris, L., et al., *American Society of Clinical Oncology 2007 update of recommendations for the use of tumor markers in breast cancer.* J Clin Oncol, 2007. **25**(33): p. 5287-312.
23. Lang, J.E., et al., *Molecular markers for breast cancer diagnosis, prognosis and targeted therapy.* J Surg Oncol, 2015. **111**(1): p. 81-90.
24. Harvey, J.M., et al., *Estrogen receptor status by immunohistochemistry is superior to the ligand-binding assay for predicting response to adjuvant endocrine therapy in breast cancer.* J Clin Oncol, 1999. **17**(5): p. 1474-81.
25. Wolff, A.C., et al., *American Society of Clinical Oncology/College of American Pathologists guideline recommendations for human epidermal growth factor receptor 2 testing in breast cancer.* J Clin Oncol, 2007. **25**(1): p. 118-45.
26. DeVita, V.T., Jr. and E. Chu, *A history of cancer chemotherapy.* Cancer Res, 2008. **68**(21): p. 8643-53.
27. Chabner, B.A. and T.G. Roberts, *Chemotherapy and the war on cancer.* Nat Rev Cancer, 2005. **5**(1): p. 65-72.
28. Selwood, K., *Side Effects of Chemotherapy*, in *Cancer in Children and Young People*. 2009, John Wiley & Sons, Ltd. p. 35-71.
29. *CRUK. How you have chemotherapy*. [cited 2016 11th August]; Available from: http://www.cancerresearchuk.org/about-cancer/type/breast-cancer/treatment/chemotherapy/about-breast-cancer-chemotherapy.
30. Untch, M., et al., *Current and future role of neoadjuvant therapy for breast cancer.* Breast, 2014. **23**(5): p. 526-37.
31. Joerger, M. and B. Thurlimann, *Chemotherapy regimens in early breast cancer: major controversies and future outlook.* Expert Rev Anticancer Ther, 2013. **13**(2): p. 165-78.
32. Kulendran, M., M. Salhab, and K. Mokbel, *Oestrogen-synthesising enzymes and breast cancer.* Anticancer Res, 2009. **29**(4): p. 1095-109.
33. Regidor, P.A., *Progesterone in Peri- and Postmenopause: A Review.* Geburtshilfe Frauenheilkd, 2014. **74**(11): p. 995-1002.
34. Blows, F.M., et al., *Subtyping of breast cancer by immunohistochemistry to investigate a relationship between subtype and short and long term survival: a collaborative analysis of data for 10,159 cases from 12 studies.* PLoS Med, 2010. **7**(5): p. e1000279.
35. Yager, J.D. and N.E. Davidson, *Estrogen carcinogenesis in breast cancer.* N Engl J Med, 2006. **354**(3): p. 270-82.
36. Daniel, A.R., C.R. Hagan, and C.A. Lange, *Progesterone receptor action: defining a role in breast cancer.* Expert review of endocrinology & metabolism, 2011. **6**(3): p. 359-369.

37. Swaby, R.F., C.G. Sharma, and V.C. Jordan, *SERMs for the treatment and prevention of breast cancer.* Rev Endocr Metab Disord, 2007. **8**(3): p. 229-39.
38. Johnston, S.J. and K.L. Cheung, *Fulvestrant - a novel endocrine therapy for breast cancer.* Curr Med Chem, 2010. **17**(10): p. 902-14.
39. Sainsbury, R., *Ovarian ablation as a treatment for breast cancer.* Surg Oncol, 2003. **12**(4): p. 241-50.
40. Brueggemeier, R.W., *Update on the use of aromatase inhibitors in breast cancer.* Expert Opin Pharmacother, 2006. **7**(14): p. 1919-30.
41. Osborn, G., et al., *Is primary endocrine therapy effective in treating the elderly, unfit patient with breast cancer?* Ann R Coll Surg Engl, 2011. **93**(4): p. 286-9.
42. Widakowich, C., et al., *Review: side effects of approved molecular targeted therapies in solid cancers.* Oncologist, 2007. **12**(12): p. 1443-55.
43. Gutierrez, C. and R. Schiff, *HER2: biology, detection, and clinical implications.* Arch Pathol Lab Med, 2011. **135**(1): p. 55-62.
44. Moasser, M.M., *The oncogene HER2: its signaling and transforming functions and its role in human cancer pathogenesis.* Oncogene, 2007. **26**(45): p. 6469-87.
45. Hudis, C.A., *Trastuzumab--mechanism of action and use in clinical practice.* N Engl J Med, 2007. **357**(1): p. 39-51.
46. A, D., *HER2-positive breast cancer: update on new and emerging agents.* The American Journal of Hematology/Oncology, 2015. **11**(4): p. 17-13.
47. Metzger-Filho, O., E.P. Winer, and I. Krop, *Pertuzumab: optimizing HER2 blockade.* Clin Cancer Res, 2013. **19**(20): p. 5552-6.
48. Gianni, L., et al., *Efficacy and safety of neoadjuvant pertuzumab and trastuzumab in women with locally advanced, inflammatory, or early HER2-positive breast cancer (NeoSphere): a randomised multicentre, open-label, phase 2 trial.* The Lancet Oncology, 2012. **13**(1): p. 25-32.
49. Schneeweiss, A., et al., *Pertuzumab plus trastuzumab in combination with standard neoadjuvant anthracycline-containing and anthracycline-free chemotherapy regimens in patients with HER2-positive early breast cancer: a randomized phase II cardiac safety study (TRYPHAENA).* Ann Oncol, 2013. **24**(9): p. 2278-84.
50. Moreira, C. and V. Kaklamani, *Lapatinib and breast cancer: current indications and outlook for the future.* Expert Rev Anticancer Ther, 2010. **10**(8): p. 1171-82.
51. Hurvitz, S.A. and R. Kakkar, *Role of lapatinib alone or in combination in the treatment of HER2-positive breast cancer.* Breast Cancer (Dove Med Press), 2012. **4**: p. 35-51.
52. Valachis, A., et al., *Trastuzumab combined to neoadjuvant chemotherapy in patients with HER2-positive breast cancer: a systematic review and meta-analysis.* Breast, 2011. **20**(6): p. 485-90.
53. Kaufman, B., et al., *Trastuzumab plus anastrozole versus anastrozole alone for the treatment of postmenopausal women with human epidermal growth factor receptor 2-positive, hormone receptor-positive metastatic breast cancer: results from the randomized phase III TAnDEM study.* J Clin Oncol, 2009. **27**(33): p. 5529-37.

54. Blackwell, K.L., et al., *Randomized study of Lapatinib alone or in combination with trastuzumab in women with ErbB2-positive, trastuzumab-refractory metastatic breast cancer.* J Clin Oncol, 2010. **28**(7): p. 1124-30.
55. Blackwell, K.L., et al., *Overall survival benefit with lapatinib in combination with trastuzumab for patients with human epidermal growth factor receptor 2-positive metastatic breast cancer: final results from the EGF104900 Study.* J Clin Oncol, 2012. **30**(21): p. 2585-92.
56. Dieras, V. and T. Bachelot, *The success story of trastuzumab emtansine, a targeted therapy in HER2-positive breast cancer.* Target Oncol, 2014. **9**(2): p. 111-22.
57. Barnett, C.M., *Everolimus: targeted therapy on the horizon for the treatment of breast cancer.* Pharmacotherapy, 2012. **32**(4): p. 383-96.
58. Critchley, A.C. and H.J. Cain, *Surgical techniques in breast cancer: an overview.* Surgery (Oxford), 2016. **34**(1): p. 32-42.
59. Veronesi, U., et al., *Twenty-year follow-up of a randomized study comparing breast-conserving surgery with radical mastectomy for early breast cancer.* N Engl J Med, 2002. **347**(16): p. 1227-32.
60. Fisher, B., et al., *Twenty-year follow-up of a randomized trial comparing total mastectomy, lumpectomy, and lumpectomy plus irradiation for the treatment of invasive breast cancer.* N Engl J Med, 2002. **347**(16): p. 1233-41.
61. Veronesi, U., et al., *Comparing radical mastectomy with quadrantectomy, axillary dissection, and radiotherapy in patients with small cancers of the breast.* N Engl J Med, 1981. **305**(1): p. 6-11.
62. Connell, P.P. and S. Hellman, *Advances in radiotherapy and implications for the next century: a historical perspective.* Cancer Res, 2009. **69**(2): p. 383-92.
63. Polgar, C. and T. Major, *Current status and perspectives of brachytherapy for breast cancer.* Int J Clin Oncol, 2009. **14**(1): p. 7-24.
64. Kunkler, I.H., et al., *Personalisation of Radiotherapy for Breast Cancer*, in *Personalized Treatment of Breast Cancer*, M. Toi, et al., Editors. 2016, Springer Japan: Tokyo. p. 131-149.
65. *Effect of radiotherapy after breast-conserving surgery on 10-year recurrence and 15-year breast cancer death: meta-analysis of individual patient data for 10 801 women in 17 randomised trials.* The Lancet, 2011. **378**(9804): p. 1707-1716.
66. *Effect of radiotherapy after mastectomy and axillary surgery on 10-year recurrence and 20-year breast cancer mortality: meta-analysis of individual patient data for 8135 women in 22 randomised trials.* The Lancet, 2014. **383**(9935): p. 2127-2135.
67. *Effects of radiotherapy and of differences in the extent of surgery for early breast cancer on local recurrence and 15-year survival: an overview of the randomised trials.* The Lancet, 2005. **366**(9503): p. 2087-2106.
68. *Favourable and unfavourable effects on long-term survival of radiotherapy for early breast cancer: an overview of the randomised trials.* The Lancet, 2000. **355**(9217): p. 1757-1770.
69. Bondiau, P.Y., et al., *Phase 1 clinical trial of stereotactic body radiation therapy concomitant with neoadjuvant chemotherapy for breast cancer.* Int J Radiat Oncol Biol Phys, 2013. **85**(5): p. 1193-9.

70. *CRUK. About breast cancer radiotherapy*. [cited 2016 11th August]; Available from: http://www.cancerresearchuk.org/about-cancer/type/breast-cancer/treatment/radiotherapy/about-breast-cancer-radiotherapy.
71. Darby, S.C., et al., *Risk of ischemic heart disease in women after radiotherapy for breast cancer.* N Engl J Med, 2013. **368**(11): p. 987-98.
72. Shah, C., et al., *Cardiac dose sparing and avoidance techniques in breast cancer radiotherapy.* Radiother Oncol, 2014. **112**(1): p. 9-16.
73. Bucci, M.K., A. Bevan, and M. Roach, 3rd, *Advances in radiation therapy: conventional to 3D, to IMRT, to 4D, and beyond.* CA Cancer J Clin, 2005. **55**(2): p. 117-34.
74. Williams, N.R., et al., *Intraoperative radiotherapy for breast cancer.* Gland Surg, 2014. **3**(2): p. 109-19.
75. Adair, T. and J. Montani, *Overview of Angiogenesis*, in *Angiogenesis*. 2010, Morgan and Claypool Life Sciences.
76. Tannock, I.F., *The relation between cell proliferation and the vascular system in a transplanted mouse mammary tumour.* British Journal of Cancer, 1968. **22**(2): p. 258-273.
77. Thomlinson, R.H. and L.H. Gray, *The Histological Structure of Some Human Lung Cancers and the Possible Implications for Radiotherapy.* British Journal of Cancer, 1955. **9**(4): p. 539-549.
78. Chung, A.S., J. Lee, and N. Ferrara, *Targeting the tumour vasculature: insights from physiological angiogenesis.* Nat Rev Cancer, 2010. **10**(7): p. 505-14.
79. Vaupel, P., et al., *Hypoxia in breast cancer: role of blood flow, oxygen diffusion distances, and anemia in the development of oxygen depletion.* Adv Exp Med Biol, 2005. **566**: p. 333-42.
80. Ribatti, D., et al., *The structure of the vascular network of tumors.* Cancer Lett, 2007. **248**(1): p. 18-23.
81. Brown, J.M. and W.R. Wilson, *Exploiting tumour hypoxia in cancer treatment.* Nat Rev Cancer, 2004. **4**(6): p. 437-47.
82. Bertout, J.A., S.A. Patel, and M.C. Simon, *The impact of O2 availability on human cancer.* Nat Rev Cancer, 2008. **8**(12): p. 967-75.
83. Vaupel, P. and A. Mayer, *Hypoxia in Tumors: Pathogenesis-Related Classifi cation, Characterization of Hypoxia Subtypes, and Associated Biological and Clinical Implications*, in *Oxygen Transport to Tissue XXXV*, S.V. Huffel, et al., Editors. 2013, Springer-Verlag New York. p. 19-25.
84. Bayer, C., et al., *Acute versus chronic hypoxia: why a simplified classification is simply not enough.* Int J Radiat Oncol Biol Phys, 2011. **80**(4): p. 965-8.
85. Brown, J.M., *Evidence for acutely hypoxic cells in mouse tumours, and a possible mechanism of reoxygenation.* Br J Radiol, 1979. **52**(620): p. 650-6.
86. Chaplin, D.J., P.L. Olive, and R.E. Durand, *Intermittent blood flow in a murine tumor: radiobiological effects.* Cancer Res, 1987. **47**(2): p. 597-601.
87. Horsman, M.R., et al., *Imaging hypoxia to improve radiotherapy outcome.* Nat Rev Clin Oncol, 2012. **9**(12): p. 674-87.
88. Koch, C.J., et al., *Mechanisms of blood flow and hypoxia production in rat 9L-epigastric tumors.* Tumor Microenviron Ther, 2013. **1**: p. 1-13.

89. Dewhirst, M.W., et al., *Quantification of longitudinal tissue pO2 gradients in window chamber tumours: impact on tumour hypoxia.* Br J Cancer, 1999. **79**(11-12): p. 1717-22.
90. Vaupel, P., M. Hockel, and A. Mayer, *Detection and characterization of tumor hypoxia using pO2 histography.* Antioxid Redox Signal, 2007. **9**(8): p. 1221-35.
91. Hammond, E.M., et al., *The meaning, measurement and modification of hypoxia in the laboratory and the clinic.* Clin Oncol (R Coll Radiol), 2014. **26**(5): p. 277-88.
92. Krohn, K.A., J.M. Link, and R.P. Mason, *Molecular imaging of hypoxia.* J Nucl Med, 2008. **49 Suppl 2**: p. 129S-48S.
93. Vaupel, P., et al., *Oxygenation of human tumors: evaluation of tissue oxygen distribution in breast cancers by computerized O2 tension measurements.* Cancer Res, 1991. **51**(12): p. 3316-22.
94. Hohenberger, P., et al., *Tumor oxygenation correlates with molecular growth determinants in breast cancer.* Breast Cancer Research and Treatment, 1998. **48**(2): p. 97-106.
95. Okunieff, P., et al., *Oxygen tension distributions are sufficient to explain the local response of human breast tumors treated with radiation alone.* Int J Radiat Oncol Biol Phys, 1993. **26**(4): p. 631-6.
96. Auer, F., et al., *Technical improvement of pO(2) measurements in breast cancer: investigation of the feasibility in patients and in vitro validation of the method.* Strahlenther Onkol, 2007. **183**(5): p. 265-70.
97. Okunieff, P., et al., *Tumor oxygen measurements and personalized medicine.* Adv Exp Med Biol, 2013. **765**: p. 195-201.
98. Tredan, O., et al., *Drug resistance and the solid tumor microenvironment.* J Natl Cancer Inst, 2007. **99**(19): p. 1441-54.
99. Bedford, J.S. and J.B. Mitchell, *The effect of hypoxia on the growth and radiation response of mammalian cells in culture.* The British Journal of Radiology, 1974. **47**(562): p. 687-696.
100. Yoshiba, S., et al., *Hypoxia induces resistance to 5-fluorouracil in oral cancer cells via G(1) phase cell cycle arrest.* Oral Oncol, 2009. **45**(2): p. 109-15.
101. Hubbi, M.E. and G.L. Semenza, *Regulation of cell proliferation by hypoxia-inducible factors.* Am J Physiol Cell Physiol, 2015. **309**(12): p. C775-82.
102. Gray, L.H., et al., *The concentration of oxygen dissolved in tissues at the time of irradiation as a factor in radiotherapy.* Br J Radiol, 1953. **26**(312): p. 638-48.
103. Okunieff, P., B. Fenton, and Y. Chen, *Past, present, and future of oxygen in cancer research.* Adv Exp Med Biol, 2005. **566**: p. 213-22.
104. Eriksson, D. and T. Stigbrand, *Radiation-induced cell death mechanisms.* Tumour Biol, 2010. **31**(4): p. 363-72.
105. DeBerardinis, R.J. and N.S. Chandel, *Fundamentals of cancer metabolism.* Science Advances, 2016. **2**(5): p. e1600200.
106. Pavlova, N.N. and C.B. Thompson, *The Emerging Hallmarks of Cancer Metabolism.* Cell Metab, 2016. **23**(1): p. 27-47.
107. Alberts, B., et al., *Cell Chemistry and Biosynthesis*, in *Molecular Biology of the Cell*. 2002, New York: Garland Science.

108. Champ, P., R. Harvey, and D. Ferrier, *Glycolysis*, in *Lippincott's Illustrated Reviews Biochemistry*. 2008, Lippincott Williams and Wilkins.
109. Champ, P., R. Harvey, and D. Ferrier, *Bioenergetics and Oxidative Phosphorylation*, in *Lippincott's Illustrated Reviews Biochemistry*. 2008, Lippincott Williams and Wilkins.
110. Champ, P., R. Harvey, and D. Ferrier, *Tricarboxylic Acid Cycle* in *Lippincott's Illustrated Reviews Biochemistry*. 2008, Lippincott Williams and Wilkins.
111. Chandel, N.S., et al., *Cellular respiration during hypoxia. Role of cytochrome oxidase as the oxygen sensor in hepatocytes.* J Biol Chem, 1997. **272**(30): p. 18808-16.
112. Masoud, G.N. and W. Li, *HIF-1alpha pathway: role, regulation and intervention for cancer therapy.* Acta Pharm Sin B, 2015. **5**(5): p. 378-89.
113. Huang, L.E., et al., *Regulation of hypoxia-inducible factor 1alpha is mediated by an O2-dependent degradation domain via the ubiquitin-proteasome pathway.* Proc Natl Acad Sci U S A, 1998. **95**(14): p. 7987-92.
114. Epstein, A.C.R., et al., *C. elegans EGL-9 and Mammalian Homologs Define a Family of Dioxygenases that Regulate HIF by Prolyl Hydroxylation.* Cell, 2001. **107**(1): p. 43-54.
115. Bruick, R.K. and S.L. McKnight, *A conserved family of prolyl-4-hydroxylases that modify HIF.* Science, 2001. **294**(5545): p. 1337-40.
116. Ivan, M., et al., *Biochemical purification and pharmacological inhibition of a mammalian prolyl hydroxylase acting on hypoxia-inducible factor.* Proc Natl Acad Sci U S A, 2002. **99**(21): p. 13459-64.
117. Maxwell, P.H., et al., *The tumour suppressor protein VHL targets hypoxia-inducible factors for oxygen-dependent proteolysis.* Nature, 1999. **399**(6733): p. 271-5.
118. Jaakkola, P., et al., *Targeting of HIF-alpha to the von Hippel-Lindau ubiquitylation complex by O2-regulated prolyl hydroxylation.* Science, 2001. **292**(5516): p. 468-72.
119. Kallio, P.J., et al., *Regulation of the hypoxia-inducible transcription factor 1alpha by the ubiquitin-proteasome pathway.* J Biol Chem, 1999. **274**(10): p. 6519-25.
120. Chilov, D., et al., *Induction and nuclear translocation of hypoxia-inducible factor-1 (HIF-1): heterodimerization with ARNT is not necessary for nuclear accumulation of HIF-1alpha.* J Cell Sci, 1999. **112 (Pt 8)**: p. 1203-12.
121. Semenza, G.L., et al., *Hypoxia-inducible nuclear factors bind to an enhancer element located 3' to the human erythropoietin gene.* Proceedings of the National Academy of Sciences of the United States of America, 1991. **88**(13): p. 5680-5684.
122. Keith, B., R.S. Johnson, and M.C. Simon, *HIF1alpha and HIF2alpha: sibling rivalry in hypoxic tumour growth and progression.* Nat Rev Cancer, 2012. **12**(1): p. 9-22.
123. Makino, Y., et al., *Inhibitory PAS domain protein is a negative regulator of hypoxia-inducible gene expression.* Nature, 2001. **414**(6863): p. 550-4.
124. Jiang, B.H., et al., *Transactivation and inhibitory domains of hypoxia-inducible factor 1alpha. Modulation of transcriptional activity by oxygen tension.* J Biol Chem, 1997. **272**(31): p. 19253-60.

125. Pugh, C.W., et al., *Activation of hypoxia-inducible factor-1; definition of regulatory domains within the alpha subunit.* J Biol Chem, 1997. **272**(17): p. 11205-14.
126. Arany, Z., et al., *An essential role for p300/CBP in the cellular response to hypoxia.* Proc Natl Acad Sci U S A, 1996. **93**(23): p. 12969-73.
127. Ema, M., et al., *Molecular mechanisms of transcription activation by HLF and HIF1alpha in response to hypoxia: their stabilization and redox signal-induced interaction with CBP/p300.* Embo j, 1999. **18**(7): p. 1905-14.
128. Ruas, J.L., L. Poellinger, and T. Pereira, *Functional analysis of hypoxia-inducible factor-1 alpha-mediated transactivation. Identification of amino acid residues critical for transcriptional activation and/or interaction with CREB-binding protein.* J Biol Chem, 2002. **277**(41): p. 38723-30.
129. Mahon, P.C., K. Hirota, and G.L. Semenza, *FIH-1: a novel protein that interacts with HIF-1alpha and VHL to mediate repression of HIF-1 transcriptional activity.* Genes Dev, 2001. **15**(20): p. 2675-86.
130. Lando, D., et al., *FIH-1 is an asparaginyl hydroxylase enzyme that regulates the transcriptional activity of hypoxia-inducible factor.* Genes Dev, 2002. **16**(12): p. 1466-71.
131. Tian, Y.M., et al., *Differential sensitivity of hypoxia inducible factor hydroxylation sites to hypoxia and hydroxylase inhibitors.* J Biol Chem, 2011. **286**(15): p. 13041-51.
132. Stolze, I.P., et al., *Genetic analysis of the role of the asparaginyl hydroxylase factor inhibiting hypoxia-inducible factor (FIH) in regulating hypoxia-inducible factor (HIF) transcriptional target genes [corrected].* J Biol Chem, 2004. **279**(41): p. 42719-25.
133. Lando, D., et al., *Asparagine hydroxylation of the HIF transactivation domain a hypoxic switch.* Science, 2002. **295**(5556): p. 858-61.
134. Semenza, G.L., *Targeting HIF-1 for cancer therapy.* Nat Rev Cancer, 2003. **3**(10): p. 721-32.
135. Bardos, J.I. and M. Ashcroft, *Hypoxia-inducible factor-1 and oncogenic signalling.* Bioessays, 2004. **26**(3): p. 262-9.
136. Zhong, H., et al., *Modulation of hypoxia-inducible factor 1alpha expression by the epidermal growth factor/phosphatidylinositol 3-kinase/PTEN/AKT/FRAP pathway in human prostate cancer cells: implications for tumor angiogenesis and therapeutics.* Cancer Res, 2000. **60**(6): p. 1541-5.
137. Fukuda, R., et al., *Insulin-like growth factor 1 induces hypoxia-inducible factor 1-mediated vascular endothelial growth factor expression, which is dependent on MAP kinase and phosphatidylinositol 3-kinase signaling in colon cancer cells.* J Biol Chem, 2002. **277**(41): p. 38205-11.
138. Lu, H., R.A. Forbes, and A. Verma, *Hypoxia-inducible factor 1 activation by aerobic glycolysis implicates the Warburg effect in carcinogenesis.* J Biol Chem, 2002. **277**(26): p. 23111-5.
139. De Saedeleer, C.J., et al., *Lactate activates HIF-1 in oxidative but not in Warburg-phenotype human tumor cells.* PLoS One, 2012. **7**(10): p. e46571.
140. Weidemann, A. and R.S. Johnson, *Biology of HIF-1alpha.* Cell Death Differ, 2008. **15**(4): p. 621-7.

141. Semenza, G.L., et al., *Transcriptional regulation of genes encoding glycolytic enzymes by hypoxia-inducible factor 1.* J Biol Chem, 1994. **269**(38): p. 23757-63.
142. Mathupala, S.P., A. Rempel, and P.L. Pedersen, *Glucose catabolism in cancer cells: identification and characterization of a marked activation response of the type II hexokinase gene to hypoxic conditions.* J Biol Chem, 2001. **276**(46): p. 43407-12.
143. Iyer, N.V., et al., *Cellular and developmental control of O2 homeostasis by hypoxia-inducible factor 1 alpha.* Genes Dev, 1998. **12**(2): p. 149-62.
144. Chen, C., et al., *Regulation of glut1 mRNA by hypoxia-inducible factor-1. Interaction between H-ras and hypoxia.* J Biol Chem, 2001. **276**(12): p. 9519-25.
145. O'Rourke, J.F., et al., *Identification of hypoxically inducible mRNAs in HeLa cells using differential-display PCR. Role of hypoxia-inducible factor-1.* Eur J Biochem, 1996. **241**(2): p. 403-10.
146. Maxwell, P.H., et al., *Hypoxia-inducible factor-1 modulates gene expression in solid tumors and influences both angiogenesis and tumor growth.* Proc Natl Acad Sci U S A, 1997. **94**(15): p. 8104-9.
147. Denko, N.C., *Hypoxia, HIF1 and glucose metabolism in the solid tumour.* Nat Rev Cancer, 2008. **8**(9): p. 705-13.
148. Kim, J.W., et al., *HIF-1-mediated expression of pyruvate dehydrogenase kinase: a metabolic switch required for cellular adaptation to hypoxia.* Cell Metab, 2006. **3**(3): p. 177-85.
149. Papandreou, I., et al., *HIF-1 mediates adaptation to hypoxia by actively downregulating mitochondrial oxygen consumption.* Cell Metab, 2006. **3**(3): p. 187-97.
150. Mazzon, M., et al., *A mechanism for induction of a hypoxic response by vaccinia virus.* Proc Natl Acad Sci U S A, 2013. **110**(30): p. 12444-9.
151. Jiang, Y., et al., *The Effect of Silencing HIF-1alpha Gene in BxPC-3 Cell Line on Glycolysis-Related Gene Expression, Cell Growth, Invasion, and Apoptosis.* Nutr Cancer, 2015. **67**(8): p. 1314-23.
152. Patel, M.S. and L.G. Korotchkina, *Regulation of mammalian pyruvate dehydrogenase complex by phosphorylation: complexity of multiple phosphorylation sites and kinases.* Exp Mol Med, 2001. **33**(4): p. 191-7.
153. Zhang, S., et al., *The pivotal role of pyruvate dehydrogenase kinases in metabolic flexibility.* Nutr Metab (Lond), 2014. **11**(1): p. 10.
154. Tello, D., et al., *Induction of the mitochondrial NDUFA4L2 protein by HIF-1alpha decreases oxygen consumption by inhibiting Complex I activity.* Cell Metab, 2011. **14**(6): p. 768-79.
155. Fukuda, R., et al., *HIF-1 regulates cytochrome oxidase subunits to optimize efficiency of respiration in hypoxic cells.* Cell, 2007. **129**(1): p. 111-22.
156. Zhang, H., et al., *HIF-1 inhibits mitochondrial biogenesis and cellular respiration in VHL-deficient renal cell carcinoma by repression of C-MYC activity.* Cancer Cell, 2007. **11**(5): p. 407-20.
157. Zhang, H., et al., *Mitochondrial autophagy is an HIF-1-dependent adaptive metabolic response to hypoxia.* J Biol Chem, 2008. **283**(16): p. 10892-903.
158. Warburg, O., *The Metabolism of Carcinoma Cells.* The Journal of Cancer Research, 1925. **9**(1): p. 148-163.

159. Racker, E., *Bioenergetics and the Problem of Tumor Growth: An understanding of the mechanism of the generation and control of biological energy may shed light on the problem of tumor growth.* American Scientist, 1972. **60**(1): p. 56-63.
160. Warburg, O., *On the origin of cancer cells.* Science, 1956. **123**(3191): p. 309-14.
161. Weinhouse, S., *The Warburg hypothesis fifty years later.* Z Krebsforsch Klin Onkol Cancer Res Clin Oncol, 1976. **87**(2): p. 115-26.
162. Fantin, V.R., J. St-Pierre, and P. Leder, *Attenuation of LDH-A expression uncovers a link between glycolysis, mitochondrial physiology, and tumor maintenance.* Cancer Cell, 2006. **9**(6): p. 425-34.
163. Bonnet, S., et al., *A mitochondria-K+ channel axis is suppressed in cancer and its normalization promotes apoptosis and inhibits cancer growth.* Cancer Cell, 2007. **11**(1): p. 37-51.
164. Gatenby, R.A. and R.J. Gillies, *Why do cancers have high aerobic glycolysis?* Nat Rev Cancer, 2004. **4**(11): p. 891-9.
165. Ying, H., et al., *Oncogenic Kras maintains pancreatic tumors through regulation of anabolic glucose metabolism.* Cell, 2012. **149**(3): p. 656-70.
166. Vander Heiden, M.G., L.C. Cantley, and C.B. Thompson, *Understanding the Warburg effect: the metabolic requirements of cell proliferation.* Science, 2009. **324**(5930): p. 1029-33.
167. Locasale, J.W. and L.C. Cantley, *Metabolic flux and the regulation of mammalian cell growth.* Cell Metab, 2011. **14**(4): p. 443-51.
168. Pfeiffer, T., S. Schuster, and S. Bonhoeffer, *Cooperation and Competition in the Evolution of ATP-Producing Pathways.* Science, 2001. **292**(5516): p. 504-507.
169. Chang, C.H., et al., *Metabolic Competition in the Tumor Microenvironment Is a Driver of Cancer Progression.* Cell, 2015. **162**(6): p. 1229-41.
170. Ho, P.C., et al., *Phosphoenolpyruvate Is a Metabolic Checkpoint of Anti-tumor T Cell Responses.* Cell, 2015. **162**(6): p. 1217-28.
171. Gullino, P.M., S.H. Clark, and F.H. Grantham, *THE INTERSTITIAL FLUID OF SOLID TUMORS.* Cancer Res, 1964. **24**: p. 780-94.
172. Kilburn, D.G., M.D. Lilly, and F.C. Webb, *The energetics of mammalian cell growth.* J Cell Sci, 1969. **4**(3): p. 645-54.
173. Joshi, S., et al., *The Genomic Landscape of Renal Oncocytoma Identifies a Metabolic Barrier to Tumorigenesis.* Cell Rep, 2015. **13**(9): p. 1895-908.
174. Weinberg, F., et al., *Mitochondrial metabolism and ROS generation are essential for Kras-mediated tumorigenicity.* Proc Natl Acad Sci U S A, 2010. **107**(19): p. 8788-93.
175. Tan, A.S., et al., *Mitochondrial genome acquisition restores respiratory function and tumorigenic potential of cancer cells without mitochondrial DNA.* Cell Metab, 2015. **21**(1): p. 81-94.
176. Israelsen, W.J., et al., *PKM2 isoform-specific deletion reveals a differential requirement for pyruvate kinase in tumor cells.* Cell, 2013. **155**(2): p. 397-409.
177. Fan, T.W., et al., *Altered regulation of metabolic pathways in human lung cancer discerned by (13)C stable isotope-resolved metabolomics (SIRM).* Mol Cancer, 2009. **8**: p. 41.

178. Hensley, C.T., et al., *Metabolic Heterogeneity in Human Lung Tumors.* Cell, 2016. **164**(4): p. 681-94.
179. Davidson, S.M., et al., *Environment Impacts the Metabolic Dependencies of Ras-Driven Non-Small Cell Lung Cancer.* Cell Metab, 2016. **23**(3): p. 517-28.
180. Maftouh, M., et al., *Synergistic interaction of novel lactate dehydrogenase inhibitors with gemcitabine against pancreatic cancer cells in hypoxia.* Br J Cancer, 2014. **110**(1): p. 172-82.
181. Stincone, A., et al., *The return of metabolism: biochemistry and physiology of the pentose phosphate pathway.* Biol Rev Camb Philos Soc, 2014.
182. Patra, K.C. and N. Hay, *The pentose phosphate pathway and cancer.* Trends Biochem Sci, 2014. **39**(8): p. 347-54.
183. Miclet, E., et al., *NMR spectroscopic analysis of the first two steps of the pentose-phosphate pathway elucidates the role of 6-phosphogluconolactonase.* J Biol Chem, 2001. **276**(37): p. 34840-6.
184. Fan, J., et al., *Quantitative flux analysis reveals folate-dependent NADPH production.* Nature, 2014. **510**(7504): p. 298-302.
185. Boros, L.G., et al., *Oxythiamine and dehydroepiandrosterone inhibit the nonoxidative synthesis of ribose and tumor cell proliferation.* Cancer Res, 1997. **57**(19): p. 4242-8.
186. Mailloux, R.J., S.L. McBride, and M.E. Harper, *Unearthing the secrets of mitochondrial ROS and glutathione in bioenergetics.* Trends Biochem Sci, 2013. **38**(12): p. 592-602.
187. Balaban, R.S., S. Nemoto, and T. Finkel, *Mitochondria, oxidants, and aging.* Cell, 2005. **120**(4): p. 483-95.
188. Circu, M.L. and T.Y. Aw, *Reactive oxygen species, cellular redox systems, and apoptosis.* Free Radic Biol Med, 2010. **48**(6): p. 749-62.
189. Mari, M., et al., *Mitochondrial glutathione, a key survival antioxidant.* Antioxid Redox Signal, 2009. **11**(11): p. 2685-700.
190. Sullivan, L.B. and N.S. Chandel, *Mitochondrial reactive oxygen species and cancer.* Cancer & Metabolism, 2014. **2**: p. 17.
191. Wang, C., et al., *Identification of transaldolase as a novel serum biomarker for hepatocellular carcinoma metastasis using xenografted mouse model and clinic samples.* Cancer Lett, 2011. **313**(2): p. 154-66.
192. Fischer, A., *Amino-acid metabolism of tissue cells in vitro.* Biochemical Journal, 1948. **43**(4): p. 491-497.
193. Eagle, H., et al., *The growth response of mammalian cells in tissue culture to L-glutamine and L-glutamic acid.* J Biol Chem, 1956. **218**(2): p. 607-16.
194. Kovacevic, Z., *The pathway of glutamine and glutamate oxidation in isolated mitochondria from mammalian cells.* Biochem J, 1971. **125**(3): p. 757-63.
195. DeBerardinis, R.J. and T. Cheng, *Q's next: the diverse functions of glutamine in metabolism, cell biology and cancer.* Oncogene, 2010. **29**(3): p. 313-24.
196. Lacey, J.M. and D.W. Wilmore, *Is glutamine a conditionally essential amino acid?* Nutr Rev, 1990. **48**(8): p. 297-309.
197. Wise, D.R. and C.B. Thompson, *Glutamine addiction: a new therapeutic target in cancer.* Trends Biochem Sci, 2010. **35**(8): p. 427-33.

198. Reitzer, L.J., B.M. Wice, and D. Kennell, *Evidence that glutamine, not sugar, is the major energy source for cultured HeLa cells.* J Biol Chem, 1979. **254**(8): p. 2669-76.
199. DeBerardinis, R.J., et al., *Beyond aerobic glycolysis: transformed cells can engage in glutamine metabolism that exceeds the requirement for protein and nucleotide synthesis.* Proc Natl Acad Sci U S A, 2007. **104**(49): p. 19345-50.
200. Le, A., et al., *Tumorigenicity of hypoxic respiring cancer cells revealed by a hypoxia-cell cycle dual reporter.* Proc Natl Acad Sci U S A, 2014. **111**(34): p. 12486-91.
201. Fan, J., et al., *Glutamine-driven oxidative phosphorylation is a major ATP source in transformed mammalian cells in both normoxia and hypoxia.* Mol Syst Biol, 2013. **9**: p. 712.
202. Le, A., et al., *Glucose-independent glutamine metabolism via TCA cycling for proliferation and survival in B cells.* Cell Metab, 2012. **15**(1): p. 110-21.
203. van Geldermalsen, M., et al., *ASCT2/SLC1A5 controls glutamine uptake and tumour growth in triple-negative basal-like breast cancer.* Oncogene, 2016. **35**(24): p. 3201-8.
204. Kung, H.N., J.R. Marks, and J.T. Chi, *Glutamine synthetase is a genetic determinant of cell type-specific glutamine independence in breast epithelia.* PLoS Genet, 2011. **7**(8): p. e1002229.
205. Eales, K.L., K.E. Hollinshead, and D.A. Tennant, *Hypoxia and metabolic adaptation of cancer cells.* Oncogenesis, 2016. **5**: p. e190.
206. Perez-Escuredo, J., et al., *Monocarboxylate transporters in the brain and in cancer.* Biochim Biophys Acta, 2016. **1863**(10): p. 2481-2497.
207. Sonveaux, P., et al., *Targeting lactate-fueled respiration selectively kills hypoxic tumor cells in mice.* J Clin Invest, 2008. **118**(12): p. 3930-42.
208. Kennedy, K.M., et al., *Catabolism of exogenous lactate reveals it as a legitimate metabolic substrate in breast cancer.* PLoS One, 2013. **8**(9): p. e75154.
209. Pavlides, S., et al., *The reverse Warburg effect: aerobic glycolysis in cancer associated fibroblasts and the tumor stroma.* Cell Cycle, 2009. **8**(23): p. 3984-4001.
210. Martinez-Outschoorn, U.E., et al., *Tumor cells induce the cancer associated fibroblast phenotype via caveolin-1 degradation: implications for breast cancer and DCIS therapy with autophagy inhibitors.* Cell Cycle, 2010. **9**(12): p. 2423-33.
211. Galbiati, F., et al., *Targeted downregulation of caveolin-1 is sufficient to drive cell transformation and hyperactivate the p42/44 MAP kinase cascade.* The EMBO Journal, 1998. **17**(22): p. 6633-6648.
212. Nieman, K.M., et al., *Adipocytes promote ovarian cancer metastasis and provide energy for rapid tumor growth.* Nat Med, 2011. **17**(11): p. 1498-503.
213. Swietach, P., et al., *The chemistry, physiology and pathology of pH in cancer.* Philos Trans R Soc Lond B Biol Sci, 2014. **369**(1638): p. 20130099.
214. Schonichen, A., et al., *Considering protonation as a posttranslational modification regulating protein structure and function.* Annu Rev Biophys, 2013. **42**: p. 289-314.
215. Webb, B.A., et al., *Dysregulated pH: a perfect storm for cancer progression.* Nat Rev Cancer, 2011. **11**(9): p. 671-7.

216. Robergs, R.A., F. Ghiasvand, and D. Parker, *Biochemistry of exercise-induced metabolic acidosis.* Am J Physiol Regul Integr Comp Physiol, 2004. **287**(3): p. R502-16.
217. Boron, W.F., *Sharpey-Schafer lecture: gas channels.* Exp Physiol, 2010. **95**(12): p. 1107-30.
218. Boron, W.F., et al., *Intrinsic CO2 permeability of cell membranes and potential biological relevance of CO2 channels.* Chemphyschem, 2011. **12**(5): p. 1017-9.
219. Pinheiro, C., et al., *Role of monocarboxylate transporters in human cancers: state of the art.* J Bioenerg Biomembr, 2012. **44**(1): p. 127-39.
220. Gorbatenko, A., et al., *Regulation and roles of bicarbonate transporters in cancer.* Front Physiol, 2014. **5**: p. 130.
221. Imtaiyaz Hassan, M., et al., *Structure, function and applications of carbonic anhydrase isozymes.* Bioorg Med Chem, 2013. **21**(6): p. 1570-82.
222. Neri, D. and C.T. Supuran, *Interfering with pH regulation in tumours as a therapeutic strategy.* Nat Rev Drug Discov, 2011. **10**(10): p. 767-77.
223. Swietach, P., et al., *New insights into the physiological role of carbonic anhydrase IX in tumour pH regulation.* Oncogene, 2010. **29**(50): p. 6509-21.
224. Swietach, P., et al., *The role of carbonic anhydrase 9 in regulating extracellular and intracellular ph in three-dimensional tumor cell growths.* J Biol Chem, 2009. **284**(30): p. 20299-310.
225. Parks, S.K., J. Chiche, and J. Pouyssegur, *Disrupting proton dynamics and energy metabolism for cancer therapy.* Nat Rev Cancer, 2013. **13**(9): p. 611-23.
226. Potter, C.P. and A.L. Harris, *Diagnostic, prognostic and therapeutic implications of carbonic anhydrases in cancer.* Br J Cancer, 2003. **89**(1): p. 2-7.
227. Liao, S.Y., M.I. Lerman, and E.J. Stanbridge, *Expression of transmembrane carbonic anhydrases, CAIX and CAXII, in human development.* BMC Dev Biol, 2009. **9**: p. 22.
228. Wykoff, C.C., et al., *Expression of the Hypoxia-Inducible and Tumor-Associated Carbonic Anhydrases in Ductal Carcinoma in Situ of the Breast.* The American Journal of Pathology, 2001. **158**(3): p. 1011-1019.
229. Trastour, C., et al., *HIF-1alpha and CA IX staining in invasive breast carcinomas: prognosis and treatment outcome.* Int J Cancer, 2007. **120**(7): p. 1451-8.
230. Kaya, A.O., et al., *Hypoxia inducible factor-1 alpha and carbonic anhydrase IX overexpression are associated with poor survival in breast cancer patients.* J buon, 2012. **17**(4): p. 663-8.
231. Tafreshi, N.K., et al., *Evaluation of CAIX and CAXII Expression in Breast Cancer at Varied O2 Levels: CAIX is the Superior Surrogate Imaging Biomarker of Tumor Hypoxia.* Mol Imaging Biol, 2016. **18**(2): p. 219-31.
232. Olive, P.L., et al., *Carbonic anhydrase 9 as an endogenous marker for hypoxic cells in cervical cancer.* Cancer Res, 2001. **61**(24): p. 8924-9.
233. Mayer, A., M. Hockel, and P. Vaupel, *Carbonic anhydrase IX expression and tumor oxygenation status do not correlate at the microregional level in locally advanced cancers of the uterine cervix.* Clin Cancer Res, 2005. **11**(20): p. 7220-5.

234. Hedley, D., et al., *Carbonic anhydrase IX expression, hypoxia, and prognosis in patients with uterine cervical carcinomas.* Clin Cancer Res, 2003. **9**(15): p. 5666-74.
235. Kaluz, S., et al., *Transcriptional control of the tumor- and hypoxia-marker carbonic anhydrase 9: A one transcription factor (HIF-1) show?* Biochim Biophys Acta, 2009. **1795**(2): p. 162-72.
236. Pastorekova, S., S. Parkkila, and J. Zavada, *Tumor‐associated Carbonic Anhydrases and Their Clinical Significance.* 2006. **42**: p. 167-216.
237. Pastorek, J. and S. Pastorekova, *Hypoxia-induced carbonic anhydrase IX as a target for cancer therapy: from biology to clinical use.* Semin Cancer Biol, 2015. **31**: p. 52-64.
238. Toei, M., R. Saum, and M. Forgac, *Regulation and isoform function of the V-ATPases.* Biochemistry, 2010. **49**(23): p. 4715-23.
239. Forgac, M., *Vacuolar ATPases: rotary proton pumps in physiology and pathophysiology.* Nat Rev Mol Cell Biol, 2007. **8**(11): p. 917-29.
240. Slepkov, E.R., et al., *Structural and functional analysis of the Na+/H+ exchanger.* Biochem J, 2007. **401**(3): p. 623-33.
241. Boedtkjer, E., L. Bunch, and S.F. Pedersen, *Physiology, pharmacology and pathophysiology of the pH regulatory transport proteins NHE1 and NBCn1: similarities, differences, and implications for cancer therapy.* Curr Pharm Des, 2012. **18**(10): p. 1345-71.
242. Wykoff, C.C., et al., *Hypoxia-inducible expression of tumor-associated carbonic anhydrases.* Cancer Res, 2000. **60**(24): p. 7075-83.
243. Ivanov, S., et al., *Expression of Hypoxia-Inducible Cell-Surface Transmembrane Carbonic Anhydrases in Human Cancer.* The American Journal of Pathology, 2001. **158**(3): p. 905-919.
244. Tafreshi, N.K., et al., *Noninvasive detection of breast cancer lymph node metastasis using carbonic anhydrases IX and XII targeted imaging probes.* Clin Cancer Res, 2012. **18**(1): p. 207-19.
245. Ulmasov, B., et al., *Purification and kinetic analysis of recombinant CA XII, a membrane carbonic anhydrase overexpressed in certain cancers.* Proceedings of the National Academy of Sciences of the United States of America, 2000. **97**(26): p. 14212-14217.
246. Pastorekova, S., J. Kopacek, and J. Pastorek, *Carbonic anhydrase inhibitors and the management of cancer.* Curr Top Med Chem, 2007. **7**(9): p. 865-78.
247. Wakabayashi, S., et al., *Kinetic dissection of two distinct proton binding sites in Na+/H+ exchangers by measurement of reverse mode reaction.* J Biol Chem, 2003. **278**(44): p. 43580-5.
248. Fafournoux, P., J. Noel, and J. Pouyssegur, *Evidence that Na+/H+ exchanger isoforms NHE1 and NHE3 exist as stable dimers in membranes with a high degree of specificity for homodimers.* J Biol Chem, 1994. **269**(4): p. 2589-96.
249. Hisamitsu, T., et al., *Dimeric interaction between the cytoplasmic domains of the Na+/H+ exchanger NHE1 revealed by symmetrical intermolecular cross-linking and selective co-immunoprecipitation.* Biochemistry, 2004. **43**(34): p. 11135-43.
250. Lawrence, S.P., G.D. Holman, and F. Koumanov, *Translocation of the Na+/H+ exchanger 1 (NHE1) in cardiomyocyte responses to insulin and energy-status signalling.* Biochem J, 2010. **432**(3): p. 515-23.

251. Besson, P., et al., *Regulation of Na+/H+ exchanger gene expression: mitogenic stimulation increases NHE1 promoter activity.* Am J Physiol, 1998. **274**(3 Pt 1): p. C831-9.
252. Akram, S., et al., *Reactive oxygen species-mediated regulation of the Na+-H+ exchanger 1 gene expression connects intracellular redox status with cells' sensitivity to death triggers.* Cell Death Differ, 2006. **13**(4): p. 628-41.
253. Yang, X., et al., *Expression and modulation of Na+/H+ exchanger 1 gene in hepatocellular carcinoma: A potential therapeutic target.* Journal of Gastroenterology and Hepatology, 2011. **26**(2): p. 364-370.
254. Shimoda, L.A., et al., *HIF-1 regulates hypoxic induction of NHE1 expression and alkalinization of intracellular pH in pulmonary arterial myocytes.* Am J Physiol Lung Cell Mol Physiol, 2006. **291**(5): p. L941-9.
255. Yang, X., et al., *Inhibition of Na(+)/H(+) exchanger 1 by 5-(N-ethyl-N-isopropyl) amiloride reduces hypoxia-induced hepatocellular carcinoma invasion and motility.* Cancer Lett, 2010. **295**(2): p. 198-204.
256. Rios, E.J., et al., *Chronic hypoxia elevates intracellular pH and activates Na+/H+ exchange in pulmonary arterial smooth muscle cells.* Am J Physiol Lung Cell Mol Physiol, 2005. **289**(5): p. L867-74.
257. Smith, A.N., et al., *Vacuolar H+-ATPase d2 subunit: molecular characterization, developmental regulation, and localization to specialized proton pumps in kidney and bone.* J Am Soc Nephrol, 2005. **16**(5): p. 1245-56.
258. Toyomura, T., et al., *From lysosomes to the plasma membrane: localization of vacuolar-type H+ -ATPase with the a3 isoform during osteoclast differentiation.* J Biol Chem, 2003. **278**(24): p. 22023-30.
259. Martinez-Zaguilan, R., et al., *Vacuolar-type H(+)-ATPases are functionally expressed in plasma membranes of human tumor cells.* Am J Physiol, 1993. **265**(4 Pt 1): p. C1015-29.
260. Sennoune, S.R., et al., *Vacuolar H+-ATPase in human breast cancer cells with distinct metastatic potential: distribution and functional activity.* Am J Physiol Cell Physiol, 2004. **286**(6): p. C1443-52.
261. Sennoune, S.R. and R. Martinez-Zaguilan, *Vacuolar H(+)-ATPase signaling pathway in cancer.* Curr Protein Pept Sci, 2012. **13**(2): p. 152-63.
262. Hernandez, A., et al., *Intracellular proton pumps as targets in chemotherapy: V-ATPases and cancer.* Curr Pharm Des, 2012. **18**(10): p. 1383-94.
263. Pérez-Sayáns, M., et al., *Measurement of ATP6V1C1 expression in brush cytology samples as a diagnostic and prognostic marker in oral squamous cell carcinoma.* Cancer Biology & Therapy, 2014. **9**(12): p. 1057-1064.
264. Otero-Rey, E.M., et al., *Intracellular pH regulation in oral squamous cell carcinoma is mediated by increased V-ATPase activity via over-expression of the ATP6V1C1 gene.* Oral Oncol, 2008. **44**(2): p. 193-9.
265. Torigoe, T., et al., *Enhanced expression of the human vacuolar H+-ATPase c subunit gene (ATP6L) in response to anticancer agents.* J Biol Chem, 2002. **277**(39): p. 36534-43.
266. Murakami, T., et al., *Elevated expression of vacuolar proton pump genes and cellular PH in cisplatin resistance.* Int J Cancer, 2001. **93**(6): p. 869-74.

267. Gerweck, L.E. and K. Seetharaman, *Cellular pH gradient in tumor versus normal tissue: potential exploitation for the treatment of cancer.* Cancer Res, 1996. **56**(6): p. 1194-8.
268. Gillies, R.J., et al., *MRI of the tumor microenvironment.* J Magn Reson Imaging, 2002. **16**(4): p. 430-50.
269. Harguindey, S., et al., *Proton transport inhibitors as potentially selective anticancer drugs.* Anticancer Res, 2009. **29**(6): p. 2127-36.
270. Gupta, G.P. and J. Massague, *Cancer metastasis: building a framework.* Cell, 2006. **127**(4): p. 679-95.
271. Stock, C. and A. Schwab, *Protons make tumor cells move like clockwork.* Pflugers Arch, 2009. **458**(5): p. 981-92.
272. Ludwig, F.T., A. Schwab, and C. Stock, *The Na+ /H+ -exchanger (NHE1) generates pH nanodomains at focal adhesions.* J Cell Physiol, 2013. **228**(6): p. 1351-8.
273. Srivastava, J., et al., *Structural model and functional significance of pH-dependent talin-actin binding for focal adhesion remodeling.* Proc Natl Acad Sci U S A, 2008. **105**(38): p. 14436-41.
274. Orlichenko, L.S. and D.C. Radisky, *Matrix metalloproteinases stimulate epithelial-mesenchymal transition during tumor development.* Clin Exp Metastasis, 2008. **25**(6): p. 593-600.
275. Rofstad, E.K., et al., *Acidic extracellular pH promotes experimental metastasis of human melanoma cells in athymic nude mice.* Cancer Res, 2006. **66**(13): p. 6699-707.
276. Harashima, H., N. Dissmeyer, and A. Schnittger, *Cell cycle control across the eukaryotic kingdom.* Trends Cell Biol, 2013. **23**(7): p. 345-56.
277. Malumbres, M. and M. Barbacid, *Cell cycle, CDKs and cancer: a changing paradigm.* Nat Rev Cancer, 2009. **9**(3): p. 153-66.
278. Pouyssegur, J., et al., *Cytoplasmic pH, a key determinant of growth factor-induced DNA synthesis in quiescent fibroblasts.* FEBS Lett, 1985. **190**(1): p. 115-9.
279. Putney, L.K. and D.L. Barber, *Na-H exchange-dependent increase in intracellular pH times G2/M entry and transition.* J Biol Chem, 2003. **278**(45): p. 44645-9.
280. Lagadic-Gossmann, D., L. Huc, and V. Lecureur, *Alterations of intracellular pH homeostasis in apoptosis: origins and roles.* Cell Death Differ, 2004. **11**(9): p. 953-61.
281. Matsuyama, S., et al., *Changes in intramitochondrial and cytosolic pH: early events that modulate caspase activation during apoptosis.* Nat Cell Biol, 2000. **2**(6): p. 318-25.
282. Holahan, E.V., P.K. Stuart, and W.C. Dewey, *Enhancement of Survival of CHO Cells by Acidic pH after X Irradiation.* Radiation Research, 1982. **89**(2): p. 433-435.
283. Rottinger, E.M., M. Mendonca, and L.E. Gerweck, *Modification of pH induced cellular inactivation by irradiation-glial cells.* Int J Radiat Oncol Biol Phys, 1980. **6**(12): p. 1659-62.
284. Freeman, M.L., et al., *The effect of pH on hyperthermic and x ray induced cell killing.* Int J Radiat Oncol Biol Phys, 1981. **7**(2): p. 211-6.

285. Freeman, M.L. and E. Sierra, *An acidic extracellular environment reduces the fixation of radiation damage.* Radiat Res, 1984. **97**(1): p. 154-61.
286. Lee, H.S., et al., *Radiation-induced apoptosis in different pH environments in vitro.* Int J Radiat Oncol Biol Phys, 1997. **38**(5): p. 1079-87.
287. Ojeda, F., et al., *Radiation-Induced Apoptosis in Thymocytes: pH Sensitization.* Zeitschrift für Naturforschung C. A Journal of Biosciences, 1996. **51**(5-6): p. 432-434.
288. DiPaola, R.S., *To arrest or not to G(2)-M Cell-cycle arrest : commentary re: A. K. Tyagi et al., Silibinin strongly synergizes human prostate carcinoma DU145 cells to doxorubicin-induced growth inhibition, G(2)-M arrest, and apoptosis. Clin. cancer res., 8: 3512-3519, 2002.* Clin Cancer Res, 2002. **8**(11): p. 3311-4.
289. Park, H.J., et al., *Influence of Environmental pH on G2-Phase Arrest Caused by Ionizing Radiation.* Radiation Research, 2003. **159**(1): p. 86-93.
290. Wojtkowiak, J.W., et al., *Drug resistance and cellular adaptation to tumor acidic pH microenvironment.* Mol Pharm, 2011. **8**(6): p. 2032-8.
291. Mahoney, B.P., et al., *Tumor acidity, ion trapping and chemotherapeutics.* Biochemical Pharmacology, 2003. **66**(7): p. 1207-1218.
292. Tacar, O., P. Sriamornsak, and C.R. Dass, *Doxorubicin: an update on anticancer molecular action, toxicity and novel drug delivery systems.* J Pharm Pharmacol, 2013. **65**(2): p. 157-70.
293. Altan, N., et al., *Defective acidification in human breast tumor cells and implications for chemotherapy.* J Exp Med, 1998. **187**(10): p. 1583-98.
294. Schindler, M., et al., *Defective pH regulation of acidic compartments in human breast cancer cells (MCF-7) is normalized in adriamycin-resistant cells (MCF-7adr).* Biochemistry, 1996. **35**(9): p. 2811-7.
295. Raghunand, N., et al., *Enhancement of chemotherapy by manipulation of tumour pH.* Br J Cancer, 1999. **80**(7): p. 1005-11.
296. Gerweck, L.E., S. Vijayappa, and S. Kozin, *Tumor pH controls the in vivo efficacy of weak acid and base chemotherapeutics.* Mol Cancer Ther, 2006. **5**(5): p. 1275-9.
297. Thews, O., et al., *Impact of extracellular acidity on the activity of P-glycoprotein and the cytotoxicity of chemotherapeutic drugs.* Neoplasia, 2006. **8**(2): p. 143-52.
298. Lotz, C., et al., *Role of the tumor microenvironment in the activity and expression of the p-glycoprotein in human colon carcinoma cells.* Oncol Rep, 2007. **17**(1): p. 239-44.
299. Breedveld, P., et al., *The Effect of Low pH on Breast Cancer Resistance Protein (ABCG2)-Mediated Transport of Methotrexate, 7-Hydroxymethotrexate, Methotrexate Diglutamate, Folic Acid, Mitoxantrone, Topotecan, and Resveratrol in In Vitro Drug Transport Models.* Molecular Pharmacology, 2006. **71**(1): p. 240-249.
300. McDonald, P.C. and S. Dedhar, *Carbonic anhydrase IX (CAIX) as a mediator of hypoxia-induced stress response in cancer cells.* Subcell Biochem, 2014. **75**: p. 255-69.
301. McDonald, P.C., et al., *Recent Developments in Targeting Carbonic Anhydrase IX for Cancer Therapeutics.* Oncotarget, 2012. **3**(1): p. 84-97.

302. Ilie, M., et al., *High levels of carbonic anhydrase IX in tumour tissue and plasma are biomarkers of poor prognostic in patients with non-small cell lung cancer.* Br J Cancer, 2010. **102**(11): p. 1627-35.
303. Choschzick, M., et al., *Overexpression of carbonic anhydrase IX (CAIX) is an independent unfavorable prognostic marker in endometrioid ovarian cancer.* Virchows Arch, 2011. **459**(2): p. 193-200.
304. Haapasalo, J.A., et al., *Expression of carbonic anhydrase IX in astrocytic tumors predicts poor prognosis.* Clin Cancer Res, 2006. **12**(2): p. 473-7.
305. van Kuijk, S.J., et al., *Prognostic Significance of Carbonic Anhydrase IX Expression in Cancer Patients: A Meta-Analysis.* Front Oncol, 2016. **6**: p. 69.
306. Hussain, S.A., et al., *Hypoxia-regulated carbonic anhydrase IX expression is associated with poor survival in patients with invasive breast cancer.* Br J Cancer, 2007. **96**(1): p. 104-9.
307. Lou, Y., et al., *Targeting tumor hypoxia: suppression of breast tumor growth and metastasis by novel carbonic anhydrase IX inhibitors.* Cancer Res, 2011. **71**(9): p. 3364-76.
308. Gut, M.O., et al., *Gastric hyperplasia in mice with targeted disruption of the carbonic anhydrase gene Car9.* Gastroenterology, 2002. **123**(6): p. 1889-903.
309. Gieling, R.G. and K.J. Williams, *Carbonic anhydrase IX as a target for metastatic disease.* Bioorg Med Chem, 2013. **21**(6): p. 1470-6.
310. Gieling, R.G., et al., *Antimetastatic effect of sulfamate carbonic anhydrase IX inhibitors in breast carcinoma xenografts.* J Med Chem, 2012. **55**(11): p. 5591-600.
311. McDonald, P.C., S.C. Chafe, and S. Dedhar, *Overcoming Hypoxia-Mediated Tumor Progression: Combinatorial Approaches Targeting pH Regulation, Angiogenesis and Immune Dysfunction.* Front Cell Dev Biol, 2016. **4**: p. 27.
312. Supuran, C.T., *Carbonic anhydrases: novel therapeutic applications for inhibitors and activators.* Nat Rev Drug Discov, 2008. **7**(2): p. 168-81.
313. Pettersen, E.O., et al., *Targeting tumour hypoxia to prevent cancer metastasis. From biology, biosensing and technology to drug development: the METOXIA consortium.* J Enzyme Inhib Med Chem, 2015. **30**(5): p. 689-721.
314. Surfus, J.E., et al., *Anti-renal-cell carcinoma chimeric antibody G250 facilitates antibody-dependent cellular cytotoxicity with in vitro and in vivo interleukin-2-activated effectors.* J Immunother Emphasis Tumor Immunol, 1996. **19**(3): p. 184-91.
315. Davis, I.D., et al., *A phase I multiple dose, dose escalation study of cG250 monoclonal antibody in patients with advanced renal cell carcinoma.* Cancer Immunity : a Journal of the Academy of Cancer Immunology, 2007. **7**: p. 13.
316. Siebels, M., et al., *A clinical phase I/II trial with the monoclonal antibody cG250 (RENCAREX(R)) and interferon-alpha-2a in metastatic renal cell carcinoma patients.* World J Urol, 2011. **29**(1): p. 121-6.
317. Stillebroer, A.B., et al., *Phase 1 radioimmunotherapy study with lutetium 177-labeled anti-carbonic anhydrase IX monoclonal antibody girentuximab in patients with advanced renal cell carcinoma.* Eur Urol, 2013. **64**(3): p. 478-85.

318. Muselaers, C.H., et al., *Phase 2 Study of Lutetium 177-Labeled Anti-Carbonic Anhydrase IX Monoclonal Antibody Girentuximab in Patients with Advanced Renal Cell Carcinoma.* Eur Urol, 2016. **69**(5): p. 767-70.
319. Guler, O.O., G. De Simone, and C.T. Supuran, *Drug design studies of the novel antitumor targets carbonic anhydrase IX and XII.* Curr Med Chem, 2010. **17**(15): p. 1516-26.
320. Dubois, L., et al., *Targeting carbonic anhydrase IX by nitroimidazole based sulfamides enhances the therapeutic effect of tumor irradiation: a new concept of dual targeting drugs.* Radiother Oncol, 2013. **108**(3): p. 523-8.
321. Rami, M., et al., *Hypoxia-targeting carbonic anhydrase IX inhibitors by a new series of nitroimidazole-sulfonamides/sulfamides/sulfamates.* J Med Chem, 2013. **56**(21): p. 8512-20.
322. Loo, S.Y., et al., *NHE-1: a promising target for novel anti-cancer therapeutics.* Curr Pharm Des, 2012. **18**(10): p. 1372-82.
323. Cardone, R.A., V. Casavola, and S.J. Reshkin, *The role of disturbed pH dynamics and the Na+/H+ exchanger in metastasis.* Nat Rev Cancer, 2005. **5**(10): p. 786-95.
324. Reshkin, S.J., M.R. Greco, and R.A. Cardone, *Role of pHi, and proton transporters in oncogene-driven neoplastic transformation.* Philos Trans R Soc Lond B Biol Sci, 2014. **369**(1638): p. 20130100.
325. Yun, C.H., et al., *Leu143 in the putative fourth membrane spanning domain is critical for amiloride inhibition of an epithelial Na+/H+ exchanger isoform (NHE-2).* Biochem Biophys Res Commun, 1993. **193**(2): p. 532-9.
326. Szabo, E.Z., et al., *Kinetic and pharmacological properties of human brain Na(+)/H(+) exchanger isoform 5 stably expressed in Chinese hamster ovary cells.* J Biol Chem, 2000. **275**(9): p. 6302-7.
327. Matthews, H., M. Ranson, and M.J. Kelso, *Anti-tumour/metastasis effects of the potassium-sparing diuretic amiloride: an orally active anti-cancer drug waiting for its call-of-duty?* Int J Cancer, 2011. **129**(9): p. 2051-61.
328. Harguindey, S., et al., *Cariporide and other new and powerful NHE1 inhibitors as potentially selective anticancer drugs – an integral molecular/biochemical/metabolic/clinical approach after one hundred years of cancer research.* Journal of Translational Medicine, 2013. **11**(1): p. 1-17.
329. Palandoken, H., et al., *Amiloride peptide conjugates: prodrugs for sodium-proton exchange inhibition.* J Pharmacol Exp Ther, 2005. **312**(3): p. 961-7.
330. Reshkin, S.J., R.A. Cardone, and S. Harguindey, *Na+-H+ exchanger, pH regulation and cancer.* Recent Pat Anticancer Drug Discov, 2013. **8**(1): p. 85-99.
331. Fais, S., et al., *Targeting vacuolar H+-ATPases as a new strategy against cancer.* Cancer Res, 2007. **67**(22): p. 10627-30.
332. Sennoune, S.R., D. Luo, and R. Martinez-Zaguilan, *Plasmalemmal vacuolar-type H+-ATPase in cancer biology.* Cell Biochem Biophys, 2004. **40**(2): p. 185-206.
333. Spugnini, E.P., et al., *Proton channels and exchangers in cancer.* Biochim Biophys Acta, 2015. **1848**(10 Pt B): p. 2715-26.
334. Luciani, F., et al., *Effect of proton pump inhibitor pretreatment on resistance of solid tumors to cytotoxic drugs.* J Natl Cancer Inst, 2004. **96**(22): p. 1702-13.

335. Capecci, J. and M. Forgac, *The function of vacuolar ATPase (V-ATPase) a subunit isoforms in invasiveness of MCF10a and MCF10CA1a human breast cancer cells.* J Biol Chem, 2013. **288**(45): p. 32731-41.
336. Cotter, K., et al., *Activity of plasma membrane V-ATPases is critical for the invasion of MDA-MB231 breast cancer cells.* J Biol Chem, 2015. **290**(6): p. 3680-92.
337. Werner, G., et al., *Metabolic products of microorganisms. 224. Bafilomycins, a new group of macrolide antibiotics. Production, isolation, chemical structure and biological activity.* J Antibiot (Tokyo), 1984. **37**(2): p. 110-7.
338. Toshima, K., et al., *Total Synthesis of Bafilomycin A1.* The Journal of Organic Chemistry, 1997. **62**(10): p. 3271-3284.
339. Bowman, E.J., et al., *The bafilomycin/concanamycin binding site in subunit c of the V-ATPases from Neurospora crassa and Saccharomyces cerevisiae.* J Biol Chem, 2004. **279**(32): p. 33131-8.
340. Fernandes, F., et al., *Binding assays of inhibitors towards selected V-ATPase domains.* Biochim Biophys Acta, 2006. **1758**(11): p. 1777-86.
341. Wang, Y., T. Inoue, and M. Forgac, *Subunit a of the yeast V-ATPase participates in binding of bafilomycin.* J Biol Chem, 2005. **280**(49): p. 40481-8.
342. Bowman, B.J. and E.J. Bowman, *Mutations in subunit C of the vacuolar ATPase confer resistance to bafilomycin and identify a conserved antibiotic binding site.* J Biol Chem, 2002. **277**(6): p. 3965-72.
343. Teplova, V.V., et al., *Bafilomycin A1 is a potassium ionophore that impairs mitochondrial functions.* J Bioenerg Biomembr, 2007. **39**(4): p. 321-9.
344. Moriyama, Y., et al., *Evidence for a common binding site for omeprazole and N-ethylmaleimide in subunit A of chromaffin granule vacuolar-type H(+)-ATPase.* Biochem Biophys Res Commun, 1993. **196**(2): p. 699-706.
345. Sabolic, I., et al., *H(+)-ATPases of renal cortical and medullary endosomes are differentially sensitive to Sch-28080 and omeprazole.* Am J Physiol, 1994. **266**(6 Pt 2): p. F868-77.
346. Der, G., *An overview of proton pump inhibitors.* Gastroenterol Nurs, 2003. **26**(5): p. 182-90.
347. Kastelein, F., et al., *Proton pump inhibitors reduce the risk of neoplastic progression in patients with Barrett's esophagus.* Clin Gastroenterol Hepatol, 2013. **11**(4): p. 382-8.
348. Ferrari, S., et al., *Proton pump inhibitor chemosensitization in human osteosarcoma: from the bench to the patients' bed.* J Transl Med, 2013. **11**: p. 268.
349. Spugnini, E.P., et al., *Lansoprazole as a rescue agent in chemoresistant tumors: a phase I/II study in companion animals with spontaneously occurring tumors.* J Transl Med, 2011. **9**: p. 221.
350. Wang, B.Y., et al., *Intermittent high dose proton pump inhibitor enhances the antitumor effects of chemotherapy in metastatic breast cancer.* J Exp Clin Cancer Res, 2015. **34**: p. 85.
351. Das, V., et al., *Pathophysiologically relevant in vitro tumor models for drug screening.* Drug Discov Today, 2015. **20**(7): p. 848-55.
352. Vargo-Gogola, T. and J.M. Rosen, *Modelling breast cancer: one size does not fit all.* Nat Rev Cancer, 2007. **7**(9): p. 659-72.

353. Hickman, J.A., et al., *Three-dimensional models of cancer for pharmacology and cancer cell biology: capturing tumor complexity in vitro/ex vivo.* Biotechnol J, 2014. **9**(9): p. 1115-28.
354. Katz, E., et al., *Targeting of Rac GTPases blocks the spread of intact human breast cancer.* Oncotarget, 2012. **3**(6): p. 608-19.
355. Ward, C., et al., *Evaluation of carbonic anhydrase IX as a therapeutic target for inhibition of breast cancer invasion and metastasis using a series of in vitro breast cancer models.* Oncotarget, 2015. **6**(28): p. 24856-70.
356. Manning, H.C., J.R. Buck, and R.S. Cook, *Mouse Models of Breast Cancer: Platforms for Discovering Precision Imaging Diagnostics and Future Cancer Medicine.* J Nucl Med, 2016. **57 Suppl 1**: p. 60S-8S.
357. Edmondson, R., et al., *Three-dimensional cell culture systems and their applications in drug discovery and cell-based biosensors.* Assay Drug Dev Technol, 2014. **12**(4): p. 207-18.
358. Hutmacher, D.W., *Biomaterials offer cancer research the third dimension.* Nat Mater, 2010. **9**(2): p. 90-3.
359. Fitzgerald, K.A., et al., *Life in 3D is never flat: 3D models to optimise drug delivery.* J Control Release, 2015. **215**: p. 39-54.
360. Weiswald, L.B., D. Bellet, and V. Dangles-Marie, *Spherical cancer models in tumor biology.* Neoplasia, 2015. **17**(1): p. 1-15.
361. Achilli, T.M., J. Meyer, and J.R. Morgan, *Advances in the formation, use and understanding of multi-cellular spheroids.* Expert Opin Biol Ther, 2012. **12**(10): p. 1347-60.
362. Jamieson, L.E., D.J. Harrison, and C.J. Campbell, *Chemical analysis of multicellular tumour spheroids.* Analyst, 2015. **140**(12): p. 3910-20.
363. Leek, R., et al., *Methods: Using Three-Dimensional Culture (Spheroids) as an In Vitro Model of Tumour Hypoxia.* Adv Exp Med Biol, 2016. **899**: p. 167-96.
364. Hirschhaeuser, F., et al., *Multicellular tumor spheroids: an underestimated tool is catching up again.* J Biotechnol, 2010. **148**(1): p. 3-15.
365. Kramer, N., et al., *In vitro cell migration and invasion assays.* Mutat Res, 2013. **752**(1): p. 10-24.
366. Brown, L.F., et al., *Vascular stroma formation in carcinoma in situ, invasive carcinoma, and metastatic carcinoma of the breast.* Clin Cancer Res, 1999. **5**(5): p. 1041-56.
367. Gillet, J.-P., et al., *Redefining the relevance of established cancer cell lines to the study of mechanisms of clinical anti-cancer drug resistance.* Proceedings of the National Academy of Sciences, 2011. **108**(46): p. 18708-18713.
368. Daniel, V.C., et al., *A primary xenograft model of small-cell lung cancer reveals irreversible changes in gene expression imposed by culture in vitro.* Cancer Res, 2009. **69**(8): p. 3364-73.
369. Leeper, A.D., et al., *Determining tamoxifen sensitivity using primary breast cancer tissue in collagen-based three-dimensional culture.* Biomaterials, 2012. **33**(3): p. 907-15.
370. de Visser, K.E., A. Eichten, and L.M. Coussens, *Paradoxical roles of the immune system during cancer development.* Nat Rev Cancer, 2006. **6**(1): p. 24-37.

371. Lakshmi Narendra, B., et al., *Immune system: a double-edged sword in cancer.* Inflamm Res, 2013. **62**(9): p. 823-34.
372. Li, Y., et al., *Catalysis and pH Control by Membrane-associated Carbonic Anhydrase IX in MDA-MB-231 Breast Cancer Cells.* The Journal of Biological Chemistry, 2011. **286**(18): p. 15789-15796.
373. Lucien, F., et al., *Hypoxia-Induced Invadopodia Formation Involves Activation of NHE-1 by the p90 Ribosomal S6 Kinase (p90RSK).* PLoS ONE, 2011. **6**(12): p. e28851.
374. Ditte, P., et al., *Phosphorylation of Carbonic Anhydrase IX Controls Its Ability to Mediate Extracellular Acidification in Hypoxic Tumors.* Cancer Research, 2011. **71**(24): p. 7558.
375. Holliday, D.L. and V. Speirs, *Choosing the right cell line for breast cancer research.* 2011(1465-542X (Electronic)).
376. Gaffney, E.V., *A cell line (HBL-100) established from human breast milk.* Cell and Tissue Research, 1982. **227**(3): p. 563-568.
377. Skehan, P., et al., *New colorimetric cytotoxicity assay for anticancer-drug screening.* J Natl Cancer Inst, 1990. **82**(13): p. 1107-12.
378. Voigt, W., *Sulforhodamine B Assay and Chemosensitivity*, in *Chemosensitivity: Volume 1 In Vitro Assays*, R.D. Blumenthal, Editor. 2005, Humana Press: Totowa, NJ. p. 39-48.
379. Vichai, V. and K. Kirtikara, *Sulforhodamine B colorimetric assay for cytotoxicity screening.* Nat Protoc, 2006. **1**(3): p. 1112-6.
380. Fricker, S.P., *The application of sulforhodamine B as a colorimetric endpoint in a cytotoxicity assay.* Toxicology in Vitro, 1994. **8**(4): p. 821-822.
381. Mocellin, S. and M. Provenzano, *RNA interference: learning gene knock-down from cell physiology.* Journal of Translational Medicine, 2004. **2**(1): p. 39.
382. *siRNA resuspension protocol*. [cited 2017 6.3.17]; Available from: http://dharmacon.gelifesciences.com/uploadedFiles/Resources/basic-sirna-resuspension-protocol.pdf.
383. Dharmacon. *siRNA transfection protocol*. 6.3.17]; Available from: http://dharmacon.gelifesciences.com/uploadedFiles/Resources/basic-dharmafect-protocol.pdf.
384. Mahmood, T. and P.-C. Yang, *Western Blot: Technique, Theory, and Trouble Shooting.* North American Journal of Medical Sciences, 2012. **4**(9): p. 429-434.
385. QIAGEN, *RNeasy Mini Handbook*. 2012.
386. *Illumina TotalPrep RNA amplification Kit Manual*. 2011.
387. Raleigh, J.A., et al., *Comparisons among Pimonidazole Binding, Oxygen Electrode Measurements, and Radiation Response in C3H Mouse Tumors.* Radiation Research, 1999. **151**(5): p. 580-589.
388. Bussink, J., et al., *Effects of nicotinamide and carbogen on oxygenation in human tumor xenografts measured with luminescense based fiber-optic probes.* Radiother Oncol, 2000. **57**(1): p. 21-30.
389. Ljungkvist, A.S., et al., *Changes in tumor hypoxia measured with a double hypoxic marker technique.* Int J Radiat Oncol Biol Phys, 2000. **48**(5): p. 1529-38.

390. Pogue, B.W., et al., *Estimation of Oxygen Distribution in RIF-1 Tumors by Diffusion Model-Based Interpretation of Pimonidazole Hypoxia and Eppendorf Measurements.* Radiation Research, 2001. **155**(1): p. 15-25.
391. Gandomkar, Z., P. Brennan, and C. Mello-Thoms, *Computer-based image analysis in breast pathology.* Journal of Pathology Informatics, 2016. **7**(1): p. 43-43.
392. Braun, M., et al., *Quantification of protein expression in cells and cellular subcompartments on immunohistochemical sections using a computer supported image analysis system.* Histol Histopathol, 2013. **28**(5): p. 605-10.
393. Winum, J.Y., et al., *Ureido-substituted sulfamates show potent carbonic anhydrase IX inhibitory and antiproliferative activities against breast cancer cell lines.* Bioorg Med Chem Lett, 2012. **22**(14): p. 4681-5.
394. Fan, S.H., et al., *AGPAT9 suppresses cell growth, invasion and metastasis by counteracting acidic tumor microenvironment through KLF4/LASS2/V-ATPase signaling pathway in breast cancer.* Oncotarget, 2015. **6**(21): p. 18406-17.
395. von Schwarzenberg, K., et al., *Mode of cell death induction by pharmacological vacuolar H+-ATPase (V-ATPase) inhibition.* J Biol Chem, 2013. **288**(2): p. 1385-96.
396. Supino, R., et al., *Biological effects of a new vacuolar-H,-ATPase inhibitor in colon carcinoma cell lines.* Ann N Y Acad Sci, 2009. **1171**: p. 606-16.
397. Turturro, F., et al., *Troglitazone Acts on Cellular pH and DNA Synthesis through a Peroxisome Proliferator-Activated Receptor γ-Independent Mechanism in Breast Cancer-Derived Cell Lines.* Clinical Cancer Research, 2004. **10**(20): p. 7022.
398. Amith, S.R., et al., *The Na(+) /H(+) exchanger (NHE1) as a novel co-adjuvant target in paclitaxel therapy of triple-negative breast cancer cells.* Oncotarget, 2015. **6**(2): p. 1262-1275.
399. Reshkin, S.J., et al., *Phosphoinositide 3-Kinase Is Involved in the Tumor-specific Activation of Human Breast Cancer Cell Na+/H+Exchange, Motility, and Invasion Induced by Serum Deprivation.* Journal of Biological Chemistry, 2000. **275**(8): p. 5361-5369.
400. Hinton, A., et al., *Function of a subunit isoforms of the V-ATPase in pH homeostasis and in vitro invasion of MDA-MB231 human breast cancer cells.* J Biol Chem, 2009. **284**(24): p. 16400-8.
401. Masereel, B., *An overview of inhibitors of Na+/H+ exchanger.* European Journal of Medicinal Chemistry, 2003. **38**(6): p. 547-554.
402. Bowman, E.J., A. Siebers, and K. Altendorf, *Bafilomycins: a class of inhibitors of membrane ATPases from microorganisms, animal cells, and plant cells.* Proceedings of the National Academy of Sciences, 1988. **85**(21): p. 7972-7976.
403. Duivenvoorden, W.C., et al., *Inhibition of carbonic anhydrase IX (CA9) sensitizes renal cell carcinoma to ionizing radiation.* Oncol Rep, 2015. **34**(4): p. 1968-76.
404. Doyen, J., et al., *Knock-down of hypoxia-induced carbonic anhydrases IX and XII radiosensitizes tumor cells by increasing intracellular acidosis.* Frontiers in Oncology, 2013. **2**(199).

405. Paglin, S., et al., *A novel response of cancer cells to radiation involves autophagy and formation of acidic vesicles.* Cancer Res, 2001. **61**(2): p. 439-44.
406. Balcer-Kubiczek, E.K., *Apoptosis in radiation therapy: a double-edged sword.* Exp Oncol, 2012. **34**(3): p. 277-85.
407. Gross, M.W., et al., *Calibration of misonidazole labeling by simultaneous measurement of oxygen tension and labeling density in multicellular spheroids.* Int J Cancer, 1995. **61**(4): p. 567-73.
408. Laurent, J., et al., *Multicellular tumor spheroid models to explore cell cycle checkpoints in 3D.* BMC Cancer, 2013. **13**(1): p. 1-12.
409. Mohanty, C., et al., *Massive induction of apoptosis of multicellular tumor spheroids by a novel compound with a calmodulin inhibitor-like mechanism.* journal of Cancer Therapeutics and Research, 2013. **2**(1).
410. Richard, D.E., et al., *p42/p44 mitogen-activated protein kinases phosphorylate hypoxia-inducible factor 1alpha (HIF-1alpha) and enhance the transcriptional activity of HIF-1.* J Biol Chem, 1999. **274**(46): p. 32631-7.
411. Choi, Y.J., et al., *HIF-1α modulation by topoisomerase inhibitors in non-small cell lung cancer cell lines.* Journal of Cancer Research and Clinical Oncology, 2009. **135**(8): p. 1047-1053.
412. Suzuki, H., A. Tomida, and T. Tsuruo, *Dephosphorylated hypoxia-inducible factor 1alpha as a mediator of p53-dependent apoptosis during hypoxia.* Oncogene, 2001. **20**(41): p. 5779-88.
413. Warfel, N.A., et al., *CDK1 stabilizes HIF-1α via direct phosphorylation of Ser668 to promote tumor growth.* Cell Cycle, 2013. **12**(23): p. 3689-3701.
414. Fuady, J.H., et al., *Estrogen-dependent downregulation of hypoxia-inducible factor (HIF)-2alpha in invasive breast cancer cells.* Oncotarget, 2016. **7**(21): p. 31153-65.
415. Minet, E., et al., *ERK activation upon hypoxia: involvement in HIF-1 activation.* FEBS Lett, 2000. **468**(1): p. 53-8.
416. Holmquist-Mengelbier, L., et al., *Recruitment of HIF-1alpha and HIF-2alpha to common target genes is differentially regulated in neuroblastoma: HIF-2alpha promotes an aggressive phenotype.* Cancer Cell, 2006. **10**(5): p. 413-23.
417. Wiesener, M.S., et al., *Induction of endothelial PAS domain protein-1 by hypoxia: characterization and comparison with hypoxia-inducible factor-1alpha.* Blood, 1998. **92**(7): p. 2260-8.
418. Janssen, H.L., et al., *Differentiation-associated staining with anti-pimonidazole antibodies in head and neck tumors.* Radiother Oncol, 2004. **70**(1): p. 91-7.
419. Chiche, J., et al., *Hypoxia-inducible carbonic anhydrase IX and XII promote tumor cell growth by counteracting acidosis through the regulation of the intracellular pH.* Cancer Res, 2009. **69**(1): p. 358-68.
420. Morris, J.C., et al., *Targeting hypoxic tumor cell viability with carbohydrate-based carbonic anhydrase IX and XII inhibitors.* J Med Chem, 2011. **54**(19): p. 6905-18.
421. Eom, K.Y., et al., *The Expression of Carbonic Anhydrase (CA) IX/XII and Lymph Node Metastasis in Early Breast Cancer.* Cancer Res Treat, 2016. **48**(1): p. 125-32.

422. Gatenby, R.A., et al., *Cellular adaptations to hypoxia and acidosis during somatic evolution of breast cancer.* British Journal of Cancer, 2007. **97**(5): p. 646-653.
423. Andersen, A.P., et al., *Roles of acid-extruding ion transporters in regulation of breast cancer cell growth in a 3-dimensional microenvironment.* Molecular Cancer, 2016. **15**(1): p. 1-18.
424. Hachem, J.P., et al., *Extracellular pH Controls NHE1 expression in epidermis and keratinocytes: implications for barrier repair.* J Invest Dermatol, 2005. **125**(4): p. 790-7.
425. http://www.uniprot.org/uniprot/P38606. [cited 2016 20th September].
426. Indelicato, M., et al., *Role of hypoxia and autophagy in MDA-MB-231 invasiveness.* J Cell Physiol, 2010. **223**(2): p. 359-68.
427. Munoz-Najar, U.M., et al., *Hypoxia stimulates breast carcinoma cell invasion through MT1-MMP and MMP-2 activation.* Oncogene, 2006. **25**(16): p. 2379-92.
428. Swietach, P., et al., *Tumor-associated carbonic anhydrase 9 spatially coordinates intracellular pH in three-dimensional multicellular growths.* J Biol Chem, 2008. **283**(29): p. 20473-83.
429. McIntyre, A., et al., *Carbonic anhydrase IX promotes tumor growth and necrosis in vivo and inhibition enhances anti-VEGF therapy.* Clin Cancer Res, 2012. **18**(11): p. 3100-11.
430. Janicke, R.U., et al., *Caspase-3 is required for DNA fragmentation and morphological changes associated with apoptosis.* J Biol Chem, 1998. **273**.
431. Kagawa, S., et al., *Deficiency of caspase-3 in MCF7 cells blocks Bax-mediated nuclear fragmentation but not cell death.* Clinical cancer research, 2001. **7**(5): p. 1474-1480.
432. Yang, X.-H., et al., *Reconstitution of Caspase 3 Sensitizes MCF-7 Breast Cancer Cells to Doxorubicin- and Etoposide-induced Apoptosis.* Cancer Research, 2001. **61**(1): p. 348.
433. Li, Y., et al., *Expression and Activity of Carbonic Anhydrase IX Is Associated With Metabolic Dysfunction in MDA-MB-231 Breast Cancer Cells.* Cancer investigation, 2009. **27**(6): p. 613-623.
434. Ohta, T., et al., *Bafilomycin A1 induces apoptosis in the human pancreatic cancer cell line Capan-1.* J Pathol, 1998. **185**(3): p. 324-30.
435. Nakashima, S., et al., *Vacuolar H+-ATPase inhibitor induces apoptosis via lysosomal dysfunction in the human gastric cancer cell line MKN-1.* J Biochem, 2003. **134**(3): p. 359-64.
436. Geraghty, R., et al., *Guidelines for the use of cell lines in biomedical research.* British journal of cancer, 2014. **111**(6): p. 1021-1046.
437. Wenger, S.L., et al., *Comparison of established cell lines at different passages by karyotype and comparative genomic hybridization.* Bioscience reports, 2004. **24**(6): p. 631-639.
438. Chou, T.-C., *Theoretical basis, experimental design, and computerized simulation of synergism and antagonism in drug combination studies.* Pharmacological reviews, 2006. **58**(3): p. 621-681.
439. Foucquier, J. and M. Guedj, *Analysis of drug combinations: current methodological landscape.* Pharmacology research & perspectives, 2015. **3**(3).

440. Franken, N.A., et al., *Clonogenic assay of cells in vitro.* Nature protocols, 2006. **1**(5): p. 2315-2319.
441. Ho, W.Y., et al., *Development of Multicellular Tumor Spheroid (MCTS) Culture from Breast Cancer Cell and a High Throughput Screening Method Using the MTT Assay.* PLOS ONE, 2012. **7**(9): p. e44640.
442. Wen, Z., et al., *A spheroid-based 3-D culture model for pancreatic cancer drug testing, using the acid phosphatase assay.* Brazilian Journal of Medical and Biological Research, 2013. **46**(7): p. 634-642.
443. Zhang, X., et al., *3D Spheroid Culture Enhances the Expression of Antifibrotic Factors in Human Adipose-Derived MSCs and Improves Their Therapeutic Effects on Hepatic Fibrosis.* Stem cells international, 2016. **2016**.
444. Munshi, A., M. Hobbs, and R.E. Meyn, *Clonogenic Cell Survival Assay*, in *Chemosensitivity: Volume 1 In Vitro Assays*, R.D. Blumenthal, Editor. 2005, Humana Press: Totowa, NJ. p. 21-28.
445. Yuan, Y., et al., *Cobalt inhibits the interaction between hypoxia-inducible factor-alpha and von Hippel-Lindau protein by direct binding to hypoxia-inducible factor-alpha.* J Biol Chem, 2003. **278**(18): p. 15911-6.
446. Sakamoto, T. and M. Seiki, *Mint3 enhances the activity of hypoxia-inducible factor-1 (HIF-1) in macrophages by suppressing the activity of factor inhibiting HIF-1.* J Biol Chem, 2009. **284**(44): p. 30350-9.
447. Sabeh, F., et al., *Secreted Versus Membrane-anchored Collagenases: RELATIVE ROLES IN FIBROBLAST-DEPENDENT COLLAGENOLYSIS AND INVASION.* Journal of Biological Chemistry, 2009. **284**(34): p. 23001-23011.
448. Sakamoto, T. and M. Seiki, *A membrane protease regulates energy production in macrophages by activating hypoxia-inducible factor-1 via a non-proteolytic mechanism.* J Biol Chem, 2010. **285**(39): p. 29951-64.
449. Pahwa, S., M.J. Stawikowski, and G.B. Fields, *Monitoring and Inhibiting MT1-MMP during Cancer Initiation and Progression.* Cancers, 2014. **6**(1): p. 416-435.
450. Han, J., et al., *Interaction of Mint3 with Furin regulates the localization of Furin in the trans-Golgi network.* J Cell Sci, 2008. **121**(Pt 13): p. 2217-23.
451. Sakamoto, T., D. Niiya, and M. Seiki, *Targeting the Warburg effect that arises in tumor cells expressing membrane type-1 matrix metalloproteinase.* J Biol Chem, 2011. **286**(16): p. 14691-704.
452. Pulyaeva, H., et al., *MT1-MMP correlates with MMP-2 activation potential seen after epithelial to mesenchymal transition in human breast carcinoma cells.* Clin Exp Metastasis, 1997. **15**(2): p. 111-20.
453. MacDougall, J.R. and L.M. Matrisian, *Targets of extinction: identification of genes whose expression is repressed as a consequence of somatic fusion between cells representing basal and luminal mammary epithelial phenotypes.* J Cell Sci, 2000. **113 (Pt 3)**: p. 409-23.
454. Petrella, B.L., J. Lohi, and C.E. Brinckerhoff, *Identification of membrane type-1 matrix metalloproteinase as a target of hypoxia-inducible factor-2 alpha in von Hippel-Lindau renal cell carcinoma.* Oncogene, 2005. **24**(6): p. 1043-52.

455. Li, Y., et al., *Expression and activity of carbonic anhydrase IX is associated with metabolic dysfunction in MDA-MB-231 breast cancer cells.* Cancer Invest, 2009. **27**(6): p. 613-23.
456. Hernandez-Barrantes, S., et al., *Binding of active (57 kDa) membrane type 1-matrix metalloproteinase (MT1-MMP) to tissue inhibitor of metalloproteinase (TIMP)-2 regulates MT1-MMP processing and pro-MMP-2 activation.* J Biol Chem, 2000. **275**(16): p. 12080-9.
457. Lee, S.H. and M. Hannink, *Molecular mechanisms that regulate transcription factor localization suggest new targets for drug development.* Adv Drug Deliv Rev, 2003. **55**(6): p. 717-31.
458. Depping, R., et al., *Nuclear translocation of hypoxia-inducible factors (HIFs): Involvement of the classical importin α/β pathway.* Biochimica et Biophysica Acta (BBA) - Molecular Cell Research, 2008. **1783**(3): p. 394-404.
459. Moroz, E., et al., *Real-Time Imaging of HIF-1α Stabilization and Degradation.* PLoS ONE, 2009. **4**(4): p. e5077.
460. Ree, A.H., et al., *Regulation of tissue-degrading factors and in vitro invasiveness in progression of breast cancer cells.* Clin Exp Metastasis, 1998. **16**(3): p. 205-15.
461. Hyseni, A., et al., *Subcellular FIH-1 expression patterns in invasive breast cancer in relation to HIF-1α expression.* Cellular Oncology (Dordrecht), 2011. **34**(6): p. 565-570.
462. Tan, E.Y., et al., *Cytoplasmic location of factor-inhibiting hypoxia-inducible factor is associated with an enhanced hypoxic response and a shorter survival in invasive breast cancer.* Breast Cancer Res, 2007. **9**(6): p. R89.
463. Bhattacharya, S., et al., *Functional role of p35srj, a novel p300/CBP binding protein, during transactivation by HIF-1.* Genes Dev, 1999. **13**(1): p. 64-75.
464. Freedman, S.J., et al., *Structural basis for negative regulation of hypoxia-inducible factor-1alpha by CITED2.* Nat Struct Biol, 2003. **10**(7): p. 504-12.
465. Yoon, H., et al., *CITED2 controls the hypoxic signaling by snatching p300 from the two distinct activation domains of HIF-1alpha.* Biochim Biophys Acta, 2011. **1813**(12): p. 2008-16.
466. Rouleau, M., et al., *PARP inhibition: PARP1 and beyond.* Nat Rev Cancer, 2010. **10**(4): p. 293-301.
467. Kaufmann, S.H., et al., *Specific proteolytic cleavage of poly(ADP-ribose) polymerase: an early marker of chemotherapy-induced apoptosis.* Cancer Res, 1993. **53**(17): p. 3976-85.
468. Rami, M., et al., *Hypoxia-Targeting Carbonic Anhydrase IX Inhibitors by a New Series of Nitroimidazole-Sulfonamides/Sulfamides/Sulfamates.* Journal of Medicinal Chemistry, 2013. **56**(21): p. 8512-8520.
469. Zatovicova, M., et al., *Ectodomain shedding of the hypoxia-induced carbonic anhydrase IX is a metalloprotease-dependent process regulated by TACE/ADAM17.* Br J Cancer, 2005. **93**(11): p. 1267-76.
470. Zatovicova, M. and S. Pastorekova, *Modulation of cell surface density of carbonic anhydrase IX by shedding of the ectodomain and endocytosis.* Acta Virol, 2013. **57**(2): p. 257-64.

471. Vidlickova, I., et al., *Apoptosis-induced ectodomain shedding of hypoxia-regulated carbonic anhydrase IX from tumor cells: a double-edged response to chemotherapy.* BMC Cancer, 2016. **16**: p. 239.
472. Hektoen, H.H., et al., *Sulfamate inhibitor S4 influences carbonic anhydrase IX ectodomain shedding in colorectal carcinoma cells.* J Enzyme Inhib Med Chem, 2016. **31**(5): p. 779-86.
473. Meijer, T.W., et al., *Tumor microenvironmental changes induced by the sulfamate carbonic anhydrase IX inhibitor S4 in a laryngeal tumor model.* PLoS One, 2014. **9**(9): p. e108068.
474. Scozzafava, A. and C.T. Supuran, *Carbonic anhydrase and matrix metalloproteinase inhibitors: sulfonylated amino acid hydroxamates with MMP inhibitory properties act as efficient inhibitors of CA isozymes I, II, and IV, and N-hydroxysulfonamides inhibit both these zinc enzymes.* J Med Chem, 2000. **43**(20): p. 3677-87.
475. DeRose, Y.S., et al., *Tumor grafts derived from women with breast cancer authentically reflect tumor pathology, growth, metastasis and disease outcomes.* Nat Med, 2011. **17**(11): p. 1514-20.
476. Dean, J.L., et al., *Therapeutic response to CDK4/6 inhibition in breast cancer defined by ex vivo analyses of human tumors.* Cell Cycle, 2012. **11**(14): p. 2756-61.
477. Mao, Y., et al., *Stroma Cells in Tumor Microenvironment and Breast Cancer.* Cancer metastasis reviews, 2013. **32**(0): p. 303-315.
478. Chan, M.C., et al., *Tuning the Transcriptional Response to Hypoxia by Inhibiting Hypoxia-inducible Factor (HIF) Prolyl and Asparaginyl Hydroxylases.* Journal of Biological Chemistry, 2016. **291**(39): p. 20661-20673.
479. Gieling, R.G., et al., *Inhibition of carbonic anhydrase activity modifies the toxicity of doxorubicin and melphalan in tumour cells in vitro.* J Enzyme Inhib Med Chem, 2013. **28**(2): p. 360-9.
480. van Kuijk, S.J., et al., *The Sulfamate Small Molecule CAIX Inhibitor S4 Modulates Doxorubicin Efficacy.* PLoS One, 2016. **11**(8): p. e0161040.
481. Federici, C., et al., *Lansoprazole and carbonic anhydrase IX inhibitors sinergize against human melanoma cells.* J Enzyme Inhib Med Chem, 2016: p. 1-7.
482. Sabeh, F., et al., *Tumor cell traffic through the extracellular matrix is controlled by the membrane-anchored collagenase MT1-MMP.* J Cell Biol, 2004. **167**(4): p. 769-81.
483. Espi, M.d.L.V., *Characterization of the mechanism by which carbonic anhydrase IX facilitates tumour growth and metastasis*. 2015, The University of British Columbia.
484. Goh, W., I. Sleptsova-Freidrich, and N. Petrovic, *Use of proton pump inhibitors as adjunct treatment for triple-negative breast cancers. An introductory study.* J Pharm Pharm Sci, 2014. **17**(3): p. 439-46.
485. Jin, U.H., et al., *The aryl hydrocarbon receptor ligand omeprazole inhibits breast cancer cell invasion and metastasis.* BMC Cancer, 2014. **14**: p. 498.
486. De Milito, A., et al., *Proton pump inhibitors induce apoptosis of human B-cell tumors through a caspase-independent mechanism involving reactive oxygen species.* Cancer Res, 2007. **67**(11): p. 5408-17.

487. De Milito, A., et al., *pH-dependent antitumor activity of proton pump inhibitors against human melanoma is mediated by inhibition of tumor acidity.* Int J Cancer, 2010. **127**(1): p. 207-19.
488. Zhang, S., Y. Wang, and S.J. Li, *Lansoprazole induces apoptosis of breast cancer cells through inhibition of intracellular proton extrusion.* Biochem Biophys Res Commun, 2014. **448**(4): p. 424-9.